



2022 Grid Energy Storage Technology Cost and Performance Assessment

Vilayanur Viswanathan, Kendall Mongird, Ryan Franks,
Xiaolin Li, Vincent Sprenkle*, Pacific Northwest National
Laboratory.

Richard Baxter, Mustang Prairie Energy

* vincent.sprenkle@pnnl.gov

Technical Report

Publication No. PNNL-33283

August 2022

Disclaimer

This report was prepared as an account of work sponsored by an agency of the United States government. Neither the United States government nor any agency thereof, nor any of their employees, makes any warranty, express or implied, or assumes any legal liability or responsibility for the accuracy, completeness, or usefulness of any information, apparatus, product, or process disclosed, or represents that its use would not infringe privately owned rights. Reference herein to any specific commercial product, process, or service by trade name, trademark, manufacturer, or otherwise does not necessarily constitute or imply its endorsement, recommendation, or favoring by the United States government.

Acknowledgments

The Energy Storage Grand Challenge (ESGC) is a crosscutting effort managed by the Department of Energy's Research Technology Investment Committee. The project team would like to acknowledge the support, guidance, and management of Paul Spitsen from the DOE Office of Strategic Analysis, ESGC Policy and Valuation Track Lead and Eric Hsieh from the DOE Office of Electricity, ESGC Technology Development Track Lead in the development and execution of this assessment for the ESGC.

Other DOE contributors to acknowledge include Kara Podkaminer (Office of Strategic Analysis); Sunita Satyapal, Neha Rustagi, Ned Stetson and Eric Miller (Hydrogen and Fuel Cell Technologies); Sam Bockenbauer (Water Power Technologies); David Howell and Steven Boyd (Vehicle Technologies); Avi Shultz, Vijaykumar Rajgopal, Andru Prescod, Andrew Dawson (Solar Energy Technologies); Stephen Hendrickson (Office of Technology Transitions); Hugh Ho (Office of Strategic Planning and Policy); and Vinod Siberry (Office of Electricity). Input data for this work were derived from the energy storage pricing surveys supported by the DOE Office of Electricity Energy Storage Program under the guidance of Dr. Imre Gyuk.

Additional support for this effort was provided by Nate Blair, Chad Hunter, Vignesh Ramasamy, Chad Augustine, Greg Stark, Margaret Mann, Vicky Putsche, and David Feldman of the National Renewable Energy Laboratory; Vladimir Koritarov and Susan Babinec at Argonne National Laboratory; Brennan Smith at Oak Ridge National Laboratory; and Elsie Puig Santana, Tim Wolf, Andrea Starr, Shannon Bates, Matt Paiss, Charlie Vartanian, Daiwon Choi, Jan Haigh, and Mark Weimar at Pacific Northwest National Laboratory.

The authors also wish to acknowledge the significant contributions and insight provided by the industry partners referenced in the assessment.

Foreword to 2022 Report

The Department of Energy's (DOE) Energy Storage Grand Challenge (ESGC) is a comprehensive program to accelerate the development, commercialization, and utilization of next-generation energy storage technologies and sustain American global leadership in energy storage. The program is organized around five crosscutting pillars (Technology Development, Manufacturing and Supply Chain, Technology Transitions, Policy and Valuation, and Workforce Development) that are critical to achieving the ESGC's 2030 goals. Foundational to these efforts is the need to fully understand the current cost structure of energy storage technologies and identify the research and development opportunities that can impact further cost reductions. The second edition of the Cost and Performance Assessment continues ESGC's efforts of providing a standardized approach to analyzing the cost elements of storage technologies, engaging industry to identify these various cost elements, and projecting 2030 costs based on each technology's current state of development. This data-driven assessment of the current status of energy storage technologies is essential to track progress toward the goals described in the ESGC and inform the decision-making of a broad range of stakeholders.

As with last year, not all energy storage technologies are being addressed in the report due to the breadth of technologies available and their various states of development. Future efforts will continue to expand the list of energy storage technologies covered while providing any significant updates to cost and performance data for previous technologies.

Note that since data for this report was obtained in the year 2021, the comparison charts have the year 2021 for current costs. Due to intra-annual uncertainty, the reported costs may have changed by the time this report was released. The cost estimates provided in the report are not intended to be exact numbers but reflect a representative cost based on ranges provided by various sources for the examined technologies.

The 2022 Cost and Performance Assessment includes five additional features comprising of additional technologies & durations, changes to methodology such as battery replacement & inclusion of decommissioning costs, and updating key performance metrics such as cycle & calendar life.

1. The 2020 Cost and Performance Assessment provided installed costs for six energy storage technologies: lithium-ion (Li-ion) batteries, lead-acid batteries, vanadium redox flow batteries, pumped storage hydro, compressed-air energy storage, and hydrogen energy storage. The assessment adds zinc batteries, thermal energy storage, and gravitational energy storage.
2. The 2020 Cost and Performance Assessment provided the levelized cost of energy. The 2022 Cost and Performance Assessment provides the levelized cost of storage (LCOS). The two metrics determine the average price that a unit of energy output would need to be sold at to cover all project costs inclusive of taxes, financing, operations and maintenance, and others. However, shifting toward LCOS as a separate metric allows for the inclusion of storage-specific components and terminology that can be more accurately defined when compared to the levelized cost of energy calculation. This includes the cost to charge the storage system as well as augmentation and replacement of the storage block and power equipment. The LCOS offers a way to comprehensively compare the true cost of owning and operating various storage assets and creates better alignment with the new Energy Storage Earthshot (<https://www.energy.gov/eere/long-duration-storage-shot>).

3. This report incorporates an increase in Li-ion iron phosphate and nickel manganese cobalt Li-ion cycle life and calendar life based on input from industry partners.
4. Recycling and decommissioning are included as additional costs for Li-ion, redox flow, and lead-acid technologies.
5. The 2020 Cost and Performance Assessment analyzed energy storage systems from 2 to 10 hours. The 2022 Cost and Performance Assessment analyzes storage system at additional 24- and 100-hour durations. In September 2021, DOE launched the Long-Duration Storage Shot which aims to reduce costs by 90% in storage systems that deliver over 10 hours of duration within one decade. The analysis of longer duration storage systems supports this effort.¹

¹ <https://www.energy.gov/eere/long-duration-storage-shot>

Executive Summary

As growth and evolution of the grid storage industry continues, it becomes increasingly important to examine the various technologies and compare their costs and performance on an equitable basis. As part of the Energy Storage Grand Challenge, Pacific Northwest National Laboratory is leading the development of a detailed cost and performance database for a variety of energy storage technologies that is easily accessible and referenceable for the entire energy storage stakeholder community. This work aims to: 1) update cost and performance values and provide current cost ranges; 2) increase fidelity of the individual cost categories comprising a technology; 3) provide cost ranges and estimates for storage cost projections in 2030; and 4) develop an online website to make energy storage cost and performance data easily accessible and updatable for the stakeholder community. This research effort will periodically update tracked performance metrics and cost estimates as the storage industry continues its rapid pace of technological advancement.

During the preparation of the Phase 2 report, global supply chain disruptions led to volatility in costs for many categories of goods, including materials and components for energy storage systems. The disruption to energy storage materials and components is the result of the confluence of two global factors, plus the nascent nature of some new technologies and vendors.

First, the COVID-19 pandemic initially slowed manufacturing and shipping as work was suspended and worker safety precautions and protocols were enacted. Subsequently, consumption patterns changed as consumers shifted expenditures from services to goods. The increased consumption of goods resulted in higher competition and prices for freight shipping, scarcity of shipping containers, and delays at marine, roadway, and railway freight ports and depots. This confluence of shock in and response to supply chain disruption is anticipated to continue in the near term, adding a degree of uncertainty and volatility to current and near-future costs for energy storage systems (Doll, 2021; Lee & Tian, 2021).

Note that since data for this report was obtained in the year 2021, the comparison charts have the year 2021 for current costs. In addition, the energy storage industry includes many new categories of technology, plus new intermediate companies in the supply chain for both new and established technologies. Supply chains become more resilient as the number of suppliers and users of a material or component increase and there is a transition from one-off or intermittent ordering to continuous ordering due to ongoing production. Some technologies and supply chain nodes in the energy storage system industry have not yet reached this turning point of commercial maturity, which results in further exacerbating supply chain disruptions and, in turn, increased near-term cost and cost volatility.

Phase 2 of this initiative includes cost and performance metrics for most commercially available energy storage technologies across various energy-to-power ratios:

- Lithium-ion (Li-ion): lithium iron phosphate (LFP) batteries
- Li-ion: Li-ion nickel manganese cobalt (NMC) batteries
- Lead-acid batteries
- Vanadium redox flow batteries (RFBs)
- Diabatic Compressed-air energy storage (CAES)

- Pumped storage hydropower (PSH)
- Hydrogen energy storage system (HESS) (bidirectional)
- Zinc-based batteries
- Gravity energy storage
- Thermal energy storage

Note that diabatic CAES and some of the thermal energy storage technologies considered are not zero emission technologies, since they use fuel such as natural gas in the discharge cycle. Additional storage technologies will be incorporated in later phases of this research effort to capture emerging storage technologies of interest to the Department of Energy and other stakeholders.

In addition to current cost estimates and projections, the research team aimed to develop a cohesive framework to organize and aggregate the cost categories for energy storage systems (ESSs). This framework helps eliminate current inconsistencies associated with specific component costs (e.g., battery storage block vs. battery packs used in electric vehicles) and enables equitable comparisons between and among technologies, while using data from industry participants. The definitions and breakdown of these components has been reviewed by multiple energy storage experts in the technology developer community and national laboratories.

Cost and performance information was compiled for the defined categories and components based on conversations with technology developers and industry stakeholders, literature, commercial datasets, and reported storage costs for systems deployed across the United States. A range of detailed cost and performance estimates is presented for 2021 and projected out to 2030 for each technology. Current cost estimates provided in this report reflect the derived point estimate based on available data² from the reference sources listed above with estimated ranges for each studied technology.

In addition to ESS installed costs, a levelized cost of storage (LCOS) value for each technology is also provided to better compare the complete cost of each ESS over its project life, inclusive of any major overhauls and replacements required to maintain operation. The LCOS measures the price that a unit of energy output from the storage asset would need to be sold at to cover all project costs inclusive of taxes, financing costs, operations and maintenance, and others. It offers a way to comprehensively compare the true cost of owning and operating various storage assets.

Each technology was modeled for a specific set of power and duration combinations, depicted in Figure ES-1. Batteries were modeled for all cost and power durations considered. Other technologies were modeled specifically in high-power and longer duration applications assumed to be representative of their likely use cases and enable comparisons between and among technologies. For example, PSH and CAES primarily serve longer durations, but a duration of 4 hours at power levels of 100 MW and 1,000 MW is included to provide a comparison point at a shorter duration with other technologies and capture

² Depending on technology and category, the derived point estimate corresponds to the average after removing outliers (Li-ion and zinc storage block, CAES, PSH), professional judgment (balance of system), single estimate (lead-acid module), or consensus values (power conversion system). Hence, whether the value is average, median, or point estimate depends on the cost category and technology. We have therefore used “derived point estimate” since no single word can describe what the estimates represent. Point estimates within this document refer to the value residing within the upper and lower bounds of the cost range as the most representative cost.

uses in projects developed in the past. It is important to note that the cost and power combinations depicted in Figure ES-1 are not exhaustive of all use cases for each of the technologies modeled, but were chosen to allow for consistent evaluations of LCOS across systems.

	1 MW						10 MW						100 MW						1,000 MW									
	2	4	6	8	10	24	100	2	4	6	8	10	24	100	2	4	6	8	10	24	100	2	4	6	8	10	24	100
Lithium-ion LFP																												
Lithium-ion NMC																												
Lead Acid																												
Vanadium Redox Flow																												
Zinc																												
PSH																												
CAES																												
Hydrogen																												
Thermal																												
Gravitational																												

Figure ES-1. Power Capacity (MW) and Energy Duration (hr) Coverage Table by Technology

Key findings from this analysis include the following:

- PSH, the dominant grid storage technology, has a projected cost estimate of \$263/kWh for a 100 MW, 10-hour installed system. The most significant cost components are the reservoir (\$76/kWh) and powerhouse (\$742/kW). For a 24-hour system, the total installed cost is reduced to \$143/kWh.
- Battery grid storage solutions, which have seen significant growth in deployments in the past decade, have projected 2021 costs for fully installed 100 MW, 10-hour battery systems of: Li-ion LFP (\$356/kWh), Li-ion NMC (\$405/kWh), vanadium RFB (\$385/kWh), and lead-acid (\$409/kWh). Zinc-based systems are not available at the 100 MW scale; for a 10 MW, 10-hour system, the total installed cost for 2021 is \$449/kWh, putting it at a higher cost than the other systems at the same scale.
- Diabatic CAES is estimated to be the lowest cost storage technology on an installed cost basis at durations ≥ 4 hours (\$295/kWh for a 100 MW, 4 hour system, \$122/kWh for a 100 MW, 10 hour system). At 100 MW, 4 hours, LFP has the second lowest installed cost at \$385/kWh, followed by NMC (\$435/kWh) and lead-acid (\$447/kWh). At the 10 hour duration, PSH is projected to be the second lowest cost storage technology (\$263/kWh) at the same scale, followed by thermal and hydrogen. At 1,000 MW, while CAES retains its lowest cost status, thermal and gravitational storage move up in ranking, especially at 10 hour duration, with thermal nearly tied with PSH, followed by gravitational. For 1,000 MW, 100-hour duration, CAES is the lowest cost, closely followed by hydrogen, with PSH and thermal next, followed by gravitational, with batteries lagging far behind. Figures ES-2 and ES-3 show the total installed ESS costs by power capacity, duration, and technology for 2021 and 2030.
- Regarding projected 2030 installed ESS costs, for 100 MW, 4 hour systems, LFP (\$291/kWh) and CAES (\$295/kWh) installed costs are nearly the same, whereas CAES is significantly lower at 10 hours due to low cavern cost. At durations greater than 10 hours, HESS installed cost is just below CAES for both 100 MW and 1,000 MW systems. At 100 MW, 100 hours, CAES and HESS

systems are estimated at \$18/kWh and \$15/kWh, respectively followed by thermal and PSH, at \$73/kWh and \$83/kWh, respectively, with battery costs much higher just as in 2021.

- Diabatic CAES provides the lowest LCOS at durations ≥ 4 hours mainly due to the lower unit energy cost for caverns. At 1,000 MW, 10 hours, the LCOS for CAES is \$0.10/kWh followed closely by PSH (\$0.11/kWh) and gravitational (\$0.13/kWh), with lead-acid and hydrogen at the high end at \$0.33/kWh and \$0.35/kWh, respectively. HESS offers the highest LCOS at 10 hours due to its higher power equipment cost and lower round-trip efficiency but gets more competitive at higher durations due to low cavern cost.
- As duration increases, the LCOS for all technologies decreases to a minimum at 10 hours followed by an increase at higher durations because their annual discharge energy throughput is limited by the number of cycles they can perform in a year (less than one cycle per day for the 24- and 100-hour durations). For technologies with a lower unit energy cost for the storage block (SB) (CAES, PSH, hydrogen, thermal), the LCOS increase at high durations is less than for batteries, which have higher unit energy cost for the SB. Since calendar life is limiting for 100-hour duration, choice of lead-acid batteries with lower cycle life and lower SB capital cost, is expected to lower the LCOS at high durations.

Major findings from this analysis are shown in Figures ES-2 and ES-3. Values presented show the derived point estimates for total installed ESS cost (\$/kWh) by technology, power capacity (MW), and duration (hr)³. Figure ES-2 provides estimates for 2021, while ES-3 shows estimates for 2030. LCOS estimates for 100 MW and 1,000 MW systems across all durations are shown in ES-4. This chart, along with comparisons across additional power capacities is provided in the Levelized Cost of Storage section.

³ The total installed cost divided by rated energy gives \$/kWh, while the total installed cost divided by rated power gives \$/kW for the system

2021 Total Installed Cost Comparison, \$/kWh

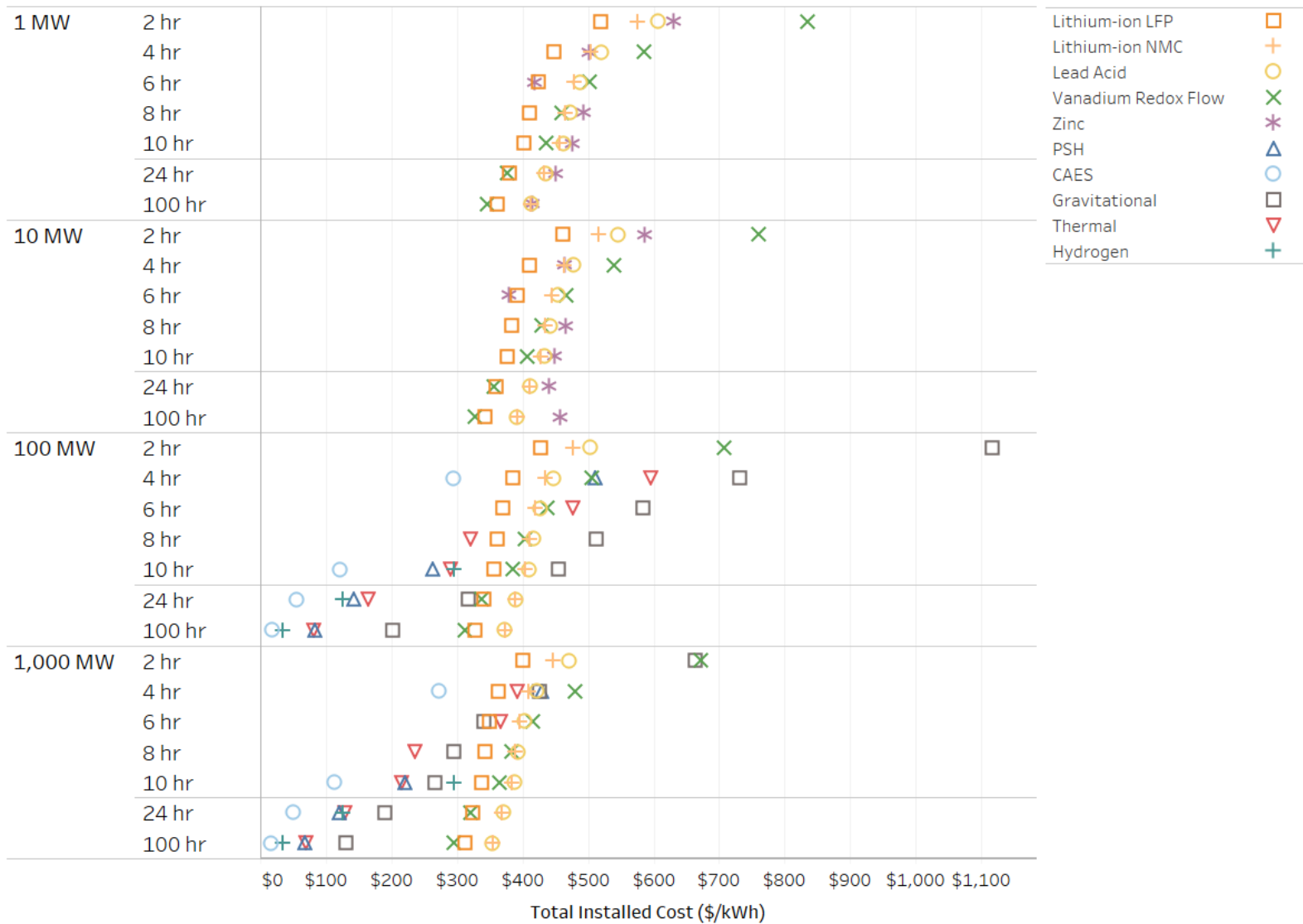


Figure ES-2. Comparison of Total Installed ESS Cost Estimates by Technology, 2021 Values

2030 Total Installed Cost Comparison, \$/kWh

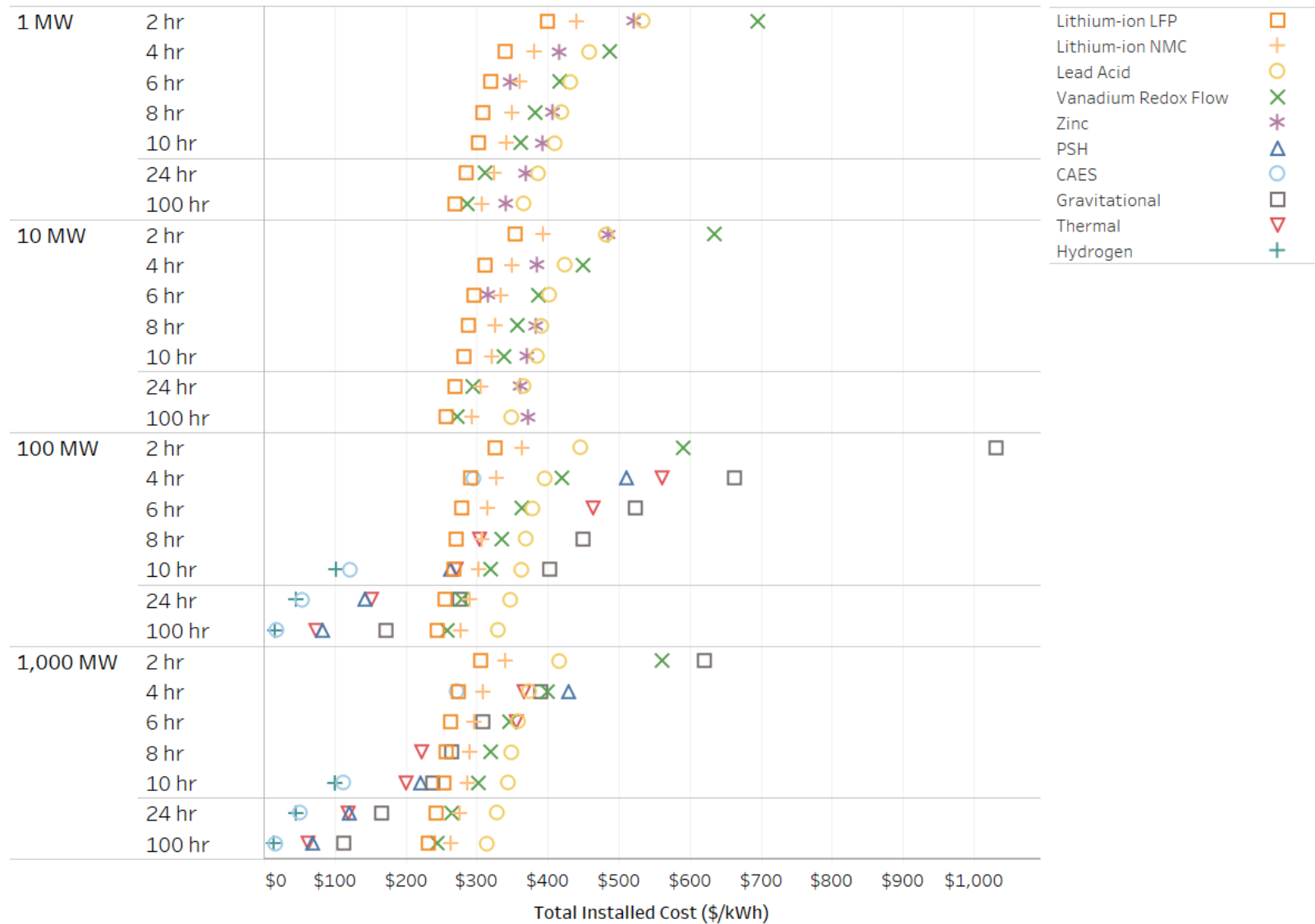


Figure ES-3. Comparison of Total Installed ESS Cost Point Estimates by Technology, 2030 Values

2021 LCOS (\$/kWh) Comparison - 100 MW & 1,000 MW

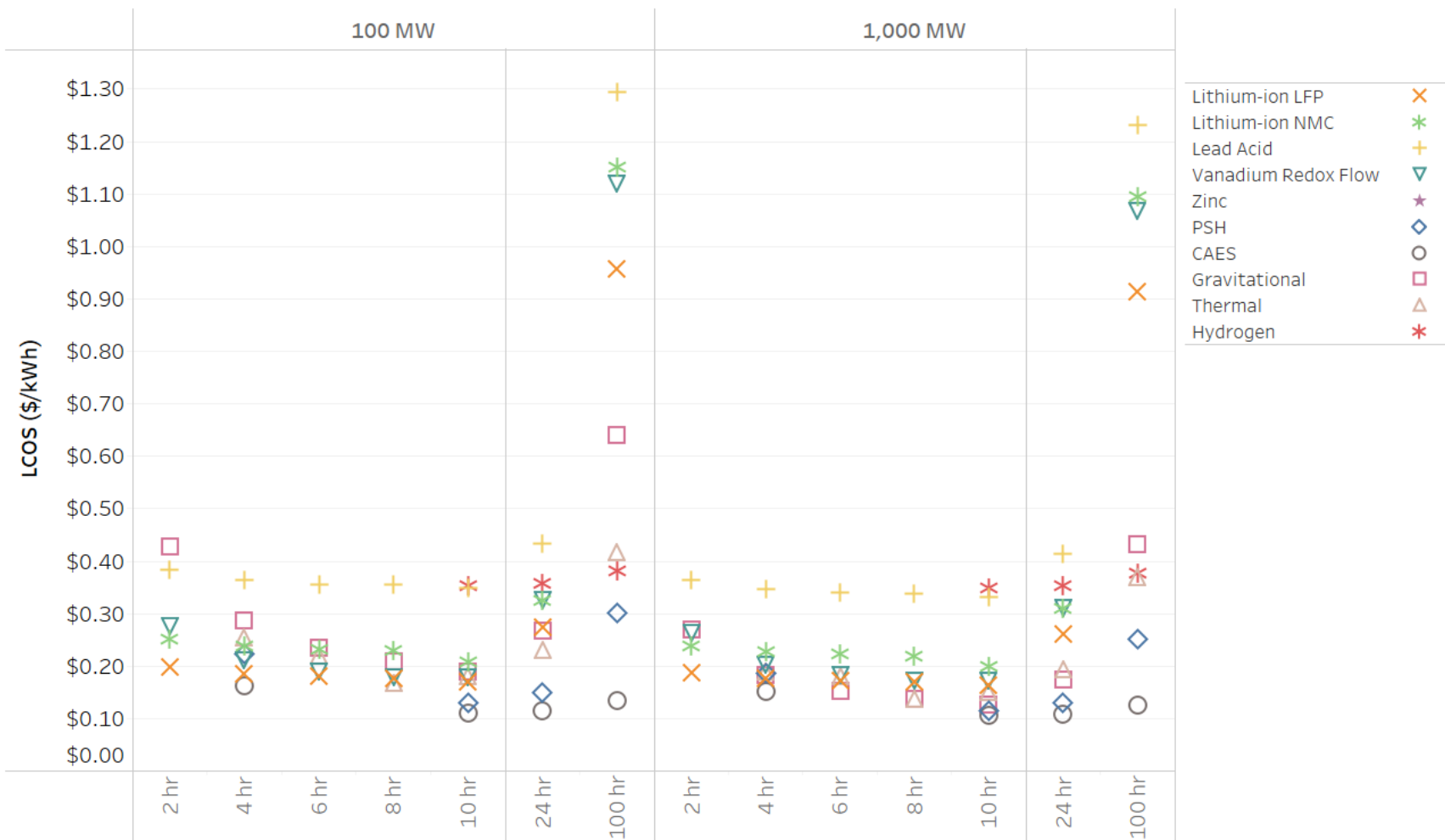


Figure ES-4. Comparison of LCOS (\$/kWh) by Technology, Power Capacity, and Duration

Table of Contents

Acknowledgments.....	ii
Foreword to 2022 Report	iii
Executive Summary.....	v
Acronyms	xix
1 Introduction	1
2 Terminology	5
2.1 Organization and Categorization of Cost and Performance Categories	5
2.2 Definitions of Cost Components and Performance Metrics	8
3 Learning Rates vs. Fixed Percent Decline for 2030	11
4 Results by Technology	12
4.1 Lithium-ion Batteries	12
4.1.1 Capital Costs.....	12
4.1.2 Operating Costs.....	17
4.1.3 Decommissioning Costs	18
4.1.4 Performance Metrics	19
4.1.5 Results.....	22
4.2 Lead-Acid Batteries	28
4.2.1 Capital Cost	28
4.2.2 Operating Costs.....	28
4.2.3 Decommissioning Costs	28
4.2.4 Performance Metrics	29
4.2.5 Results.....	32
4.3 Vanadium Redox Flow Batteries	35
4.3.1 Capital Cost	35
4.3.2 Operating Costs.....	38
4.3.3 Decommissioning Costs	39
4.3.4 Performance Metrics	40
4.3.5 Results.....	41
4.4 Zinc-Based Batteries.....	44
4.4.1 Capital Cost	44
4.4.2 Operating Costs.....	51
4.4.3 Decommissioning Costs	54
4.4.4 Performance Metrics	54
4.4.5 Results.....	58
4.5 Compressed-Air Energy Storage	60

4.5.1	Capital Cost	61
4.5.2	Operating Costs.....	62
4.5.3	Decommissioning Costs	62
4.5.4	Performance Metrics	62
4.5.5	Results	63
4.6	Pumped Storage Hydropower	65
4.6.1	Capital Cost	66
4.6.2	Operating Costs.....	66
4.6.3	Decommissioning Costs	67
4.6.4	Performance Metrics	67
4.6.5	Results	67
4.7	Gravity Energy Storage	69
4.7.1	Capital Cost	71
4.7.2	Operating Costs.....	76
4.7.3	Performance Parameters	77
4.7.4	Results	79
4.8	Thermal Energy Storage.....	81
4.8.1	Capital Cost	89
4.8.2	Operating Costs.....	103
4.8.3	Decommissioning Costs	105
4.8.4	Performance Metrics	105
4.8.5	Results	107
4.9	Hydrogen.....	109
4.9.1	Capital Cost	110
4.9.2	Operating Costs.....	111
4.9.3	Decommissioning Costs	111
4.9.4	Performance Metrics	111
4.9.5	Results	112
5	Comparative Results	115
5.1	Total Installed Cost.....	115
5.2	Performance Parameters	118
6	Levelized Cost of Storage	120
6.1	Methodology.....	120
6.1.1	Overview	120
6.1.2	Assumptions and Parameters	121
6.1.3	Cycles Per Day and Annual Discharge Methodology	123
6.1.4	Depth of Discharge and Cycle Life Assumptions.....	124

6.1.5	Augmentation, Replacement, and Warranty Methodology	126
6.2	Results	127
6.2.1	2021 LCOS Values.....	127
6.2.2	2030 LCOS Values.....	131
6.3	Sensitivity Analyses	134
6.3.1	Recycling Cost	134
6.3.2	Extended Economic Life	135
7	Conclusion.....	136
8	References	139
	Appendix 1: LCOS Methodology and Definitions.....	149

List of Figures

Figure 1.1 Power Capacity (MW) and Energy Duration (hr) Coverage Table by Technology	2
Figure 2.1. ESSs and Performance Metrics	5
Figure 2.2 ESSs Included in Total Installed Cost for each Storage Technology.....	7
Figure 4.1. Ratio of 2030 to 2021 Costs Based on Learning Rate	17
Figure 4.2. Discharge Energy Throughput as a Function of DOD for Li-ion Batteries.....	21
Figure 4.3. 2021 and 2030 Installed Costs and Performance Parameters – LFP	24
Figure 4.4. 2021 and 2030 Total Installed Costs Ranges – LFP	25
Figure 4.5. 2021 and 2030 Installed Costs and Performance Parameters – NMC.....	26
Figure 4.6. 2021 and 2030 Total Installed Costs Ranges – NMC.....	27
Figure 4.7. Cycles as a Function of DOD for Lead-Acid Systems and Associated Trendline	31
Figure 4.8. 2021 and 2030 Installed Costs and Performance Parameters – Lead-Acid	33
Figure 4.9. 2021 and 2030 Total Installed Costs Ranges – Lead-Acid.....	34
Figure 4.10. 2021 and 2030 Installed Costs and Performance Parameters – Vanadium RFB	42
Figure 4.11. 2021 and 2030 Total Installed Costs Ranges – Vanadium RFB	43
Figure 4.12. 2021 and 2030 Installed Costs and Performance Parameters – Zinc	59
Figure 4.13. 2021 and 2030 Total Installed Costs Ranges – Zinc	60
Figure 4.14. 2021 and 2030 Installed Costs and Performance Parameters – CAES.....	64
Figure 4.15. 2021 and 2030 Total Installed Costs Ranges – CAES.....	65
Figure 4.16. 2021 and 2030 Installed Costs and Performance Parameters – PSH	68
Figure 4.17. 2021 and 2030 Total Installed Costs Ranges – PSH	69
Figure 4.18. 2021 and 2030 Installed Costs and Performance Parameters – Gravitational.....	80
Figure 4.19. 2021 and 2030 Total Installed Costs Ranges – Gravitational.....	81
Figure 4.20 Distribution of capital costs for solar salt-based thermal energy storage for a 100 MW, 8 hour plant based on the steam cycle	84
Figure 4.21 Schematic of Baseline Gen3 System using sand particles as thermal storage media and sCO ₂ as working fluid (used with permission).	87
Figure 4.22 Schematic of a Pumped Hydro Energy Storage System – used with permission (Echogen Power Systems; Held & Brennan, 2021).	91
Figure 4.23 Schematic of LAES System © Highview Power Storage, Inc. all rights reserved – used with permission. (Highview Power, 2021; Riley, 2021)	96
Figure 4.24 Schematic of the Liquid Air Combined-Cycle System 9: combustion turbine, 7 gas (air) turbine, 14 low-temperature turbine for organic Rankine cycle; used with permission (Conlon, 2022)...	97
Figure 4.25. 2021 and 2030 Total Installed Cost Estimates – Thermal.....	108
Figure 4.26. 2021 and 2030 Total Installed Cost Ranges – Thermal.....	109
Figure 4.27. 2021 and 2030 Installed Costs and Performance Parameters – Hydrogen	113
Figure 4.28. 2021 and 2030 Total Installed Costs Ranges – Hydrogen.....	114

Figure 5.1. Comparison of Total Installed ESS Cost Point Estimates by Technology, 2021 Values.....	116
Figure 5.2. Comparison of Total Installed ESS Cost Point Estimates by Technology, 2030 Values.....	117
Figure 5.3. RTE vs. Calendar Life for 100 MW, 10-hour Systems.....	119
Figure 5.4 RTE vs. Cycles at 80% Depth of Discharge	119
Figure 6.1. Example SB Augmentation and Replacement Schedule	127
Figure 6.2. LCOS Results for 1 MW and 10 MW Storage Systems, 2021 Values	129
Figure 6.3. LCOS Results for 100 MW and 1,000 MW Storage Systems, 2021 Values	130
Figure 6.4. LCOS Results for 1 MW and 10 MW Storage Systems, 2030 Values	132
Figure 6.5. LCOS Results for 100 MW and 1,000 MW Storage Systems, 2030 Values	133
Figure 6.6. Sensitivity Analysis Results Showing Net Cost Increase due to Recycling Costs by Power Capacity (MW) and Duration (hr)	134
Figure 6.7. Sensitivity Analysis Results for Extended Economic Life on LCOS Value	135

List of Tables

Table 4.1. Learning Rates Used to Establish Li-ion 2030 Capital Cost and Fixed O&M Ranges.....	16
Table 4.2. Cycles at Specified DOD for Li-ion LFP and NMC.....	19
Table 4.3. Cycles at Specified DOD for Li-ion LFP and NMC Using DOD Correction	22
Table 4.4. Li-ion DC-DC and AC-AC RTE Values	22
Table 4.5. Assumed DOD and Cycle Life for Lead-Acid Systems by Duration (hr)	30
Table 4.6. Lead-Acid DC-DC and AC-AC RTE Values	31
Table 4.7. Redox Flow Battery Component Cost for 2021 for 10 MW at Various Durations	37
Table 4.8. RFB Component Cost for 2030 for 10 MW at Various Durations.....	38
Table 4.9. RFB DC-DC and AC-AC RTE Values.....	41
Table 4.10. Composite Ni-Zn Capital Costs, 2021	46
Table 4.11. Composite Zinc-Bromine Capital Costs, 4-hour Duration, 2021 Systems	46
Table 4.12. Capital Cost for 1MW and 10 MW Zinc-Air SB and BOS, 2021 Systems	47
Table 4.13. Composite Zinc BESS SB Costs (\$/kWh) by Power Capacity and Duration, 2021	49
Table 4.14. Composite Zinc BESS SB Costs (\$/kWh) by Power Capacity and Duration, 2030	49
Table 4.15. Composite Zinc BESS SBOS Costs (\$/kWh) by Power Capacity and Duration, 2021	50
Table 4.16. Zinc BESS SBOS Costs (\$/kWh) by Power Capacity and Duration, 2030	50
Table 4.17. Composite Zinc BESS Total Installed Costs (\$/kWh) by Power Capacity and Duration, 2021..	51
Table 4.18. Composite Zinc BESS Total Installed Costs (\$/kWh) by Power Capacity and Duration, 2030..	51
Table 4.19. Composite Ni-Zn Fixed O&M Values, 2021 and 2030	52
Table 4.20. Composite Zinc-Bromine Fixed O&M Values, 2021 and 2030	52
Table 4.21. Zinc-air Fixed O&M Values, 2021 and 2030	53
Table 4.22. Composite Zinc BESS Fixed O&M (\$/kW-year) Values by Power Capacity and Duration, 2021	53
Table 4.23. Composite Ni-Zn Performance Parameters, 2021 and 2030	55
Table 4.24. Composite Zinc-Bromine Performance Parameters, 2021 and 2030	55
Table 4.25. Composite Zinc BESS RTE (%) by Power Capacity and Duration, 2021 and 2030	56
Table 4.26. Composite Zinc BESS Cycle Life by Duration, 2021 and 2030	57
Table 4.27. Composite Zinc BESS Calendar Life (years) by Duration, 2021 and 2030	57
Table 4.28. Cavern Costs for CAES from Various Sources.....	61
Table 4.29. PSH O&M Costs by Category for 10-hour Systems	66
Table 4.30. 2021 Capital Costs for Pressurized-Water Gravitational Energy Storage	73
Table 4.31. Power Equipment Cost (\$/kW) for All Gravity Storage Technologies.....	74
Table 4.32. SB and BOS Cost (\$/kWh) for All Gravity Storage Technologies.	74
Table 4.33. Total Installed Cost (\$/kWh) for All Gravity Storage Technologies.....	75
Table 4.34. Composite Costs for Gravitational Storage, Year 2030	76

Table 4.35. O&M Costs (\$/kW-year) for Various Gravity Technologies	77
Table 4.36. Composite Weight-based System Performance Parameters, 2021 and 2030.....	77
Table 4.37. Composite Pressurized-Water-based System Performance Parameters, 2021 and 2030.....	78
Table 4.38. Composite Gravity Storage Performance Parameters, 2021 & 2030	78
Table 4.39. PHES Composite Capital Costs	92
Table 4.40. Sensible Heat-based Thermal Composite Capital Costs.....	94
Table 4.41. Liquid Air Thermal Composite Capital Costs	98
Table 4.42. Composite Thermal SB and BOS Costs (\$/kWh) by Power Capacity and Duration.....	101
Table 4.43. Composite Thermal Power Equipment Costs (\$/kW)	101
Table 4.44. Composite Thermal Total Installed Costs (\$/kWh) by Duration	102
Table 4.45. Composite PHES Fixed O&M (\$/kW-yr), 2021 and 2030	103
Table 4.46. Composite Conventional Thermal Storage Fixed O&M (\$/kW-yr), 2021 and 2030 ^a	104
Table 4.47. Composite Liquid Air Thermal Storage Fixed O&M (\$/kW-yr), 2021 and 2030.....	104
Table 4.48. Fixed O&M Costs for Thermal Storage Technologies and Composite Values by Duration....	105
Table 4.49. Composite PHES Performance Parameters for 2021 and 2030	106
Table 4.50. Composite Conventional Thermal Performance Parameters for 2021 and 2030.....	106
Table 4.51. Composite Liquid Air Performance Parameters for 2021 and 2030	107
Table 4.52. Composite Performance Parameters for Thermal Systems, 2021 and 2030.....	107
Table 4.53. Hydrogen DC-DC and AC-AC RTE Values	112
Table 6.1. Financial Parameters and Assumptions	121
Table 6.2. Assumed Project Life and Construction Period for Each Energy Storage Technology.....	122
Table 6.3. Required Rest Time (hours) for Battery Systems by Duration	124
Table 6.4. DOD Assumptions by Storage Technology and Duration.....	125
Table 6.5. Augmentation, Replacement, and Warranty Schedule by Technology	126
Table A4.1. WACC Equation Variable List and Definition	150

Acronyms

AC	alternating current
Ah	ampere-hour
BESS	battery energy storage system
BMS	battery management system
BOP	balance of plant
BOS	balance of system
C&C	controls and communication
CAES	compressed-air energy storage
CFF	construction finance factor
CRF	capital recovery factor
CSP	concentrating solar power
DC	direct current
DOD	depth of discharge
DOE	U.S. Department of Energy
EIC	electricals, instrumentation, and controls
EPC	engineering, procurement, and construction
ESGC	Energy Storage Grand Challenge
ESS	energy storage system
HESS	hydrogen energy storage system
HEX	heat exchanger
HVAC	heating, ventilation, and air conditioning
kWe	kilowatt electric
kWh	kilowatt-hour
kWhe	kilowatt-hour electric
kWht	kilowatt-hour thermal
LAES	liquid air energy storage
LCOS	levelized cost of storage
LFP	lithium-ion iron phosphate
Li-ion	lithium-ion
MACRS	modified accelerated cost recovery system
MWh	megawatt-hour
MWt	megawatt thermal
NEMA	National Electrical Manufacturers Association
Ni-Zn	nickel-zinc

NMC	nickel manganese cobalt
NREL	National Renewable Energy Laboratory
O&M	operations and maintenance
OEM	original equipment manufacturer
PCS	power conversion system
PEM	polymer electrolyte membrane
PHES	pumped heat energy storage
PNNL	Pacific Northwest National Laboratory
PSH	pumped storage hydro
RFB	redox flow battery
RTE	round-trip efficiency
SB	storage block
SBOS	storage balance of system
SOC	state of charge
TRL	technology readiness level
USP	uninterruptable power source
WACC	weighted average cost of capital

2022 Grid Energy Storage Cost and Performance Assessment

1 Introduction

Energy storage and its impact on the grid and transportation sectors have expanded globally in recent years as storage costs continue to fall and new opportunities are defined across a variety of industry sectors and applications. Electrification of the transportation sector is being driven by the availability of lower cost, higher performance lithium-ion (Li-ion) batteries for electric vehicles and is being actively tracked and advanced by the Department of Energy's (DOE's) Energy Efficiency and Renewable Energy Vehicle Technologies Office and other commercial entities. Grid-scale energy storage, however, lacks the stringent power and weight constraints of electric vehicles, enabling a multitude of storage technologies to compete to provide current and emerging grid flexibility services.

As growth and evolution of the grid storage industry continues, it becomes increasingly important to examine the various technologies and compare their costs and performance on an equitable basis. As part of the Energy Storage Grand Challenge (ESGC), Pacific Northwest National Laboratory (PNNL) is leading the development of a detailed cost and performance database for a variety of energy storage technologies that is easily accessible and referenceable for the entire energy stakeholder community. This work is based on previous storage cost and performance research at PNNL funded by DOE's HydroWIRES Initiative (Mongird et al., 2019). This work aims to: 1) provide a detailed analysis of the all-in costs for energy storage technologies, from basic components to connecting the system to the grid; 2) update and increase fidelity of the individual cost elements comprising a technology; 3) provide cost ranges and estimates for storage cost projections in 2030; and 4) develop an online website to make energy storage cost and performance metrics easily accessible and updatable for the stakeholder community. This research effort will periodically update tracked performance metrics and cost estimates as the storage industry continues its rapid pace of technological advances. Due to intra-annual uncertainty, the reported costs may have changed by the time this report was released. The cost estimates provided in the report are not intended to be exact numbers but reflect a representative cost based on ranges provided by various sources for the examined technologies.

The analysis was done for energy storage systems (ESSs) across various power levels and energy-to-power ratios. The power and energy duration combinations for each technology provided in the 2022 report are shown in Figure 1.1. The power and duration choices reflect a combination of their current and potential future applications, and also include selections to enable comparisons between categories. For example, pumped storage hydro (PSH) and compressed-air energy storage (CAES) primarily serve longer durations, but a duration of 4 hours at power levels of 100 MW and 1,000 MW are included to provide a comparison point at a shorter duration with other technologies and capture uses in projects developed in the past.

	1 MW							10 MW							100 MW							1,000 MW							
	2	4	6	8	10	24	100	2	4	6	8	10	24	100	2	4	6	8	10	24	100	2	4	6	8	10	24	100	
Lithium-ion LFP	■	■	■	■	■	■	■	■	■	■	■	■	■	■	■	■	■	■	■	■	■	■	■	■	■	■	■	■	■
Lithium-ion NMC	■	■	■	■	■	■	■	■	■	■	■	■	■	■	■	■	■	■	■	■	■	■	■	■	■	■	■	■	■
Lead Acid	■	■	■	■	■	■	■	■	■	■	■	■	■	■	■	■	■	■	■	■	■	■	■	■	■	■	■	■	■
Vanadium Redox Flow	■	■	■	■	■	■	■	■	■	■	■	■	■	■	■	■	■	■	■	■	■	■	■	■	■	■	■	■	■
Zinc	■	■	■	■	■	■	■	■	■	■	■	■	■	■															
PSH															■	■							■	■	■	■	■	■	■
CAES															■	■							■	■	■	■	■	■	■
Hydrogen																							■	■	■	■	■	■	■
Thermal															■	■	■	■	■	■	■	■	■	■	■	■	■	■	■
Gravitational															■	■	■	■	■	■	■	■	■	■	■	■	■	■	■

Figure 1.1 Power Capacity (MW) and Energy Duration (hr) Coverage Table by Technology

Phase 2 of this initiative includes cost and performance metrics for the following energy storage technologies across the energy-to-power ratios indicated above:

- Li-ion: Li-ion iron phosphate (LFP) batteries
- Li-ion: Li-ion nickel manganese cobalt (NMC) batteries
- Lead-acid batteries
- Vanadium redox flow batteries (RFBs)
- Diabatic CAES
- PSH
- Hydrogen energy storage system (HESS) (bidirectional)
- Zinc-based batteries
- Gravity energy storage
- Thermal energy storage

Additional storage technologies will be incorporated in future phases to capture newer technologies of interest to DOE and other stakeholders.

In addition to cost estimates and projections, this work aims to develop a cohesive framework to organize and aggregate cost and performance metrics for ESSs. An ESS may include numerous stakeholders including intermediate sellers and buyers (e.g., vendors, distributors, resellers, developers, financial interests, electric service provider, and operators). Cost metrics are approached from the viewpoint of the final downstream entity in the energy storage project, ultimately representing the final project cost. This framework helps eliminate current inconsistencies associated with specific cost categories (e.g., energy storage racks vs. energy storage modules). Over the past year, this framework has been socialized with industry and the research community with only minor revisions.

Cost and performance information was compiled for the defined categories and components based on conversations with developers and industry stakeholders, literature, commercial datasets, and real-world storage costs for systems deployed across the United States. A range of detailed cost and performance estimates are presented for 2021 and projected out to 2030 for each technology.

Current cost estimates provided in this report reflect the derived point estimate based on available data from the reference sources listed above with estimated ranges for each studied technology. In addition to ESS installed costs, a \$/kWh levelized cost of storage (LCOS) value for each technology is also provided to better compare the complete cost of each ESS over the duration of its project life, inclusive of any major overhauls and replacements required to maintain operation. The LCOS measures the cost that a unit of energy output from the storage asset would need to be sold at to cover all project costs inclusive of taxes, financing, operations and maintenance, and others. It offers a way to comprehensively compare the true cost of owning and operating various storage assets.

Cycle life is one of the most important metrics that determines LCOS, particularly for battery technologies. Specification sheets from developers show Li-ion cycle life data obtained at 1C charge and discharge rates. Hence, about 10 cycles per day are possible corresponding to test duration of 3 years for 10,950 cycles. Additionally, the cycle life is estimated by extrapolating data obtained for a limited number of cycles in the 1000-4500 cycles range, restricting test duration further to 0.25-1 year. Hence, calendar life limitation doesn't come into play for reported cycle life data. However, during operation, most warranties limit the user to one full 100% depth of discharge (DOD) equivalent cycle per day. Therefore, for batteries to reach the same number of 10,500 reported cycles, they would have to cycle 10 times longer, or 30 years, which is much greater than the calendar life for Li-ion batteries. This would require derating the cycle life reported in specification sheets.

For lead-acid batteries, cycling is not done at such high rates. The cycle life is sufficiently small so that even at one cycle per day, the battery life is limited to 3-4 years of operation, where calendar aging doesn't have a significant impact. Plus, the duration for each cycle at 80% DOD is approximately 20 hours for an 8-hour discharge rate, close to one cycle per day. The smallest discharge duration considered is 2 hours at 50% DOD, which requires 6 hours per cycle (4 cycles per day). Testing in the laboratory would be completed in one year (for 1460 cycles) as opposed to the 2 years it would take based on the warranty conditions not to exceed one 100% equivalent DOD cycle per day. Hence, the calendar life related aging is not expected to have a big impact for lead-acid batteries.

In the field while providing various grid services, energy storage systems do not continuously charge or discharge. At times they remain idle if there are no grid services that offer sufficient value for the system to operate thus reducing the capacity factor⁴ (Hunter et al., In Press; Hunter et al., 2021). The capacity factor depends on the following variables:

- Type and penetration of renewables in the region
- Annual load and generation profiles for the region
- Allowable annual energy throughput for the ESS
- Duration of the ESS (Energy to power ratio)
- Round trip efficiency (RTE)

Regions with high wind penetration may require the ESS to charge at night, while regions with high solar PV penetration will require the ESS to charge during the day. The region-specific annual load and

⁴ Capacity factor is the ratio of the total time the storage system is engaged over the actual available time. Capacity factor for charge is the percent of time the ESS is being charged, while the capacity factor for discharge is the percent of time the ESS is being discharged.

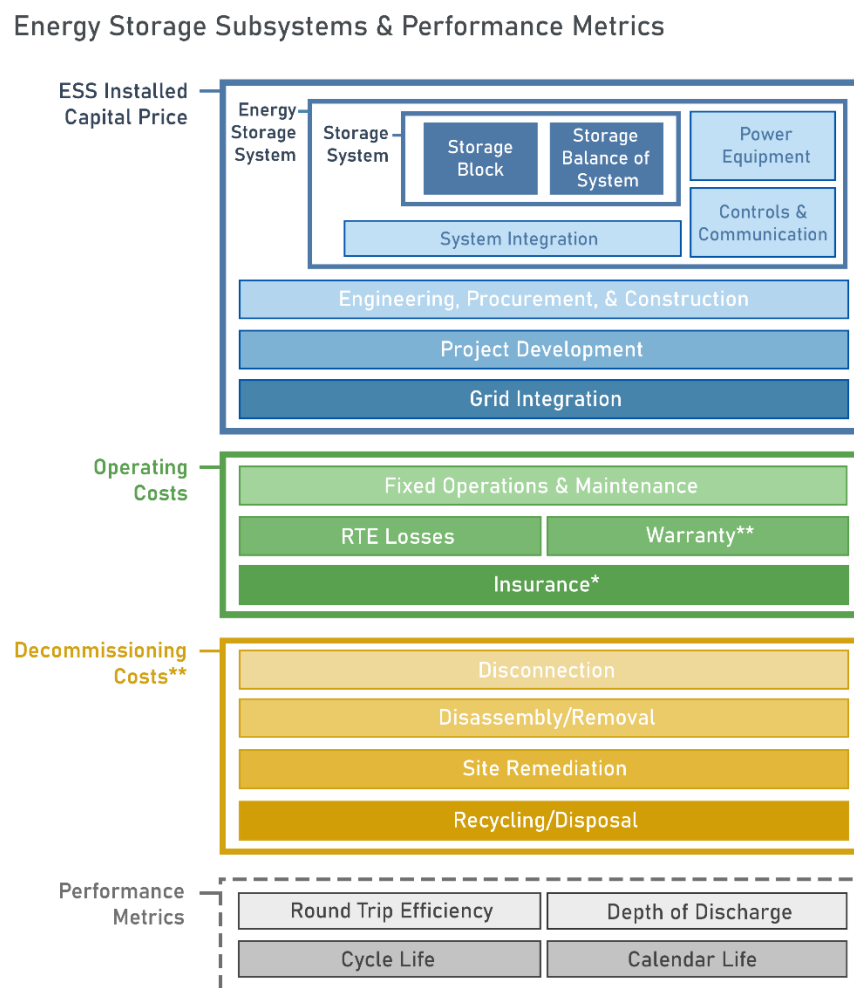
generation profiles further affect the charge and discharge periods and durations. The charge duration will depend on the hours of over-generation, the charge efficiency and the rated energy capacity of the storage system. The discharge duration depends on the periods of under-generation and the rated energy capacity. For storage systems with separate charge and discharge powertrains, there is flexibility of oversizing the charge powertrain to capture excess renewable energy in less time. Due to the complexity associated with region-specific load and generation profiles, this study has developed a simplified approach to estimate charge and discharge capacity factors as described below.

The allowable annual cumulative discharge energy is limited to 365 discharges at 100% DOD (or one full discharge per day). At the 80% DOD used in this analysis, the maximum number of cycles allowed per day is $1/0.8$ or 1.25 cycles. The total time needed to complete each cycle depends on the ESS duration and RTE. For example, for a 2-h ESS with 0.8 RTE, the ESS operates for 4.5 hours each cycle (2 hours discharge, 2.5 hours charge), or 5.6 hours in a day (4.5 hours/cycle x 1.25 cycles/day). This corresponds to a capacity factor of 23% for charge and discharge combined. For a 10-hour storage system with the same RTE, the ESS operates for 22.5 hours in each cycle, for a combined capacity factor of 94%.

2 Terminology

2.1 Organization and Categorization of Cost and Performance Categories

For the 2020 report, the research team compiled information on various cost components for a range of energy storage technologies and produced a cohesive breakdown of items that is consistent and tractable across multiple storage types. Figure 2.1 displays an updated schematic of the cost and performance categorization that resulted from that effort.



* Estimates for these components are not included at this time in technology-specific findings
 ** Estimates for these components are available for a limited subset of storage technologies at this time

Figure 2.1. ESSs and Performance Metrics

It should be noted that this schematic has been designed to capture a practical level of granularity for the costs of ESS. For a battery energy storage system (BESS), the storage block (SB) corresponds to battery modules and racks, flow battery stacks, electrolyte, and tanks, while the storage balance of

system (SBOS) consists of containers; heating, ventilation, and air conditioning (HVAC); safety disconnects; fire extinguishers; and pumps, valves, and pipes. For other technologies, like PSH and CAES plants, these cost elements (SB and SBOS) are aggregated to capture the costs associated with reservoirs and caverns, respectively. For PSH and CAES systems, additional cost elements such as power equipment, controls and communication (C&C), and system integration corresponding to electromechanical equipment/powertrain and powerhouse/power island construction are aggregated. While engineering, procurement and construction (EPC) and project development costs are typically included in CAES system costs, these are captured in a catch-all contingency fee cost component for PSH. For HESS, the SB is represented by the electrolyzer, stationary fuel cell, and cavern, while the balance of system (BOS) is represented by the compressor, humidifiers, and air and fuel delivery system. A table of how the cost components compare (following the diagram for total installed cost in Figure 2.1) is shown in Figure 2.2 with further resolution of subcomponents of each energy storage subsystem or cost component.⁵

⁵ Cost component and energy storage subsystem are used interchangeably

		Li-ion	Lead-acid	Zinc	Redox Flow	Hydrogen	PSH	Gravitational	CAES	Thermal	
ESS Installed Cost	Storage System	Storage Block	Li-ion modules in racks	Lead-acid modules in racks	Zinc modules in racks	Stacks & Electrolyte Tanks	Electrolyzer, Fuel Cell Stacks, & Cavern	Reservoir(s)	Bricks, Pistons, & Mine Shaft	Cavern	Storage Media, Tanks, & Insulation
		Balance of System	Container, Cabling, Switchgear, & HVAC			Pumps & Piping	Blowers, Humidifiers, Mass Flow Controllers, & Compressors		Cranes, Valves, & Seals		Valves, Pipes, Pumps, & Insulation
	Energy Storage System (ESS)	Power Equipment	Power Conversion System & DC-DC Converter				Rectifier & Inverter	Electromechanical Powertrain - Pumps/Turbines, Motors/Generators & Powerhouse Construction	Electromechanical Powertrain - Pumps/Turbines, Motors/Generators, & Powerhouse Construction (as required)	Power Island with Electromechanical Powertrain - Compressors, Turbines and Generators	Charging hardware, Compressors, Turbines, Generators, Steam System Balance of Plant
		Controls & Communication	Controls/Energy Management System							Included in Storage System and Power Equipment Costs	Electrical, Instrumentation, & Controls (Sometimes included in Power Equipment Costs)
		System Integration	System Integration			Included in above Costs					Included in Storage System & Power Equipment Costs
	Engineering Procurement and Construction (EPC)		EPC					Included in above ESS Costs	EPC Fee, Project Development, & Grid Integration	Included in above ESS Costs	EPC Fee, Project Development, & Grid Integration
	Project Development		Project Development					Contingency Fees*			
	Grid Integration		Grid Integration								

* Contingency fees cover costs from unanticipated risks and/or indirect costs

Figure 2.2 ESSs Included in Total Installed Cost for each Storage Technology

2.2 Definitions of Cost Components and Performance Metrics

Defining cost component parameters is necessary to effectively break down system costs in a consistent way. Failing to do so leads to inconsistent results and a misunderstanding of the estimates being produced. The list below aims to provide clarity and defines each of the cost items that appear in Figure 2.2. For categories and parameters for non-BESS technologies, information is included in the individual technology sections analysis.

- **ESS Installed Cost Components**

- i) **SB (\$/kilowatt-hour [kWh])** – includes the unit energy cost for the energy component of the ESS, for example, battery module, rack, and battery management system (BMS) for BESS; electrolyzer, fuel cell stacks, and cavern for HESS; bricks, mass cars, mined shaft, and pressurized water for gravitational storage; and storage medium, tank, and insulation for thermal storage.
- ii) **SBOS (\$/kWh)** – includes supporting cost components for the SB with container, cabling, switchgear, flow battery pumps, and HVAC for BESS; blowers, humidifiers, mass flow controllers, and compressors for HESS; cranes, valves, and seals for gravitational storage; and valves, pipes, pumps, and insulation for thermal storage.
- iii) **Storage System (\$/kWh)** – this is the sum of the SB and SBOS costs and is the appropriate level of granularity for some storage technologies such as PSH and CAES.
- iv) **Power Equipment (\$/kilowatt [kW])** – power conversion system and direct current (DC)-DC converter for batteries, rectifier, and inverter for HESS; electromechanical powertrain and powerhouse for PSH; electromechanical powertrain with or without powerhouse for gravity-based systems; charging hardware, compressors, turbines, generators, and steam system balance of plant for thermal energy storage; and the power island with electromechanical powertrain for CAES.
- v) **Controls & Communication (C&C) (\$/kW)** – includes the energy management system for the entire ESS and is responsible for ESS operation; also referred to as electrical, instrumentation, and controls (EIC) for thermal powerplants. Typically represented as a fixed-cost scalable with respect to power.
- vi) **System Integration (\$/kWh)** – cost charged by the system integrator to integrate components of a BESS into a single-functional system. Tasks include procurement and shipment to the site of battery modules, racks with cables in place, containers, and power equipment. At the site, the modules and racks are containerized with HVAC and fire suppression installed and integrated with the power equipment to provide a turnkey system.
- vii) **EPC (\$/kWh)** – includes nonrecurring engineering costs and construction equipment as well as siting, installation, and commissioning of the ESS.
- viii) **Project Development (\$/kWh)** – costs associated with permitting, power purchase agreements, interconnection agreements, site control, and financing.

- ix) **Grid Integration (\$/kW)** – costs associated with connecting the ESS to the grid, including transformer cost, metering, and isolation breakers.
- **Operating Costs**
 - i) **Fixed Operations & Maintenance (O&M) (\$/kW-year)⁶** – includes all costs necessary to keep the storage system operational throughout its life that do not fluctuate based on energy throughput, such as planned maintenance, parts, and labor and benefits for staff. This also includes major overhaul-related maintenance which may depend on energy throughput or occurs at fixed time intervals.
 - ii) **Round-Trip Efficiency (RTE) Losses (\$/kWh)** – Round-trip efficiency is simply the ratio of energy discharged to the grid from a starting state of charge to the energy received from the grid to bring the ESS to the same starting state of charge. RTE is < 1 due to losses related to thermal management, auxiliary power consumption, electrochemical losses, power conversion losses, powertrain-related electromechanical losses, energy conversion losses, self-discharge, evaporation, stored heat or gas/air leakage losses. This value for RTE losses is estimated through the cost of the additional electricity and fuel required per kWh of energy discharged due to the losses described.
 - iii) **Warranty (\$/kWh-year)** – annual fees to the equipment provider for contractual performance of quality of materials and equipment and performance assurance of designated lifespan.
 - iv) **Insurance (\$/kWh)** – insurance fees to hold a policy to cover unknown and/or unexpected risks. The terms of this cost may depend on developer reputation, project complexity, location, and financial strength.
- **Decommissioning Costs**
 - i) **Disconnection, Disassembly, Removal, and Site Remediation (\$/kWh)** – costs associated with the disconnection, disassembly, removal, and site remediation. These costs may vary widely based on whether the ESS is in the built environment or outside the built environment, how far materials must be transported, and whether site remediation is necessary.
 - ii) **Recycling and Disposal (\$/kWh)** – net costs associated with recycling and disposing of components less any costs recouped from sale of materials. The value of recouped materials is typically measured in cents/pound.
- **Performance Metrics**
 - i) **Duration (hours)** – the ratio of rated energy to rated power of the ESS.
 - ii) **RTE (%)** – the electrical⁷ energy that is discharged to the grid (after accounting for all the losses listed in RTE losses) as a percentage of the total energy⁸ used to charge the ESS. Note

⁶ In this report, the O&M variable cost of \$0.0005/kWh related to consumables used in the 2020 report has been removed due to lack of clarity of source materials.

⁷ This work considers only electrical energy output during discharge

⁸ Except for hybrid thermal energy storage, this work considers only electricity input during charge.

- that RTE for a fixed-system design depends on operating conditions such as charge-discharge power, ambient temperature, state of charge (SOC) range.
- iii) **Depth of Discharge (DOD) (%)** – the energy discharged as a percentage of the rated energy capacity of the storage system.
 - iv) **Cycles (#)** – each charge and discharge corresponds to a half cycle, with a charge-discharge pair corresponding to one cycle.
 - v) **End of Life** – the condition at which the ESS can no longer provide a minimum required percent of its rated power or energy. As an example, for Li-ion batteries, the end of life is when its available energy is less than 60% of rated energy.
 - vi) **Cycle Life (#)** – is the total number of cycles that an ESS can provide before reaching end of life; is a function of DOD for nonflow BESS.
 - vii) **Calendar Life (years)** – defined as the maximum duration after which the ESS reaches end of life regardless of operating conditions. For BESS considered in this report, calendar life can depend on the ambient temperature, pressure, humidity, and SOC at which the battery is stored.

It should be noted that some of these items have not been separately considered in this analysis due to current unavailability of data. Warranty, insurance, decommissioning, disassembly, removal, site remediation, and recycling and disposal costs are not well documented in the literature for all technologies and accordingly the values for these metrics have low accuracy.

In this report, warranty costs are included for vanadium RFB and NMC Li-ion BESSs based on industry feedback. Recycling and disposal costs are calculated for LFP, Li-ion NMC, vanadium RFB, and lead-acid batteries as the inverse physical operation of construction and thus a recurrence of the cost of the EPC costs, minus the value of the recoverable materials specific to these battery systems. Some of the costs associated with these items may be partially included in other cost estimates based on the business process used in an ESS (e.g., part of the cost of decommissioning may be embedded in a capital cost quoted by a developer), but the capability to estimate them separately is not available at this time. However, recycling and disposal is a cost component that will grow in importance due to financial, risk, and environmental considerations. Analysis of the warranty, insurance, decommissioning, disassembly, removal, and site remediation components will be pursued in later phases of this continued research effort as more information becomes available. Additionally, future efforts will attempt to expand the list of performance characteristics tracked to provide a more complete assessment of each technology's capabilities.

3 Learning Rates vs. Fixed Percent Decline for 2030

Typically, learning rates have been used to project cost reductions as manufacturing output increases. Using the learning rate approach requires knowledge of two parameters: 1) future demand and 2) the correct learning rate. Historical analysis of mature energy technologies can be used to better inform the expected rate of cost reduction as manufacturing capacity increases. For example, learning rate for established technologies such as combustion turbines are reported at 20% for up to cumulative deployments of 1,000 MW, followed by a lowering to 10% for deployments up to 100,000 MW (Gritsevskiy & Nakićenovi, 2000). Photovoltaics and wind turbines also have the 20% learning rate curve for deployments up to 800 MW and 2,000 MW, respectively. However, during the initial stages of deployment, all three technologies show a lower learning rate based on the lower slope of cost drop vs. deployment, which was not quantified but appear to be 10% for gas turbines and lower for photovoltaics. This gap was addressed by Wei, Smith, and Sohn (2017), who determined the learning rate for cost is relatively flat initially, followed by a steep curve corresponding to the 20% learning rate upon attaining a minimum deployment threshold to benefit from scale, then by a lower learning rate as deployments increase further.

This work uses the same learning rates for Li-ion, lead-acid, and flow batteries as used in the 2020 ESGC report. Learning rates can be used for technologies such as Li-ion batteries that have a 10-year period of deployment history in the transportation and grid storage sectors. For RFBs and lead-acid batteries, due to uncertainties in deployment, learning rates are not directly applicable. In the 2020 report, learning rates were assumed for these technologies, while using the estimated Li-ion deployment. The same approach was followed in this report. For example, the nominal DC SB learning rate for RFBs is set at 4.5%, 1.5% for lead-acid batteries, compared to 10% for Li-ion batteries, corresponding to cost drops of 17%, 6%, and 35%, respectively. For the rest of the categories for battery-based systems, the learning rates were kept the same for all batteries as described in the ESGC 2020 report.

Due to the uncertainties in both anticipated deployments and the correct learning rate to use during the initial phase, this work assumes a fixed-cost drop for zinc batteries, gravity, and thermal storage systems. For example, a 20% cost drop in DC SB and 10% drop in DCBOS was assumed for zinc batteries, while keeping the cost drops for power equipment in line with Li-ion BESS, while system integration, EPC, and project development costs are maintained at 90% of Li-ion BESS 2030 values.

4 Results by Technology

4.1 Lithium-ion Batteries

Li-ion batteries are one of the most widely used technologies for consumer electronics and electric vehicle applications due to their high energy density⁹ and cycling performance. These systems store electrical energy in electrodes that can accommodate lithium within their host lattice or matrix, called intercalation or insertion compounds. Presently, most commercial Li-ion batteries consist of a graphite anode, a lithium-containing transition metal oxide or phosphate cathode, and a nonaqueous Li-ion-conducting liquid electrolyte. When using a graphite anode, cells are often characterized by the different cathode materials used (e.g., LiCoO_2 , $\text{LiNi}_x\text{Mn}_y\text{Co}_z\text{O}_2$ [NMC], $\text{LiNi}_x\text{Co}_y\text{Al}_z\text{O}_2$ [NCA], or LiFePO_4 [LFP]). The basic cell components are packaged in a cylindrical, prismatic or pouch format to form the basic repeating unit.

For large-scale stationary storage systems, costs for Li-ion can be analyzed at various levels including the DC SB (groups of cells and associated wiring and racking), and the DC BOS. Costs for DC SB and equipment comprising ESSs are tracked and available from multiple sources with this report focused on quantifying the additional costs of system integration, EPC, project development, grid integration, and operations required for a functional energy storage deployment. Current cost data were obtained from several sources and with developer interviews. 2030 cost projections were accomplished by using defined learning rates for the various cost components. For a detailed description of the methodology used, see the 2020 Cost and Performance Report.

New information and methodology changes included for 2021 estimates are provided below. The Li-ion battery technology is mature and has been commercially deployed for grid-scale storage.

4.1.1 Capital Costs

Li-ion battery systems have experienced sustained cost declines over the last few years resulting from a variety of drivers—component cost decline, system integration improvements, and deployment advancements. As the industry moves aggressively into larger deployments, new factors from across the supply chain are expected to impact the forward cost track of battery systems. These include lithium battery material supply availability, competition with other markets (electric vehicle), and the growing sophistication of battery systems. More specifically, for individual customers, forward cost trends are expected to change for different customer segments as pricing/purchasing power dynamics begin to impact differences in final system costs.

Overall, these trends will combine to drive average costs slightly lower over the next few years for Li-ion-based systems. However, this average decline is based on an expansion of larger systems garnering the majority of cost decline. Systems for smaller deployments are not expected to experience significant cost decline due to the producer's pricing power, lack of individual customer's purchasing power, and increased competition from other customers willing to buy in larger quantities. The costs of a project, including the cost of capital, can vary depending on the ESSs being stand-alone or used in combination

⁹ In this work, energy density is used as proxy for both gravimetric and volumetric energy density.

with other assets, the variability and risk of the revenue stream, and the established relationships between developers and capital providers (Odayar, 2021).

Finally, an important distinction when dealing with lithium battery pricing is product vs. project costs. Because the usage profile will impact the amount of augmentation and/or replacement required by the battery project to meet performance requirements for the necessary applications, this report makes a distinction between capital costs (up front) vs. levelized costs (project lifetime). This distinction rises in importance when comparing different energy storage technologies that have widely different usable life in cycles or years over the project life. Therefore, although most of the industry talks about battery pricing in capital cost metrics (\$/kWh), it is critically important to recognize that these systems are evaluated within a project framework; comparing two purchase costs cannot differentiate between batteries with different usable lifespans related to different degradation characteristics, different O&M costs, costs related to RTE losses, and decommissioning costs to meet performance requirements through the end of life.

There are two main chemistries that dominate stationary Li-ion energy storage projects: LFP and NMC. LFP-based modules continue to be roughly 10% less expensive on a \$/kWh basis than NMC-based modules. Due to safety considerations, the maximum SOC for NMC is typically limited to 90%, while this restriction does not apply to LFP (Choi, 2021); the SB and BOS costs for NMC are divided by 0.9 to reflect this.

One key difference in the LCOS of systems between LFP and NMC is the cycle life as a function of DOD, resulting in increased costs for augmentation and replacement in NMC. A second key difference that I shows up in the LCOS between the two systems is the end-of-life costs. NMC cells have a higher value in the recycling stream due to the nickel and cobalt content. Since the recycling market is still evolving, it is difficult to say what that difference will be as projects reach their end of life, but it is expected that there will remain a difference to end-of-life costs between the two chemistries due to the market value of the recyclable metals.

The sustained cost decline of Li-ion DC modules over the last few years changed in 2021, stemming from a variety of factors. Commodity price increases, continued competition from vehicle markets, increasing design requirements related to fire protection engineering, permitting, and conformance assessment, and lack of availability leaves few customers able to expect advantageous pricing in the near term. Changes in this last year point toward increasing upward pressure on costs overall. However, these recent market changes are occurring in a fluid market, with a wide range of trends still possible. It is important to note two issues about current anecdotal rising price quotes in the press. First, these recently quoted system prices are for future deployments and not units that are being deployed today. Second, these price quotes are not standing offers to all potential customers but capital cost snapshots for particular customers in an environment where other project cost components outside of capital costs are not mentioned. Final project costs to customers can still remain far above what most customers expect based on pricing sheets and quotes that are not specific to time period or project.

Commodity prices for battery materials increased in 2021 as the demand for lithium battery systems rose for the stationary market as well as the much larger vehicle market. Exacerbating the overall demand for these commodity materials is the overall disruptions in supply chain logistics resulting from global supply and demand fluctuations caused by the COVID-19 pandemic (Odayar, 2021). These

disruptions cause the loss of the efficiency gains in the supply chain logistics, erasing some of the cost decline over the last few years.

The availability of cells is typically never questioned, yet has been and will continue to be a vexing issue driving pricing volatility for the stationary energy storage industry for many years to come. Cells used in electric vehicles and ESSs are produced at the same manufacturing facility. Since the demand for battery systems from the vehicle market and the scale of that market is approximately ten times that of the stationary market—battery original equipment manufacturers (OEM) put the vehicle market first in priority for any available production capacity. For the last few years, manufacturers have been typically sold out of battery modules¹⁰ on a rolling 6 to 12 month basis, making availability of cells difficult and driving cost increases for the stationary storage market with smaller orders.

Power conversion systems (inverters and related equipment) have risen in cost since 2020 due primarily to the increase in material commodity prices. Other items have also played a role in the recent cost increase, including improvements in software and competition from solar and industrial markets for equipment. The impact of purchasing power continues to remain; customers willing to purchase larger volumes of equipment continue to receive 10% to 20% price breaks.

Many in the industry continue to look to system integration costs for areas of cost reductions; however, there are pressures in this segment that could increase costs. First, the demand for more sophisticated engineering design and assembly requirements increases the early engineering costs that must be recouped. These design revisions are ongoing, incorporating new generations of OEM modules and new containerization strategies that can require hundreds of thousands or a million dollars of non-recurring engineering cost depending on the scale of the system. An important aspect of these designs are the thermal management issues. The increased energy density of battery modules, combined with closer packing in cabinets threatens to raise the operating temperature of the storage systems, especially at durations less than 4 hours, to a point that is expected to adversely affect the lifespan of the cells and modules. Transition to liquid cooling systems can support these technical requirements, but at an increase in costs (Saft, 2021). More stringent requirements for safety and conformance testing to standards are also driving additional costs. Finally, material costs have increased in the last 12 months, erasing much of the cost reductions that have been made over the last few years. In all, these integration costs pressures are expected to dampen any expectation for continued cost reductions and leave the possibility for cost increases over the next two to three years if some of these trends continue. However, because of the dynamic nature of the market, no trends, up or down, can simply be applied for the next two to three years without additional review.

The EPC cost of an energy storage deployment will vary widely based on the needs of construction, but there is an added level of variability due to the relatively early stage of the industry in the project development arena. Project development costs and EPC costs are based on the number of hours of design effort required, including fixed amounts (project management, certifications, etc.) and a scalable component (size and complexity of the project). When dealing with energy storage deployments, there are also technology-specific differences stemming from the type of storage medium, including weight,

¹⁰ For some vendors a cell is the smallest repeating unit, for most vendors a module consisting of multiple cells connected in a series or parallel arrangement is the smallest repeating unit from the end user's perspective.

level of chemical safety, and site-specific logistics and planning that could require additional design efforts.

Another cost issue that is based on the specific energy storage technology is the physical complexity of the system. The modularity of the technology allows smaller systems to be collected into standardized energy blocks that can be replicated with larger systems. For outdoor deployments, many storage technologies have a standard design arrangement combining these modular storage building blocks into either 20- or 40-foot enclosures or containers. In addition, cabinet designs are becoming increasingly prevalent. The evolution of enclosures, from walk-in spaces equipped with standard access doors and interior accessible equipment to cabinets where there is no interior occupiable space and all equipment is accessed from the exterior, has been driven by several factors. One factor is additional life safety requirements in the model fire codes for occupiable spaces, another is requirements for the UL9540 product safety standard. As fire and explosion testing is a required component of product listing, performing this destructive testing on representative samples is facilitated in a standardized modular cabinet design as opposed to in one-off enclosure designs. This leads to ease of validation of consistent fire safety system requirements for the cabinet, simpler overall plant design and costs, and reliable listing requirements in the fire codes (Paiss, 2021). Indoor deployments are also based on these standard rack systems allowing for lower cost requirements. ESSs that have a lower degree of modularity for a similar system rating (power or energy) can have a large degree of non-recurring engineering costs.

Finally, the experience of the EPC firm with energy storage technologies will also have an impact on the engineering design costs. A system with significant modular layout will allow the firm to utilize previous design efforts on future project work, lowering the cost for these subsequent deployments. The ability to use prior engineering efforts in subsequent deployments is an ongoing challenge for engineering firms to avoid nonrecurring expenses.

Procurement costs for ESSs have both direct and indirect cost elements. Depending on the sourcing locations for the equipment, the shipping costs can be easily determined. Of increasing concern for system deployments is the growing breakdown in global supply chain logistics affecting shipments from overseas. This breakdown is a result of global supply and demand fluctuations caused by the COVID-19 pandemic, which are anticipated to persist for one to two more years.

Beyond increasing direct costs, shipping disruptions also make the potential for construction schedule slippage far more realistic. Although not directly connected, sourcing decisions also include possible tariffs on components that increase imported costs. For these reasons, significant effort is being made by a number of EPC and project development firms to find alternative and domestic sources of equipment to avoid tariffs, supply disruptions, and impact of domestic disruptions in the country of origin, and have supply guarantees for production and business planning (Baxter, 2021b).

Construction costs are the area of most variability for overall EPC costs and hold out the promise for greatest areas of cost reduction. These costs are driven by where and how the unit is deployed and the experience of those doing the work. The deployment location of the ESS is the first-level driver for construction costs. Deployment locations can come in either urban, suburban, or rural locations, with a generally increasing cost as the location goes to higher population density environments. The site type is another driver that entails either a greenfield (a vacant site where no prior development work has been done), making the cost estimate for deployment straightforward, or a brownfield site (previously

developed). The type and extent of previous construction at the brownfield site will determine if remediation costs are necessary or if some of the existing changes to the site be adapted for the new project, lowering the costs. Finally, the placement of the system at the site will have an impact on construction costs. Here, the choice is either inside an existing building, inside a purpose-built building, next to an existing structure, or free standing away from existing structures. Inside an existing building will typically be the most expensive option (per kWh of system) especially if retrofitting is required for electrical cabling, HVAC, safety, etc. As the deployment moves toward the easier and unencumbered location, the complexity and hence construction costs will decline.

The companies involved in project construction include both the EPC firm and the electrical contractors. Experience of the EPC firm is based on its project management abilities for energy storage projects, while the important electrical contractor experience is in deploying the particular technology from the specific original equipment manufacturer (OEM) used. A good working relationship between the firms is critical not for just following the plan as stated, but for the electrical contractor to provide feedback to the EPC firm about issues with the actual deployment, which can reduce slippage of the timetable as unexpected items come up. Finally, the level of experience of the two firms in the state or region is important to provide familiarity with local codes and ordinances and working relationships with the authorities having jurisdiction. This cannot be overstated; failing to follow the specific codes and inspection timetables is a risk to the EPC's schedule.

As mentioned in the engineering discussion, the modularity of the technology helps in the construction of the facility. The ability to replicate efforts enables a reduction in the complexity of project management, while modularity of the equipment also reduces the number and types of on-site equipment needed to handle the systems during installation.

A few additions and modifications were made for the 2022 report, including the extension of power capacity to 1,000 MW and energy duration coverage to include 24- and 100-hour systems for both LFP and NMC. The extension to these durations follows the scaling methodology outlined in the Li-ion section of the 2020 report wherein information on components of capital expenditure at specific power and energy was obtained from industry reports, interviews with developers and industry participants, and national laboratory subject matter experts and then synthesized. Trends in capital costs for components as a function of energy and power capacity were established to then interpolate data to estimate the capital costs for the listed power and energy levels in this report.

In addition to including cost and performance parameters for the higher power level of 1,000 MW and longer durations, the same learning rates from the 2020 report were used as shown in Table 4.1, with the basis for these learning rates provided in pages 7-12 of the 2020 report (Mongird et al., 2020a).

Table 4.1. Learning Rates Used to Establish Li-ion 2030 Capital Cost and Fixed O&M Ranges

Component	Low Cost	Point Estimate Cost	High Cost
DC SB (\$/kWh)	14%	10%	7%
DC SBOS (\$/kWh)	10%	7%	4%
DC-DC converter (\$/kW)	7%	3%	2%
Power conversion system PCS (\$/kW)	7%	3%	2%
C&C (\$/kW)	10%	7%	4%
System integration (\$/kWh)	6%	4%	2%
EPC (\$/kWh)	6%	4%	2%

Component	Low Cost	Point Estimate Cost	High Cost
Project Development (\$/kWh)	6%	4%	2%
Grid Integration (\$/kW)	6%	4%	2%
Fixed O&M (\$/kW/year)	6%	4%	2%

The ratio of 2030 costs to 2021 costs was calculated using annual demand estimates for 2021 and 2030 from (BNEF, 2020) and is shown in Figure 4.1.

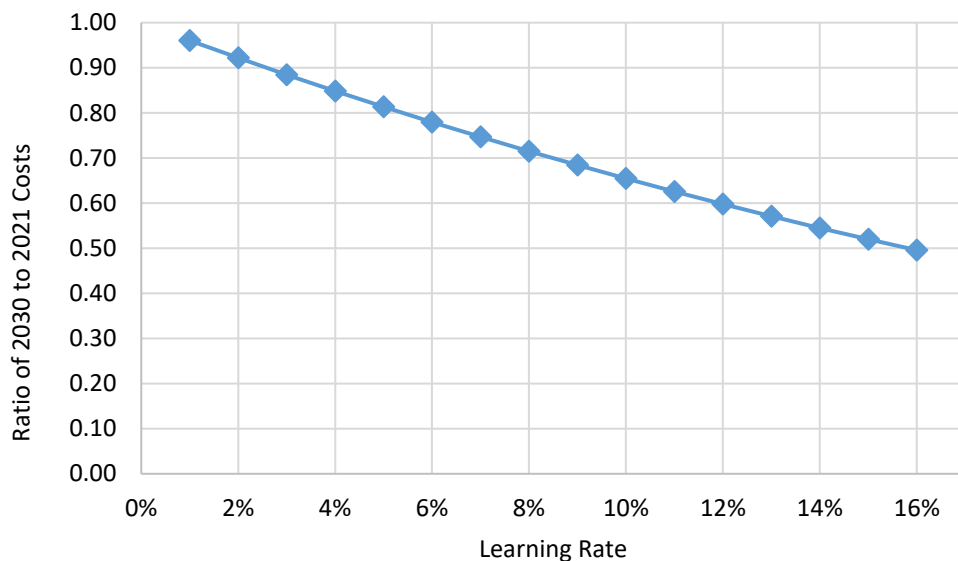


Figure 4.1. Ratio of 2030 to 2021 Costs Based on Learning Rate

4.1.2 Operating Costs

4.1.2.1 Fixed Operations and Maintenance

A fixed O&M of 0.43% of the direct capital cost for SB, SBOS and power equipment was retained for the 2022 analysis, consistent with the 2020 analysis (Mongird et al., 2020b). This fixed O&M cost covers yearly minor maintenance including inspections, filter replacements, alignments, and in some cases software upgrades. In addition, however, the 2021 fixed O&M cost estimate for all battery systems considered in this report also includes major refurbishment for power equipment components. This cost is assumed to be 30% of the power equipment (\$/kWh) and is incurred every 10 years of the project life (Austin, 2021; Vartanian, 2021). The major refurbishment costs include augmentation of subsystems of the power conversion equipment and the labor associated with it. The total fixed O&M cost for Li-ion LFP is approximately \$4.59/kW-year for a 10 MW, 4-hour system and \$5.11/kW-year for NMC.

4.1.2.2 Warranty

Li-ion LFP batteries are not expected to incur an additional warranty cost over the project lifetime, though there are some instances where such costs are incurred, with warranty terms of 10-15 years or 10,000 cycles at 80% DOD (Atlas ESS, 2020; SimpliPhi Power, 2019). Li-ion NMC systems, however, are expected to require an additional warranty purchase after an initial included warranty expires (Baxter, 2021b). Within this analysis, the warranty cost for Li-ion NMC systems is expected to occur on an annual

basis. There is assumed to be an initial warranty included with each SB that expires four years after purchase (Baxter, 2021a), so the warranty cost specified here is incurred four years after project start and after each DC SB rack augmentation across the entire project life. This cost is estimated to be approximately \$3/kWh-year for NMC systems in 2021.

4.1.3 Decommissioning Costs

4.1.3.1 Disconnection, Disassembly, Removal, and Site Remediation

Li-ion ESSs reaching the end of life can be left in place and secured, have the battery modules removed while leaving the rest of the system in place, or be completely deconstructed. The cost components of end-of-life treatment can include disconnection and preparation for removal of the electrical and communications system; removal of the battery modules; rental of equipment including cranes, forklifts, and telehandlers; transportation of ESS parts off site (Hickley, 2021); and recycling of the PCS, container, and transformer. A specialized high-voltage electrician may be required, which accounts for \$0.15–\$0.25 per pound of battery module (Kahl, 2021). In addition, post-removal site work may be necessary and involve grading and top-layer soil removal. However, each site has different attributes by nature of its size, ownership structure, and construction including being indoors or outdoors. As a result, the net recycling and disposal cost is modeled as the initial EPC cost minus the money recouped from material of the battery modules during recycling.

Transportation is typically accomplished by over-road truck and/or train. A truckload can fit approximately 18 tons of battery modules. Transportation costs from site to recycler vary by distance from \$1,000–\$2,000 (\$0.45–\$0.90 per pound) regionally up to \$8,000–\$10,000 (\$3.60–\$4.50 per pound) per truckload for transportation across the continental United States. There is lack of experience in end-of-life issues in ESSs. In some instances, the system minus the DC SB and any other hazardous materials could be left in place or left to the subsequent energy storage developer or landowner to handle accordingly. Only the DC SB is considered in transportation.

4.1.3.2 Recycling

Li-ion recycling is driven by two factors. First, there is a growing emphasis on cradle-to-grave and cradle-to-cradle environmental responsibility and ensuring that social and environmental impacts are minimized throughout the entire lifespan of a project, including end of life. Second, as the demand for Li-ion batteries increases through their use in electric vehicles, consumer electronics, and ESSs, upstream supply lines for battery manufacturing, including mining, face constraints. Recycling of Li-ion batteries and the extraction of lithium, as well as valuable commodity metals including manganese, cobalt, and nickel, help mitigate these supply line constraints (Westlake, 2021).

While large-scale recycling of ESSs is a relatively new field, there are a number of third-party recycling operations pursuing large-scale operations. Recyclers employ proprietary processes to disassemble modules and use one or more methods of mechanical separation, hydrolysis, or pyrolysis. Pricing for recycling at this time is on a project-by-project basis as business models are established, including off-take agreements for the resultant commodity metals, and recyclers look to establish incumbency in the market (Hickley, 2021).

The money recouped for LFP differs from the money recouped from NMC because LFP batteries contain lesser amounts of recoverable metal having value. As a result, LFP currently costs the owner of an ESS a

net of \$0.50 to \$0.70 per pound to recycle, which is forecast to trend to \$0 by 2030. NMC batteries currently cost the owner of an ESS \$0 net to recycle as the transportation costs on average are offset by the value of the metals extracted. Factors that will influence these costs in the future include increasing supply chain and operations efficiencies and commodity costs of metals (Hickley, 2021; Kahl, 2021).

As a result, recycling and disposal costs for LFPs are calculated based on weight of the DC storage block in 2021 and \$0 in 2030. Cost-effective recycling of LFPs has already been accomplished in China due to the presence of a market for black mass from domestic demand from battery manufacturers (Spangenberg, 2021). The weight of LFP modules is 4.42 pounds per kWh on average (Kane, 2021). Recycling and disposal costs for NMCs are calculated as \$0 currently and in 2030. The weight of NMC modules is 2.55 pounds per kWh on average (Kane, 2021; Chem, 2016).

4.1.4 Performance Metrics

4.1.4.1 Calendar Life

In the 2020 report, calendar life for both LFP and NMC Li-ion systems was stated as 10 years. The 2022 report takes additional information from long-term laboratory work (Saft, 2021) and product data into account (Baxter, 2021b) to establish new calendar lives of 16 years for LFP and 13 years for NMC. The calendar life is unchanged for 2030.

4.1.4.2 Cycle Life

Cycle life is analyzed as a function of DOD, with DOD having a wide range based on the grid service. In the 2020 report, a cycle life of 2,000 cycles was used for LFP and 1,200 cycles was used for NMC until the DC SB reached end of life corresponding to 80% of its rated energy capacity. Laboratory data (Saft, 2021) on the degradation of energy capacity with cycling was obtained for LFP and NMC and is shown in Table 4.2. **Error! Reference source not found.** Note that available energy as a function of cycles is expected to be linear up to 50% of rated energy for LFP and 60% for NMC, after which the available energy is expected to drop sharply (Saft, 2021). For simplicity, our work assumes linearity up to 60% of rated energy for both LFP and NMC, and assigns end-of-life condition when available energy is 60% rated energy.

Table 4.2. Cycles at Specified DOD for Li-ion LFP and NMC

DOD Provided (%)	Average DOD (%)	LFP Cycles to end of life ¹¹	LFP 100% DOD Equivalent Cycles	Corrected LFP 100% DOD Equivalent Cycles based on Average DOD	NMC Cycles to end of life	NMC 100% DOD Equivalent Cycles	Corrected NMC 100% DOD Equivalent Cycles based on Average DOD
100	80	4,800	4,800	3,840	3,040	3,040	2,432
80	70	6,000	4,800	4,200	4,000	3,200	2,800
60	60	8,000	4,800	4,800	5,573	3,344	3,344
30	30	32,000	9,600	9,600	40,533	12,160	12,160
5	5	192,000	9,600	9,600	608,000	30,400	30,400

¹¹ End of life is when available energy at full charge is 60% of rated energy.

The cycles are converted to equivalent cycles at 100% DOD as shown in **Error! Reference source not found.**¹². The number of equivalent cycles at 100% DOD is identical for LFP in the 100% to 60% DOD range, while for NMC it increases by 5% at 80% DOD and 10% at 60% DOD over the 100% DOD value. Since available energy as a function of cycles is linear up to 60% of rated energy, this implies that after 6,000 cycles at 80% DOD for LFP, half the battery life is still available for discharge down to end of life, as long as discharge is done at DOD < 80%, ending at DOD of 60%. In other words, the battery discharged at 80% DOD provides twice the cumulative discharge energy throughput to the same end-of-life condition as a battery discharged at 60% DOD, which is not realistic.

It is our hypothesis that cycle life data provided at $\geq 60\%$ DOD are measured until end of life is reached corresponding to available energy at full charge equal to 60% of rated energy. For example, at a reported DOD of 100%, each subsequent cycle yields lower discharge energy to ensure end-of-discharge conditions¹³ are not violated, and cycling is continued until end of life is reached (60% of rated energy). Clearly, DOD decreases with each cycle, finishing at 60%, or an average of 80% DOD (average of 100% and 60%). Similarly, for the cycle life data corresponding to reported DOD of 80%, the average DOD is 70%. Note that the cumulative energy throughput using the average DOD at $> 60\%$ DOD decreases due to average DOD being lower than the reported DOD.¹⁴ The corrected 100% DOD equivalent cycles based on average DOD is also provided in Table 4.2.

With the reported DOD at $> 60\%$ corrected to average DOD as described above, it is determined that the cumulative throughput at 70% average DOD (cycling at 80% DOD to end of life) is 9% and 15% higher than that at 80% average DOD (cycling at 100% DOD to end of life) for LFP and NMC, respectively, while the cumulative throughput at 60% DOD is 25% and 37% higher than that at 80% average DOD for LFP and NMC, respectively. This is more in line with the expectation that cumulative discharge energy throughput increases with a decrease in DOD.

At high DOD, LFP cumulative throughput is higher, 58% higher at 80% average DOD and 44% at 60% DOD, whereas at low DOD the reverse is true, with NMC throughput 27% higher at 30% DOD and 217% higher at 5% DOD. These results are shown in

Figure 4.2 with crossover occurring at an estimated 50% DOD.

¹² This table also shows average DOD as explained later in this paragraph.

¹³ Such as a minimum cell or module voltage, minimum SOC for a string.

¹⁴ Cumulative energy throughput = DOD*Rated Energy*number of cycles, average DOD < reported DOD for DOD > 60%

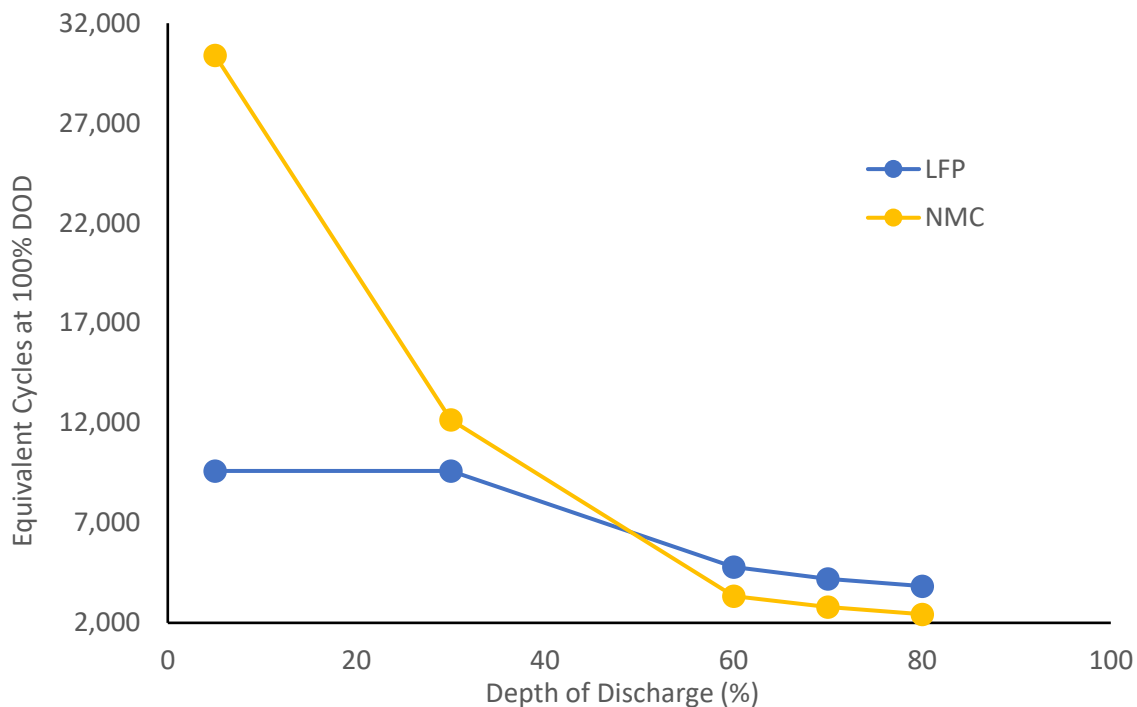


Figure 4.2. Discharge Energy Throughput as a Function of DOD for Li-ion Batteries

As seen in Table 4.3, the cycle life at 80% DOD for LFP and NMC is 2,400 and 1,520 cycles, respectively, after which available energy at full charge is < 80% of rated energy. Note that at the end of cycling at 80% DOD, the battery state of health is halfway been the initial 100% and the 0% state of health reached at end of life when available energy is 60% of rated energy. Based on these findings, an augmentation approach has been described in the LCOS section, with DOD going forward set to energy withdrawn corresponding to 60% of rated energy of the system. When the energy content of the augmented battery decreases to 60% of system rated energy, additional augmentation is done until the desired plant life of 20-25 years is reached.

NMC cycle life was reported at 90% DOD (6,000 cycles) and 80% DOD (8,000 cycles)¹⁵ to end-of-life condition of 70% of rated energy (Kokam, 2020), which upon adjustment of reported DOD corresponds to 3,750 and 4,667 cycles respectively at 80% DOD, with the same throughput available up to end-of-life condition of 60% rated energy. 6,000 cycles were projected¹⁶ at 100% DOD to end-of-life condition of 80% of rated energy (Samsung SDI, 2018). These numbers are much higher than the 1,520 cycles shown in Table 4.3. For the low end of the LCOS, NMC batteries will be assigned 4,805 cycles¹⁷ at 80% DOD to 80% rated energy, halfway to end of life, with the same additional energy throughput available to end of life of 60% of rated energy.

¹⁵ The number of cycles tested is not reported

¹⁶ 4,500 cycles were tested

¹⁷ Average of 3750, 4667 and 6000 cycles

For LFP, 2,475-6,250 cycles were estimated (after adjusting the reported DOD) at 80% DOD to 80% rated energy (ESS, 2020; Lithionics Battery, 2019; Lithium Werks, 2019; SimpliPhi Power, 2019; Zhongeng Technology, 2019), with the same throughput available to end of life of 60% of rated energy, with only one developer reporting the number of cycles tested (Zhongeng Technology, 2019). For the low end of the LCOS, LFP batteries will be assigned 4550¹⁸ cycles at 80% DOD to 80% rated energy, halfway to end of life, with the same additional throughput available to end of life of 60% of rated energy.

Note that the high cycle life reported for both NMC and LFP is partly due to accelerated testing where several cycles are done per day, reducing calendar aging related effects. However, during operation, most warranties limit the user to one full 100% DOD equivalent cycle per day. The reported cycle life is also an extrapolation of limited number of cycles the batteries are actually subjected to. Due to these reasons, the numbers shown in Table 4.3 are used for the point estimate of LCOS, with the higher reported cycle life assigned to the low end of the LCOS calculation. The cycle life is assumed to increase by 10% by 2030.

Table 4.3. Cycles at Specified DOD for Li-ion LFP and NMC Using DOD Correction

Average DOD	LFP Cycles to State Where Remaining Energy Equals Energy at Average DOD	NMC Cycles to State Where Remaining Energy Equals Energy at Average DOD
80%	2,400	1,520
70%	4,500	3,000
60%	8,000	5,573
30%	32,000	40,533
5%	192,000	608,000

4.1.4.3 Round-trip Efficiency

Table 4.4 provides information on the conversion from DC-DC RTE to alternating current (AC)-AC RTE inclusive of inverter and transformer efficiency losses. The RTE used in this report for the final summary table as well as the value used in the LCOS calculations is the AC-AC RTE inclusive of inverter and transformer RTE. The RTE is increased by two percentage points for 2030.

Table 4.4. Li-ion DC-DC and AC-AC RTE Values

Technology	DC-DC RTE		AC-AC RTE at Inverter Level ^a		AC-AC RTE at Transformer Level ^b	
	2021	2030	2021	2030	2021	2030
LFP	89.55%	91.63%	86.00%	88.00%	82.59%	84.52%
NMC	89.55%	91.63%	86.00%	88.00%	82.59%	84.52%

^a Assumes a bidirectional inverter RTE of (0.98)²

^b Assumes a transformer RTE of (0.98)²

4.1.5 Results

Figure 4.3 and Figure 4.4 show the 2021 and 2030 total installed cost and performance parameters for 1 MW and 10 MW; 2-, 4-, 10-, and 24-hour systems; and the installed cost ranges for all power capacity and energy durations, respectively, for Li-ion LFP. Figure 4.5 and Figure 4.6 show the 2021 and 2030

¹⁸ Average of reported cycle numbers, excluding 2475 cycles, an outlier.

total installed cost and performance parameters for 1 MW and 10 MW; 2-, 4-, 10-, and 24-hour systems; and the installed cost ranges for all power capacity and energy durations, respectively, for NMC.

2021 & 2030 Lithium-ion LFP
Installed Costs & Performance Parameters

ESS Installed Cost		ESS	Storage System	1 MW								10 MW							
				2 hr		4 hr		10 hr		24 hr		2 hr		4 hr		10 hr		24 hr	
				2021	2030	2021	2030	2021	2030	2021	2030	2021	2030	2021	2030	2021	2030	2021	2030
			DC Storage Block (\$/kWh)	\$184.94	\$121.02	\$182.27	\$119.28	\$178.80	\$117.00	\$175.54	\$114.87	\$176.21	\$115.31	\$173.67	\$113.64	\$170.36	\$111.48	\$167.25	\$109.45
			DC Storage BOS (\$/kWh)	\$45.55	\$34.01	\$42.38	\$31.64	\$40.06	\$29.92	\$38.75	\$28.93	\$43.40	\$32.41	\$40.38	\$30.15	\$38.17	\$28.50	\$36.92	\$27.57
			Power Equipment (\$/kW)	\$84.65	\$74.88	\$84.65	\$74.88	\$84.65	\$74.88	\$84.65	\$74.88	\$73.05	\$64.62	\$73.05	\$64.62	\$73.05	\$64.62	\$73.05	\$64.62
			C&C (\$/kW)	\$40.01	\$29.87	\$40.01	\$29.87	\$40.01	\$29.87	\$40.01	\$29.87	\$7.75	\$5.78	\$7.75	\$5.78	\$7.75	\$5.78	\$7.75	\$5.78
			Systems Integration (\$/kWh)	\$56.56	\$47.99	\$50.16	\$42.56	\$45.87	\$38.92	\$43.73	\$37.10	\$51.62	\$43.80	\$46.66	\$39.59	\$43.24	\$36.69	\$41.48	\$35.19
			EPC (\$/kWh)	\$69.88	\$59.29	\$61.20	\$51.92	\$55.44	\$47.04	\$52.64	\$44.67	\$62.33	\$52.88	\$56.18	\$47.67	\$51.97	\$44.10	\$49.80	\$42.26
			Project Development (\$/kWh)	\$83.85	\$71.15	\$73.43	\$62.31	\$66.53	\$56.45	\$63.17	\$53.60	\$74.79	\$63.46	\$67.42	\$57.20	\$62.37	\$52.92	\$59.76	\$50.71
			Grid Integration (\$/kW)	\$30.94	\$26.25	\$30.94	\$26.25	\$30.94	\$26.25	\$30.94	\$26.25	\$24.81	\$21.05	\$24.81	\$21.05	\$24.81	\$21.05	\$24.81	\$21.05
			Total Installed Cost (\$/kWh)	\$518.59	\$398.98	\$448.34	\$340.46	\$402.25	\$302.42	\$380.32	\$284.63	\$461.15	\$353.58	\$410.70	\$311.11	\$376.67	\$282.83	\$359.62	\$268.98
			Total Installed Cost (\$/kW)	\$1,037	\$798	\$1,793	\$1,362	\$4,023	\$3,024	\$9,128	\$6,831	\$922	\$707	\$1,643	\$1,244	\$3,767	\$2,828	\$8,631	\$6,456
Operating Costs																			
			Fixed O&M (\$/kW-yr)	\$3.17	\$2.69	\$5.05	\$4.28	\$10.59	\$8.99	\$23.30	\$19.77	\$2.79	\$2.37	\$4.59	\$3.89	\$9.87	\$8.38	\$21.98	\$18.65
Decommissioning Costs																			
			Recycling/Disposal (\$/kWh)	\$2.65	\$0.00	\$2.65	\$0.00	\$2.65	\$0.00	\$2.65	\$0.00	\$2.65	\$0.00	\$2.65	\$0.00	\$2.65	\$0.00	\$2.65	\$0.00
Performance Parameters																			
			RTE (%)	83%	85%	83%	85%	83%	85%	83%	85%	83%	85%	83%	85%	83%	85%	83%	85%
			Cycle Life (#)*	2,400	2,640	2,400	2,640	2,400	2,640	2,400	2,640	2,400	2,640	2,400	2,640	2,400	2,640	2,400	2,640
			Calendar Life (yrs)	16	16	16	16	16	16	16	16	16	16	16	16	16	16	16	16
			DOD (%)	80%	80%	80%	80%	80%	80%	80%	80%	80%	80%	80%	80%	80%	80%	80%	80%

* Cycle Life (#) represents available cycles until remaining energy is equivalent to average DOD (%).

Figure 4.3. 2021 and 2030 Installed Costs and Performance Parameters – LFP

Total Installed Cost (\$/kWh) Ranges - Lithium-ion LFP

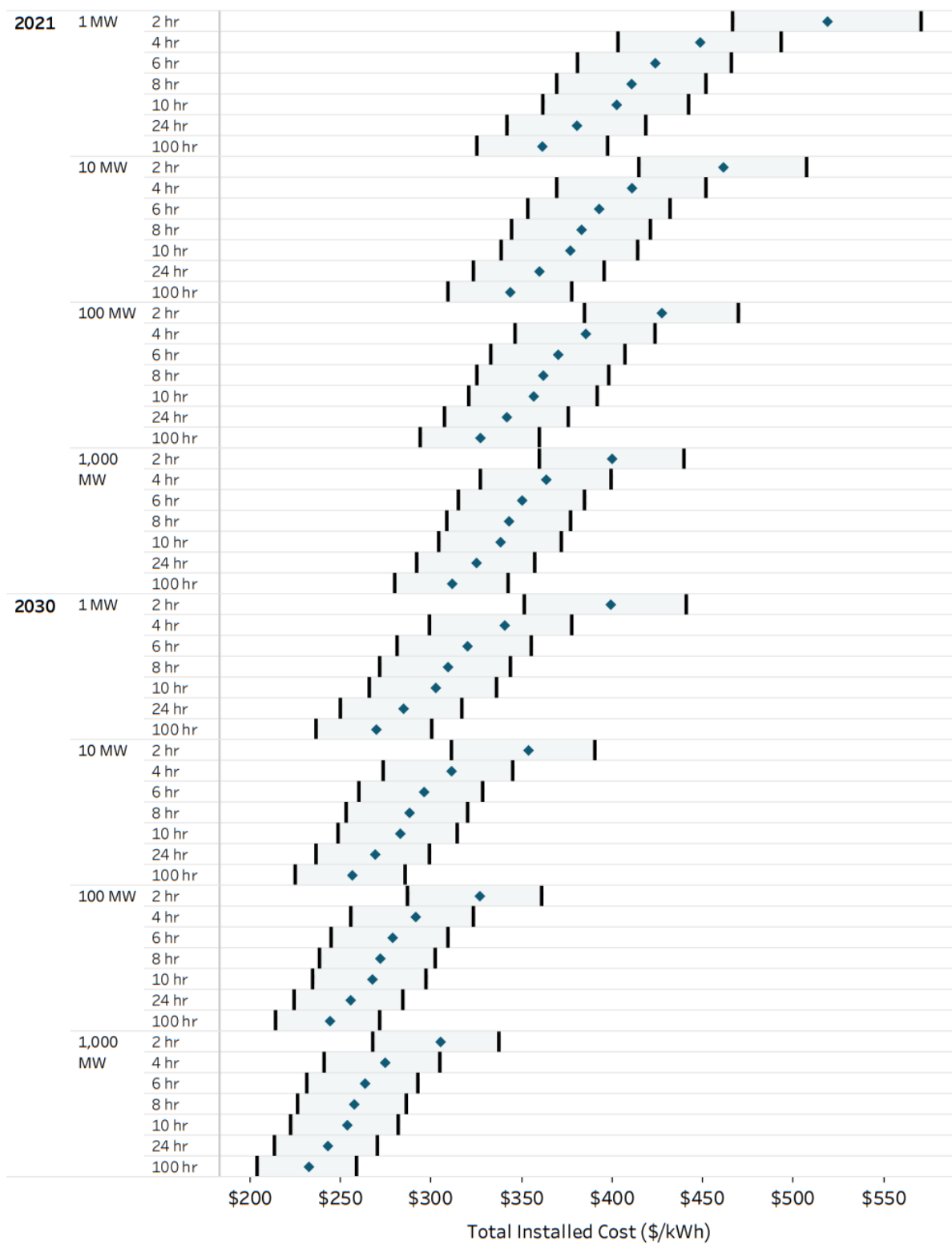


Figure 4.4. 2021 and 2030 Total Installed Costs Ranges – LFP

2021 & 2030 Lithium-ion NMC
Installed Costs & Performance Parameters

ESS Installed Cost	ESS	Storage System	1 MW								10 MW							
			2 hr		4 hr		10 hr		24 hr		2 hr		4 hr		10 hr		24 hr	
			2021	2030	2021	2030	2021	2030	2021	2030	2021	2030	2021	2030	2021	2030	2021	2030
		DC Storage Block (\$/kWh)	\$218.71	\$143.12	\$215.55	\$141.05	\$211.44	\$138.36	\$207.59	\$135.84	\$208.29	\$136.30	\$205.28	\$134.33	\$201.37	\$131.77	\$197.70	\$129.37
		DC Storage BOS (\$/kWh)	\$44.76	\$33.42	\$41.32	\$30.85	\$38.86	\$29.02	\$37.50	\$28.00	\$42.65	\$31.85	\$39.37	\$29.40	\$37.02	\$27.65	\$35.73	\$26.68
		Power Equipment (\$/kW)	\$84.65	\$74.88	\$84.65	\$74.88	\$84.65	\$74.88	\$84.65	\$74.88	\$73.05	\$64.62	\$73.05	\$64.62	\$73.05	\$64.62	\$73.05	\$64.62
		C&C (\$/kW)	\$40.01	\$29.87	\$40.01	\$29.87	\$40.01	\$29.87	\$40.01	\$29.87	\$7.75	\$5.78	\$7.75	\$5.78	\$7.75	\$5.78	\$7.75	\$5.78
		Systems Integration (\$/kWh)	\$63.16	\$53.59	\$56.61	\$48.03	\$52.15	\$44.25	\$49.89	\$42.33	\$57.88	\$49.11	\$52.78	\$44.78	\$49.22	\$41.76	\$47.33	\$40.16
		EPC (\$/kWh)	\$77.79	\$66.00	\$68.93	\$58.48	\$62.98	\$53.44	\$60.03	\$50.94	\$69.84	\$59.26	\$63.53	\$53.90	\$59.14	\$50.18	\$56.82	\$48.22
		Project Development (\$/kWh)	\$93.35	\$79.21	\$82.71	\$70.18	\$75.58	\$64.13	\$72.04	\$61.13	\$83.81	\$71.11	\$76.23	\$64.68	\$70.97	\$60.21	\$68.19	\$57.86
		Grid Integration (\$/kW)	\$30.94	\$26.25	\$30.94	\$26.25	\$30.94	\$26.25	\$30.94	\$26.25	\$24.81	\$21.05	\$24.81	\$21.05	\$24.81	\$21.05	\$24.81	\$21.05
		Total Installed Cost (\$/kWh)	\$575.57	\$440.85	\$504.01	\$381.35	\$456.57	\$342.30	\$433.53	\$323.69	\$515.28	\$393.36	\$463.58	\$349.95	\$428.28	\$320.72	\$410.17	\$306.09
		Total Installed Cost (\$/kW)	\$1,151	\$882	\$2,016	\$1,525	\$4,566	\$3,423	\$10,405	\$7,769	\$1,031	\$787	\$1,854	\$1,400	\$4,283	\$3,207	\$9,844	\$7,346
Operating Costs																		
		Fixed O&M (\$/kW-year)	\$3.45	\$2.93	\$5.60	\$4.75	\$11.95	\$10.14	\$26.48	\$22.46	\$3.06	\$2.60	\$5.11	\$4.34	\$11.16	\$9.47	\$25.00	\$21.21
		Warranty (\$/kWh-yr)	\$3.28	\$2.15	\$3.23	\$2.12	\$3.17	\$2.08	\$3.11	\$2.04	\$3.12	\$2.04	\$3.08	\$2.01	\$3.02	\$1.98	\$2.97	\$1.94
Performance Parameters																		
		RTE (%)	83%	85%	83%	85%	83%	85%	83%	85%	83%	85%	83%	85%	83%	85%	83%	85%
		Cycle Life (#)*	1,520	1,672	1,520	1,672	1,520	1,672	1,520	1,672	1,520	1,672	1,520	1,672	1,520	1,672	1,520	1,672
		Calendar Life (yrs)	13	13	13	13	13	13	13	13	13	13	13	13	13	13	13	13
		DOD (%)	80%	80%	80%	80%	80%	80%	80%	80%	80%	80%	80%	80%	80%	80%	80%	80%

* Cycle Life (#) represents available cycles until remaining energy is equivalent to average DOD (%).

Figure 4.5. 2021 and 2030 Installed Costs and Performance Parameters – NMC

Total Installed Cost (\$/kWh) Ranges - Lithium-ion NMC

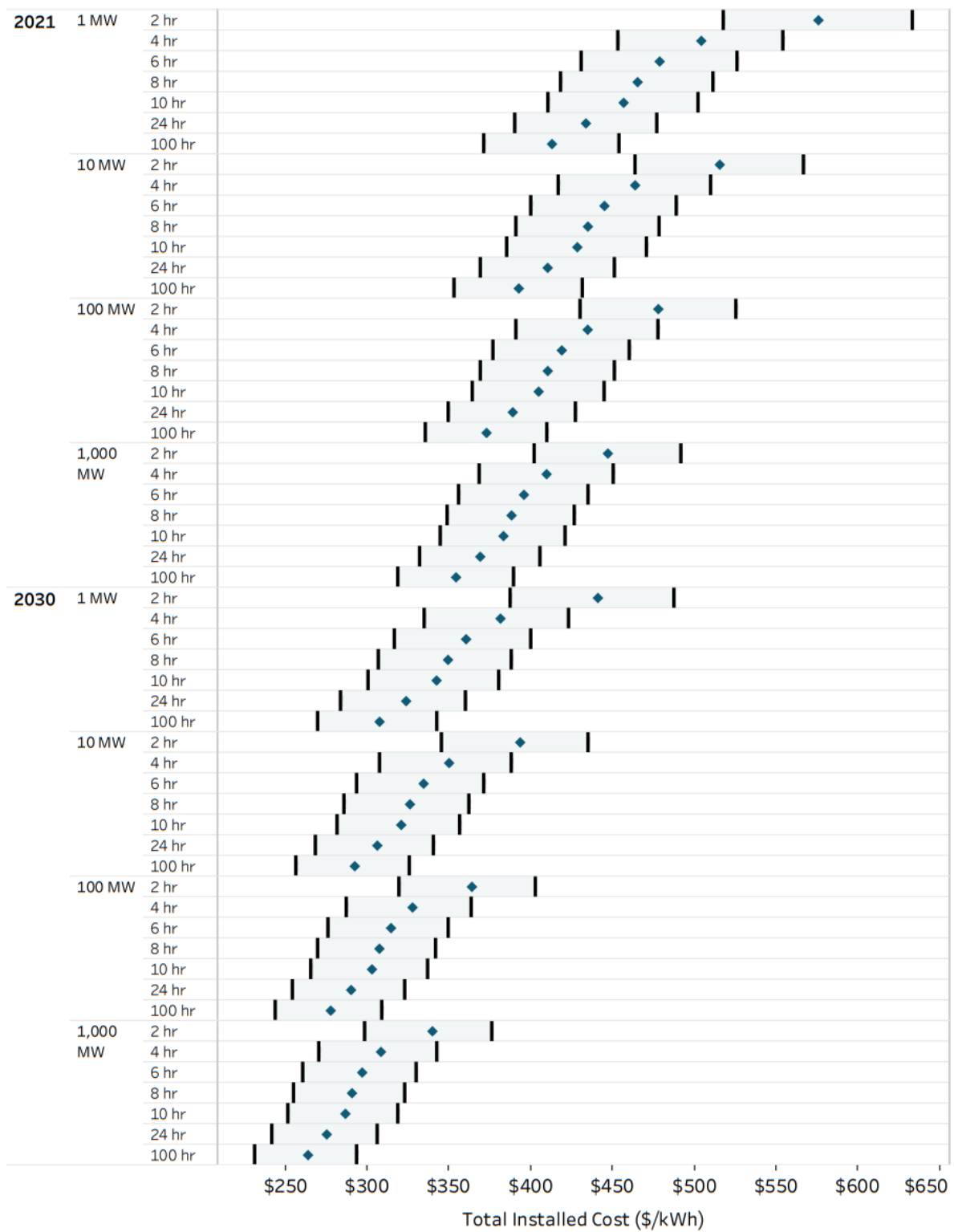


Figure 4.6. 2021 and 2030 Total Installed Costs Ranges – NMC

4.2 Lead-Acid Batteries

4.2.1 Capital Cost

Lead-acid SB cost estimates for 2021 are significantly different from those provided in 2020 (\$171/kWh for a 10 MW, 4-hr system in 2020 report vs. \$235/kWh in 2021). The 2020 costs corresponded to repeat units consisting of 12-volt monoblocs or modules, which cost \$100/kWh, with rack cost estimated at \$71/kWh. While the capital cost is quite attractive, these batteries have a low cycle life, providing 520 cycles at 80% DOD. Longer cycle life is obtained when using battery strings with single cells as the repeat units (Raiford, 2020), mainly attributed to thicker grids and more uniform cell-to-cell temperature distribution with minimal hot spots. Hence, for 2021, lead-acid batteries comprising single cells as repeat units with longer cycle life are used. Other cost components were estimated to be the same as those presented in the 2020 analysis (Mongird et al., 2020b).

The cost range (low and high estimates) for 2021 was 0.94 to 1.06 times the nominal values for each category. In the 2020 report, learning rates were chosen for lead-acid SB and BOS, while using annual deployment projections for Li-ion battery storage systems, since 2021 and 2030 estimated deployment volumes for lead-acid BESS are not known. The same approach is followed for the 2022 report as well, with learning rates for SB and SBOS left unchanged. For all other cost components, the percentage drop for 2030 follows that associated with the learning rates included for Li-ion, using Li-ion volume deployments.

The lead-acid battery technology is mature and has been commercially deployed for grid-scale storage. Estimates for four durations at 1 and 10 MW can be found in Figure 4.8.

4.2.2 Operating Costs

4.2.2.1 Fixed Operations and Maintenance

Estimation of fixed O&M costs for lead-acid systems follow the methodology of the 2020 report and is calculated as 0.43% of total installed costs (\$/kW). An additional 30% power equipment overhaul cost is incurred every 10 years across the project life, following the same methodology described in the Li-ion section. The final fixed O&M cost for a 10 MW lead-acid system, therefore, is estimated to be in the range of approximately \$4 to \$115/kW-year depending on duration for 2021, with learning rate assumed to be the same as for the Li-ion system. Estimates for four durations at 1 and 10 MW can be found in Figure 4.8.

4.2.2.2 Warranty

No warranty or other operating costs are included in estimates for lead-acid batteries at this time. While lead-acid DC SB vendors may include a warranty in their cost, total project warranty costs are not a well-developed business model.

4.2.3 Decommissioning Costs

4.2.3.1 Disconnection, Disassembly, Removal, and Site Remediation

Lead-acid ESSs reaching the end of life can be left in place and secured, have the battery modules removed while leaving the rest of the system in place, or be completely deconstructed. The cost

components of end-of-life treatment includes disconnection and preparation for removal of electrical and communications systems; removal of the battery modules; rental of equipment including cranes, forklifts, and telehandlers; transportation of equipment off site; and recycling of the PCS, container, and transformer. In addition, post-removal site work may be necessary and involve grading and top-layer soil removal. In one case of an 850 kWh ESS that costs are known for disconnection, disassembly, removal, and site remediation, costs totaled \$247,723 (Buchanan, 2021). However, each site may have different attributes by nature of its size, ownership structure, and construction including being indoors or outdoors. As a result, the net recycling and disposal costs are modeled as the initial EPC cost minus the money recouped from material of the battery modules during recycling.

4.2.3.2 Recycling and Disposal

Lead-acid battery recycling is a mature industry with many applications having defined return processes and supply chain routes. Automotive, marine, industrial, and forklift batteries are commonly recycled. OEM battery manufacturers and third-party recycling centers accept batteries at the end of their life and use mechanical and chemical processes to recover lead. From 10-12% of the initial cost of lead-acid battery modules is recoverable through these methods (Buchanan, 2021).

4.2.4 Performance Metrics

4.2.4.1 Calendar Life

The calendar life of a lead-acid battery kept on float at 25°C is estimated at 14 years (Dufo-López, Cortés-Arcos, Artal-Sevil, & Bernal-Agustín, 2021). Note that for uninterruptible power source (UPS) applications, the batteries are kept in a fully charged state, which drops their calendar life to 5 years at the same temperature (Zhang et al., 2017). The calendar life for 2021 for a lead-acid system is assumed to be 12 years in this report and remains consistent with the 2020 estimate. This value is not expected to change by 2030.

4.2.4.2 Cycle Life

Lead-acid battery cycle life depends on the repeat unit, with 12-volt module cycle life significantly lower than single-cell cycle life (Raiford, 2020). In the 2020 report, the lower capital cost and lower cycle life of 12-volt modules were used, while in this report, single-cell values are used (Raiford, 2020). Additional information on single-cell cycle life was available from (BAES), which was 17-21% higher than the reported single-cell cycle life. These values were used to estimate the low end of the LCOS. As explained earlier, due to cycle life limitations, calendar aging does not play as important a role as for Li-ion batteries, hence the reported cycle life is not derated.

While lead-acid battery technology is considered mature, significant industry research and development has focused on improving the performance and durability required for grid-scale applications. Lead-acid cycle life is highly dependent on DOD. The ampere-hour (Ah) capacity for most lead-acid batteries are rated at the 50- to 100-hour rate, hence cycling them at 100% DOD corresponds to a discharge duration of 50 to 100 hours.

At lower discharge durations (or higher rates), a smaller percent of the rated Ah capacity is available. **Error! Reference source not found.** Table 4.5 shows the maximum DOD possible for the durations considered in this study using available energy as percent of rated energy at various durations (C&D Technologies). The DODs have been adjusted lower for durations of 2-10 hours to account for increase

in battery resistance over its life, with adjustment increasing at lower duration or higher rate. Cycle life is left unchanged for 2030.

Table 4.5. Assumed DOD and Cycle Life for Lead-Acid Systems by Duration (hr)

Duration (hr)	Maximum DOD (%)	Adjusted DOD (%)	Cycles
2	61.0%	58.0%	1,951
4	70.6%	68.1%	1,634
6	77.0%	75.0%	1,470
8	81.6%	79.9%	1,371
10	86.2%	80.0%	1,370
24	98.5%	80.0%	1,370
100	102.5%	80.0%	1,370

One additional consideration is that lead-acid batteries degrade faster when stored at low SOC for a prolonged time due to irreversible sulfation of the electrodes. While a DOD of > 98% is possible for 24- and 100-hour discharge, it may be advisable to limit the DOD to 80% for both durations to avoid prolonged stay at < 20% SOC. Lead-acid batteries reach end of life when the available energy at full charge decreases to 80% of rated energy. At DOD > 80%, augmentation would be needed once available energy at full charge decreases to a point where this DOD cannot be sustained. To avoid the need to estimate the number of cycles at DOD > 80% for which this DOD can be sustained, and to avoid the need for augmentation, the DOD is capped at 80%, so that the DC SB is replaced at end of life.

Figure 4.7 shows the relationship between DOD and cycle life and the associated trendline for a single-cell system (Raiford, 2020). It is assumed that the cycle life provided at 100% DOD corresponds to operation until available energy at full charge is less than or equal to 80% of rated energy. This operation corresponds to an average DOD of 90%, hence the cycle life provided at 100% DOD is assigned a DOD of 90%. The cycle life at the durations of interest using the proposed DODs is obtained from Figure 4-7. The cycle life of 1,370 cycles at 80% DOD corresponds to a cumulative throughput of 57% of an LFP battery at the same DOD and end-of-life condition,¹⁹ in line with findings in Dufo-López et al. (2021).

Compared to the 2020 estimates for 12-volt battery modules (Mongird et al., 2020b), the cycle life at each DOD is twice as high for single cells.

¹⁹ Available energy equals 80% of rated energy

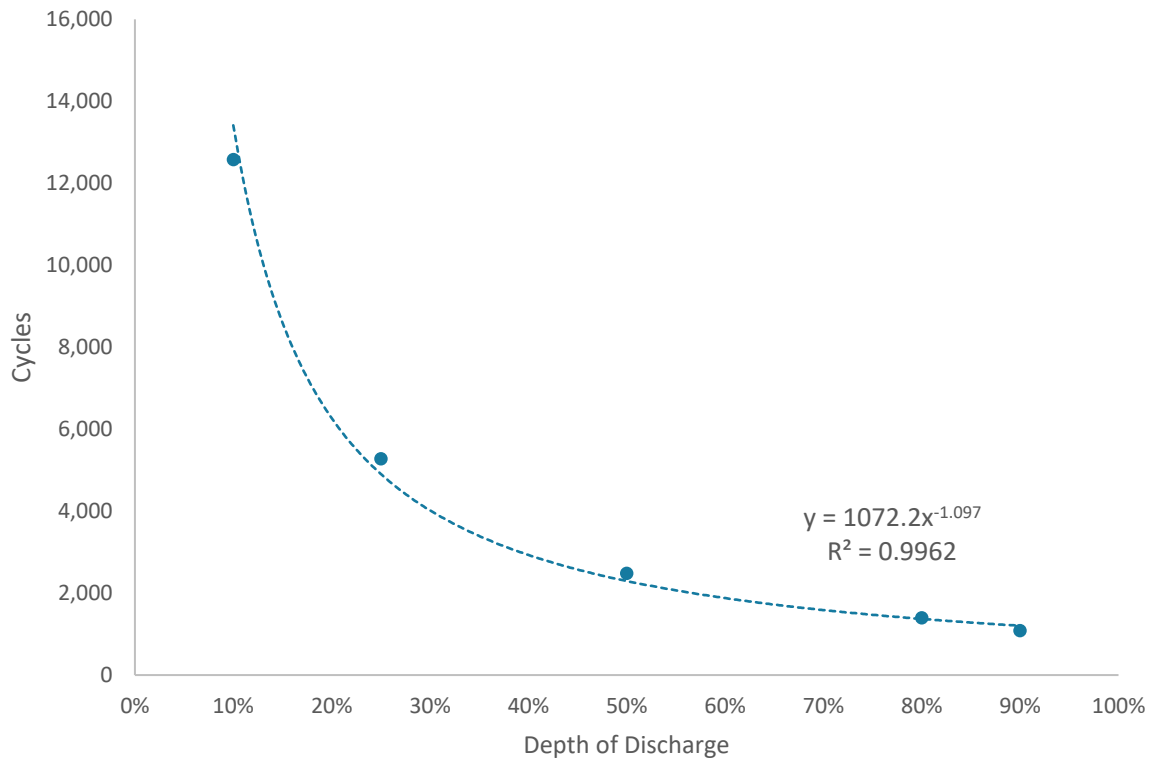


Figure 4.7. Cycles as a Function of DOD for Lead-Acid Systems and Associated Trendline

4.2.4.3 Round-trip Efficiency

Table 4.6 provides information on the conversion from DC-DC RTE to AC-AC RTE for lead-acid. The RTE used in this report for the final summary table, as well as the value used in the LCOS calculations later, is the AC-AC RTE inclusive of bidirectional inverter and transformer RTE. RTE values are left unchanged for 2030.

Table 4.6. Lead-Acid DC-DC and AC-AC RTE Values

Duration (hr)	DC-DC RTE		AC-AC RTE at Inverter Level ^a		AC-AC RTE at Transformer Level ^b	
	2021	2030	2021	2030	2021	2030
2	77%	77%	74%	74%	71%	71%
4	79%	79%	76%	76%	73%	73%
6	82%	82%	79%	79%	76%	76%
8	84%	84%	81%	81%	77%	77%
10	85%	85%	82%	82%	78%	78%
24	86%	86%	83%	83%	79%	79%
100	87%	87%	84%	84%	80%	80%

^a. Assumes a two-way inverter efficiency of (.98)²

^b. Assumes a two-way transformer efficiency of (.98)²

4.2.5 Results

Figure 4.8 and Figure 4.9 show the 2021 and 2030 total installed cost and performance parameters for 1 MW and 10 MW; 2-, 4-, 10-, and 24-hour systems; and the installed cost ranges for all power capacity and energy durations, respectively, for lead-acid.

2021 & 2030 Lead Acid
Installed Costs & Performance Parameters

ESS Installed Cost		ESS	Storage System	1 MW								10 MW							
				2 hr		4 hr		10 hr		24 hr		2 hr		4 hr		10 hr		24 hr	
				2021	2030	2021	2030	2021	2030	2021	2030	2021	2030	2021	2030	2021	2030	2021	2030
ESS Installed Cost	ESS	Storage System	DC Storage Block (\$/kWh)	\$251.08	\$236.19	\$247.28	\$232.62	\$242.35	\$227.98	\$237.72	\$223.63	\$238.68	\$224.53	\$235.07	\$221.13	\$230.38	\$216.72	\$225.98	\$212.58
			DC Storage BOS (\$/kWh)	\$50.22	\$37.50	\$49.46	\$36.93	\$48.47	\$36.19	\$47.54	\$35.50	\$47.74	\$35.64	\$47.01	\$35.11	\$46.08	\$34.40	\$45.20	\$33.75
			Power Equipment (\$/kW)	\$154.86	\$137.00	\$154.86	\$137.00	\$154.86	\$137.00	\$154.86	\$137.00	\$133.00	\$117.65	\$133.00	\$117.65	\$133.00	\$117.65	\$133.00	\$117.65
			C&C (\$/kW)	\$40.01	\$29.88	\$40.01	\$29.88	\$40.01	\$29.88	\$40.01	\$29.88	\$7.75	\$5.79	\$7.75	\$5.79	\$7.75	\$5.79	\$7.75	\$5.79
			Systems Integration (\$/kWh)	\$54.54	\$46.28	\$47.36	\$40.18	\$42.61	\$36.15	\$40.32	\$34.21	\$49.65	\$42.13	\$43.92	\$37.26	\$40.07	\$33.99	\$38.14	\$32.36
			EPC (\$/kWh)	\$60.90	\$51.67	\$52.09	\$44.20	\$46.58	\$39.53	\$44.01	\$37.34	\$56.66	\$48.08	\$48.95	\$41.53	\$44.06	\$37.39	\$41.75	\$35.42
			Project Development (\$/kWh)	\$77.13	\$65.44	\$66.74	\$56.62	\$59.92	\$50.85	\$56.66	\$48.07	\$69.46	\$58.94	\$61.52	\$52.20	\$56.20	\$47.68	\$53.54	\$45.43
			Grid Integration (\$/kW)	\$30.94	\$26.25	\$30.94	\$26.25	\$30.94	\$26.25	\$31.94	\$27.10	\$24.81	\$21.05	\$24.81	\$21.05	\$24.81	\$21.05	\$24.81	\$21.05
Total Installed Cost (\$/kWh)				\$606.78	\$533.64	\$519.38	\$458.84	\$462.52	\$410.01	\$435.70	\$386.84	\$544.97	\$481.56	\$477.86	\$423.35	\$433.33	\$384.63	\$411.50	\$365.56
Total Installed Cost (\$/kW)				\$1,214	\$1,067	\$2,078	\$1,835	\$4,625	\$4,100	\$10,457	\$9,284	\$1,090	\$963	\$1,911	\$1,693	\$4,333	\$3,846	\$9,876	\$8,773
Operating Costs																			
Fixed O&M (\$/kW-yr)				\$4.61	\$3.96	\$7.13	\$6.09	\$14.53	\$12.37	\$31.46	\$26.74	\$4.05	\$3.47	\$6.44	\$5.50	\$13.48	\$11.47	\$29.57	\$25.13
Decommissioning Costs																			
Recycling/Disposal (\$/kWh)				\$33.28	\$25.69	\$24.89	\$18.61	\$19.93	\$14.45	\$17.86	\$12.74	\$30.41	\$23.38	\$23.09	\$17.21	\$18.72	\$13.55	\$16.89	\$12.04
Performance Parameters																			
RTE (%)				71%	71%	73%	73%	78%	78%	79%	79%	71%	71%	73%	73%	78%	78%	79%	79%
Cycle Life (#)*				1,951	1,951	1,634	1,634	1,370	1,370	1,370	1,370	1,951	1,951	1,634	1,634	1,370	1,370	1,370	1,370
Calendar Life (yrs)				12	12	12	12	12	12	12	12	12	12	12	12	12	12	12	12
DOD (%)				58%	58%	68%	68%	80%	80%	80%	80%	58%	58%	68%	68%	80%	80%	80%	80%

* Cycle Life (#) represents available cycles until remaining energy is equivalent to average DOD (%).

Figure 4.8. 2021 and 2030 Installed Costs and Performance Parameters – Lead-Acid

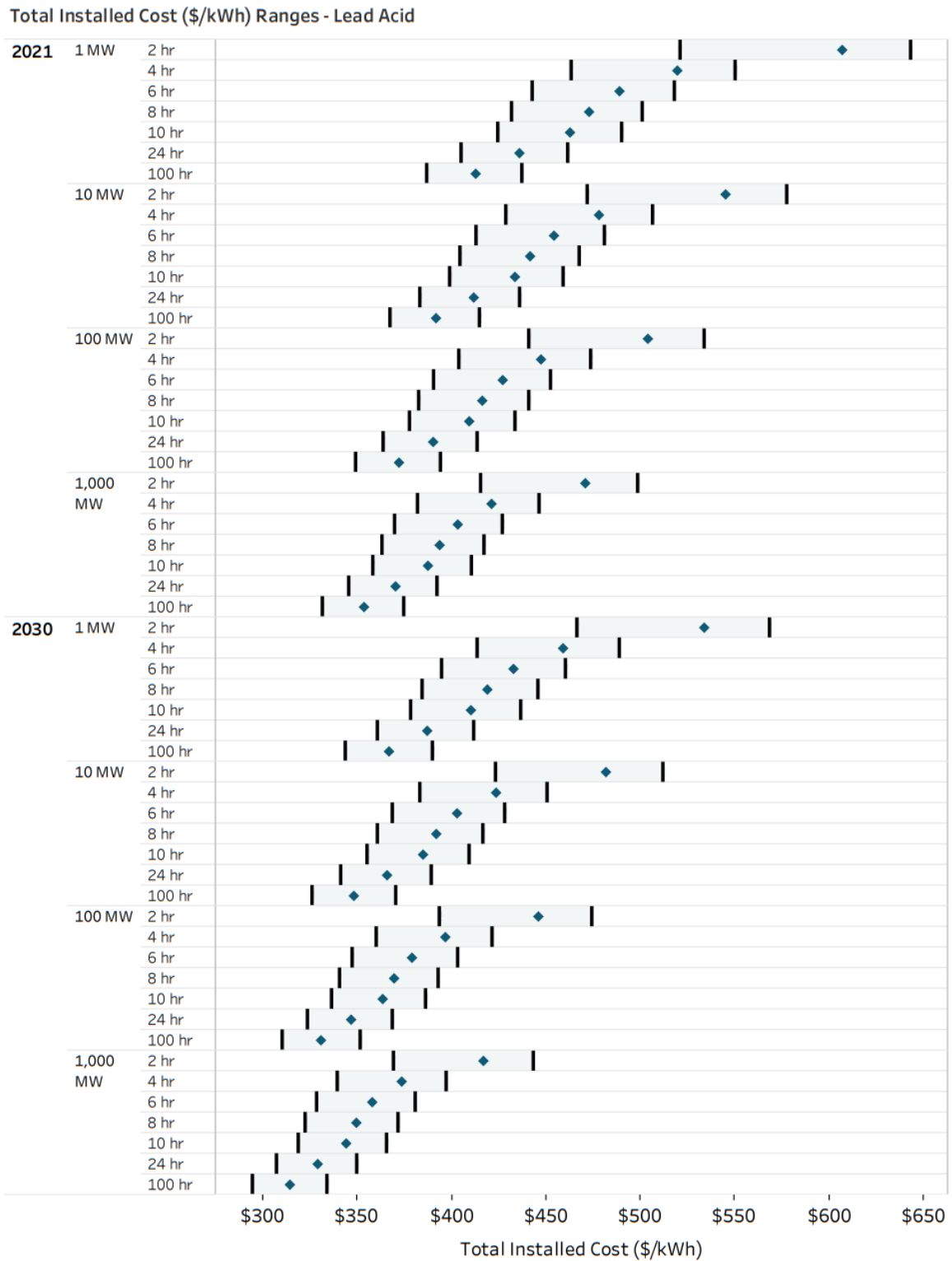


Figure 4.9. 2021 and 2030 Total Installed Costs Ranges – Lead-Acid

4.3 Vanadium Redox Flow Batteries

An RFB is a unique type of rechargeable battery architecture in which the energy is stored in one or more soluble redox couples contained in external electrolyte tanks (Yang et al., 2011). Liquid electrolytes are pumped from the storage tanks through electrodes where the chemical energy in the electrolyte is converted to electrical energy (discharge) or vice versa (charge). The electrolytes flowing through the cathode and anode are often different and referred to as catholyte and anolyte, respectively. Between the anode and cathode compartments is a membrane (or separator) that selectively allows cross-transport of a charge-carrying species (e.g., H^+ , Cl^-) to complete the electrochemical reaction. Mixed-acid electrolytes have a wider SOC operating range of 10-90% (Cipriano, 2021) compared to conventional sulfuric-acid-based electrolytes with an SOC range of 10-80% (Mittal, 2021), leading to higher vanadium utilization. This, coupled with their higher concentration, results in an energy density twice that of conventional sulfuric-acid-based batteries, resulting in lower cost (Cipriano, 2021). At lower SOC, battery performance suffers during discharge, while at higher SOC, bipolar plate corrosion (Mittal, 2021) and gassing (Cipriano, 2021) reduce stack and electrolyte life, respectively.

Depending on stack design, the RFB can provide as much as twice its rated power for up to one hour (Torikai & SHIBATA, 2021). While some systems do not provide rated power across the entire SOC range, most developers include additional electrolyte in the tank to ensure the rated power is sustained across the 0–100% SOC range. Note that the actual SOC range as seen by the BMS would be in a tighter range such as 10-90%, with SOC excursions beyond this range prevented to ensure performance and reliability, with minimal need for electrolyte balancing (Cipriano, 2021; Mittal, 2021; Watson, 2021).

In traditional battery designs like Li-ion, the stored energy is directly related to the amount of electrode material and increasing the power capacity of these systems also increases the energy capacity and vice versa as more cells are added. In RFB systems, the power and energy capacity can be varied separately. The power (kW) of the system is determined by the size of the electrodes, number of cells in a stack, and number of stacks in the battery system, whereas the energy storage capacity (kWh) is determined by the concentration and total volume of the electrolyte. Both energy and power can be easily adjusted for storage from a few hours to days, depending on the application. This flexibility makes RFB an attractive technology for a variety of grid-scale applications with a wide range of power and energy needs. Using the same stack power capacity, increasing durations (energy levels) are accommodated by increasing the electrolyte quantity, while an application requiring greater power for the same energy content can be met by simply adding more stacks, and an application requiring greater power and energy is met by increasing the stack count and electrolyte volume. The vanadium redox flow battery technology is mature and has been commercially deployed for grid-scale storage.

4.3.1 Capital Cost

This section summarizes qualitative and quantitative input from several developers on drivers for lower cost such as various grades and sources of vanadium, electrolyte leasing models, SOC range of operation (how that impacts capital cost of power equipment as well as DC SB cost), business models such as vertical integration that enable manufacturing and logistics efficiencies, simplification in system integration, and streamlining of project development costs.

Capital cost information from the 2020 ESGC report was supplemented by information from (Cipriano, 2021; Mittal, 2021). Some of the cost reduction drivers for the energy subcomponent of the SB are using cheaper low-metallurgical-grade vanadium coupled with an ultrapurification step (Cipriano, 2021), use of fly ash from petroleum coke burned in a gasifier (Mittal, 2021) and spent catalyst from refineries (Perles, 2021). Drivers for cost reduction for the SB power component are improvement in power density (Cipriano, 2021; Reed et al., 2016), use of microporous separator instead of fluorinated membranes (Mittal, 2021), limiting the upper SOC to avoid corrosion of bipolar plates with stack replacement restricted to components closer to the positive end of a string (Mittal, 2021).

One of the limitations of RFB systems in the past has been the limited SOC range over which rated power is sustained during charge and discharge, with gas evolution at high SOC an additional cause for concern related to electrolyte degradation. Operation at extreme SOCs and temperatures also lead to precipitation of active species in both compartments, which is mitigated by use of mixed-acid electrolyte (Li et al., 2010). A workaround has been to add additional electrolyte (Watson, 2021) to restrict the SOC range to 20–75% for conventional sulfuric-acid electrolyte (Mittal, 2021), and to 10–90% for mixed-acid electrolyte (Cipriano, 2021). Note that from the end user's perspective, the allowable SOC range is 0–100%, where rated power is available during charge and discharge, with the BMS ensuring the battery operates within the real SOC range. The actual energy content of the electrolyte is 25% higher than rated energy for mixed-acid electrolyte and 82% higher for sulfuric-acid electrolyte. An added benefit of operating in this narrow SOC range is that the maximum span for voltage during a full charge-discharge cycle is limited to 30%, avoiding the need for a DC-DC converter (Mittal, 2021; Watson, 2021). Shunt current related limitations for maximum DC voltage is solved by having separate electrolyte tanks for each series-connected repeating unit of block consisting of parallel connected stacks, with each stack limited to ~50-volt DC (Mittal, 2021). The nominal operating voltage reported by one developer is 1,000-volt DC, with a planned shift toward 1,500-volt DC (Brown, 2021). In this report, for the low range of the cost estimate, it is assumed that a DC-DC converter is not needed, with potential for removing the need for such a converter once sufficient data are available.

Use of low-metallurgical-grade vanadium pentoxide coupled with operation in the 10–90% SOC range allows reduction in electrolyte cost from \$180/kWh to \$105/kWh for mixed-acid electrolyte (Cipriano, 2021), while use of sulfuric-acid-based electrolyte and operation in the 20–75% SOC regime corresponds to electrolyte cost of \$150/kWh (Mittal, 2021).

There are several potential mines, such as the Maracás Menchen Mine located in Brazil, producing 12,000 metric tons of V_2O_5 annually (Largo, 2021; Perles, 2021). Primary production also extends to stone coal, a carbonaceous shale with < 1% V_2O_5 content, with China producing 4,800 metric tons in 2020. Secondary production includes vanadium-bearing slag from steel production containing 14–24% V_2O_5 , coal ash and catalyst to refine vanadium-bearing crude oil (Perles, 2021). While crude oil production is expected to decrease over time, production is moving toward sour crude with greater vanadium content, which is expected to keep the cost-effective supply intact for several years (Perles, 2021). The other source of vanadium is recovery of metals such as Mo, Co, Ni, W, Cr, and V from high-strength steel, where vanadium content is expected to be as high as 20%. Electrolyte leasing models are also being explored where the electrolyte cost may be shifted to an annual O&M cost (Delamarche, 2018; Stover, 2021).

Vertical integration is an approach followed by some developers where vanadium supply, electrolyte manufacture, and stack development are under the same corporate structure (Minopoli, 2021; Stover, 2021). As an example, VRB Energy manufactures stacks in China while leveraging on vanadium resources in central China, with a 100 MW, 500 MWh system using 2 MW, 12 MWh systems as repeat unit planned for construction for Hubei Central District, as part of a Giga Technology requirement from the local government (Stover, 2021). Largo Clean Energy mines V_2O_5 , purifies the electrolyte and manufactures stacks in-house (Watson, 2021).

Cost reduction pathways include using high density polyethylene tanks which are not containerized, while the stacks are containerized in National Electrical Manufacturers Association NEMA 3 rated containers, with secondary containment provided by raised edges around the concrete pad (Watson, 2021). Such layouts are possible for indoor installation as well, contingent upon the roof being sufficiently high. Cost reductions of up to 30% are anticipated for 10 hour duration, with larger reductions possible at longer durations.

System integration is simplified with containers fully populated with stacks, tanks, electrolytes, and balance of plant (BOP) in the factory and shipped globally (Torikai & SHIBATA, 2021). Some developers consider the low Wh/kg and Wh/L as a benefit, since this increases the thermal mass, limiting the maximum temperature increase in the event of a short circuiting of electrolyte tank contents (Schoenfeldt, 2021). The battery developer, site owner, financiers, and electrolyte suppliers work together as project developers, with opportunities to streamline processes with experience (Schumacher, Rupprecht, & Kayaalp, 2021).

The ratio of average or point estimates for DC SB and BOS for the 2022 report to 2020 report for year 2021 was 0.94-0.95, associated with the lower electrolyte cost due to use of vanadium of low metallurgical grade (Cipriano, 2021) and lower stack cost using microporous separator (Mittal, 2021). The high-cost values were the same, since the additional data obtained for the report were lower for these components. The low end of the range for DC SB was 77% of corresponding 2020 values, related to low electrolyte cost for low-metallurgical-grade vanadium, while the BOS was 48% of 2020 cost, related to a lower percentage (12.5%) of the lower SB cost. This results in installed capital cost 74–79% of 2020 costs.

Table 4.7 shows the cost components for the year 2021 for 10 MW systems across the 2–100 hour duration.

Table 4.7. Redox Flow Battery Component Cost for 2021 for 10 MW at Various Durations

Component	Duration (hr)						
	2	4	6	8	10	24	100
DC SB, \$/kWh	352	263	234	219	210	190	179
DC BOS, \$/kWh	70	53	47	44	42	38	36
DC-DC converter, \$/kW	60	60	60	60	60	60	60
PCS, \$/kW	73	73	73	73	73	73	73
EMS \$/kW	7.8	7.8	7.8	7.8	7.8	7.8	7.8
System Integration, \$/kWh	74	53	46	42	40	35	32
EPC, \$/kWh	85	61	52	48	46	40	37
PD, \$/kWh	98	70	60	56	53	46	43
Grid Integration, \$/kW	25	25	25	25	25	25	25

Single-point, low and high estimates for both reports were obtained using the same learning rates for all components. The only exception is for the 2022 report, low cost for SB was obtained using an electrolyte cost of \$50/kWh assuming vanadium recovery from coal ash, which drops the SB cost significantly, especially at long durations.

Note that the percentage drop for doubling of volume at a fixed learning rate is different for both reports, since the estimated volume deployments²⁰ have been updated for the 2022 report and there are only 9 years to 2030 for the current report versus 10 years for the 2030 reports. Due to these two factors, the percentage drop in the year 2030 is lower for the 2022 report at the same learning rate.

Note that the single-point and high estimates for 2030 for both reports are obtained by using the same learning rates. The low estimate SB cost for 2022 report is 77% of the 2020 report cost for 2-hour duration and 55% at 100-hour duration. This translates to installed capital cost ratio of 77–87% of 2020 report cost.

Table 4.8 shows the cost components for the year 2030 for 10 MW systems across the 2–100 hour duration.

Table 4.8. RFB Component Cost for 2030 for 10 MW at Various Durations

Component	Duration						
	2	4	6	8	10	24	100
DC Module, \$/kWh	292	219	194	182	175	158	148
DC BOS, \$/kWh	53	39	35	33	31	28	27
DC-DC converter, \$/kW	53	53	53	53	53	53	53
PCS, \$/kW	65	65	65	65	65	65	65
EMS \$/kW	6	6	6	6	6	6	6
System Integration, \$/kWh	62	45	39	36	34	30	27
EPC, \$/kWh	72	51	45	41	39	34	32
PD, \$/kWh	83	59	51	47	45	39	36
Grid Integration, \$/kW	21	21	21	21	21	21	21

4.3.2 Operating Costs

4.3.2.1 Fixed Operations and Maintenance

O&M is typically done by storage owner, utility, or the EPC contractor, with the O&M staff training and stocking up critical parts (Schumacher et al., 2021). One model involves creating a joint venture with a mining company to divide O&M scope. The battery developer ensures critical parts are kept on site and is responsible for servicing the DC battery annually through an O&M contract with an EPC firm, with the site owner paying for spare parts and services (Schumacher et al., 2021). Electronic parts such as sensors are trouble points and require scheduled and unscheduled maintenance. Electronic parts within the PCS also are known to fail (Stover, 2021). Annual maintenance includes top-off and balancing of electrolyte

²⁰ In the 2020 report, learning rates were chosen for RFB SB and BOS, while using annual deployment projections for Li-ion battery storage systems. The same approach is followed for 2022 report as well, with learning rates for SB and SBOS left unchanged.

(Stover, 2021), calibration of sensors, vibration analysis of pumps, and replacement of pumps and valves (Watson, 2021). Most of the stack degradation is restricted to cells near the positive end, allowing reuse of majority of the stack (Mittal, 2021). The O&M as a percent of direct capital cost of the DC SB and DC BOS is estimated at 0.45% (Watson, 2021).

As with Li-ion and lead-acid batteries, there are not many examples in the literature of O&M costs that provide substantial clarity for RFB systems. For this study, the fixed O&M is set to 0.43% of direct capital cost, as described in the Li-ion section. In addition, the cost of power equipment augmentation (30% of power equipment cost) is incurred every 10 years over the life of the system and included in fixed O&M. Therefore, the final fixed O&M cost for RFB systems is assumed to be \$6.66/kW-year for a 10 MW, 4-hour system in 2021.

4.3.2.2 Warranty

Vanadium RFBs are estimated to have a warranty cost of 2.5% of the DC SB and DC BOS, excluding the cost of the electrolyte (Baxter, 2021b). This annual cost then ranges between \$1.25–\$2.59/kWh-year. This warranty cost is expected to be incurred every year of the project life, with a period ranging from 10–25 years (Brown, 2021; Vartanian, 2021)

4.3.3 Decommissioning Costs

4.3.3.1 Disconnection, Disassembly, Removal, and Site Remediation

Vanadium RFB ESSs reaching the end of life can have the electrolyte and/or stacks removed while leaving the rest of the system in place, or be completely deconstructed (Vartanian, 2021). The cost categorization of end-of-life treatment includes disconnection and preparation for removal of electrical and communications systems; removal of the tanks, stacks, and electrolyte; rental of equipment including cranes, forklifts, and telehandlers; transportation of equipment off site; and recycling of the PCS, container, and transformer. In addition, post-removal site work may be necessary and involve grading and top-layer soil removal. However, few systems have reached the end of their life and gone through a recycling process. As a result, the net recycling and disposal costs are modeled as the initial EPC cost constituting a reversal of construction costs minus the money recouped from material of the battery modules during recycling.

4.3.3.2 Recycling and Disposal

With standard recycling processes used for sheet metals, plastics, and electronics, 95% of material can be recycled (Brown, 2021). The vanadium found within the electrolyte is most desired in recycling a system. In 2021, the price of vanadium pentoxide (V_2O_5) reached a high of \$12.80 per pound (Vanadium Price, 2021) and supplies remain constrained from limited vanadium production methods and its use in other industrial processes including metal alloys. The money recouped during recycling is calculated as the percentage of vanadium within the electrolyte by weight corresponding to the amount of electrolyte present in the system as calculated by Crawford et al. (2015) and Stover (2021). In the leasing model, the electrolyte is leased by the end user. At the end of the project life, the developer takes possession of the electrolyte at no cost to the user (Watson, 2021). Disposal of the rest of the system is the responsibility of the storage owner/user, including recycling of stacks which have no residual value. Including the money recouped from recycling the vanadium, the net recycling and disposal cost for an RFB system is assumed to be \$36.50/kWh for a 10 MW, 4-hour system.

4.3.4 Performance Metrics

The RFB can provide two times its rated power for one hour (Torikai & SHIBATA, 2021); however, to take advantage of this, the power equipment rating needs to be chosen to accommodate twice the DC rated power. An unintended consequence of this is that the bidirectional converter ends up operating at low percent of its rated power under normal operation. Some vendors propose using a hybrid approach with a high-power Li-ion battery to provide pulse power; in that context, the ability of the RFB to provide twice its rated power may result in cost reduction by avoiding use of the high-power Li-ion battery.

4.3.4.1 Calendar and Cycle Life

Compared to other electrochemical battery systems, RFBs typically have longer lifespans due to being less sensitive to temperature as long as the electrolyte temperature is maintained within the operating envelop and avoiding material stresses experienced by other battery systems during cycling.

The calendar and cycle life for the electrolyte is typically unlimited. One developer reported a cumulative 3 million operating hours for 100 installed systems operating globally, with 1% degradation after 7,000 cycles on average (Urban, Brunner, & Oldacre, 2021), while another indicated electrolyte degradation of 1% over 25 years (Stover, 2021) and > 100,000 cycles were reported with minimal electrolyte degradation (Sumitomo Electric Industries; Sumitomo Electric Industries).

The calendar life for stacks typically falls between 10–20 years, though most estimates place it in the middle of those two values (Aquino, Zuelch, & Koss, 2017; EASE, 2016; May, Davidson, & Monahov, 2018). Such numbers are overly simplistic since stack aging depends on the conditions the stack is subjected to. For example, if the electrolyte in the stack is fully charged, the stack components degrade faster (Brown, 2021). One developer reported replacing 20% of stacks after 10 years to meet agreed upon performance levels (Schoenfeldt, 2021), while another replaces all the stacks after 10 years (Brown, 2021). Stack calendar life depends on manufacturing quality control to ensure stack component tolerances are met. If the BMS does not measure individual cell voltages, out of tolerance stacks are replaced within the 25-year plant life. In some systems, stack design allows replacement of cells closer to the positive end of the stack where degradation is greater, thus allowing reuse of the remaining cells (Mittal, 2021). One developer reports no degradation after 5-6 years of use in the field, with accelerated tests²¹ estimating stack life of 25 years (Watson, 2021).

Pumps have a mean time before failure of 12–13 years but are typically replaced every 10 years as part of scheduled maintenance (Stover, 2021). The calendar life used in this report for RFB stacks is 12 years, after which stacks and pumps are replaced.

4.3.4.2 Round-trip Efficiency

To improve RTE, pumps with variable frequency drive are used. The batteries have two modes: standby and charge-discharge. During standby, the electrolyte flow is maintained at a very low level to ensure stack cells are wetted and ready to ramp in power as needed, thus reducing auxiliary power consumption, while during normal operation, electrolyte flow is maintained at a higher rate (Stover, 2021). Some developers during standby operate the pump once every 12 hours to ensure the stacks stay

²¹ Stacks are designed for one cycle per day to last 25 years or 9125 cycles. Accelerated testing involves cycling s for multiple cycles each day till the design 9125 cycles.

wet, again reducing auxiliary consumption (Brown, 2021). These result in DC-DC RTE excluding auxiliary consumption of 78–80% (Minopoli, 2021; Mittal, 2021) and system efficiency of 70% (SumiomoElectric Industries). In some instance, the DC-DC RTE includes auxiliary power consumption, and varies from 78–82%, the lower value corresponding to higher thermal load to cool the stacks (Watson, 2021).

The RTE for RFBs is assumed to be consistent with the RTE presented in the 2020 report at the DC-DC level. For the system AC-AC RTE, the 2020 report included the bidirectional inverter RTE, but did not include the transformer RTE; for this report, the transformer RTE is also included in system AC-AC RTE . Table 4.9 provides information on the conversion from DC-DC RTE to AC-AC RTE. The RTE used in this report for the final summary table, as well as the value used in the LCOS calculations, is the AC-AC RTE inclusive of inverter and transformer RTE.

Table 4.9. RFB DC-DC and AC-AC RTE Values

DC-DC RTE ^a		AC-AC RTE at Inverter Level ^b		AC-AC RTE at Transformer Level ^c	
2021	2030	2021	2030	2021	2030
71%	71%	68%	68%	65%	65%

^a Includes auxiliary power consumption and DC-DC converter RTE

^b Assumes a bidirectional inverter RTE of $(0.98)^2$

^c Assumes a transformer RTE of $(0.98)^2$

4.3.5 Results

Figure 4.10 and Figure 4.11 show the 2021 and 2030 total installed cost and performance parameters for 1 MW and 10 MW; 2-, 4-, 10-, and 24-hour systems; and the installed cost ranges for all power capacities and durations for vanadium RFB.

2021 & 2030 Vanadium Redox Flow
Installed Costs & Performance Parameters

		Storage System	1 MW								10 MW									
			2 hr		4 hr		10 hr		24 hr		2 hr		4 hr		10 hr		24 hr			
			2021	2030	2021	2030	2021	2030	2021	2030	2021	2030	2021	2030	2021	2030	2021	2030		
ESS Installed Cost	ESS	DC Storage Block (\$/kWh)	\$369.30	\$306.96	\$276.59	\$229.89	\$220.96	\$183.66	\$199.32	\$165.67	\$351.72	\$292.34	\$263.42	\$218.95	\$210.44	\$174.91	\$189.83	\$157.79		
		DC Storage BOS (\$/kWh)	\$73.86	\$55.15	\$55.32	\$41.31	\$44.19	\$33.00	\$39.86	\$29.77	\$70.34	\$52.53	\$52.68	\$39.34	\$42.09	\$31.43	\$37.97	\$28.35		
		Power Equipment (\$/kW)	\$154.86	\$137.00	\$154.86	\$137.00	\$154.86	\$137.00	\$154.86	\$137.00	\$133.00	\$117.65	\$133.00	\$117.65	\$133.00	\$117.65	\$133.00	\$117.65		
		C&C (\$/kW)	\$40.00	\$29.87	\$40.00	\$29.87	\$40.00	\$29.87	\$40.00	\$29.87	\$7.80	\$5.82	\$7.80	\$5.82	\$7.80	\$5.82	\$7.80	\$5.82		
		Systems Integration (\$/kWh)	\$79.59	\$67.53	\$56.34	\$47.81	\$42.40	\$35.97	\$36.97	\$31.37	\$73.58	\$62.43	\$52.55	\$44.59	\$39.93	\$33.88	\$35.03	\$29.72		
		EPC (\$/kWh)	\$93.03	\$78.93	\$65.54	\$55.61	\$49.05	\$41.62	\$42.64	\$36.18	\$84.91	\$72.04	\$60.58	\$51.40	\$45.98	\$39.01	\$40.30	\$34.20		
		Project Development (\$/kWh)	\$106.98	\$90.77	\$75.38	\$63.96	\$56.41	\$47.87	\$49.04	\$41.61	\$97.64	\$82.85	\$69.66	\$59.11	\$52.88	\$44.87	\$46.35	\$39.33		
		Grid Integration (\$/kW)	\$30.94	\$26.25	\$30.94	\$26.25	\$30.94	\$26.25	\$30.94	\$26.25	\$25.00	\$21.21	\$25.00	\$21.21	\$25.00	\$21.21	\$25.00	\$21.21		
		Total Installed Cost (\$/kWh)			\$835.66	\$695.90	\$585.62	\$486.85	\$435.59	\$361.42	\$377.25	\$312.65	\$761.08	\$634.53	\$540.34	\$449.55	\$407.89	\$338.57	\$356.39	\$295.41
		Total Installed Cost (\$/kW)			\$1,671	\$1,392	\$2,342	\$1,947	\$4,356	\$3,614	\$9,054	\$7,504	\$1,522	\$1,269	\$2,161	\$1,798	\$4,079	\$3,386	\$8,553	\$7,090
Operating Costs																				
Fixed O&M (\$/kW-yr)			\$5.60	\$4.99	\$7.50	\$6.60	\$13.19	\$11.43	\$26.48	\$22.70	\$4.85	\$4.49	\$6.66	\$6.03	\$12.08	\$10.63	\$24.73	\$21.36		
Decommissioning Costs																				
Recycling/Disposal (\$/kWh)			\$59.27	\$50.87	\$40.26	\$34.60	\$28.86	\$24.83	\$24.42	\$21.04	\$52.75	\$45.32	\$36.50	\$31.38	\$26.74	\$23.02	\$22.95	\$19.77		
Performance Parameters																				
RTE (%)			65%	65%	65%	65%	65%	65%	65%	65%	65%	65%	65%	65%	65%	65%	65%			
Cycle Life (#)			Unlimited		Unlimited		Unlimited		Unlimited		Unlimited		Unlimited		Unlimited		Unlimited			
Calendar Life (yrs)			12	12	12	12	12	12	12	12	12	12	12	12	12	12	12			
DOD (%)			80%	80%	80%	80%	80%	80%	80%	80%	80%	80%	80%	80%	80%	80%	80%			

Figure 4.10. 2021 and 2030 Installed Costs and Performance Parameters – Vanadium RFB

Total Installed Cost (\$/kWh) Ranges - Vanadium Redox Flow

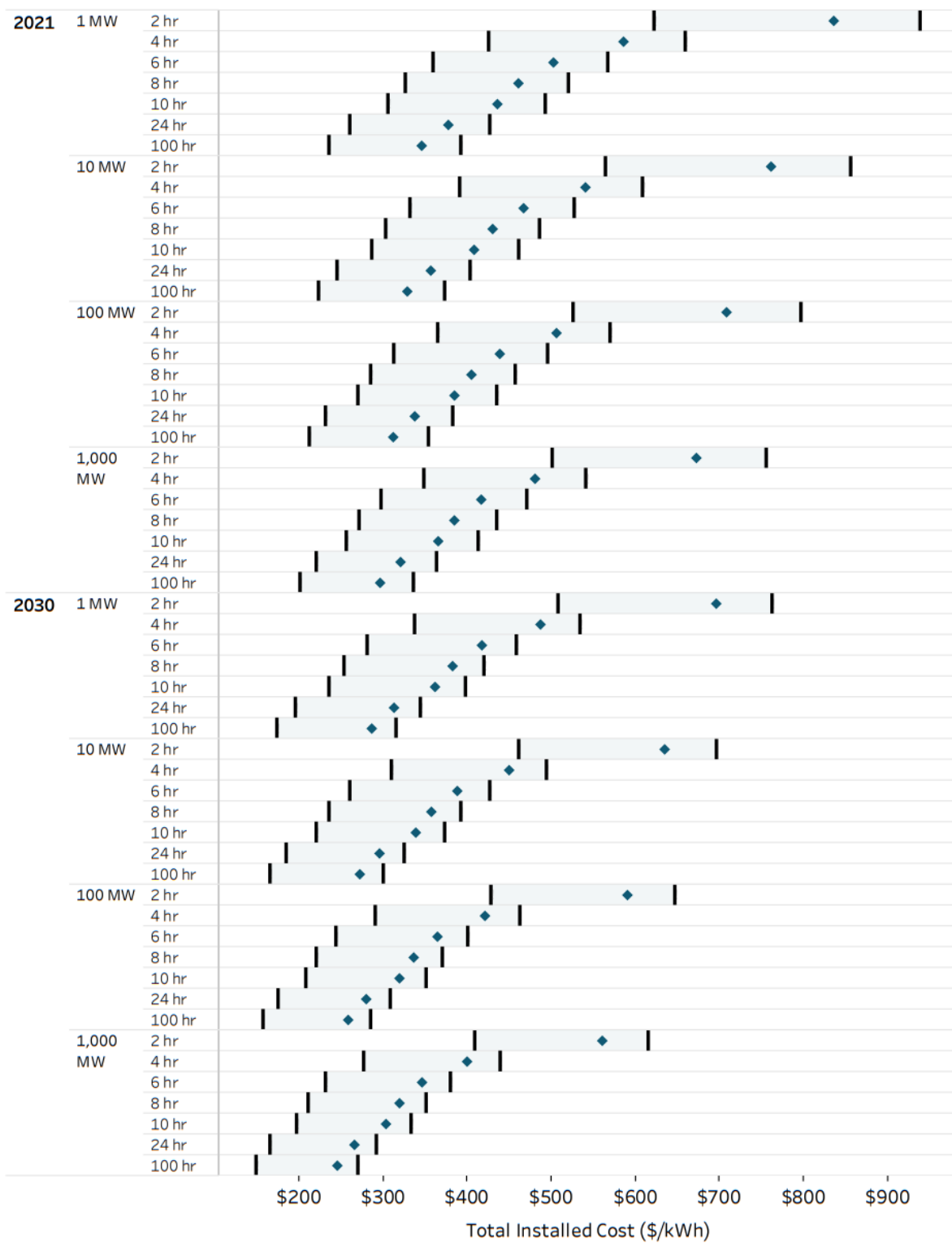


Figure 4.11. 2021 and 2030 Total Installed Costs Ranges – Vanadium RFB

4.4 Zinc-Based Batteries

There are several technologies and configurations that employ metallic zinc as the battery anode. For this study, four zinc-based technologies were analyzed: nickel-zinc (Ni-Zn), zinc-bromine (in flow and static designs), and zinc-air. The component costs and performance were analyzed for each technology based on developer specifications with additional projections made to match the power and duration targets for this study. High-level details on developer-provided information for the zinc technologies are given below:

- Ni-Zn – one developer-provided information for 2 hours, another for 2 and 4 hours, while a third developer-provided information for 2-100 hours.
- Zinc-bromine (flow) – information was available only from one developer at the 4-hour rate.
- Zinc-bromine (nonflow) – information was available only from one developer at the 4-hour rate. The same unit energy cost was applicable for 3-12 hour durations as well.
- Zinc-air – information was available only from one developer for 8-100 hour duration.

Since most zinc-based manufacturers have not deployed systems rated at > 10 MW, the study for zinc-based technology is limited to 10 MW.

Due to the significant differences among the zinc technologies considered, the available information from developers on cost, O&M, and performance have a wide range. While for the BESS technologies addressed in Phase 1, this work has used a nominal scaling factor for higher power and energy content, for zinc-based technologies, due to data provided by most developers restricted to only one or two durations, this scaling factor is not applied, with data provided by each vendor for various durations retained as is.

A new trend in the Ni-Zn industry is to leverage lead-acid manufacturing efficiencies and use equipment and plants designed for lead-acid manufacture. This involves investment by lead-acid equipment manufacturers in Ni-Zn manufacturing (International, 2021) and Ni-Zn manufacturers actively seeking out lead-acid plants for Ni-Zn manufacturing (Burz, Macher, & Baker, 2021). There is potential to use some of this equipment for other nonflow zinc-based chemistries as well.

4.4.1 Capital Cost

There is a wide range of DC SB capital cost, ranging from \$200/kWh to \$450/kWh. The cost decreased with increasing duration, mainly because at higher duration, the zinc-air flow battery costs were very low, at \$51/kWh for 100-hour duration. Where data from only one developer is available for one duration, the low and high costs are estimated using factors of 0.9 and 1.1, respectively.

While several products have DC voltages well below the operating range of ~600–800 volts DC for a standard 480 V AC bidirectional inverter, this study assumes no such voltage limitations (Anwer, Cowles, & Yadav, 2021), and uses power equipment costs corresponding to Li-ion ESS, without the use of DC-DC converter to boost the voltage.

Zinc-based batteries have lower footprint and weight than lead-acid and flow batteries while being on par in terms of safety, thus not requiring fire suppression systems. Thermal management is also

relatively simple, removing the need for heating, ventilation, and air conditioning (HVAC). Hence, system integration, EPC, and project development costs are estimated to be 90% of Li-ion BESS costs both in 2021 and 2030. Note that, except for one developer that provided EPC and project development cost, and another that provided project development cost, there was sparse information.

For levelized cost analysis, the low, high, and average values provided for each power and energy combination are used. High RTE, cycle, and calendar life are paired with low capital and O&M costs, and vice versa. Due to each developer within and across chemistries providing data for different durations at each power level, the capital cost, O&M, and LCOS results as a function of duration are not expected to follow a smooth profile.

For 2030 prices, one nickel-zinc developer anticipates a 50% price drop, a zinc-bromine developer anticipates a 59% price drop while a nickel-zinc developer anticipated a 6% price drop. As stated in Section 3, the learning rate approach is not used here due to the low levels of deployments, which can lead to unrealistically high-cost reductions even at low learning rates due to multiple doublings in deployment possible from a very low base. Due to the uncertainties in both anticipated deployments and the correct learning rate to use during the initial phase, this work assumes a 20% cost drop in DC SB, and a 10% drop in DC BOS cost, significantly lower than the corresponding numbers for Li-ion BESS at 35% and 25% respectively, due to the uncertainty in deployment of this technology. The power equipment cost assumed to be in line with Li-ion BESS. The RTE is increased by 4 percentage points with a 10% increase in cycle life.

4.4.1.1 Nickel-Zinc

The basic Ni-Zn battery consists of a metallic zinc anode, potassium hydroxide electrolyte, and a nickel-based cathode. The open circuit voltage of the electrochemical couple is 1.73 volts. For the DC SB, the technology is able to utilize traditional lead-acid manufacturing methods and formats, e.g., Group 31²² (Battery Equivalents; Plautz, 2021) for the basic cell and module construction. The BOS consists of container, cables, disconnect switches, circuit breaker. A typical configuration has the cells and modules housed in racks in a standard shipping container with HVAC, with rack cost including cables.

Most Ni-Zn systems being developed today are rated for 2–4 hour discharge durations with power ratings ranging from 100 kW to 1 MW (Burz et al., 2021; Eguchi, 2021; Plautz, 2021). The power equipment cost is assumed to be the same as for Li-ion BESS. Due to the high safety of this system, systems integration, EPC, and project development costs are assumed to be 90% of corresponding costs for a Li-ion BESS. Use of a ceramic separator further adds to safety (Eguchi, 2021). It should be noted that for smaller scale commercial systems (e.g., 100 kW, 200 kWh), an additional PCS cost may be added in the form of a DC-DC converter to increase the battery output voltage to the threshold needed for bidirectional 480-volt AC inverters.

Note that the largest N-Zn battery is at the module level, with no pilot-scale testing or demonstrations conducted. Hence these costs have not been validated through real grid-scale system deployment and testing.

As stated earlier, for 2030, this report assumes a 20% cost drop in DC SB and a 10% drop in DC BOS cost, while power equipment costs are maintained the same as for a Li-ion BESS for both 2021 and 2030.

²² Group 31 refers to the specific physical dimension (e.g. ~13 x 6.8 x 9.44 inches) of the battery format. Group 31 batteries are one of the most common formats and are used in transportation and off-the-grid applications.

System integration, EPC, and project development costs are maintained at 90% of corresponding costs for a Li-ion BESS for 2020 and 2030.

Table 4.10 shows composite capital costs by component for Ni-Zn systems for 2021.

Table 4.10. Composite Ni-Zn Capital Costs, 2021

Cost Component	Value	Source
SB (\$/kWh)	197-450	Burz et al. (2021); Eguchi (2021); Plautz (2021)
BOS (\$/kWh)	30-50	
Power Equipment (\$/kW)	200-300 ^a	
C&C	\$100/kW, \$25/kWh	
System Integration (\$/kWh)	100	Eguchi (2021)
EPC (\$/kWh)	50	
Project Development (\$/kWh)	50	
Grid Integration (\$/kW)	100	

^a\$300/kW includes transformer costs.

4.4.1.2 Zinc-Bromine For example

Zinc-bromine technology has a relatively high technology readiness level (TRL),²³ with 2-4 MWh systems currently being built (Hickey, 2021) or deployed as pilot systems (Richey, 2021). The DC SB cost ranges from \$190–346/kWh, while the DC BOS cost ranges from \$50–95/kWh, the higher cost corresponding to the flow battery (Hickey, 2021) possibly due to BOP-related component costs such as pumps, pipes, and electrolyte tanks. The system architecture also varies, with the flow battery consisting of 48-volt DC repeat units connected in parallel, with a DC-DC converter used to interface with a bidirectional inverter. This results in a 40% higher cost for the power equipment. This architecture may be tied to mitigation of shunt current losses in flow battery systems. For this analysis, power equipment costs for Li-ion BESS was used for zinc-based technologies, with the assumption that the considerable work done to mitigate shunt current losses in RFBs can be leveraged. System integration, EPC, and project development costs were in a relatively tight range. System integration costs are especially low since the modules can be shipped at 0% SOC, avoiding safety issues. For this study, the costs for these categories are assigned 90% of Li-ion BESS costs due to the relative safety of these systems.

For 2030, the DC SB cost is reduced by 20% and BOS cost is reduced by 10%, while power equipment costs are maintained the same as for a Li-ion BESS. System integration, EPC, and project development costs are maintained at 90% of corresponding costs for a Li-ion BESS. The RTE is increased by 4 percentage points with a 10% increase in cycle life.

Table 4.11 shows composite 2021 cost performance results for 4-hour zinc-bromine ESSs (Hickey, 2021; Richey, 2021).

Table 4.11. Composite Zinc-Bromine Capital Costs, 4-hour Duration, 2021 Systems

Cost Component	Value
SB (\$/kWh)	190-346
BOS (\$/kWh)	50-95

²³ TRL is a metric used to quantify the maturity of a technology where more mature technologies correspond to higher values on a scale of 1 to 9.

Cost Component	Value
Power Equipment (\$/kW)	65-140
C&C (\$/kW)	30-50
System Integration (\$/kWh)	10-18
EPC (\$/kWh)	20-70
Project Development (\$/kWh)	20-25
Grid Integration (\$/kW)	30

4.4.1.3 Zinc-Air

The zinc-air battery system consists of two stacks, one for charge and one for discharge, and a tank to store electrolyte. During charge, the discharge zincate product is pumped to the charge stack, where zinc is loosely plated on the cathode and stripped off the electrode by continuous electrolyte flow (Solutions, 2020). The zinc regeneration has multiple zinc growth cycles followed by a flush to transfer the charged zinc particles to the storage tank. This occurs multiple times to fully convert the zincate particles to zinc. The cathode needs to be replaced at an estimated cost of \$200/kW after 20,000 hours of operation, with replacement simplified due to the modular nature of the cathode (Berron & Edley, 2021). Electrolyte slurry is stored in a tank and pumped to the discharge stack, with air scrubbed free of carbon dioxide fed to the cathode. The building block is 40 kW per system, with module voltage at 48-volt DC, similar to the zinc-bromine flow battery. Operation is at 60°C, offering potential for additional efficiency related to heat capture and use.

The DC SB consists of power stack, storage tank, and zinc regenerator stack, with the DC BOS comprising pumps (for slurry transfer), pipes, valves, thermal management system, containerization, and blowers for air feed to the fuel cell stack. The power equipment comprises a rectifier for charge and inverter for discharge. Due to the lack of cost data, the power equipment cost is assumed to be the same as for Li-ion BESS.

There have been no pilot plant scale or demonstrations done for this technology, with a 40 kW/160 kWh expected to be deployed in British Columbia and two 100 kW systems of durations 10 and 15 hours in New York state by the end of 2022 (Berron & Edley, 2021). Hence these costs have not been validated through real grid-scale system deployment and testing.

Cost information for a 10 MW system is shown in Table 4.12 (Berron & Edley, 2021). For the 1 MW and 10 MW systems, the same cost per kW is assumed, since the 40 MW manufacturing capacity planned for 2023 is set to manufacture regenerator and fuel cell stack module repeat units that can be strung together to form units with various rated power. For the longer term, the production capacity and unit storage system size are expected to increase to offer sufficient scaling related to cost reduction opportunities to enable a target cost drop to \$120/kWh at 8 hours. As discussed in the O&M section, the power stack cathode replacement cost at \$200/kW after 20,000 operating hours is included in the capital cost for our LCOS analysis.

Table 4.12. Capital Cost for 1MW and 10 MW Zinc-Air SB and BOS, 2021 Systems

Parameter	Proposed units			Value		
	Hours	8	10	24	48	100
Rated Power	MW	1 or 10				
DC SB cost	\$/kWh	208	174	94	66	51
DC BOS	\$/kWh	42	35	19	13	10

Parameter	Proposed units		Value			
2030 SB and BOS cost	\$/kWh	120 ^a				

^a2030 estimate is provided only for 8-hour duration.

Since the technology is at a pre-commercialization stage, information regarding system integration, EPC, and project development is not provided, and is assumed to be 90% of corresponding costs for Li-ion BESS.

By 2023, two 120 kW systems are expected to be deployed. Cost reductions for the year 2030 are anticipated from economies of scale, manufacturing efficiency, and performance improvement. For 2030, this report assumes a 20% cost drop in DC SB and a 10% drop in DC BOS cost, while power equipment costs are maintained the same as for a Li-ion BESS. System integration, EPC, and project development costs are maintained at 90% of corresponding costs for a Li-ion BESS. The RTE is increased by 4 percentage points with a 10% increase in cycle life.

4.4.1.4 Composite Zinc System

Four different zinc-based technologies were considered in this study. Since deployments > 10 MW are not yet common, the investigation was done for 1 and 10 MW systems. Data for Ni-Zn were available for 2 hours from one developer (Eguchi, 2021), while another provided data across the 2-100 hour regime (Burz et al., 2021), with costs about three times lower than that reported for zinc-based technology. The main drivers for this cost reduction appear to be use of the zinc wire foam as both current collector and active material (Burz et al., 2021), and leveraging lead-acid manufacturing plants and equipment to reduce production costs (Burz et al., 2021; Plautz, 2021). Data for zinc-bromine (flow and nonflow) systems were available for 4-hour duration, while zinc-air system data were available for ≥ 8 hours. This results in discontinuity of cost, O&M, and performance values across durations, lacking a smooth trend.

The zinc-bromine flow battery SB cost obtained from developers is close to twice that of the nonflow or static battery, while BOS was 50% higher, possibly due to greater complexity of the flow battery BOS and the fact that flow battery cost was provided only for 4-hour duration, where stack costs dominate SB cost. One reason for restricting the duration to 4 hours is that the zinc-bromine flow battery is a hybrid with the zinc electrode corresponding to a conventional battery, making it difficult to separate the power and energy components as one could in a conventional flow battery. In contrast, the zinc-air flow battery has separate stacks for discharge and charge, and a tank that stores the zinc/zincate particles at various SOCs. This offers the advantage of a conventional flow battery, with unit energy cost for the DC SB decreasing from \$208/kWh at the 8-hour duration to \$51/kWh at the 100-hour duration, with corresponding numbers for DC BOS at \$42/kWh and \$10/kWh. Where data from only one developer are available for one duration, the low and high costs are estimated using factors of 0.9 and 1.1.

Zinc-based systems are relatively safe due to nonflammability of the aqueous electrolyte; however, concentrated alkaline electrolyte can be hazardous (Klein & McLarnon, 1995), requiring adequate personal protection equipment. The established safety procedure followed for sealed and vented lead-acid batteries should be followed to ensure hydrogen and oxygen generated during charge and even at open circuit are vented away safely and not allowed to accumulate. Bromine, the charge product at the cathode of zinc-bromine batteries, is hazardous in liquid or gaseous state. However, bromine forms a low-soluble complex with complexing agents added to the electrolyte, reducing the amount of bromine in the aqueous electrolyte by one to two orders of magnitude (Butler, Eidler, Grimes, Klassen, & Miles,

1995). The low-soluble complex settles at the bottom of the electrolyte tank and is not in contact with the zinc electrode. Its low bromine vapor pressure further adds to safety.

The superior safety characteristics of zinc-based batteries are expected to reduce system integration, EPC, and project development costs. While a range of numbers was provided by the various developers, this work assumes these costs to be 90% of the corresponding costs for a Li-ion BESS.

Some developers provided power equipment costs, which was in the \$65–300/kW range. The wide range is due to different assumptions—some included cost of transformers (Eguchi, 2021), others assume PCS cost to be in line with Li-ion BESS (Hickey, 2021), and some used cost for a 125 kW PCS coupled with a DC-DC converter²⁴ leading to ~70% higher total cost than a Li-ion PCS (Hickey, 2021). This study uses Li-ion BESS power equipment cost for zinc-based technologies.

For 2030, the DC SB is reduced by 20% and BOS costs reduced by 10% from 2021 values, while power equipment costs are retained the same as for Li-ion BESS. System integration, EPC, and project development costs are maintained at 90% of Li-ion BESS 2030 values. The composite SB, BOS and total installed costs for 2021 and 2030 are shown in Table 4.13, Table 4.14, Table 4.15, Table 4.16, Table 4.17, and Table 4.18.

Table 4.13. Composite Zinc BESS SB Costs (\$/kWh) by Power Capacity and Duration, 2021

Technology	Power (MW)	Duration (h)	Ni-Zn	Zinc-Bromine		Zinc-air	Composite
				Flow	Nonflow		
1		2	197-450				197-450
		4	197	346	190		190-346
		6	197		190		190-197
		8	197		190	452	190-452
		10	197		190	425	190-425
		24	197			354	197-354
		100	197			315	197-315
10		2	197-450				197-450
		4	197	346	175		175-346
		6	197		175		175-197
		8	197		175	452	175-452
		10	197		175	425	175-452
		24	197			354	197-354
		100	197			315	197-315

Table 4.14. Composite Zinc BESS SB Costs (\$/kWh) by Power Capacity and Duration, 2030

Technology	Power (MW)	Duration (h)	Ni-Zn	Zinc-Bromine		Zinc-air	Composite
				Flow	Nonflow		
1		2	158-360				158-360
		4	158	277	152		152-277
		6	158		152		152-158
		8	158		152	362	152-362

²⁴ As reported by developers, zinc-bromine flow and zinc-air batteries have 48-volt DC modules connected in parallel, requiring DC-DC converters. This study assumes no such limitations exist, removing the need for a DC-DC converter.

Technology		Ni-Zn	Zinc-Bromine		Zinc-air	Composite
Power (MW)	Duration (h)		Flow	Nonflow		
	10	158		152	340	152-340
	24	158			283	197-354
	100	158			252	158-252
10	2	158-360				158-360
	4	158	277	140		140-277
	6	158		140		140-158
	8	158		140	362	140-362
	10	158		140	340	140-340
	24	158			283	158-283
	100	158			252	158-252

Table 4.15. Composite Zinc BESS SBOS Costs (\$/kWh) by Power Capacity and Duration, 2021

Technology		Ni-Zn	Zinc-Bromine		Zinc-air	Composite
Power (MW)	Duration (h)		Flow	Nonflow		
1	2	30-50				30-50
	4	30	78	50		30-78
	6	30		50		30-50
	8	30		50	42	30-50
	10	30		50	35	30-50
	24	30			19	19-30
	100	30			10	10-30
10	2	30-50				30-50
	4	30	78	28		28-78
	6	30		28		28-30
	8	30		28	42	28-42
	10	30		28	35	28-35
	24	30			19	19-30
	100	30			10	10-30

Table 4.16. Zinc BESS SBOS Costs (\$/kWh) by Power Capacity and Duration, 2030

Technology		Ni-Zn	Zinc-Bromine		Zinc-air	Composite
Power (MW)	Duration (h)		Flow	Nonflow		
1	2	27-45				27-45
	4	27	70	45		27-70
	6	27		45		27-45
	8	27		45	38	27-45
	10	27		45	32	10-45
	24	27			17	17-27
	100	27			9	9-27
10	2	27-45				27-45
	4	27	70	25		25-70
	6	27		25		25-27
	8	27		25	38	25-38
	10	27		25	32	25-32

	24	27			17	17-27
	100	27			9	9-27

Table 4.17. Composite Zinc BESS Total Installed Costs (\$/kWh) by Power Capacity and Duration, 2021

Technology		Ni-Zn	Zinc-Bromine		Zinc-air	Composite
Power (MW)	Duration (h)		Flow	Nonflow		
1	2	494-767				494-767
	4	432	629	445		432-629
	6	411		424		411-424
	8	400		413	667	400-627
	10	394		407	627	394-627
	24	377			523	377-523
	100	365			463	365-463
10	2	450				450-767
	4	407	603	398		398-603
	6	392		383		383-392
	8	384		375	667	375-667
	10	379		370	627	370-627
	24	367			523	367-523
	100				463	463

Table 4.18. Composite Zinc BESS Total Installed Costs (\$/kWh) by Power Capacity and Duration, 2030

Technology		Ni-Zn	Zinc-Bromine		Zinc-air	Composite
Power (MW)	Duration (h)		Flow	Nonflow		
1	2	355-575				355-575
	4	337	499	349		337-499
	6	329		341		329-341
	8	323		335	538	323-538
	10	321		333	508	321-508
	24	314			429	314-429
	100	308			384	308-384
10	2	336-556				336-556
	4	322	484	302		302-484
	6	317		297		297-317
	8	312		292	527	292-527
	10	311		291	498	291-498
	24	305			420	305-420
	100	300			376	300-376

4.4.2 Operating Costs

The O&M costs are in line with costs for other battery technologies, in the \$10–60/kW-year range for the 2–100 hour duration. At the low end, the nonflow zinc-bromine technology DC SB and BOS has an O&M cost of \$0.5/kW-year for 4-hour duration due to the absence of pumps and HVAC which require regular maintenance. The only anticipated O&M tasks were changing air filters and fans once in 5 years.

The average of O&M costs at each duration was used for the point estimate. Where data from only one developer was available for one duration, the low and high costs were estimated using factors of 0.9 and 1.1, respectively. The 2030 O&M costs are assumed to drop by 15%, the same as the anticipated drop for Li-ion BESS O&M costs. The basis for this assumption is that, as deployments grow, some of the O&M procedures can be streamlined, with opportunity to learn from O&M practices in the Li-ion and lead-acid industry. While this makes the case for a higher percent reduction than Li-ion BESS, there needs to be some critical deployment threshold that has to be crossed before such streamlining-related benefits can accrue.

As with the previous battery technologies, an additional fixed O&M cost is added for major overhauls related to the power equipment at 30% of power equipment costs every 10 years.

4.4.2.1 Nickel-Zinc

O&M costs depend on rated power and energy as provided by the developers. The composite 2021 and 2030 fixed O&M cost for Ni-Zn systems is provided in Table 4.19.

Table 4.19. Composite Ni-Zn Fixed O&M Values, 2021 and 2030

Cost Component	Year	Value	Source
O&M Fixed (\$/kW-year)	2021	10	Eguchi (2021)
	2030	8.5	

4.4.2.2 Zinc-Bromine Systems

The O&M for zinc-bromine systems has a very wide range between \$0.50–\$44/kW-year, with the low end corresponding to the static system. Due to the absence of external auxiliary equipment such as pumps and HVAC, the only O&M tasks anticipated are replacement of air filters and fans every five years (Richey, 2021). The flow battery system, as expected, has higher O&M cost corresponding to 2.5% of direct capital costs, in line with reported O&M cost for zinc-bromine flow batteries of 2% of capital cost (Sapient, 2020).

The composite 2021 fixed O&M cost for zinc-bromine systems is provided in Table 4.20 (Sapient, 2020).

Table 4.20. Composite Zinc-Bromine Fixed O&M Values, 2021 and 2030

Cost Component	Year	Value
O&M Fixed (\$/kW-year)	2021	0.5-44
	2030	0.425-38

4.4.2.3 Zinc-Air

O&M costs are provided as fixed and variable (Berron & Edley, 2021). Fixed O&M costs consider overhaul costs for periodic maintenance (labor) and replacement of pumps with a maximum useful lifetime of 10 years. The fixed O&M cost is assigned as 1% of the SB and BOS cost, and ranges from \$20/kW-year at 8 hours to \$61/kW-year at 100 hours. This does not fully take advantage of the fact that most of the fixed O&M cost is allocated to labor, offering opportunity for cost reductions for systems with greater power and energy content.

The zinc-air system has a 25-year lifetime, corresponding to ~9,000 cycles at one cycle per day, with cathode replacement of the discharge fuel stack after 20,000 hours of operation. The replacement cost for the cathode amounts to \$0.01/kWh, which is the variable O&M cost, calculated based on \$200/kW for cathode replacement, and 20,000 hours of operation. For this report, the cathode replacement cost has been included in the upfront capital costs for the zinc-air systems of 8 hour durations or greater. Depending on the energy-to-power ratio, the annual discharge operating hours change slightly, thus affecting the replacement intervals. Since the project lifetime is set to 20–25 years for this analysis, the cost of SB replacement, excluding discharge fuel stack cathode, is not included.

Fixed O&M costs for zinc-air systems are shown in Table 4.21.

Table 4.21. Zinc-air Fixed O&M Values, 2021 and 2030

Cost Component	Year	Value
O&M Fixed (\$/kW-year)	2021	20-61
	2030	17-52

4.4.2.4 Composite Zinc System

O&M costs for zinc systems range from a very low cost of \$0.50/kW-year (Richey, 2021) to a high of \$42.5/kW-year for zinc-bromine 4-hour RFBs (Hickey, 2021). Note that the zinc-air battery has an O&M cost of \$61/kW-year for the 100-hour system, which when converted to \$/kWh is a low \$0.60/kWh-year. Replacement costs for the cathode in the fuel cell stack for zinc-air technology are considered as capital cost expenditures and amount to \$0.01/kWh discharged. O&M costs for the year 2030 are assumed to be 85% of 2021 O&M costs as discussed earlier. Results for 2021 are shown in Table 4.22.

Table 4.22. Composite Zinc BESS Fixed O&M (\$/kW-year) Values by Power Capacity and Duration, 2021

Year	Technology Duration (h)	Ni-Zn	Zinc-Bromine		Zinc-air	Composite
			Flow	Nonflow		
2021	2	10				10
	4		42.4	0.5		0.5-43.4
	6					
	8				20	20
	10				21	21
	24				27	27
	100				61	61
2030	2	8.5				8.5
	4		36.0	0.43		0.4-36
	6					
	8				17	17
	10				17.9	17.9
	24				23	23
	100				51.9	51.9

4.4.3 Decommissioning Costs

4.4.3.1 Nickel-Zinc

The infrastructure in place for lead-acid battery recycling is a good model for Ni-Zn recycling, with metals recovery value of 25-30 cents per pound (Burz et al., 2021). Alternatives to energy-intensive pyrometallurgical processes such as hydrometallurgical processes reduce cost, carbon footprint while allowing recovering cobalt, in addition to nickel and zinc. Separation of the positive and negative electrodes for subsequent processing in separate streams further simplifies recovery (BG Materials, Undated; Materials; Plautz, 2021). Conversion of electrode current collectors, tabs, and terminals to nickel hydroxide adds to the value of the recycled product.

4.4.3.2 Zinc-Bromine

All older generations of battery modules have been recycled using an existing module recycling process (Hickey, 2021). The approach is similar to the one used in the Ni-Zn industry (BG Materials, Undated), with module disassembly, material separation into different streams, and processing/recycling of the titanium, plastic packaging, and electrolyte. Nearly all of the materials in a module are expected to be recovered, with the value from the reclaimed material expected to cover recycling cost. Specifically, zinc-bromine electrolyte recycling is a common process in the oil and gas industry, where it finds use due to its high density. Multiple companies are expected to reclaim, refurbish, and recycle end-of-life zinc-bromine solutions. Recovery of residual electrolyte is expected to pay for decommissioning costs (Hickey, 2021).

4.4.3.3 Zinc-Air

Zinc-air has a high-cost recovery at the end of life due to BOS components such as racks and piping (Berron & Edley, 2021). There is also some cost recovery from catalysts that would need to be replaced every 20,000 hours. Zinc and the electrolyte can be reused for the next system.

4.4.3.4 Composite Zinc System

There is growing experience in the area of decommissioning for zinc-based technologies (Hickey, 2021; Materials; Plautz, 2021; Richey, 2021). Regardless of the specific technology, material value recovered from recycling is expected to cover disposal costs (Hickey, 2021; Materials; Richey, 2021) and recover nearly 100% of the materials in some cases (Richey, 2021). Hydrometallurgical processes are less energy intensive than pyrometallurgical processes, while enabling recovery of cobalt, nickel, and zinc, with the cathode and anode separated and processed in separate streams processes (BG Materials, Undated). Zinc-bromine electrolyte leverages existing processes in the oil and gas industry for zinc-bromine solution recovery (Richey, 2021).

4.4.4 Performance Metrics

The RTE and cycle life for zinc systems have a wide range due to the diverse technologies included in this category. This is one of the main reasons the LCOS as a function of duration is not expected to be smooth for zinc-based energy storage.

4.4.4.1 Nickel-Zinc

Overall system efficiencies for Ni-Zn range between 71 and 88%,²⁵ with the high RTE corresponding to the ZAF system whose cells are designed for high-power UPS applications, with a DC-DC RTE of 95% (Plautz, 2021). The NGK battery RTE of 80% was provided for 2-hour duration, while the Enzinc battery RTE ranged from 71% for 2 hours to 83% for 10 hours or greater.

Cycle life for the Enzinc battery increased from 1,500 cycles for a 2-hour discharge rate to 2,000 cycles at the 8-hour and higher discharge durations. This may be due to the fact that at shorter discharge durations, the higher rate increases the operating temperature, leading to faster degradation rates. This shows there may be a benefit to using thermal management for low-duration applications. Calendar life was estimated at 15 years, which would require replacement of batteries within 15 years depending on their DOD. For 2030, the RTE is estimated to increase by 4 percentage points with a 10% increase in cycle life.

Composite nickel-zinc performance parameters are shown in Table 4.23.

Table 4.23. Composite Ni-Zn Performance Parameters, 2021 and 2030

Performance Metric	Year	Value	Source
RTE (%)	2021	71-88%	Burz et al. (2021); Eguchi (2021); Plautz (2021)
	2030	75-87%	
Cycle Life	2021	1,000-3,938 at 80% DOD	Burz et al. (2021); Eguchi (2021); Plautz (2021)
	2030	1,100-4,323 at 80% DOD	
Calendar Life (years)	2021	15	Eguchi (2021)
	2030	15	

4.4.4.2 Zinc-Bromine

The RTE is 65–75%, with cycle life of 3,650–5,000 cycles at 80% DOD. Just as for Ni-Zn technology, the cumulative energy throughput does not depend on DOD. The calendar life is in the 10–15 years range, with replacement done for flow batteries, while augmentation is an option for the Eos nonflow battery since its remaining energy decreases linearly up to a 50% of initial energy remaining. For 2030, the RTE is increased by 4 percentage points with a 10% increase in cycle life.

Composite zinc-bromine performance parameters are shown in Table 4.24.

Table 4.24. Composite Zinc-Bromine Performance Parameters, 2021 and 2030

Performance Metric	Year	Value	Source
RTE (%)	2021	65-75	Hickey (2021); Richey (2021)
	2030	69-79	
Cycle Life at 80% DOD	2021	3,650-5,000	Hickey (2021); Richey (2021)
	2030	4,015-5,500	
Calendar Life (years)	2021	10-15	Hickey (2021); Richey (2021)
	2030	10-15	

²⁵ In this work, the RTE of bidirectional inverter and transformer are set at 0.96 each, with a combined RTE of 0.92. Hence, the AC-AC RTE for the ZAF battery is estimated at $0.95 \times 0.92 = 0.88$.

4.4.4.3 Zinc-Air

The cycle life was 12,500 cycles at 100% DOD, with cumulative throughput unchanged at various DODs. The DC-DC RTE was 64%, including auxiliary losses, corresponding to AC-AC RTE of 59%. Since pumps and ancillary equipment draw the same power, RTE decreases for operation at low power levels, where the auxiliary power consumption is a high percent of charge and/or discharge power. The calendar life was 25 years in the 5-70°C range. For 2030, the RTE is increased by 4 percentage points, while cycle life is increased by 10%.

4.4.4.4 Composite Zinc System

Except for a Ni-Zn battery system using high-power cells with a DC-DC efficiency as high as 95% (translating to AC-AC RTE of 88%), the RTE was in a 65% (Hickey, 2021) to 80% (Eguchi, 2021) range for 2-to 6-hour durations. Cycle life has a wide range, from 1,000-4,000 cycles for Ni-Zn technology at 80% DOD to 4,500 cycles for zinc-bromine flow, 500 cycles for zinc-bromine nonflow and 12,500 cycles for zinc-air.

Cell design impacts RTE. The RTE for one Ni-Zn systems was 71% for a 2-hour system, increasing to 82% for an 8-hour duration (Burz et al., 2021), indicating that the design is more suitable for high energy, with lower RTE at high rate related to resistive losses. As expected, for this system cycle life also increased with duration, since higher resistive losses at low durations are expected to increase internal battery temperature, making a case for active thermal management at high rates (low durations). The zinc-air battery RTE and cycle life were constant in the 8–100 hour range at 64% and 12,500 cycles, respectively, possibly because at these low rates, there is not much room for improvement of electrochemical efficiency, and temperature-related degradation is not a factor.

Some developers provided DC-DC RTE, while other provided AC-AC RTE at the bidirectional inverter level. The RTE used in this report for the final summary table, as well as the value used in the LCOS calculations later, is the AC-AC RTE inclusive of inverter and transformer efficiency losses, with one-way efficiency for each being 0.98.

Regarding 2030 estimates, one developer expected cycle life to increase by 20 percentage points, while another developer expected RTE to increase by 7 percentage points. For the year 2030, we have set the cycle life to increase by 10% and the RTE to increase by 4 percentage points. Composite results for performance are provided in Table 4.25, Table 4.26, and Table 4.27.

Table 4.25. Composite Zinc BESS RTE (%) by Power Capacity and Duration, 2021 and 2030

Year	Technology Duration (h)	Ni-Zn	Zinc-Bromine		Zinc-air	Composite
			Flow	Nonflow		
2021	2	71-88				71-88
	4	75-88	65	75		75-88
	6	78				78
	8	82			59	59-82
	10	83			59	59-83
	24	83			59	59-83
	100	83			59	59-83
2030	2	75-92				75-92
	4	79-92	69	79		79-92

	6	82				82
	8	86			63	63-86
	10	87			63	63-86
	24	87			63	63-86
	100	87			63	63-86

Table 4.26. Composite Zinc BESS Cycle Life by Duration, 2021 and 2030

Year	Technology Duration (h)	Ni-Zn	Zinc-Bromine		Zinc-air	Composite
			Flow	Nonflow		
2021	2	1,000-1,700				1,000-1,700
	4	1,000-3,938	4,563	5,000		1,000-5,000
	6	2,000				2,000
	8	2,000			12,500	2,000-12,500
	10	2,000			12,500	2,000-12,500
	24	2,000			12,500	2000-12,500
	100	2,000			12,500	2,000-12,500
2030	2	1,100-1,870				1,100-1,870
	4	1,100-1,980	5,019	5,500		1,100-5,500
	6	2,200				2,200
	8	2,200			13,750	2,200-13,750
	10	2,200			13,750	2,200-13,750
	24	2,200			13,750	2,200-13,750
	100	2,200			13,750	2,200-13,750

Table 4.27. Composite Zinc BESS Calendar Life (years) by Duration, 2021 and 2030

Duration (h)	Ni-Zn	Zinc-Bromine		Zinc-air	Composite
		Flow	Nonflow		
2	15				15
4		10	15		10-15
6					
8				25	25
10				25	25
24				25	25
100				25	25

4.4.5 Results

Figure 4.12 and Figure 4.13 show the 2021 and 2030 total installed cost and performance parameters for 1 MW and 10 MW; 2-, 4-, 10-, and 24-hour systems; and the installed cost ranges for all power capacity and energy durations, respectively, for zinc-based batteries.

2021 & 2030 Zinc
Installed Costs & Performance Parameters

		Storage System	1 MW								10 MW							
			2 hr		4 hr		10 hr		24 hr		2 hr		4 hr		10 hr		24 hr	
			2021	2030	2021	2030	2021	2030	2021	2030	2021	2030	2021	2030	2021	2030	2021	2030
ESS Installed Cost	ESS	DC Storage Block (\$/kWh)	\$323.50	\$258.80	\$244.33	\$195.47	\$270.73	\$216.58	\$275.34	\$220.27	\$323.50	\$258.80	\$239.33	\$191.47	\$265.73	\$212.58	\$275.34	\$220.27
		DC Storage BOS (\$/kWh)	\$40.00	\$36.00	\$52.50	\$47.25	\$38.33	\$34.50	\$24.50	\$22.05	\$40.00	\$36.00	\$45.17	\$40.65	\$31.00	\$27.90	\$24.50	\$22.05
		Power Equipment (\$/kW)	\$84.65	\$74.88	\$84.65	\$74.88	\$84.65	\$74.88	\$84.65	\$74.88	\$73.05	\$64.62	\$73.05	\$64.62	\$73.05	\$64.62	\$73.05	\$64.62
		C&C (\$/kW)	\$40.01	\$29.87	\$40.01	\$29.87	\$40.01	\$29.87	\$40.01	\$29.87	\$7.75	\$5.78	\$7.75	\$5.78	\$7.75	\$5.78	\$7.75	\$5.78
		Systems Integration (\$/kWh)	\$50.91	\$43.19	\$45.15	\$38.31	\$41.28	\$35.02	\$39.36	\$33.39	\$46.45	\$39.42	\$41.99	\$35.63	\$38.92	\$33.02	\$37.33	\$31.67
		EPC (\$/kWh)	\$62.89	\$53.36	\$55.08	\$46.73	\$49.89	\$42.33	\$47.38	\$40.20	\$56.09	\$47.59	\$50.56	\$42.90	\$46.77	\$39.69	\$44.82	\$38.03
		Project Development (\$/kWh)	\$75.47	\$64.03	\$66.09	\$56.08	\$59.87	\$50.80	\$56.85	\$48.24	\$67.31	\$57.11	\$60.67	\$51.48	\$56.13	\$47.62	\$53.79	\$45.64
		Grid Integration (\$/kW)	\$30.94	\$26.25	\$30.94	\$26.25	\$30.94	\$26.25	\$30.94	\$26.25	\$24.81	\$21.05	\$24.81	\$21.05	\$24.81	\$21.05	\$24.81	\$21.05
		Total Installed Cost (\$/kWh)			\$630.57	\$520.89	\$502.05	\$416.58	\$475.67	\$392.34	\$449.91	\$369.61	\$586.16	\$484.65	\$464.13	\$384.99	\$449.11	\$369.96
Total Installed Cost (\$/kW)			\$1,261	\$1,042	\$2,008	\$1,666	\$4,757	\$3,923	\$10,798	\$8,871	\$1,172	\$969	\$1,857	\$1,540	\$4,491	\$3,700	\$10,564	\$8,675
Operating Costs																		
Fixed O&M (\$/kW-yr)			\$10.65	\$9.03	\$21.61	\$18.33	\$12.41	\$10.53	\$27.65	\$23.46	\$10.56	\$8.96	\$22.14	\$18.79	\$12.23	\$10.38	\$27.56	\$23.38
Performance Parameters																		
RTE (%)			79%	83%	74%	78%	70%	74%	69%	73%	72%	76%	69%	73%	70%	74%	69%	73%
Cycle Life (#)*			2,146	2,360	2,827	3,109	5,917	6,508	6,625	7,288	2,969	3,266	3,688	4,056	5,917	6,508	6,625	7,288
Calendar Life (yrs)			14	14	12	12	17	17	19	19	14	14	12	12	17	17	19	19
DOD (%)			80%	80%	80%	80%	80%	80%	80%	80%	80%	80%	80%	80%	80%	80%	80%	80%

* Cycle Life (#) represents available cycles until remaining energy is equivalent to average DOD (%).

Figure 4.12. 2021 and 2030 Installed Costs and Performance Parameters – Zinc

Total Installed Cost (\$/kWh) Ranges - Zinc

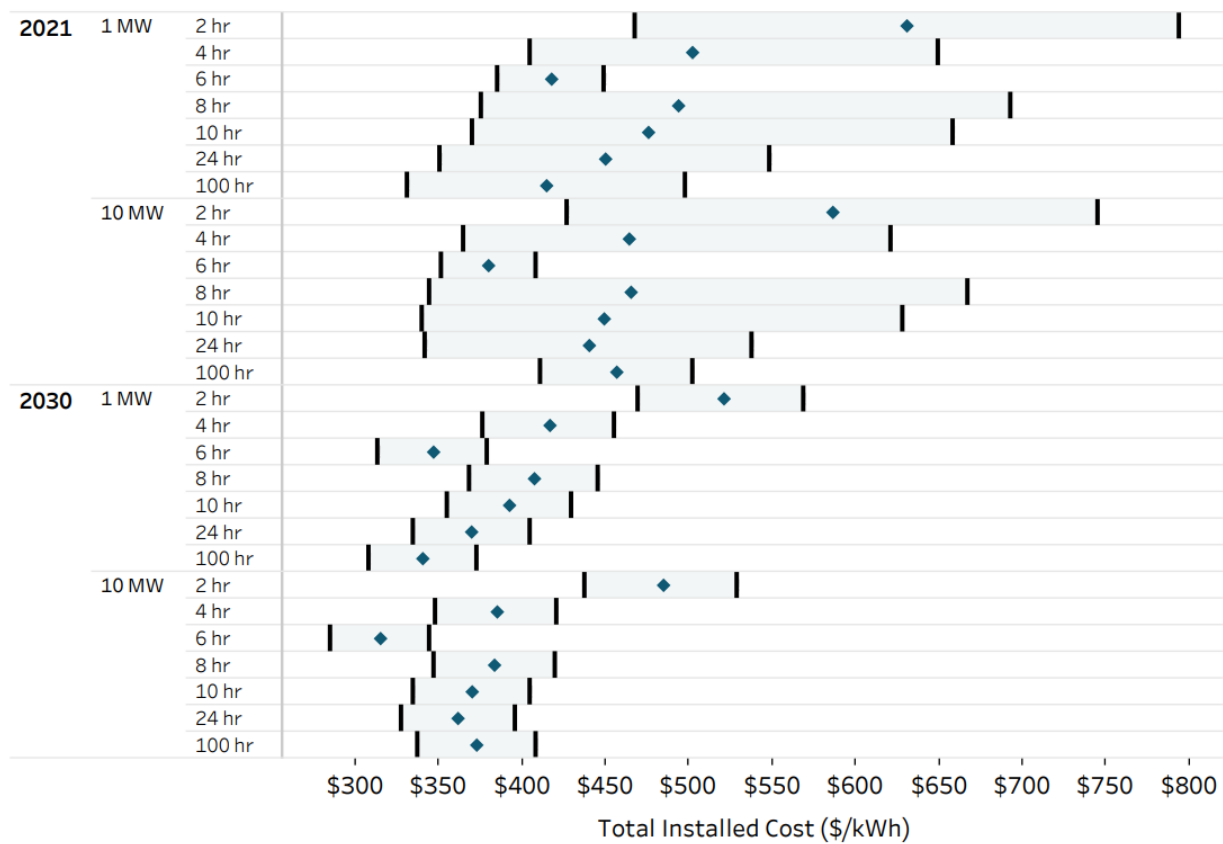


Figure 4.13. 2021 and 2030 Total Installed Costs Ranges – Zinc

4.5 Compressed-Air Energy Storage

CAES involves using electricity to compress air and store it in underground caverns. When electricity is needed, the compressed air is released and expands, passing through a turbine to generate electricity. There are various types of this technology including adiabatic systems and diabatic systems. The difference between these two configurations is that adiabatic systems capture and store the heat generated through the compression process to reuse later in the air expansion process in order to generate a larger amount of power output. For diabatic systems, the heat generated during compression is simply released. Newer applications of this technology include development of isothermal CAES. This technology removes heat across multiple stages of compression to reach a temperature closer to ambient, making it easier and more economic to store.

CAES is designed to fill markets where longer duration (12-24 hours) is needed. While CAES has been demonstrated to deliver longer duration storage, its cost effectiveness is limited by the availability and design of the caverns.

4.5.1 Capital Cost

No significant changes in cost were projected for CAES systems between 2020 and 2021. As a result, the majority of the cost and performance estimates remain the same as those provided in the 2020 report. The only capital cost update for CAES surrounds the cavern cost assumption. The fuel consumption for polymer electrolyte membrane (PEM) fuel cell system is estimated from its electrochemical efficiency of 0.507 (Hunter et al., 2021), its higher heating value of 285.8 kJ/mole (Harrison, Remick, Martin, & Hoskin, 2010), the thermoneutral potential for water decomposition of 1.482 V (Barbir, 2005), and a stoichiometric ratio of 1.3 for hydrogen (Scribner, 2017). Air consumption per kWh, along with CAES RTE were obtained from (Mongird et al., 2020b), using a molecular weight of 28.97 g/mole (Engineering ToolBox, 2014). It was determined that the required moles for air per unit energy generated for CAES is 3.39 times higher than the corresponding moles of hydrogen per unit energy. This improves upon the 2020 report assumption that the moles required would be equivalent for both air and hydrogen. However, in spite of hydrogen caverns being smaller for fixed-energy content, cavern cost per kWh of energy discharged for hydrogen can be slightly higher than for CAES due to the requirement of higher equipment grade (Howitt, 2021).

Unit energy costs were provided by different sources as shown in Table 4.28. While the first four data points are from (Mongird et al., 2020b), cost for the CAES cavern was estimated from total project costs at fixed power and various durations for adiabatic CAES, also referred to as green CAES, after subtracting costs for thermal storage, which was assigned 70% of the total cost of thermal storage and cavern (Howitt, 2021). The average cost of \$6.9/kWh was used as the single-point estimate, with low and high values of \$2.7/kWh and \$13.8/kWh, respectively.

The power island cost for adiabatic CAES was \$890/kW for a 40 MW system and \$725/kW for a 1,000 MW system, while that for a hydrogen CAES system was \$1,285/kW for a 75 MW system and \$540/kW for a 1,000 MW system (Howitt, 2021), with an average of \$860/kW, which is 75% of the sum of the power island and BOP used in the 2020 report. Considering that this difference may be assigned to BOP, which includes permitting, transmission interconnection, natural gas pipeline construction, and contingency, these numbers are considered sufficiently close to the 2020 report.

Table 4.28. Cavern Costs for CAES from Various Sources

Cavern Cost (\$/kWh)	Source
3.75	Baillie (2020)
4.3	Wright (2012)
2.7	Farley (2020)
10 ^a	
13.8	Howitt (2021)
6.9	Average

^a For bedded caverns

The scaling applied to CAES with respect to power capacity follows the same methodology as the 2020 report and is based on scaling for PSH given limited data availability. An assumption has been made that the drop in system cost with scaling for CAES is approximately half that of PSH at an 8% drop for every 10X increase in power, since PSH benefits more from scaling due to the nature of the excavation and requirements for underground powerhouse expansion. The scaling factor for various power levels was

determined by setting the 100 MW value to 1. For the CAES cavern, the scale was set to 1 for 800 MWh of storage based on data provided in the literature, with a similar 8% drop in cost for every ten times increase in storage MWh capacity (Davitti, 2018).

The 2020 report included power capacities of 100, 1000 and 10000 MW, while for this report, only 100 and 1000 MW have been included, to be in line with the power levels considered for PSH. In addition to the 4 and 10 hour durations provided in the 2020 report, the 2022 update includes 24- and 100-hour durations for both 2021 and 2030.

To determine the 2021 cost range, the powertrain-related costs are multiplied by 0.9 and 1.1, respectively, to get the low and high end of the cost range. For the cavern cost, the low and high values provided by the literature were assumed, \$2.7/kWh and \$13.8/kWh, respectively. No learning rates were assigned for year 2030 due to maturity of the technology related to powertrain and caverns.

4.5.2 Operating Costs

4.5.2.1 Fixed O&M

No substantial changes in operating costs for CAES were found between 2020 and 2021. The only adjustment included for this cost component is the inclusion of a storage-related fixed O&M cost, calculated at 0.43% of the difference in storage CAPEX (\$/kWh) required over 10 hours (14 hours for 24 hour systems). This adds an increase in fixed O&M cost of between \$0.09 and \$0.22/kW-year for 2021 for systems 24 hours and above. For the 4 hour system, a credit of <\$0.01/kW-year is added, given that the 10 hour system is the assumed baseline. In total, the fixed O&M for CAES is estimated to be \$16.12/kW-year for 100 MW systems and \$9.82/kW-year for 1,000 MW systems.

4.5.2.2 Warranty

No warranty information is included for CAES systems at this time. The limited number of CAES projects and the approach to constructing them as a civil engineering project rather than a manufactured item precludes robust warranty information being available.

4.5.3 Decommissioning Costs

Given the considerable calendar life of CAES systems, decommissioning costs are considered to be very small when considered in present value terms over 60 years or more. Often these costs are not considered upfront and limited information exists regarding estimations around decommissioning, deconstruction, or other teardown components. For these reasons, decommissioning costs for CAES are not currently considered in this phase of the analysis.

4.5.4 Performance Metrics

4.5.4.1 Calendar Life

The estimated calendar life for CAES has been extended from previous values to be 60 years in this report. The design life of building structures is typically stated as 50 years or more and the design life of large civil engineering structures is typically stated to be 100 years (Designing Buildings, 2021). The Huntorf CAES plant in Germany was constructed in 1971 and has reached 50 years of calendar life (Barbour, Undated).

4.5.4.2 Round-trip Efficiency

The RTE for CAES systems is assumed to remain consistent with the findings in the 2020 report at 52% for 2021 and 2030.

4.5.5 Results

Figure 4.14 and Figure 4.15 show the 2021 and 2030 total installed cost and performance parameters for 100 MW and 1,000 MW; 4-, 10-, 24-, and 100-hour systems; and the installed cost ranges for the above power capacity and durations, respectively, for CAES.

2021 & 2030 CAES
Installed Costs & Performance Parameters

ESS Installed Cost		ESS	Storage System	100 MW								1,000 MW							
				4 hr		10 hr		24 hr		100 hr		4 hr		10 hr		24 hr		100 hr	
				2021	2030	2021	2030	2021	2030	2021	2030	2021	2030	2021	2030	2021	2030	2021	2030
			Cavern Storage (\$/kWh)	\$7.05	\$7.05	\$6.84	\$6.84	\$6.64	\$6.64	\$6.31	\$6.31	\$6.52	\$6.52	\$6.31	\$6.31	\$6.11	\$6.11	\$5.78	\$5.78
			Turbine, Compressor, BOP, & EPC Management (\$/kW)	\$1,153	\$1,153	\$1,153	\$1,153	\$1,153	\$1,153	\$1,153	\$1,153	\$1,061	\$1,061	\$1,061	\$1,061	\$1,061	\$1,061	\$1,061	\$1,061
			Total Installed Cost (\$/kWh)	\$295.30	\$295.30	\$122.14	\$122.14	\$54.68	\$54.68	\$17.84	\$17.84	\$271.77	\$271.77	\$112.41	\$112.41	\$50.32	\$50.32	\$16.39	\$16.39
			Total Installed Cost (\$/kW)	\$1,181	\$1,181	\$1,221	\$1,221	\$1,312	\$1,312	\$1,784	\$1,784	\$1,087	\$1,087	\$1,124	\$1,124	\$1,208	\$1,208	\$1,639	\$1,639
Operating Costs																			
			Fixed O&M (\$/kW-yr)	\$16.11	\$16.11	\$16.12	\$16.12	\$16.22	\$16.22	\$18.56	\$18.56	\$9.82	\$9.82	\$9.82	\$9.82	\$9.83	\$9.83	\$10.04	\$10.04
Performance Parameters																			
			RTE (%)	52%	52%	52%	52%	52%	52%	52%	52%	52%	52%	52%	52%	52%	52%	52%	52%
			Cycle Life (#)	Unlimited		Unlimited		Unlimited		Unlimited		Unlimited		Unlimited		Unlimited		Unlimited	
			Calendar Life (yrs)	60	60	60	60	60	60	60	60	60	60	60	60	60	60	60	60
			DOD (%)	80%	80%	80%	80%	80%	80%	80%	80%	80%	80%	80%	80%	80%	80%	80%	80%

Figure 4.14. 2021 and 2030 Installed Costs and Performance Parameters – CAES

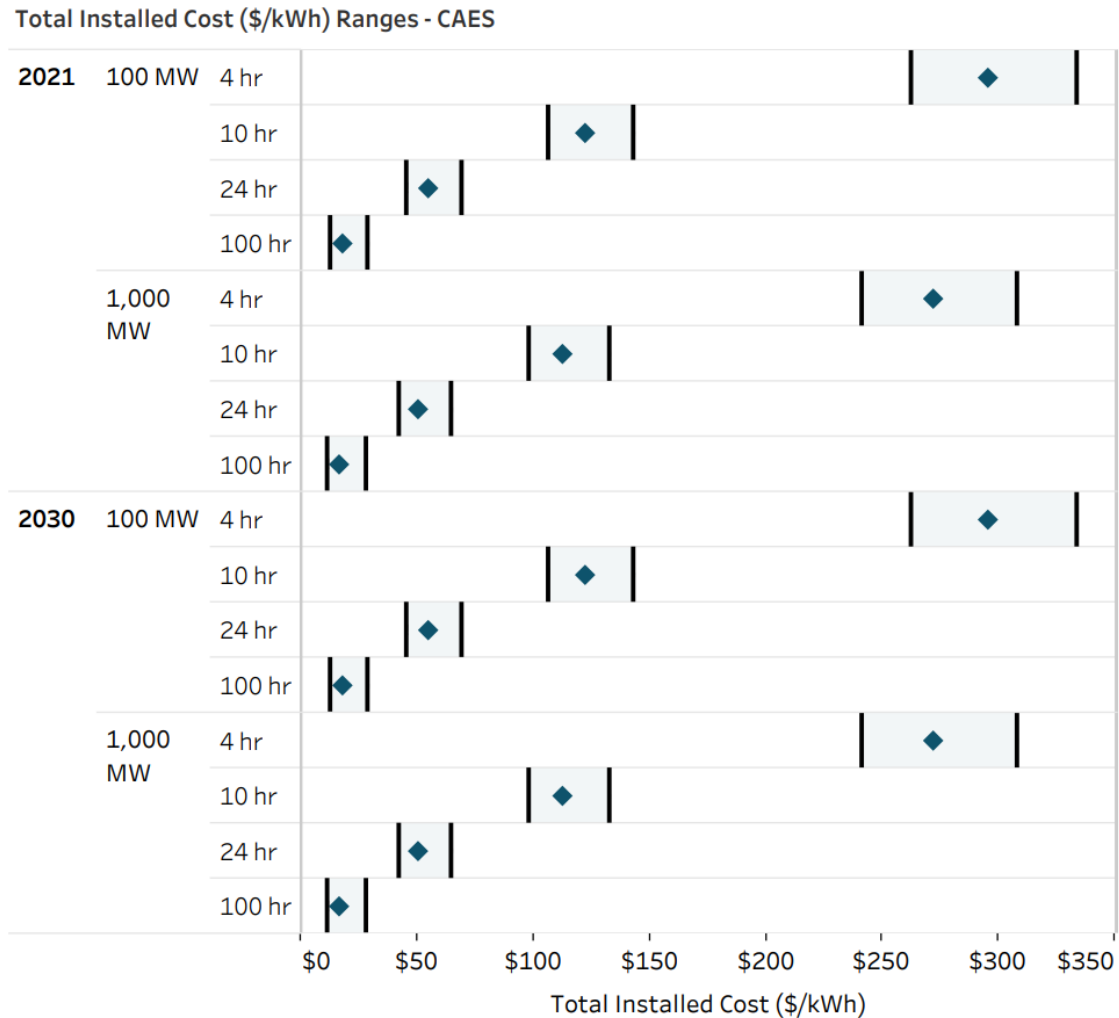


Figure 4.15. 2021 and 2030 Total Installed Costs Ranges – CAES

4.6 Pumped Storage Hydropower

As noted in the 2020 report, PSH is a mature technology that includes pumping water from a lower reservoir to a higher one where it is stored until needed. When released, water from the upper reservoir flows back down through a turbine and generates electricity. There are various configurations of this technology, including open loop (one or more of the reservoirs are connected to a natural body of water) and closed loop (reservoirs are separate from natural waterways). Existing turbine technologies also offer different features and capabilities, including fixed speed, advanced speed, and ternary.

4.6.1 Capital Cost

No significant changes were projected for PSH systems between 2020 and 2021. As a result, the majority of the cost and performance estimates remain the same as those provided previously.

Scaling with respect to MW capacity for PSH follows the same methodology as the 2020 report and was completed using data from Davitti (2018), with changes in scaling factor as described in the 2020 report. The scale factor was adjusted to reflect a 16% drop (instead of a 35% drop) in system cost in \$/kW for every 10X increase in power. The scaling factor for various power levels was determined by setting the 100 MW value to 1. As with the power-scaling factor, for the reservoir to be conservative, the scale was adjusted using data from Davitti (2018). Scale was set to 1 for 800 MWh of storage, with a 16% drop in cost for every 10X increase in storage MWh capacity. For PSH, the capital cost is multiplied by 0.9 and 1.1, respectively, to get the low and high end of the year 2021 cost range. No learning rates were assigned for year 2030 due to maturity of the technology related to powertrains.

In addition to the 4 and 10-hour durations provided in the 2020 report, the 2021 update includes 24- and 100-hour durations for 100 MW and 1,000 MW power capacity groups for both 2021 and 2030.

4.6.2 Operating Costs

4.6.2.1 Fixed O&M

The fixed O&M methodology follows that of the 2020 report but has included updated estimates with refurbishment-related costs and storage-related O&M. Fixed O&M defined by R. Miller (2020) and the National Hydropower Association (Manwaring, Mursch, & Erpenbeck, 2020) corresponds to yearly fixed-labor costs, while variable O&M corresponds to deep repair and refurbishments. However, both costs are related to labor, maintenance, and repair, and have been denoted as total fixed O&M in this study. The O&M costs are shown in Table 4.29. Note that labor costs are assumed to double for every 10X increase in power.

Table 4.29. PSH O&M Costs by Category for 10-hour Systems

Fixed O&M Component	100 MW System	1,000 MW System
Labor related (\$/kW-year)	\$15.75	\$3.15
Parts related (\$/kW-year)	\$5.59	\$5.59
Refurbishment related (\$/kW-year)	\$6.85	\$6.85
Total fixed O&M (\$/kW-year)	\$28.19	\$15.60

In addition to the above, storage-related fixed O&M has also been included. This amount is calculated in the same manner as described in the CAES section at 0.43% of the difference in storage CAPEX (reservoir construction and infrastructure [\$/kWh]) required over 10 hours (14 hours for 24 hour systems). The combination of labor related, parts related, refurbishment related, and storage-related O&M provides a fixed O&M cost range of approximately \$15-52/kW-year depending on power capacity and duration.

4.6.2.2 Warranty

No information for warranty is provided for PSH at this time. The limited number of PSH projects and the approach to constructing them as a civil engineering project rather than a manufactured item precludes robust warranty information being available.

4.6.3 Decommissioning Costs

Given the considerable calendar life of PSH systems, decommissioning costs are considered to be small when considered in present value terms over 60 years or more. Often these costs are not considered upfront and limited information exists regarding estimations around decommissioning, deconstruction, and other teardown components. For these reasons, decommissioning costs for PSH are not currently considered in this phase of the analysis.

4.6.4 Performance Metrics

4.6.4.1 Calendar Life

The estimated calendar life for PSH has been extended from previous values to be 60 years in this report. The design life of building structures is typically stated as 50 years or more and the design life of large civil engineering structures is typically stated to be 100 years (Designing Buildings, 2021). The design life of hydroelectric dams is typically assumed to be 100 years or more (EIA, 2021).

4.6.4.2 Round-trip Efficiency

RTE for PSH systems is assumed to remain consistent with the findings in the 2020 report at 80% for 2021 and 2030.

4.6.5 Results

Figure 4.16 and Figure 4.17 below show the 2021 and 2030 total installed cost and performance parameters for 100 MW and 1,000 MW; 4-hour and 10-hour systems; and the installed cost ranges for all durations, respectively, for PSH.

2021 & 2030 PSH
Installed Costs & Performance Parameters

		Storage System	100 MW				1,000 MW			
			4 hr		10 hr		4 hr		10 hr	
			2021	2030	2021	2030	2021	2030	2021	2030
ESS Installed Cost	ESS	Reservoir Construction & Infrastructure (\$/kWh)	\$81.00	\$81.00	\$76.00	\$76.00	\$68.00	\$68.00	\$64.00	\$64.00
		Powerhouse Construction & Infrastructure (\$/kW)	\$742.00	\$742.00	\$742.00	\$742.00	\$623.00	\$623.00	\$623.00	\$623.00
		Electromechanical (\$/kW)	\$467.00	\$467.00	\$467.00	\$467.00	\$392.00	\$392.00	\$392.00	\$392.00
		Contingency Fee (\$/kW)	\$511.00	\$511.00	\$656.33	\$656.33	\$429.00	\$429.00	\$551.67	\$551.67
		Total Installed Cost (\$/kWh)	\$511.00	\$511.00	\$262.53	\$262.53	\$429.00	\$429.00	\$220.67	\$220.67
		Total Installed Cost (\$/kW)	\$2,044	\$2,044	\$2,625	\$2,625	\$1,716	\$1,716	\$2,207	\$2,207
Operating Costs										
		Fixed O&M (\$/kW-yr)	\$28.10	\$28.10	\$28.19	\$28.19	\$15.58	\$15.58	\$15.59	\$15.59
Performance Parameters										
		RTE (%)	80%	80%	80%	80%	80%	80%	80%	80%
		Cycle Life (#)	Unlimited		Unlimited		Unlimited		Unlimited	
		Calendar Life (yrs)	60	60	60	60	60	60	60	60
		DOD (%)	80%	80%	80%	80%	80%	80%	80%	80%

Figure 4.16. 2021 and 2030 Installed Costs and Performance Parameters – PSH

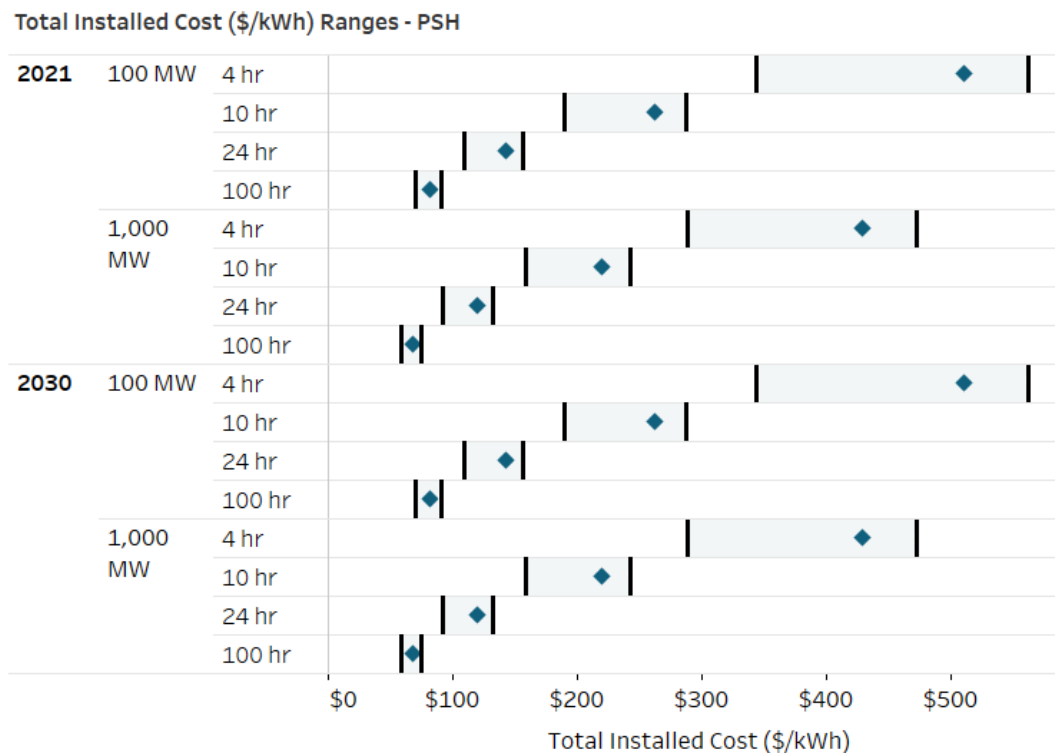


Figure 4.17. 2021 and 2030 Total Installed Costs Ranges – PSH

4.7 Gravity Energy Storage

Gravity-based ESSs can take many forms, from pressurized water that lifts a piston within a mined shaft to heavy bricks that are lifted by a crane to store energy. In each case, the stored energy is converted into kinetic energy that generates electricity using generators. The systems offer the potential for scalable energy outputs, for example doubling shaft depth increases stored energy content by a factor of four; whereas, for storage based on lifting heavy blocks, scaling with respect to energy is enabled by increasing the mass of each block. The different types of gravity ESSs covered in this section are:

- Heavy bricks lifted by cranes
- Rail-based gravity storage
- Pressurized water that lifts a heavy piston within a mined shaft with power equipment below ground
- Pressurized water that lifts a heavy piston within a mined shaft with power equipment above ground.

Gravity-based systems use stored gravitational potential energy for conversion to electricity via a generator. Energy is stored by lifting 35-ton concrete blocks using a six-arm crane powered by a motor during periods of excess electricity and electricity is generated by dropping the blocks with the motor running in reverse (John, 2019; Pedretti, 2021; Spector, 2018; Vault, 2021). The control software directs

smooth movement of the blocks considering wind conditions and inertia. A demonstration system has been running in Switzerland for a year, using a one-armed crane and 500 kg concrete blocks. The blocks are built on site using recycled building material with minimal fresh cement, keeping costs low while being environmentally viable. Per the specifications, this system has an RTE of 85–90%, a life of 30–40 years, responds within a few milliseconds, and ramps to maximum power in 2.5 seconds. The performance specifications are in line with Li-ion battery technology, while the life is two to three times higher.

Currently, 500-ton weights are used in existing mine shafts or custom-built shafts 150 to 1,500 m deep (Gravitricity, 2021), with power of 1–20 MW per shaft, and total energy content ranging from 8–192 MWh depending on the number of weights used per shaft. These weights are suspended by several cables that lift them during charge and drop them in a controlled manner during discharge. Efforts are ongoing to develop projects in Europe and South Africa using existing or custom-built shafts. The higher unit block weight lends itself to a smaller footprint, while movement of the blocks within a mineshaft offers protection from severe wind. A 250 kW demonstration unit has been commissioned using an aboveground 15 m high rig and has demonstrated a response time of 1 second from 0–100% of rated power (Gravitricity, 2021). The demonstration was completed, and the system was being decommissioned in July 2021 (Blair & Apps, 2021). An RTE of 85% and calendar life of 50 years is estimated (Gravitricity).

A 50 MW project is being developed on 20 acres in a gravel mine in Pahrump, Nevada (Storage, 2020). The project is expected to comprise of 10 multi-rail tracks, with 210 cars packed with material weighing 75,000 tons (Weed, 2021). The project targets frequency regulation and other ancillary services. Drive motors draw electricity from the grid to move the cars uphill and operate as generators when the cars descend. By increasing the number of cars, the energy content is increased. The system is scalable and ranges from 5 MW to 1 GW, with a duration of 15 minutes to 10 hours. The life is estimated at 40 years (Advanced Rail Energy Storage, Undated) with an RTE of 90% and response time of 10 and 17 seconds to full discharge and full charge, respectively (Weed, 2021).

Gravity Power (Santa Barbara, California) uses water pressure to hold a heavy piston weighing more than 8 million metric tons (Moore, 2021). When electricity is needed, the piston drops with pressurized water turning turbines and generating electricity. The piston height is set at half the shaft depth, while the distance moved along the shaft is equal to piston height. Thus, doubling shaft height increases stored energy content by a factor of four, lowering unit energy costs. A variation of this approach corresponds to piston height and diameter set equal to each other, with the distance moved along the shaft limited to half the piston height (Heindl Energy, 2021; Werner, 2021). Doubling the piston diameter results in stored energy increase by a factor of 16 (2^4). The power equipment in these technologies is similar to that used in PSH, the only difference being their location is either on the surface or underground. The RTE of these systems increases with system power capacity, as the pumps/turbines and motors/generators are more efficient at larger sizes and is in the 78.5–84% range with an estimated plant life of 60 years. These systems have not been commercially deployed or validated by a demonstration project. While the equipment used in these systems are commercially available, sealing of water within the shaft as the piston moves needs to be validated.

For this study, analysis was conducted for 100 MW and 1,000 MW systems of durations 2, 4, 6, 8, 10, 24 and 100 hours since the lowest power level for which data was provided was 50 MW.

4.7.1 Capital Cost

Cost information for various gravity-based storage systems was obtained directly from developers. For brick-based storage systems, cost and performance information was obtained for a single power output (10 MW) with two different energy outputs (40 and 2,40 MWh) (Terruzzin, 2021). From this information, costs were extrapolated for the various energy and power levels considered in this study by solving two linear equations. Note that the power equipment cost for the Energy Vault system is in line with the electromechanical powertrain cost for PSH due to location of the powertrain aboveground. Cost reduction for both components for an order of magnitude increase in power or energy at greater than a threshold of power and energy is provided (a 3% reduction in unit power cost at > 100 MW and a 3% reduction in unit energy cost at > 400 MWh).

Information on pressurized water or piston-based gravitational storage was obtained from two developers, with power equipment located either below ground or on the surface. For the system with power equipment located below ground, the energy component cost for a fixed duration of 8 hours at various power levels ranging from 125–1,250 MW in 125 MW increments was provided (Werner, 2021), from which energy costs are estimated at various energy levels by curve fitting. The power equipment was assumed to be the same as that of a PSH plant (the sum of electromechanical powertrain and powerhouse construction costs).

For the system with the powertrain located on the surface, the unit energy and power costs were provided for three power levels and two durations (50 MW, 4-hour, 200 MW, 8-hour, and 800 MW, 8-hour (Fiske, 2021), with curve fitting used to estimate unit power and energy costs for the 100 MW and 1,000 MW power levels and 2–100 hour duration. Note that while power costs were provided for 50, 200, and 800 MW, unit power cost reductions related to scaling occurs only up to power levels of 400 MW, since the largest pumps/turbines are rated at 400 MW (Fiske, 2021). Hence, curve fitting for unit power costs as a function of rated power was done using 400 MW as the power corresponding to unit power costs provided at 800 MW to estimate costs within the 50–400 MW range. Beyond 400 MW, unit power cost was kept constant. As expected, the power component costs were lower for the aboveground location of the powertrain.

One developer assigned a 10% fee on direct capital costs for planning and engineering (Werner, 2021), while the others did not provide estimates for this category. For this work, it is assumed that the EPC, project development, and grid integration costs are less than the 33% contingency fee typically used in PSH systems due to lower complexity of site selection and permitting and were set at 20% of direct costs.

For 2030, one developer estimates a 7% reduction per year in system cost (Terruzzin, 2021), while another estimates a 10% learning rate (Fiske, 2021), with an anticipated 8X increase in demand, corresponding to 73% of 2021 cost. As stated in Section 3, the learning rate approach is not used here due to the low levels of deployments, which can lead to unrealistically high-cost reductions even at low learning rates due to multiple doublings in deployment possible from a very low base. This work assigns a modest 15% cost reduction for 2030 for the SB and BOS, and no change for the power equipment, in line with our approach for PSH.

4.7.1.1 Brick-based Systems

Data was obtained from only one developer in this category (Terruzzin, 2021). The system consists of 35-ton blocks that are lifted using a six-arm crane powered by a motor during periods of excess electricity and arranged using software control (John, 2019; Pedretti, 2021; Spector, 2018; Vault, 2021). During discharge the blocks are lowered, converting their potential energy to kinetic energy using generators (motors running in reverse). Power scales with the number of arms in the crane, the size and number of motors/generators, and the speed at which the blocks are raised or lowered, while the energy scales with the weight and number of blocks, and the crane height. The blocks are made of composites of coal ash, fiberglass from decommissioned wind turbine blades, and waste tailings from mining processes. The building block for the system is a 10 MW unit ranging from 2–10 hours.

The stability of the fully charged system during high winds along with the impact of seismic events needs to be verified. Additionally, impact of high winds on crane stability needs to be considered (TECH, 2021).

Construction was completed on a commercial demonstration unit rated at 4 MW and 35 MWh in July 2020. This system is connected to Switzerland's national grid performing various grid services (Energy Vault, 2021).

Electricity is generated at 1,000 V AC,²⁶ with multiple systems connected electrically in parallel to increase power. While the developer did not provide costs for the energy and power blocks separately, the costs for a 4-hour system with rated energy of 400 MWh was < \$300/kWh, while for a 24-hour system with rated energy of 2,400 MWh, the cost was \$200/kWh. By setting the cost for 100 MW, 400 MWh and 100 MW, 2,400 MWh systems at \$300/kWh and \$200/kWh, respectively, the energy cost component is calculated to equal \$180/kWh, while the power component cost is estimated at \$480/kW.²⁷ For an order of magnitude increase in power or energy, a 3% reduction in energy cost is suggested for energy > 400 MWh and for power > 100 MW (Terruzzin, 2021).

4.7.1.2 Pressurized-Water Systems with Piston Moving Along Shaft

A deep shaft dug using standard mining techniques (Gravity Power, 2021) offers an opportunity to build the plant in urban areas as well due to low footprint. Retirement of existing powerplants offer the opportunity to retain a skilled workforce. The piston carved out of the existing rock structure reduces environment impact, as most of the material stays in place (Heindl Energy, 2021; Werner, 2021). The piston is sealed against the shaft wall by a rolling membrane that has been pressure tested at 160 bars (Heindl Energy, 2021; Werner, 2021) or a membrane seal that is fixed in place along the shaft wall (Gravity Power, 2021) to prevent shunting of water around the piston. Water pressure in the shaft is 70–80 bars at full charge (Heindl Energy, 2021; Werner, 2021).

The SB cost components consist of the piston and construction for the mined shaft that stores water at high pressure and along which the piston moves, while the BOS consists of valves and seals. The power equipment, similar to conventional PSH plants, consists of penstocks, pumps/turbines, and motors/generators, the largest size available being 400 MW (Fiske, 2021), with location aboveground (Fiske, 2021) or below ground (Heindl Energy, 2021; Werner, 2021).

²⁶ For this system, the transformer RTE needs to be accounted for to arrive at system AC-AC RTE at the distribution level.

²⁷ \$480/kW is close to the electromechanical cost for a PSH powerplant.

For the system with powertrain located below ground, the power equipment cost, which was not available, was assumed to be equal to that of a conventional PSH powerplant (\$1209/kW for 100 MW and \$1,015/kW for 1,000 MW). Cost information was provided for 8-hour systems of power levels ranging from 125–1,250 MW, along with data for piston weight, diameter (height is equal to diameter), water volume and peak pressure in the shaft, and total construction costs for the SB (Werner, 2021).²⁸ A power law was used to fit the unit energy cost data as a function of stored energy, with a cost range of \$140–\$373/kWh in the 1,000–10,000 MWh range. Note that the piston diameter equals its height and the distance traveled in the shaft is half the piston height, with stored energy proportional to d^4 , where d is the piston diameter.

For the system with power equipment located aboveground, to maximize stored energy, the piston height is set at half the depth of the shaft, with the distance the piston moves along the shaft equal to piston height (Fiske, 2021). For a constant shaft diameter, doubling the shaft depth doubles the height and weight of the piston, and doubles the distance the piston is lifted, producing four times the energy content. Since the excavation cost is roughly linear with shaft depth, doubling shaft depth increases shaft excavation cost by up to a factor of two while increasing energy content by a factor of four, halving the unit energy cost (Gravity Power, 2021). Cost/performance information for gravity powerplants rated at 50 MW/4 hours, 200 MW/8 hours, and 800 MW/8 hours are provided (Fiske, 2021). The energy costs drop from \$565/kWh at 200 MWh to \$207/kWh at 6,400 MWh. Similarly, the power equipment costs decrease from \$1,767/kW at 50 MW to \$410/kW at 800 MW.²⁹ Fitting the unit energy and power costs provided by power curves, corresponding costs were obtained for each power and duration considered in this study. Note that while power costs are provided for 50, 200, and 800 MW, since the largest pumps/turbines are rated at 400 MW, curve fitting was done using 400 MW as the power corresponding to \$410/kW, with the unit power cost kept constant beyond 400 MW rated power as explained in the Methodology section.

As a proxy for EPC fee, project development, and grid integration costs, a 10% contingency plus 5% underground design fee on the SB and a 10% contingency fee on the power equipment was estimated (Fiske, 2021). For this work, these costs are accounted for by applying a 20% markup to the sum of the SB, BOS, and power equipment costs, less than the 33% contingency for PSH since a Federal Energy Regulatory Commission hydro permit is not required. Table 4.30 shows capital costs for pressurized-water gravitational ESSs. The wide range of unit energy and power costs are related to scaling effects for both energy and power costs. These numbers need to be validated with a demonstration project. However, the pump/turbine & motor/generator equipment used is commercial, while mineshaft drilling is also an established process.

Table 4.30. 2021 Capital Costs for Pressurized-Water Gravitational Energy Storage

Cost Component (\$/kWh)	Value	Source
SB and SBOS	44-605	Fiske (2021); Heindl Energy (2021); Werner (2021)
Power Equipment	410-1,209	

²⁸ The diameter ranged from 163–290 m in the 1,000–10,000 MWh energy range, with corresponding weights of 9 and 51 tons and piston lift height ranging from 56–99 m.

²⁹ The decrease in unit power cost is attributed to turbine power being proportional to radius, while machining costs are linear with radius (Fiske, 2021).

Cost Component (\$/kWh)	Value	Source
EPC, Project Development, Grid Integration ^a	11-242	Fiske (2021)

^a It is unclear what the generated AC voltage is. May require a transformer to get to 12 kV distribution level.

Cost reductions by 2030 will depend on the learning rate and number of plants deployed. One of the developers suggested a 10% learning curve and estimates that between 2021 and 2030 three or four doublings in plant deployment could be achieved (Fiske, 2021). Thus, 2030 costs are expected to be 72.9% of the 2021 numbers for three doublings in demand. For this study, 2030 costs for gravity-based systems are set at 85% of 2021 costs due to uncertainties in deployments and the correct learning rate to use.

4.7.1.3 Composite Gravitational System

The final cost performance estimates for gravity-based systems are obtained by taking the average of values from the developers. In addition, for the LCOS study, the low-cost values were grouped with high RTE and calendar life and high-cost values with low RTE and calendar life to estimate low and high range of the LCOS values.

Power equipment costs, SB and BOS costs, and total installed costs are provided in Table 4.31, Table 4.32, and Table 4.33, respectively. Power equipment cost for the brick-based system is less than half that of the pressurized-water-based system cost at 100 MW (Table 4.31).

Table 4.31. Power Equipment Cost (\$/kW) for All Gravity Storage Technologies

Power (MW)	Heavy Bricks ^a	Pressurized Water with Underground Powertrain ^b	Pressurized Water with Aboveground Powertrain ^b	Average
100	480	1,209	1,042	910
1,000	466	1,015	410	630

^a Commercialization status: Demonstration completed

^b Commercialization status: No demonstration, uses commercialized equipment

At a fixed power, total installed costs decrease with increasing duration, decreasing from \$1,116/kWh at 2 hours to \$199/kWh for 100-hour duration at 100 MW (Table 4.33). For 1,000 MW, the corresponding numbers are \$663/kWh and \$130/kWh, respectively. Note that for the same energy content, costs for the two power levels are different. For example, the installed cost for a 100 MW, 100-hour system, at \$199/kWh, is lower than that for a 1,000 MW, 10h system (\$262/kWh). While the unit energy cost for SB and SBOS is the same, the power equipment cost is distributed over a longer duration, resulting in a lower \$/kWh contribution from the power equipment for the 100 MW, 100-hour case, in spite of the unit power cost being 35% higher for 100 MW. For similar reasons, the installed unit energy cost for a 100 MW, 24-hour system is less than half of that a 1,000 MW, 2-hour system. In summary, 100 MW gravity-based systems are attractive options at \geq 24-hour duration, while 1,000 MW systems are attractive at \geq 8-hour duration, with total installed cost of \sim \$300/kWh.

Table 4.32. SB and BOS Cost (\$/kWh) for All Gravity Storage Technologies.

Power (MW)	Duration (h)	Heavy Bricks	Pressurized Water with Underground Powertrain	Pressurized Water with Aboveground Powertrain	Average
100	2	180	712	534	475
	4	180	531	434	382
	6	175	447	385	335
	8	175	396	353	308
	10	175	360	330	288
	24	175	249	254	226
	100	175	136	166	159
1000	2	175	269	269	237
	4	175	200	219	198
	6	175	169	194	179
	8	175	149	178	167
	10	175	136	166	159
	24	175	94	128	132
	100	175	51	84	103

The energy cost component for brick-based systems is lower than that for pressurized water at rated energies < 7–9 GWh (Table 4.32). For these systems, the scaling effect with respect to energy is not as high as for pressurized water, for which energy scales with the fourth power of piston diameter when diameter equals height (Werner, 2021), or with the square of height for a fixed-piston diameter (Fiske, 2021). Due to higher scaling cost reductions for the SB and BOS for pressurized-water storage (Table 4.32), these systems become more cost effective as duration increases at fixed power. At 100 MW, the crossover duration is 85 hours (Table 4.33), beyond which pressurized water has the potential to be more cost effective. At 1,000 MW, the power equipment cost for the system with the powertrain located aboveground is close to that for the brick-based storage, while that for the system with the powertrain located underground is about two times higher. The crossover in total direct system cost for 1,000 MW occurs at a duration of 6 hours for the system with the aboveground powertrain and 12 hours for the systems with underground powertrain, below which the heavy brick-based storage system is more cost effective.

To determine low and high estimates for each 2021 capital cost component, the minimum, average, and maximum value for each power capacity and energy duration combination was taken from the data provided by the developers.

Table 4.33. Total Installed Cost (\$/kWh) for All Gravity Storage Technologies

Power (MW)	Duration (h)	Heavy Bricks	Pressurized Water with Underground Powertrain	Pressurized Water with Above Ground Powertrain	Average
100	2	504	1,579	1,266	1,116
	4	360	1,000	786	715
	6	306	778	633	572
	8	282	656	549	496
	10	267	577	495	446
	24	234	359	340	311
	100	215	178	203	199
1,000	2	489	931	568	663

	4	349	545	364	419
	6	303	406	298	335
	8	279	332	261	291
	10	265	285	236	262
	24	233	163	166	187
	100	215	74	101	130

For 2030 the SB and BOS cost is assumed to drop by 15% of 2021 costs, more conservative than the 27% drop estimated by a developer based on a 10% learning rate and three doublings in deployed volume, and more in line with the modest drops assigned for redox flow batteries and zinc-based batteries. This drop is assigned to development of lower cost bricks, optimization of piston diameter and shaft height, and development of methods for reliable sealing of the mined shafts. The power equipment cost, which consists of commercially equipment such as motors, generators, pumps and turbines, is assumed to be unchanged, in line with our approach for PSH and CAES, resulting in total system cost about 93% of 2021 cost for 100 MW, and 95% of 2021 cost for 2030 (Table 4.34).

Table 4.34. Composite Costs for Gravitational Storage, Year 2030

Power (MW)	Duration (h)	SB and BOS (\$/kWh)	Power Equipment (\$/kW)	EPC Fee, Project Development, Grid Integration (\$/kWh)	Total Installed Cost (\$/kWh)
100	2	404	910	172	1,042
	4	324	910	110	673
	6	285	910	87	535
	8	262	910	75	461
	10	245	910	67	414
	24	192	910	46	286
	100	135	910	29	184
1,000	2	202	630	103	631
	4	168	630	65	401
	6	152	630	51	319
	8	142	630	44	276
	10	135	630	40	248
	24	112	630	28	177
	100	88	630	19	123

4.7.2 Operating Costs

The O&M for piston-based storage with an underground powertrain has an estimated cost of 1.5% of capital costs (Werner, 2021), while O&M costs for system with aboveground powertrain are estimated to be less than that for a conventional PSH powerplant due to less complexity. The developer provided an estimate for PSH powerplant O&M costs as proxy for this system's O&M costs (Fiske, 2021). Note that the developer-estimated O&M cost of \$10.70/kW-year for 50–800 MW systems is less than the values of \$28.20/kW-year for 100 MW systems and \$15.60/kW-year for the 1,000 MW systems for PSH plants developed in this report. Therefore, for both piston-based systems, O&M costs developed for PSH in this report were used.

The O&M costs for various gravity technologies are shown in Table 4.35, with the last column showing composite numbers for 2021. For this study, the O&M cost for gravity-based storage systems is assumed to be equal to the average O&M costs for all three technologies.

Table 4.35. O&M Costs (\$/kW-year) for Various Gravity Technologies

Power (MW)	Duration (h)	Heavy Bricks	Pressurized Water with Underground Powertrain	Pressurized Water with Aboveground Powertrain	Composite (2021)
100	2	8	28	28	22
	4	12	28	28	23
	6	15	28	28	24
	8	19	28	28	25
	10	22	28	28	26
	24	47	28	28	34
	100	179	28	28	79
1000	2	8	16	16	13
	4	12	16	16	14
	6	15	16	16	15
	8	19	16	16	17
	10	22	16	16	18
	24	47	16	16	26
	100	179	16	16	70

Since gravity-based storage is still in the early stages of development, it is reasonable to expect some nominal decrease in O&M costs. One developer expected costs to decrease by 11% across all durations and power levels (Terruzzin, 2021). The O&M costs for 2030 were assumed to be 90% of 2021 costs.

4.7.3 Performance Parameters

Performance metrics were provided for gravity-based storage consisting of weights moved by a crane aboveground, cables located inside a mined shaft, and moving mass along an incline. For pressurized-water systems, these metrics were provided for systems with powertrain located above and below ground. The performance for gravitational storage at each power and duration was assigned the average of values provided by all developers for the corresponding power and durations.

4.7.3.1 Weight-based Systems

The RTE is estimated at 82% for brick-based systems (Terruzzin, 2021), 80–90% for weights moved along a mined shaft (Blair & Apps, 2021), and 90% for mass cars (Weed, 2021), for an average of 86%. The response time for this system is 1–17 seconds from 0–100% rated power, 1 second for weights moved along a shaft, 2.5 seconds for a brick-based system, 10 seconds to full discharge for mass cars, and 17 seconds to full charge for mass cars. There is no degradation expected with cycling, while the calendar life is estimated at 35–50 years. The composite performance parameters for weight-based gravitational storage is provided in Table 4.36.

Table 4.36. Composite Weight-based System Performance Parameters, 2021 and 2030

Performance Metric	Range	Average	Source
RTE (%)	80-90	86	Terruzzin (2021); Weed (2021); Blair and Apps (2021)
Response time (sec)	1-17	5.7	

Performance Metric	Range	Average	Source
Calendar Life (years)	35-50	41.7	Terruzzin (2021); Blair and Apps (2021)

4.7.3.2 Pressurized-Water Systems

While PSH plant discharge power decreases as water level in the upper reservoir decreases, this is not the case with the pressurized-water storage systems. The RTE was estimated to be constant at 80% across all power levels (Heindl Energy, 2017; Werner, 2021). While it is estimated to increase from 78.5% at 50 MW to 84% at 800 MW by another developer (Fiske, 2021), the increase is attributed to more efficient operation of pumps/turbines and motors/generators at higher rated power.³⁰ The dynamic response is expected to be slightly faster than that of a PSH plant of similar power output due to less inertia as a result of its shorter water conduits and the piston moving too slowly to contribute significantly to inertia (Fiske, 2021). The calendar life is assumed to be similar to PSH plants at 60 years (Fiske, 2021; Heindl Energy, 2017; Werner, 2021). Composite performance parameters for pressurized-water systems are presented in Table 4.37.

Table 4.37. Composite Pressurized-Water-based System Performance Parameters, 2021 and 2030

Performance Metric	Value	Source
RTE (%)	78.5-84 ^b	Fiske (2021); Heindl Energy (2021); Werner (2021)
Response time (s)	Slightly faster than PSH ^b	Fiske (2021)
Calendar life (years)	60	Fiske (2021); Heindl Energy (2021); Werner (2021)

^a RTE for 50 MW system is 78.5% and is 84% for 800 MW (Fiske, 2021). Average RTE is 81%.

^b PSH has response times from 5-500 seconds depending on scenario (e.g., shifting from shutdown to full load) and technology type (fixed speed, variable speed, or ternary). For the full list of response times see Mongird et al. (2020b).

4.7.3.3 Composite Gravitational System

To determine RTE and calendar life for the gravitational systems, the average was taken of values provided by various developers. No improvements in RTE or calendar life are assumed by 2030.

The RTE for all technologies is in the 80–90% range across all power levels and durations, with efficiency reported to be increasing with power levels by one developer (Fiske, 2021). For this study, an average efficiency of 83.4% at 100 MW and 84.4% at 1,000 MW is used. Calendar life for the weight-based system is estimated at 35–50 years, while for the piston-based systems is estimated to be the same as for PSH plants at 60 years, corresponding to an average of 49 years.

Composite performance parameters for gravitational storage are presented in Table 4.38.

Table 4.38. Composite Gravity Storage Performance Parameters, 2021 & 2030

Performance Metric	Value
RTE (%)	80-90 ^a
Response time (sec)	1-500 ^b
Calendar life (years)	49

^a Average of 83.4%.

^b 1–17 seconds for weight-based, 5–500 seconds for pressurized water.

³⁰ This increase in RTE likely applies to the other gravity technologies as well but has not been applied to them in this analysis.

4.7.4 Results

Figure 4.18 and Figure 4.19 show the 2021 and 2030 total installed cost and performance parameters for 100 MW and 1,000 MW; 4-, 10-, and 24-hour systems; and installed cost ranges for all durations, respectively, for gravity-based ESSs.

2021 & 2030 Gravitational
Installed Costs & Performance Parameters

ESS Installed Cost	ESS	Storage System	100 MW						1,000 MW					
			4 hr		10 hr		24 hr		4 hr		10 hr		24 hr	
			2021	2030	2021	2030	2021	2030	2021	2030	2021	2030	2021	2030
		Gravitational Capital (SB + BOS) (\$/kWh)	\$381.63	\$324.38	\$288.40	\$245.14	\$225.95	\$192.06	\$197.86	\$168.18	\$158.98	\$135.14	\$132.22	\$112.39
		Power Equipment (\$/kW)	\$910.34	\$910.34	\$910.34	\$910.34	\$910.34	\$910.34	\$630.20	\$630.20	\$630.20	\$630.20	\$630.20	\$630.20
		EPC Fee, Project Development & Grid Integration (\$/kWh)	\$121.84	\$110.39	\$75.89	\$67.24	\$52.78	\$46.00	\$71.08	\$65.15	\$44.40	\$39.63	\$31.70	\$27.73
		Total Installed Cost (\$/kWh)	\$731.05	\$662.36	\$455.32	\$403.41	\$316.66	\$275.99	\$426.49	\$390.88	\$266.41	\$237.79	\$190.17	\$166.37
		Total Installed Cost (\$/kW)	\$2,924	\$2,649	\$4,553	\$4,034	\$7,600	\$6,624	\$1,706	\$1,564	\$2,664	\$2,378	\$4,564	\$3,993
Operating Costs														
		Fixed O&M (\$/kW-yr)	\$22.80	\$20.52	\$26.22	\$23.60	\$34.37	\$30.93	\$14.28	\$12.96	\$17.77	\$16.04	\$25.92	\$23.37
Performance Parameters														
		RTE (%)	83%	83%	83%	83%	83%	83%	84%	84%	84%	84%	84%	84%
		Cycle Life (#)	Unlimited											
		Calendar Life (yrs)	49	49	49	49	49	49	49	49	49	49	49	49
		DOD (%)	80%	80%	80%	80%	80%	80%	80%	80%	80%	80%	80%	80%

Figure 4.18. 2021 and 2030 Installed Costs and Performance Parameters – Gravitational

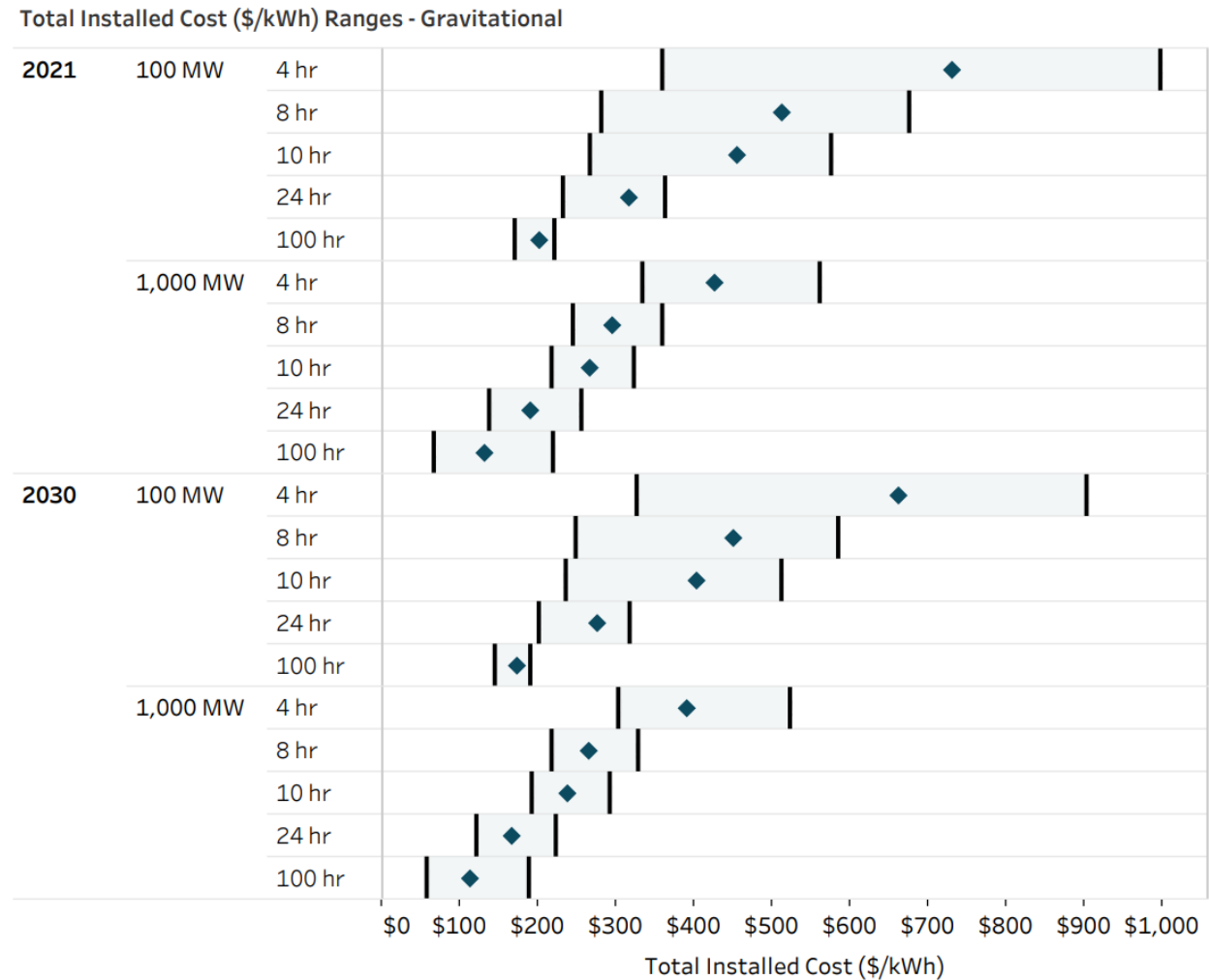


Figure 4.19. 2021 and 2030 Total Installed Costs Ranges – Gravitational

4.8 Thermal Energy Storage

Thermal energy storage comprises multiple pathways where the input and output energy is either heat or electricity. Conventional thermal storage uses concentrating solar-thermal power (CSP) to heat the storage media, which typically is a molten nitrate salt with composition 60 wt.% NaNO₃-40 wt.% KNO₃, also known as solar salt. Efforts are underway to use electrical resistive heating to replace CSP, with additional storage media considered such as crushed rock, sand, concrete, brick, or cast iron. Liquid air energy storage (LAES) involves liquefaction of air using a standard refrigeration cycle, followed by extracting stored energy by heating the liquid air, resulting in orders of magnitude higher volume, to generate electricity by driving a gas turbine.

The different types of thermal energy systems, based on how they are charge, are:

- Pumped heat energy storage (PHES) (AC in, AC out)

- Sensible heat-based thermal energy storage³¹ such as heat storage media such as molten salt, sand, concrete, thermal oil (AC in, AC out)
- LAES (AC in, AC out)
- Latent heat energy storage, which is in the applied research stage; no response was received from the developers contacted and it is not covered in this report³²
- Thermochemical energy storage, which is in the applied research stage and is not covered in this report.

All systems considered had electricity input and output. Charging is done by electricity input (heater for sensible heat, power for compressor for pumped heat storage, and power for refrigeration cycle for LAES) with an exception for some hybrid systems where fuel is also used. These additional hybrid systems, beyond CAES, are included to assess the cost and performance of molten salt and liquid air storage media integrated with gas turbines. A brief review of thermal energy storage technologies is presented and is by no means an exhaustive list of technology designs that have been proposed in the literature.

The total installed energy capacity of thermal storage was 234 GWh as of 2019, with space heating dominant, while molten-salt-based electricity storage had a 21 GWh share (IRENA, 2020) with the total numbers expected to grow to 850 GWh by 2030 at the high end, with molten-salt-based electricity storage assumed to dominate at roughly 630 GWh, of which 73 GWh are additional planned capacity, while additional deployments beyond planned capacity range from 55 to 540 GWh. While molten-salt-based storage is at the commercial stage, solid-state sensible heat (sand, concrete, rocks), high-temperature latent heat-based storage and LAES at the prototype/demonstration stage, and thermochemical storage are in the applied research stage.

Thermal storage for CSP is active where the storage medium flows between two tanks, or passive in a thermocline-type system, with a heat transfer fluid flowing through the stationary solid-state thermal energy storage medium such as concrete to exchange heat (Fernández et al., 2019). Note that all commercially deployed thermal energy storage systems for CSP are active. Active storage is direct when the storage medium also serves as the heat transfer fluid as is the case for solar tower power plants, whereas it is indirect when a synthetic oil heat transfer fluid exchanges heat with the storage medium in a heat exchanger.

Solar salt, consisting of a eutectic mixture of sodium and potassium nitrate, operates in the 290–565°C range, storing sensible heat at a capital cost of \$20–25/kWh thermal for solar salt storage media cost, (Abrams, Farzan, Lahiri, & Masiello, 2014; C. W. Forsberg, McDaniel, & Zohuri, 2021; Nunes, Queiros, Lourenco, Santos, & Castro, 2016). Temperature limits are set by the salt melting point and decomposition temperatures. The upper decomposition temperature limit may be extended by varying the salt composition and controlling gas composition over the storage tank. The hot salt is either sent directly to a steam generator or a heat transfer fluid is used to transfer heat from the salt to the steam

³¹ As explained later, the CSP is replaced with electrical heating.

³² Azelio, a Swedish developer, is actively commercially marketing a latent heat energy storage system and claims a few commercial sales.

generator. As part of a study summarizing three different pathways for DOE's Gen3 CSP roadmap, Mehos et al. (2017) describes ongoing work to develop a salt system consisting of chlorides of sodium, potassium, and magnesium with a melting point of 400°C and a decomposition temperature exceeding 1,000°C, with the operating temperature range of 500°C to 720°C (Augustine, Kesseli, & Turchi, 2020). Detailed cost breakdowns are also given for the salt and salt tanks. Note that chemically reducing conditions need to be maintained to avoid corrosion (C. Forsberg, Sabharwall, & Sowder, 2020). This chloride system was not selected to go forward for a MW-scale demonstration. However, the DOE is supporting a scaled down prototype of the chloride storage medium at the National Renewable Energy Laboratory.

Each tank has a foundation, pumps, and insulation and is instrumented to measure temperature, pressure, molten salt level, and flow rate (Bauer, Odenthal, & Bonk, 2021). The current maximum height and diameter are typically 13 m and 40 m, respectively, with storage capacity of up to 30,000 tonnes in a single tank. Research is focused on molten salts, tank design, pumps, valves, and instrumentation.

As of 2017, there were three solar tower power plants totaling 140 MW and one parabolic trough plant rated at 5 MW using solar salt as both heat transfer fluid and storage medium, also known as direct thermal storage, and 21 parabolic trough plants using a eutectic mixture of diphenyl and diphenyl oxide heating oil as heat transfer fluid and solar salt as storage medium (indirect thermal storage) with power rating in the 50-280 MW range (Fernández et al., 2019). This has grown to 12 tower projects and 34 parabolic trough projects (Kelly, 2021b). The National Renewable Energy Laboratory NREL maintains a database of operating plants (National Renewable Energy Laboratory, 2022).

The capital cost, excluding EPC management fee and project development costs for a 100 MW, 8-hour tower direct³³ thermal storage system after stripping off cost for CSP plant mirrors and towers was estimated at \$295/kWh, of which \$164/kWh (or \$1312/kW) corresponds to power block costs operating on a steam cycle (Lundy, 2020). This report provided total cost for the thermal energy storage system (which includes salt, tank, and pipe costs), BOP cost for foundation and support structure, 75% of which was assigned to tank foundation and support structure, BOP for the steam system, and BOP for the electrical, instrumentation, and controls (EIC). Note that no scaling relationship for the power block or SB was provided. **Error! Reference source not found.** shows the direct cost distribution for the various thermal energy storage components.

³³ For CSP, direct thermal storage uses solar salt storage medium as the heat transfer fluid, while indirect thermal storage uses a thermal oil as heat transfer fluid and a molten salt as storage medium

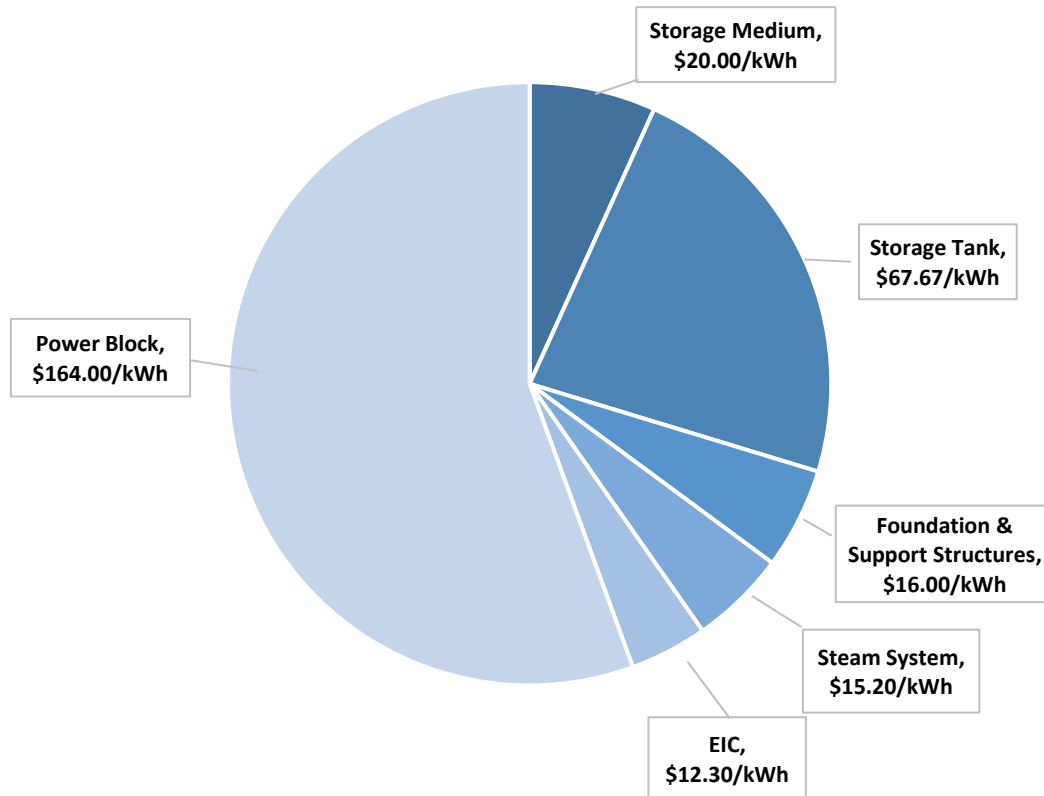


Figure 4.20 Distribution of capital costs for solar salt-based thermal energy storage for a 100 MW, 8 hour plant based on the steam cycle

Similar capital cost breakdown is not available for indirect storage systems; the first and largest indirect storage system being the 133 MW thermal, 1,000 MWh thermal Andasol plant in Spain using parabolic trough receivers and solar salt. However, storage medium and tank costs can be calculated by estimating the solar salt needed per kWh. Indirect storage has a ΔT of only 100°C, limited by thermal transfer fluid heating oil decomposition temperature of 390°C, and a heat-to-electricity efficiency of 35%, corresponding to 3.3 times the salt needs compared to directly heating the salt as in a central receiver tower. Hence, the storage medium and tank costs are expected to be 3.3 times the numbers provided in **Error! Reference source not found.** An alternative to solar salt is a eutectic mixture of potassium and sodium nitrate and sodium nitrite, widely used in the chemical process industry with the trade name HITEC®. It has a much wider operating range of 149-593°C (Coastal Chemical Co., 2022), with its lower melting point increasing the ΔT by a factor of 2.5, thus offering an opportunity to reduce capital for storage media, tank, pipes, and valves, along with O&M costs related to lower operating temperature range for these systems.

Cost savings of 34% may be possible by establishing a thermocline in a single molten salt tank system and substituting a bulk of the molten salt with low-cost crushed rock, with savings > 50% anticipated by a more complete utilization of the storage medium (Odenthal, Klasing, Knodler, Zunft, & Bauer, 2019), with a potential to reduce storage costs to \$10/kWh (C. W. Forsberg, 2020). However, scalability of this concept is yet to be tested. An alternate design replacing the single tank with a long trench filled with crushed rock with a storage capacity of 1 GWh per 10 m length (C. W. Forsberg, 2020) has the potential to drop costs further. Hot salt is fed at one end and collected in pans at the bottom, and fed to the next

section, thus establishing a thermocline. Modeling to develop design guidelines for integrating a concrete storage module with a CSP, with heat transfer fluid flowing through steel tubes is provided in (Salomoni et al., 2014). Note that thermocline-based storage has not been commercially deployed, related to thermocline degradation and associated impact on performance and utilization factor (Geissbühler, Mathur, Mularczyk, & Haselbacher, 2019a).

Thermocline degradation flattens the temperature gradients in the bed with increasing cycles, thus reducing the utilization factor for the storage medium. Numerical simulations showed that mixing of the heat transfer fluids from three ports along the height of a packed rock bed led to a 40% increase in utilization factor for molten salt as the heat transfer fluid, while a 73% increase was obtained for compressed air as heat transfer fluid for a dimensionless outflow temperature difference of 10% (Geissbühler, Mathur, Mularczyk, & Haselbacher, 2019b). Reduction in the dimensionless outflow temperature difference to 2.5% increased the corresponding utilization factors by 331% and 744%. Withdrawing or extracting the heat transfer fluid from the bottom and injecting to the top is not as effective as the mixing method. Other ways to mitigate thermocline degradation is by ensuring uniform heat transfer fluid flow, prevent axial mixing by maintaining laminar flow, and using a large height-to-diameter ratio for the tank (Ürlings & Pereira, 2020).

A 2x500 kWh_t “concrete-like” thermal storage pilot plant with Dowtherm-A heat transfer fluid was constructed and tested over two years, accumulating 6000 hours of operation without degradation of the storage medium, with good contact maintained between the medium and the heat exchange steel pipes, with charging done by electric heaters and discharge done using an air-cooled oil cooler (Hoivik et al., 2019). Progress toward commercialization is being made with a 3.1 MW_t single tank storage system using thermal oil as heat transfer and storage medium integrated with a 0.5 MWe power plant and parabolic trough solar collectors being constructed in Sao Paulo, Brazil (Ürlings & Pereira, 2020). Storing electricity in the form of thermal energy by electrical resistive heating of firebrick, cement, or concrete is under development, specifically related to providing peak power from a nuclear reactor (C. Forsberg, Stack, & McDaniel, 2021). Warm compressed air heated by waste heat produced by the reactor is further heated by thermal storage for peak electricity production via turbines, with heat transfer tubes embedded in bricks or concrete (Kelly, 2021a). The difference in thermal expansion coefficient between steel and concrete increases resistance to conduction, which is overcome by overdesign of the number of heat transfer tubes, adding to the cost (Kelly, 2021). Demonstration of a 5.4 MW, 130 MWh system by resistive heating using electricity from a renewable source connected to the Hamburg grid is ongoing (Energy, 2020). The storage medium consists of 1,000 tons of volcanic rock heated to 750°C (Collins, 2019).

For sand storage, system integration costs are expected to be similar to a gas turbine combined cycle plant, except for added costs for the particle containment silos. Since these are pre-deployment systems, EPC and project development costs are yet to be determined (Ma, Wang, Davenport, Gifford, & Martinek, 2021). The power-related cost is estimated at ~\$1,000/kW, while O&M costs are expected to be similar to a thermal generation plant; the system RTE is expected to be 50%. Discharge is done in a fluidized bed heat exchanger to heat gas/steam using a combined-cycle plant. Note that these estimated costs are from a research project and the system design, performance, and cost have not been commercially validated. Work is ongoing on a pilot plant integrating a high-temperature particle-based storage system with CSP using supercritical carbon dioxide (sCO₂) as working fluid (C. K. Ho et al., 2021). The system consists of a particle conveyor, high- and low-temperature storage tanks, and a particle-to-

sCO₂ heat exchanger. The heat exchanger and high-pressure sCO₂ flow loop are under construction. Work is also occurring on the design and development of a system using sCO₂ working fluid, which absorbs 1 MWt heat from one of three receiver sections of a central tower and exchanges the heat with a flowing silica sand bed in a heat exchanger, with the hot silica stored in a hot bed (Brayton Energy, 2021; S. D. Sullivan, 2018). The sCO₂ working fluid picks up heat from a second receiver and again exchanges heat with silica sand. This is repeated once more for a total heat transfer of 3 MWt to silica, after which the cooled sCO₂ working fluid collects 1 MWt from hot silica and is conveyed to a 0.5 MWe gas turbine simulator before returning to the receivers to repeat the process. The cooled particles, which collect in a silo, are conveyed by a skip hoist to the top of the tower.

In a variation of the above approach, sCO₂ is used to pick up heat from CSP receivers and transfer that to silica-based storage media through heat exchangers (S. Sullivan & Frinze, 2022). The ΔT for the working fluid was limited to 150°C to account for receiver material limitations at the sCO₂ pressures, which resulted in ΔT for sand of 125°C. Countercurrent flow in the heat exchangers with an approach temperature of 20°C resulted in a heat exchanger estimated cost of \$490/kWt or \$980/kWe based on \$9.8/(Wt/°C). Note that for the Air Brayton cycle, the approach temperature can be as high as 100°C, resulting in an estimated cost of \$196/kWe. Piping costs were estimated at \$25/kWe for a 100 MWe system and at \$40/kWe for a 1000 MWe system. With ΔT for storage media limited to 125°C, this resulted in an estimated storage media cost at \$30-50/ton of \$1.60/kWh, which was roughly six times the cost for sand-based storage for a ΔT of 900°C (Ma, 2021b).

A schematic for the system is shown in Figure 4.21. The power block section 1, not shown clearly, consists of turbines, recuperators, and compressors. The sCO₂ enters the turbine at 715°C and leaves the power block at 575°C. It picks up heat from heat exchanger HEX 10, with an approach temperature of 15-20°C on both ends, leaving the heat exchanger at 590°C. During the day, the sCO₂ is fed to the receivers and exchanges heat with sand particles in HEX 5 (three sets of receivers and heat exchangers). Two-thirds of the sand is stored in the hot storage tank, while one-third of sand is fed to HEX 8 to heat the sCO₂ working fluid to the turbine inlet temperature. When the CSP plant is not generating thermal energy, the working sCO₂ fluid exits HEX 9 and enters HEX 8 to pick up heat from the hot storage media to reach the turbine inlet temperature.

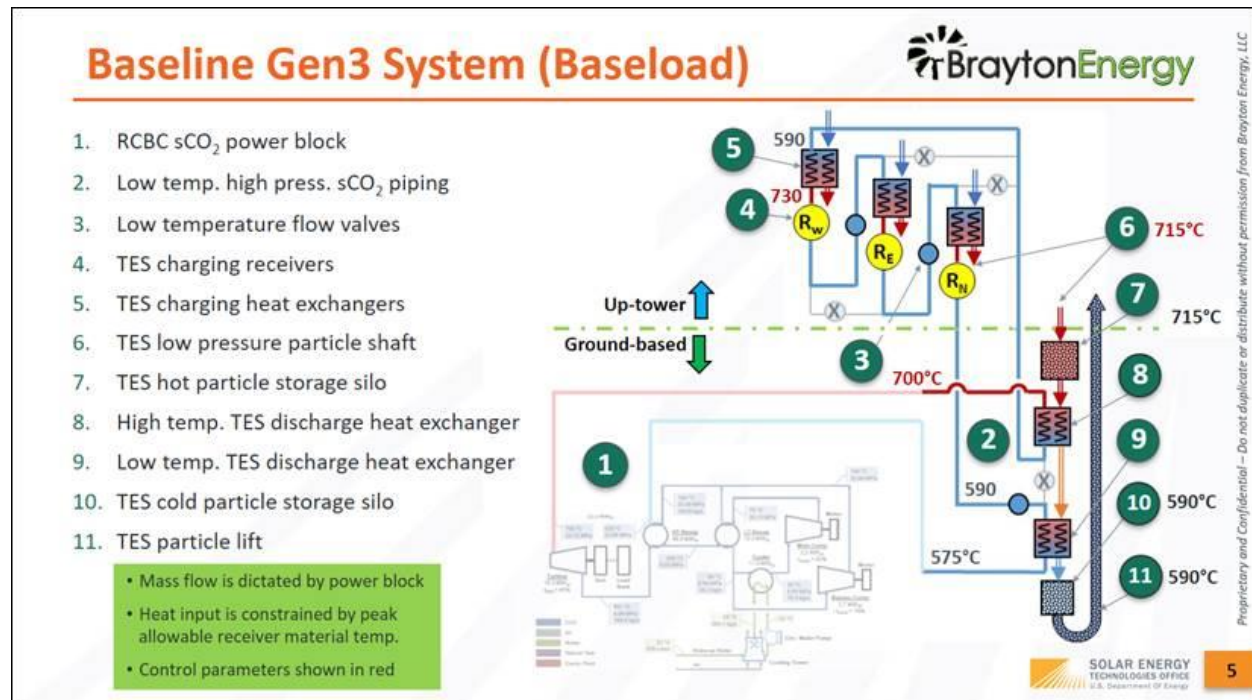


Figure 4.21 Schematic of Baseline Gen3 System using sand particles as thermal storage media and sCO₂ as working fluid (used with permission).

Extensive research has been done on optimizing receiver design to maximize thermal efficiency in CSP plants, adjusting the particle flow rate through the receiver (C. K. Ho, 2016), (Mills et al., 2022). Such details are out of scope of this work, which assumes electrical charging of the storage medium. However, sufficient details on receiver/tower design and cost are available (Albrecht, Bauer, & Ho, 2019; Gan, Wang, & Pye, 2021; C. K. Ho, 2016) for future work that may incorporate thermal energy input. The receiver/tower cost in \$/kWe had a wide range (\$149–1095/kWe) (Albrecht et al., 2019; Gan et al., 2021; C. K. Ho, 2016; C. K. Ho, Carlson, Garg, & Kumar, 2016), corresponding to an average of \$415/kWe, which is close to the DOE SunShot target of \$300/kWe (C. Ho, 2022). Ceramic particles were found to be superior to sand in terms of absorbance and resistance to wear and sintering at temperatures as high as 1000°C (C. K. Ho, 2016). The storage medium cost in \$/kWh was nearly two orders of magnitude higher than that of sand, at \$18/kWh (C. K. Ho, 2016), while the storage costs including tanks, foundation, and piping/valves was 36–39 \$/kWh (Albrecht et al., 2019; Gan et al., 2021; C. K. Ho, 2016) and \$85/kWh (C. K. Ho et al., 2016), an order of magnitude higher than cost for a corresponding silica-based storage (Ma et al., 2021). The particle-to-sCO₂ heat exchanger has a cost of \$350–500/kWe (Albrecht et al., 2019; Gan et al., 2021), five times higher than the estimated heat exchanger costs for a silica-based system (Ma et al., 2021). The power equipment cost for the sCO₂ Brayton cycle ranged from \$600–898/kWe, with an average of \$760/kWe. Since sCO₂ cycle is at least 10 years away from commercialization (S. Sullivan & Frinze, 2022), this work uses available costs for the Air Brayton cycle power block.

Solar salt has a specific heat of 1,545 J/kg °C at 600°C (Caraballo, Galán-Casado, & Serena, 2021), while cast iron, sand, concrete, and fire brick have specific capacity of 470, 830, 880 and 880 J/kg °C, respectively (The Engineering Toolbox, 2003). The costs of salt \$950–1,000/ton, concrete \$68/ton (Hume, 2020), sand \$20–46/ton (Kelly, 2021a; Ma et al., 2021), and cast iron < \$500/ton (C. W. Forsberg et al., 2021), assuming heat-to-electricity efficiency of 0.5, correspond to storage cost of \$1/kWe for

sand,³⁴ \$2.0/kWhe for concrete, \$16.9/kWhe for molten salt, and \$27.8/kWhe for cast iron for a ΔT of 275°C.

LAES is based on using the refrigeration cycle to liquefy ambient air, capturing heat from the compressors and storing it for the subsequent discharge cycle (Sciacovelli, Smitha, Navarro, Lia, & Dinga, 2016; Strahan, 2013). The compressed air is cooled by a cold storage loop, after which it undergoes isentropic expansion to form liquid air. In the discharge cycle, liquid air is preheated by the cold storage medium that has picked up heat from compressed air in the charge cycle. The heated liquid air picks up additional heat from thermal storage in a heat exchanger and is fed to turbines to generate electricity, with provision for additional heat exchangers and turbines. A 350 kW/2.5 MWh pilot was commissioned in 2011 in Heathrow, UK, and a 5 MW/15 MWh demonstration system in Manchester, UK was commissioned in 2018, with plans for 50 MW facilities in the UK and US (Sciacovelli et al., 2016; Strahan, 2013)

One LAES system developer uses a hybrid approach with a fuel-powered combustion turbine to generate electricity while also using the exhaust heat to preheat liquid air and an organic Rankine cycle working fluid, which generate electricity in separate turbine-generator sets (Conlon, 2021a; Pintail Power, 2021). A reference design was completed to estimate air consumption per MWh electricity delivered, storage tank size (200,000 cubic meters), cost to store 75,000 MWh of electricity, and cost for independent 117 MW discharge and 180 MW charge³⁵ powertrains.

PHES has an estimated TRL 3-4 (Kelly, 2021a), operating on a closed Brayton cycle to increase efficiency. The fluid inlet temperature and pressure are different for the discharge turbine and the charge compressor. Hence the compressor used during charge is different from the turbine used during discharge, since the efficiency penalty is expected to exceed cost savings benefits from using the same powertrain³⁶ (Allison, 2021; Held & Brennan, 2021). While the motor used in the charge mode can serve as a generator in the discharge mode, if the charge rate is significantly lower than the discharge rate, the motors running at partial load are not efficient. Depending on economic considerations, a single motor/generator or separate motor and generator is used, taking into consideration that equipment procurement is done such that the compressor comes with a motor, and a turbine with a generator (Held & Brennan, 2021). Electricity is used to transfer heat from cold storage to hot storage during charge, increasing the temperature difference. During power generation, heat from the hot storage tank is used to generate steam, which is fed to a steam turbine to generate power (Smith, 2021). Heating of ammonia, stored in tanks of the same size as described for liquid air storage, with air in a burner to heat molten salt may enable lower cost operation for application duration ≥ 24 hours (Klochko & Lahaye, 2021). This is an example of a potentially cost-effective hybrid system, with ammonia providing energy for long durations. While molten salt is typically used for thermal storage, since the theoretical RTE³⁷ for PHES does not depend on maximum temperature for thermal storage (Held & Brennan, 2021; Systems), sand storage medium and a low upper limit of 350°C is used, enabling use of low-cost carbon steel

³⁴ The ΔT for sand is 900°C, hence storage cost is estimated at \$0.32/kWh electric.

³⁵ The higher charge rate allows flexibility to capture electricity during off-peak hours, with the caveat this comes with added cost.

³⁶ When charge and discharge rates are different, running motors at part load reduces efficiency; further, a compressor comes with a motor and a turbine comes with a generator (Held & Brennan, 2021).

³⁷ The theoretical RTE for a PHES is $COP \cdot 1 / (COP)$, where COP is the coefficient of performance and does not depend on maximum temperature.

material for sand storage silos and conveyance with sCO₂ as working fluid (Held & Brennan, 2021). Similarities and comparison of LAES and PHES are provided in (Georgiou, Shah, & Markides, 2018; Guo, Cai, Chen, & Zhou, 2016).

While capital costs are one cost component, O&M costs affect the LCOS. The O&M contractor for thermal storage plants takes over operation after commissioning (Mehos et al., 2020) and is responsible for personnel, permit maintenance, and procurement of spare parts and supplies. Most O&M-related issues include steam generation failures, inadequate control for thermal gradients associated with startups, and leaks that can compromise process piping and valves. The O&M contractor needs to be involved during design, construction, and commissioning to ensure use of high-quality and reliability parts.

4.8.1 Capital Cost

The cost categories used in the report extend across all energy storage technologies to allow ease of data comparison. Direct costs correspond to equipment capital and installation, while indirect costs include EPC fee and project development, which include permitting, preliminary engineering design, and the owner's engineer and financing costs.

As discussed earlier, multiple storage media such as molten salt, sand, and concrete can be used for thermal storage. The storage media is assumed to be heated by electric resistance heating, followed by electricity generation using conventional thermal plant equipment with single-cycle steam systems or combined-cycled systems using gas turbines and steam turbines. Data for individual component costs for thermal storage plants such as salt, tanks, foundations, single-cycle steam system power equipment, BOP for steam, and EIC were obtained from (Lundy, 2020). Adjustments were made to tank and foundation costs to account for higher discharge energy per unit weight of salt for molten salt storage used in a combined-cycle thermal plant using fuel (Conlon, 2021b). For the stored energy block, a nominal 6% decrease was assigned for a ten times increase in energy.

For plants using combined cycle, the power equipment costs for single cycle are replaced by those for the combined cycle (Gas Turbine World, 2020; Ma et al., 2021), while retaining the BOP costs for steam and EIC.

For power equipment, the cost of single-cycle steam-based powerplants at 100 MW include a power block (\$1,312/kW), BOP for steam system (\$121.5/kW), and EIC (\$98.7/kW), which was obtained from (Lundy, 2020). Cost for combined-cycle powerplants power block was \$985/kW (Gas Turbine World, 2020; Ma et al., 2021), with the same BOP costs assigned for the steam system and EIC. An EPC fee of 10%, project development cost of 20% of direct cost, and grid integration cost of \$12/kW were assigned (Lundy, 2020).

Scaling with respect to power used costs for a combined-cycle plant power block as a function of power in the 50–1800 MW range (Gas Turbine World, 2020). The power equipment for a PHES plant was assigned the higher cost corresponding to a single-cycle steam turbine system related to separate powertrains for charge and discharge. For LAES, while the discharge powertrain costs were similar to combined-cycle plant cost, the charge cost varied depending on the ratio of charge rate to discharge rate, with a higher ratio contributing to greater cost. For systems with resistive heating, the cost for

charging hardware of \$114/kW for resistive heating was added to the power equipment cost (Capp, 2021).

For 2030 costs, one developer provided an estimated 48% reduction, while another provided a 40% cost reduction. This work assigns a modest 15% cost reduction for 2030 for the SB and BOS, and 5% for the power equipment.

4.8.1.1 Pumped Heat Energy Storage

PHES has an estimated system integration of TRL 3-4 (Kelly, 2021a). There are various system designs from different developers, and some examples are provided. The PHES operates on a closed Brayton cycle to increase efficiency in the heat engine mode with the working fluid being air (Allison, 2021), argon (Engineer, 2019) or supercritical CO₂ (Held & Brennan, 2021). Specialty equipment is needed at the targeted temperatures (Dufo-López et al., 2021). The typical hot-side temperature is 565°C when using high-temperature molten salt, allowing for use of nonexotic alloys, while the cold-side temperature of -60°C is above cryogenic temperatures, allowing use of inexpensive carbon steel (Dufo-López et al., 2021). Storage tank and BOS costs are lowered by use of lower maximum temperature for the hot storage tank, while using ice/water medium for the cold storage tank, with design considerations for minimizing exergy³⁸ (Echogen Power Systems; Held & Brennan, 2021). A schematic of a typical PHES system is shown in Figure 4.22.

To extend duration beyond 10 hours, a hybrid system is being developed that uses ammonia produced by an electric Haber-Bosch process to generate heat in a burner (Airthium)³⁹. The single tank⁴⁰ molten salt loop is heated by exhaust from the burner, which in turn heats the helium working fluid to generate electricity using a Sterling engine (Klochko & Lahaye, 2021). Large-scale liquid ammonia tanks (50 m diameter x 30 meter height, 235,000 m³) with an estimated cost of \$0.2-0.3/kWh. Table 4.39 summarizes costs for PHES, with cost information available from two developers (Echogen Power Systems, Undated; Klochko & Lahaye, 2021). A wide range of SB and BOS cost is obtained based on the ratio of molten salt to ammonia storage (Klochko & Lahaye, 2021). While the ratio of molten salt to ammonia storage as a function of duration was not provided, this study assumes storage to consist only of molten salt for all durations ≤ 10 hours,⁴¹ with 0.42 fraction of energy stored in molten salt at 24 hours and 0.1 fraction at 100 hours. The purpose for including this hybrid system with added complexity was to explore the impact on cost & performance.

As discussed earlier, separate powertrains along with separate motor (for charge) and generator (for discharge) are used for the charge and discharge cycles. Due to a lack of information on power equipment cost, the heat pump/heat engine power block cost was assumed to be the same as for a single-cycle steam thermal plant (\$1,532/kW)⁴² (Lundy, 2020), while for durations of ≥ 24 hours, the

³⁸ Exergy is the lost energy related to the difference between maximum temperature of the working fluid during charge and discharge (Echogen Power Systems).

³⁹ Molten salt storage is possible for > 10 hours. This specific example provides a cost-effective hybrid option for durations > 10h.

⁴⁰ Note that considerable work needs to be done to demonstrate single-tank concept.

⁴¹ For low durations, the power equipment cost for ammonia electrolyzer ends up dominating.

⁴² Considering the independent powertrains needed for charge and discharge, the actual costs may be higher.

electrolyzer, rectifier, and compressor costs totaling \$1,670/kW based on equipment cost for HESS (Mongird et al., 2020b) are added to the heat pump/heat engine power block cost.

A 150 kW, 600 kWh system using argon working fluid with gravel as both high- and low-temperature storage has been commissioned (Engineer, 2019), with a measured RTE of 60–65%, thus offering promise for this technology.

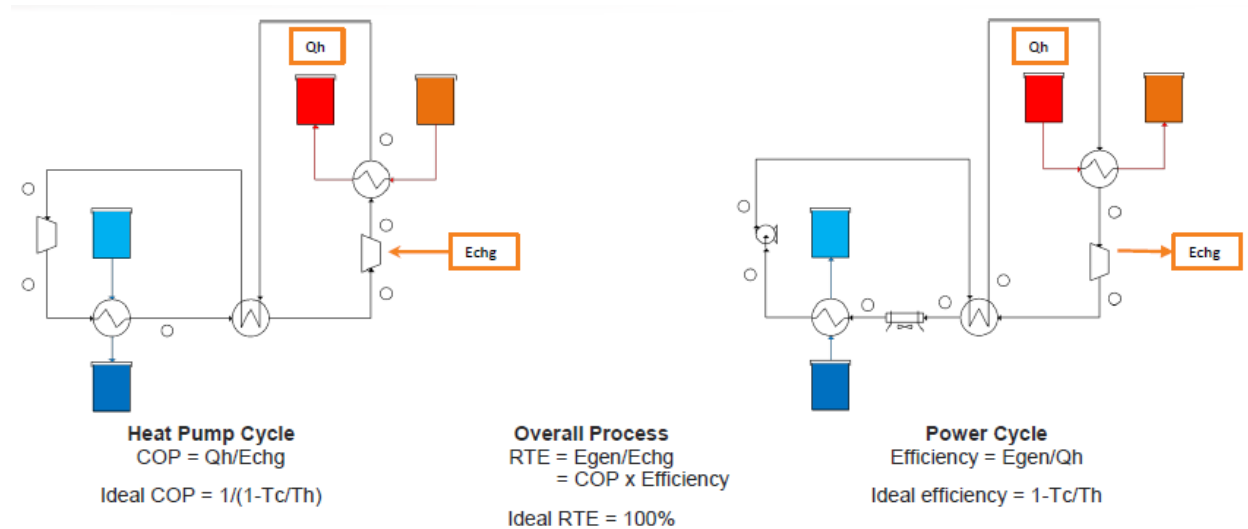


Figure 4.22 Schematic of a Pumped Hydro Energy Storage System – used with permission (Echogen Power Systems; Held & Brennan, 2021).

Installed cost as a function of duration for a 50 MWe plant is also available using sand as the hot storage medium and ice/water as the cold storage medium (Echogen Power Systems). This cost was assumed to be the same for 100 MWe. The cost for a 1,000 MWe system at each duration was estimated by taking the average of ratio of installed cost for 1,000 MW:100 MW for all other thermal storage technologies except conventional LAES, whose ratio values were not aligned with the rest. For this system, no attempt was made to back out power equipment cost and SB/BOS cost, since sufficient data are not available.⁴³ Table 4.39 provides estimated costs for PHES systems. Note that since these systems are in early stages of development, these costs have not been validated.

A 15% cost decrease was assumed for the year 2030 for the SB and BOS, in line with drops for zinc- and gravity-based systems. A nominal 5% cost decrease was assumed in the mature power equipment, related to novel use of this equipment in a variety of thermal storage options.

⁴³The storage media cost for cold and hot storage are provided at \$12/kWhe and \$1/kWhe, respectively, with tank and silo costs at \$12/kWhe. By assuming BOS costs to be a fixed percent of SB cost, and assuming 30% of direct costs for EPC fee, project development, and grid integration, the power equipment costs may be estimated, but this was not done.

Table 4.39. PHES Composite Capital Costs

Cost Component	Year	Value	Comments	Source
SB (\$/kWh)	2021	5.4-50	Higher number is for molten salt and tank, lower number for 10% energy stored in molten salt, rest in ammonia.	Klochko and Lahaye (2021)
	2030	4.6-43	85% of 2021 cost.	
BOS (\$/kWh)	2021 & 2030		Included in above cost.	Klochko and Lahaye (2021)
Power Equipment (\$/kWh)	2021	1,532- 3,202	Assume the same cost as that of a steam cycle with BOP for steam system and for EIC. For 24h and 100h, electrolyzer, rectifier, compressor costs added.	Lundy (2020), Mongird et al. (2020b)
	2030	1,454-3,042	95% of 2021 cost.	
EPC fee (\$/kWh)	2021 & 2030	10% of above direct costs		
Project Development (\$/kWh)	2021 & 2030	20% of direct costs		
Grid Integration (\$/kW)	2021 & 2030	11.3-12.0	11.3 at 1000 MW, 12 at 100 MW.	
Total System Cost (\$/kWh)	2021	19-348	Both extremes are for system with sand as hot storage and ice/water as cold storage, with high cost at 100 4h duration, and low cost at 1000 MW, 100h duration.	Echogen Power Systems (Undated)
	2030	18-218		

4.8.1.2 Sensible Heat-Based Thermal Storage with AC In, AC Out

Multiple storage media such as molten salt, sand, and concrete can be used for thermal storage. For this work, the storage media is assumed to be heated by electrical resistance heating, followed by electricity generation using conventional thermal plant equipment with single-cycle steam systems or combined-cycled systems using gas turbines and steam turbines. Data for a thermal direct storage plant using CSP was used by substituting CSP with electrical heating (Lundy, 2020). A hybrid system using fuel input to drive a combustion turbine and superheat the steam is also considered (Conlon, 2021b). For plants using combined cycle, the power equipment costs for single steam cycle are replaced by combined-cycle system power equipment costs (Gas Turbine World, 2020; Ma et al., 2021), while retaining the BOP costs for steam and EIC from (Lundy, 2020).

The SB has a wide cost range of \$4–88/kWh. The lower end corresponds to sand storage at \$4/kWh, less than 10% of which is for sand material, with the remaining costs related to silo and foundation (Ma, 2021b). The higher end of this range corresponds to high-temperature molten salt storage as part of a generic single-cycle steam system at \$88/kWh, inclusive of molten salt comprising 22% of this cost, the remaining assigned to storage tanks and pipes. Concrete SB cost of \$16–33/kWh comprises concrete medium cost, which is estimated at \$1.8/kWh based on specific heat, material cost per ton, RTE and

temperature difference of 300°C between charged and discharged state, container cost of \$15/kWh, along with steel tube system cost ranging from \$15/kWh at 4 hours to \$0.6/kWh at 100 hours.

Sand-based systems have estimated a low BOS cost at \$0.33/kWh for the energy component that includes skip hoist, motor, drum brake, pulleys, and insulation, and power-related BOS cost of \$72/kW, inclusive of pressurized fluidized bed and cyclone costs totaling \$72/kW (Ma et al., 2021), which become significant at lower durations, contributing \$9/kWh out of a total \$9.33/kWh at 8-hour duration. The BOS for concrete and low-temperature molten salt-based storage systems are similar at \$6–7/kWh, while the BOS costs for high-temperature molten salt was higher at \$9–16/kWh, tied to higher foundation costs for the tanks.

The power equipment costs include heating equipment of \$113.5/kW (Capp, 2021) in addition to costs for a single-cycle or combined-cycle thermal powerplant, with lower costs corresponding to the combined-cycle plant. Within each technology, the \$/kW costs for 1,000 MW systems were lower than 100 MW systems due to scaling effects discussed earlier. The power equipment costs fall within the \$835–1,645/kW range, with the lower value corresponding to 1,000 MW combined-cycle system and the higher value corresponding to 100 MW single-cycle system.

As expected, the EPC fee and project development costs have a wide range, from \$4–135/kWh. Table 4.40 reports these costs individually. This wide range is due to scaling effects related to power at 1,000 MW and low impact of power equipment at high duration corresponding to the low end of the range. This range is in line with the ratio of the longest to shortest duration considered for this technology (100h/4h).

2030 cost projections were not provided. A nominal 15% cost drop was assumed for SB + BOS, in line with drops for zinc- and gravity-based systems.

4.8.1.3 Liquid Air Energy Storage

The LAES technology uses energy stored in liquefied air to drive gas turbines to generate power, and has a high TRL with 350 kW, 2.5 MWh and 5MW, 15 MWh demonstrations commissioned (Capp, 2021; Riley, 2021). Liquefaction of air follows standard refrigeration principles. Two examples are provided, one of which also uses fuel input.

4.8.1.3.1 LAES System Example AC In, AC Out

This LAES system consists of a refrigeration (charge) system, storage vessels, and a turbine generator (discharge) system (Highview Power, 2021; Riley, 2021). During charge, a refrigeration cycle running on grid electricity cools air and condenses it to liquid at cryogenic temperatures. The liquid air is stored in insulated low-pressure vessels. Heat generated during compression in the refrigeration cycle is recovered via a heat exchanger and stored in the heat storage media. Cooling in the refrigeration system is supplemented with cold supplied from the cold storage media. During discharge, the liquid air is pumped from the liquid air vessel to high pressure using a cryogenic pump and warmed in a heat exchanger to close to ambient temperature. The cold release from the cryogenic high-pressure air is captured in a recirculating flow of dry air. The dry air is thus cooled and conveyed to the cold thermal storage, which stores the cold for later delivery to the refrigeration system in the next charge cycle. The warmed high-pressure air is further heated in a heat exchanger with heat from the hot storage media.

Table 4.40. Sensible Heat-based Thermal Composite Capital Costs⁴⁴

	Sand Combined Cycle	Sand Combined Cycle	Ceramic Particles Combined Cycle ⁴⁵	Generic Single Steam Cycle with High T Molten Salt	Combined Cycle with Low T Molten Salt ⁴⁶	Concrete Single Cycle	Composite	Comments
Source	Ma (2021a), Ma (2021b)	(S. Sullivan & Frinze, 2022)	(Albrecht et al., 2019; Gan et al., 2021; C. K. Ho, 2016; C. K. Ho et al., 2016)	Lundy (2020)	Conlon (2021b)	Capp (2021)		
Power, MW	100, 1000		100, 1000	100, 1000	100, 1000	100, 1000	100, 1000	
Durations (h)	8-100		8-100	10-100	10-100	4-100	4-100	
Storage Medium	Sand		Ceramic	High T MS	Low T MS	Concrete		
Delta T (deg C)	900		900	275	275	275	100-900	
Power Generation Cycle Type	Combined cycle (air and steam)		Combined cycle (air and steam) ⁴⁷	Single cycle (steam)	Combined cycle – (gas and steam)	Single cycle (steam)		
SB \$/kWhe	3.4-3.8	3.4-3.8	43-49	49-88	33-38	16-33	4-88	Direct costs. Storage medium ranges from sand, low-temperature molten salt, concrete.
BOS (\$/kWhe)	1.0-9.3	2.7-28.0	3.6-41.5	9-16	6.3-7	5.8-6.8	0.3-16	Direct costs. Sand conveyance, heat

⁴⁴ No financing costs have been considered.

⁴⁵ Storage media, foundation, tank, piping/valves, heat exchanger (which is included in balance of system cost) obtained from Source

⁴⁶ includes fuel input for power generation via combustion turbine and to provide exhaust heat for heating water and to produce super-heated steam

⁴⁷ The technology uses sCO₂ power cycle which is at least 10 years away from commercialization, hence an Air Brayton combined cycle assumed

	Sand Combined Cycle	Sand Combined Cycle	Ceramic Particles Combined Cycle ⁴⁵	Generic Single Steam Cycle with High T Molten Salt	Combined Cycle with Low T Molten Salt ⁴⁶	Concrete Single Cycle	Composite	Comments
								exchangers, pipes, valves.
Power Equipment (\$/kWe)	850-1,335	850-1,335	850-1,335	1,030-1,645	835-1,320	1,030-1,645	835-1,645	Direct costs. Higher end of cost based on single-cycle steam systems; lower end based on combined cycle.
EPC Fee (\$/kWh)	1.3-18.0	1.5-19.9	5.5-25.8	10-27	5-18	3-45	1-45	Indirect costs - 10% of direct costs.
PD (\$/kWh)	2.6-36	2.9-39.8	11.1-51.6	20-54	10-35	6-90	2.6-90	Indirect costs include preliminary engineering design, owner's engineer and permitting. 20% of direct costs.
Grid Integration (\$/kW)	11.3-12	11.3-12	11.3-12.0	11.3-12	11.3-12	11.3-12	11.3-12	

The resulting hot, high-pressure air is fed to a turbine and expanded in multiple stages of expansion and reheat using heat from the heat storage media. The nearly three orders of magnitude expansion drives the turbine generator and returns AC electrical power to the grid. The storage of heat and cold enhances system efficiency, which is estimated at 50-55%. Pilot demonstrations have been conducted in Heathrow, UK (350 kW, 2.5 MWh) and Manchester UK (5 MW, 15 MWh) (Sciacovelli et al., 2016; Strahan, 2013). Construction has begun of a 50 MW, 300 MWh commercial system, also in Manchester, UK, and multiple projects are in development in Europe and the United States (Highview Power, 2021; Riley, 2021).

Energy cost for SB and BOS was provided at \$180/kWh, while power component cost, inclusive of BOP and EIC, were provided at 800/kW for charge powertrain and \$800/kW for discharge. The discharge hardware cost was estimated at 1000 MW using the ratio of power block cost for a combined-cycle plant as discussed earlier. Costs included the EPC fee, which was stated to be 5% of direct costs, while project development costs were proposed as 15% of direct cost. BOP, EIC, and EPC costs are already included in the numbers provided.

For this work, the EPC was set at 10% of direct cost and project development was set at 20% of direct cost. Figure 4.23 shows a schematic of the LAES system.

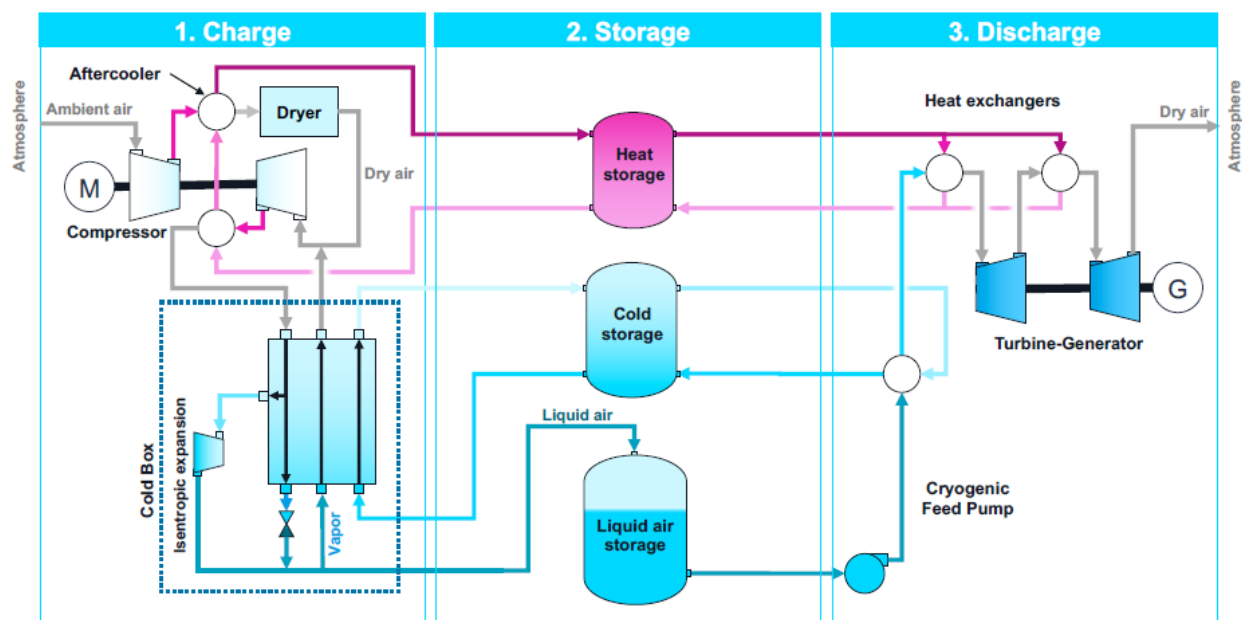


Figure 4.23 Schematic of LAES System © Highview Power Storage, Inc. all rights reserved – used with permission. (Highview Power, 2021; Riley, 2021)

4.8.1.3.2 Liquid Air Combined-Cycle Example (AC + Fuel In, AC Out)

Liquid air combined-cycle technology uses liquid air at atmospheric pressure as the storage medium (Conlon, 2021a; Pintail Power, 2021). The liquid air is produced by conventional cryogenic refrigeration equipment driven by electric motors for charging with renewable power. This technology uses fuel input in the discharge cycle to generate electricity and heat air for power generation in air turbine and the organic Rankine cycle working fluid for power generation in the low-temperature turbine. It uses commercially available equipment and processes adapted from the power and liquefied natural gas

industries to maximize the energy produced during discharge per unit of liquid air to reduce the size and cost of capital-intensive cryogenic refrigeration equipment and storage tanks. The hybrid approach is considered in this study to evaluate the impact of additional fuel input on cost and performance.

During discharge, the liquid air is pressurized and re-gasified to produce power in a cascade of three power cycles coupled by heat exchangers: a combustion turbine, an air turbine, and a low-temperature organic Rankine cycle. The wide operating temperature range of the power cycles, from about 1850 K in the combustion turbine to about 150 K in the condensing section of the organic Rankine cycle reduces the specific air consumption.

A reference design projects specific air consumption of 2.65 cubic meters per MWh of electricity discharged (Conlon, 2021a). A 200,000 cubic meter cryogenic storage tank, a common size for liquefied natural gas, could store 75,000 MWh of discharge energy on 2.5 acres of land. The estimated cost of the storage tank is \$72 million or about \$1/kWh. For energy needs less than 75 GWh, it is assumed in this report that a tank half the size is available at 60% of the cost.

In the reference design, each 117 MW discharge train has an estimated installed cost of \$175 million and a 180 MW charging train with the same liquid capacity has an estimated cost of \$390 million. The number of charging and discharging trains can be independently varied to suit the availability of renewable power and the need for dispatchable energy. During discharge, the combustion turbine consumes approximately 4.5 MJ/MWh of fuel (natural gas, hydrogen, or a distillate), roughly half the fuel consumption of a simple-cycle dispatchable resource and reducing specific air consumption (Conlon, 2021a; Pintail Power, 2021).

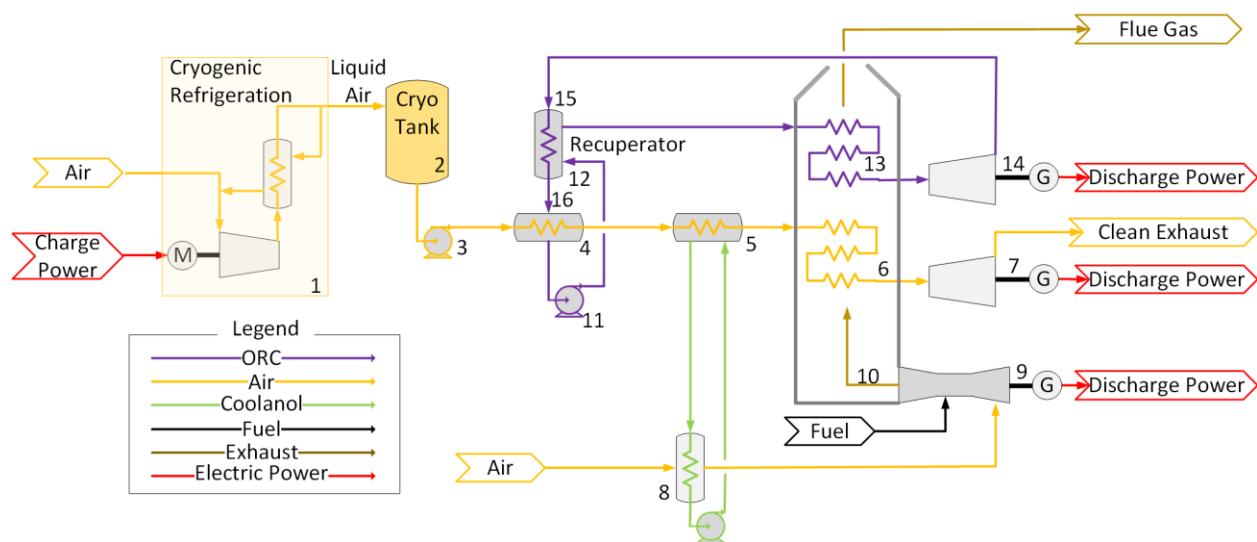


Figure 4.24 Schematic of the Liquid Air Combined-Cycle System 9: combustion turbine, 7 gas (air) turbine, 14 low-temperature turbine for organic Rankine cycle; used with permission (Conlon, 2022).

4.8.1.3.3 Composite Costs for Liquid Air Energy Storage

Estimated cost for SB and BOS was provided along with power equipment cost to enable estimation of installed costs across power levels and durations of interest (Conlon, 2021a; Highview Power, 2021; Pintail Power, 2021; Riley, 2021). The powertrain for one approach was simpler (Highview Power, 2021;

Riley, 2021), resulting in lower unit power costs, while use of combustion turbine removed the need for hot and cold storage, reducing unit energy costs (Conlon, 2021a; Pintail Power, 2021).

Due to the relatively low TRL of thermal ESSs, only nominal cost drops were assigned for 2030 costs. The SB and BOS costs were reduced by 15%, in line with drops for zinc- and gravity-based systems, while power equipment costs were reduced by 5% and O&M costs by 10%. The EPC fee and project developments costs are estimated using 10% and 20% respectively of direct costs. Liquid air thermal storage composite capital costs are provided in Table 4.41.

Table 4.41. Liquid Air Thermal Composite Capital Costs

	Year	AC-in, AC-out	Hybrid AC+ Fuel in, AC-out	Composite	Comments
Source		Highview Power (2021); Riley (2021)	Conlon (2021a); Pintail Power (2021)		
Power, MW		100, 1000	100, 1000	100, 1000	
Durations (h)		6-100	10-100	4-100	
Storage medium		Liquid air	Liquid air		
Power generation cycle type		Gas turbine	Gas turbine (multiple)		Hybrid example uses fuel as well to generate power and provide preheating and additional heating.
SB and BOS (\$/kWe)	2021	157-194	1.2-45	1-194	Liquid air tank, insulation, heat storage, cold storage.
	2030	133-175	1-38	1-175	85% of 2021 cost.
Power Equipment (\$/kWe)	2021	956-1,600	2,355-2,817	956-2,817	Motor, compressor, generator, turbine, heat exchanger, recuperator. Both provided power equipment costs inclusive of BOP and EIC.
	2030	908-1,577	2,237-2,676	908-2,676	95% of 2021 cost.
EPC fee (\$/kWh) ^a	2021	8-201	2.5-33	2.5-201	10% of direct costs used for Pintail Power, Highview Power proposed 5%.
	2030	7-181	2.3-30	2.3-181	10% of above direct costs.
Project Development (\$/kWh) ^a	2021	30-84	5-65	5-84	20% of direct costs used for both, Highview Power proposed 15%.
	2030	27-76	4.5-59	4.5-76	20% of direct costs.
Grid Integration (\$/kW) ^b	2021	11.3-12	11.3-12	11.3-12	Standard value used for all thermal technologies.
	2030	11.3-12	11.3-12	11.3-12	Unchanged from 2021
Total System Cost \$/kWh	2021	198-546	32-426	32-546	Lack of hot storage tank for Pintail Power reduces cost at high duration.
	2030	178-491	29-384	29-491	90% of 2021 costs.

^a Lundy (2020); Riley (2021)

^b Lundy (2020)

4.8.1.4 Composite Thermal Energy Storage

Among thermal energy storage technologies only molten salt storage is commercialized and pilot plant demonstration done for LAES systems. The rest of the technologies are at various stages of development and hence the numbers provided by developers have to be caveated and distinguished between deployed vs. nondeployed. Note that even for nondeployed technologies, several components such as heat exchangers, turbines, compressors, and liquefied natural gas storage tanks are commercially available.

The overarching finding is that electric heating of various thermal storage media followed by power generation offers a viable pathway toward cost-effective sensible heat-based thermal storage. The benchmark commercially deployed solar salt is the most expensive among storage media, with its higher maximum temperature associated with higher costs for storage tanks, foundations, valves, and piping. Lower cost alternatives at lower technology readiness levels are being pursued such as a yet to be commercially deployed hybrid liquid salt combined-cycle system that uses a lower temperature molten salt to generate steam that is further heated to superheated steam from a combustion turbine exhaust, which also preheats feedwater. Sand-based systems and thermoclines have not been deployed commercially and offer the promise of lower capital cost.

LAES using a simple powertrain and hot/cold storage to improve system efficiency, with successful pilot plant demonstrations, is at a high TRL. A future alternative is a combined-cycle approach that uses a more complex powertrain. This design includes an organic Rankine cycle and offers potential cost savings by using exhaust heat from a combustion turbine to both preheat and heat the liquefied air along with heating the organic Rankine cycle working fluid, removing the need for hot and cold storage.

PHES systems are at a low TRL, and cost details for the powertrain are not available and hence assumed equal to that of a steam turbine power block. While the technology has not been deployed, the storage media used ranges from commercially deployed solar salt to sand, while the power block uses motors, generators, compressors, and turbines that are commercially available. The costs associated with this technology need to be validated through pilot plant demonstrations followed by commercial deployment.

The SB and BOS, power equipment, and total installed cost comparison across various technologies are provided in **Error! Reference source not found.**, Table 4.43, and Table 4.44, respectively. As discussed earlier, EPC fees and project development costs are set at 10% and 20% of direct costs, respectively.

For the 4-hour duration, data were restricted to concrete-based systems, while the 6-hour duration includes conventional liquid air storage, with PHES and sand-based storage costs available for 8 hours and information for 10-, 24-, and 100-hour durations available for all technologies.

The power equipment costs for various technologies at 100 and 1,000 MW are shown in Table 4.43. For systems other than liquid air, costs depend on whether the discharge powertrain is based on single-cycle steam (high-temperature molten salt, concrete) or combined cycle (sand, low-temperature molten salt), with the latter having lower \$/kW costs. LAES systems need separate charge and discharge power trains, corresponding to higher unit power costs. For the conventional LAES, with liquid air and hot and cold storage, assumptions were made regarding unit energy and power costs such that direct capital costs including EPC fee were equal to the costs provided, hence these costs may have some unavoidable

inaccuracies (Riley, 2021). Note that there is some lack of clarity on powertrain costs for PHES, with costs assumed in this work to be similar to single-cycle steam plant.

As shown in **Error! Reference source not found.**, SB and BOS costs for sand-based systems are the lowest, with concrete-based systems next in line, followed by low-temperature molten salt systems. Sand-based systems are lower in cost across all power levels and durations (Table 4.44). In the 10-24 hour range, concrete-based and low-temperature thermal salt storage are equally cost effective behind sand-based storage, with the lower SB and BOS costs for concrete-based systems compensated by the lower power equipment costs for low-temperature molten salt systems. As duration increases, at 100 hours, SB and BOS cost for concrete-based systems are two times lower than for low-temperature molten salt, since the cost of embedded steel tubes within concrete blocks is distributed over a larger energy content. This is reflected in lower total system costs as well (Table 4.44).

LAES is competitive at 100 hours when combined with a combustion turbine for additional power generation along with use of its hot exhaust to preheat the liquefied air.⁴⁸ For conventional LAES, the added cost of hot and cold storage increases SB and BOS costs (Table 4.42), and makes it the most expensive across all power and energy levels, with conventional solar salt thermal storage next in line, followed by PHES (Table 4.44). PHES is especially effective at 100 hours when combined with ammonia, lowering the SB and BOS costs (Table 4.42**Error! Reference source not found.**), with system cost equal to concrete-based storage (Table 4.44). The caveats here are that PHES has a low TRL and ammonia is burned in the boiler with associated emissions.

In summary, sand-based storage, followed by concrete-based and low-temperature molten salt,⁴⁹ offer the cost-effective alternatives to the benchmark commercially deployed solar salt system across the power levels and durations explored. Liquid air needs hot, cold, and liquid air storage to be cost effective. The unit energy costs for these storage media and associated containment vessels need to be decreased. A workaround is using fuel for preheating to remove the need for hot storage and eliminate cold storage by not capturing cold from liquid air during the preheating process, at the expense of efficiency and using fossil fuel for the discharge heating and power generation.

No information was available for anticipated price drops for the year 2030. A nominal 15% drop for SB + BOS was assumed, in line with drops for zinc- and gravity-based systems. This price drop is associated with use of molten salt with lower melting point, which leads to greater specific energy or lower BOS cost associated with lower operating temperature range, improvements in sand conveyance system, reducing thermocline degradation with associated improved utilization of storage medium. While power equipment costs for gravity-based storage were assumed to remain unchanged considering the mature status of the associated equipment, a nominal 5% price drop was assigned to thermal storage power equipment considering the complexity of the charge-discharge processes, which allows room for some cost drop as these processes are better understood and streamlined.

⁴⁸ 20% lower cost than concrete-based storage because fuel is used to provide the required heating as opposed to using hot thermal storage.

⁴⁹ Requires fossil fuel for power generation and heating feedwater with hot exhaust.

Table 4.42. Composite Thermal SB and BOS Costs (\$/kWh) by Power Capacity and Duration

Power (MW)	Duration (hr)	PHES ^a	Sand ^a	Sensible Heat Based		Concrete ^a	Liquid Air		Composite
				Generic Single-Cycle Steam with High T Molten Salt ^b	Combined Cycle with Low T Molten Salt ^a		Conventional ^c	With Fuel ^a	
100	4					39.9			39.9
	6					34.5	193.5	45.0	34.5-193.5
	8	50.0	13.2			31.8	191.3	18.8	18.8-191.3
	10	50.0	11.3	103.7	64.2	30.1	189.5	4.5	4.5-189.5
	24	26.5	7.0	101.3	62.7	26.0	183.0		7.0-183
	100	6.4	4.6	97.5	60.3	23.1	172.7		4.6-172.7
1,000	4					39.0			39.0
	6					33.9	176.3	4.5	4.5-176.3
	8	50.00	12.9			29.9	174.3	1.9	1.9-174.3
	10	50.00	11.1	97.5	60.3	28.3	172.7	1.2	1.2-172.7
	24	21.40	6.8	95.2	58.9	24.4	166.8	45.0	6.8-166.8
	100	5.40	4.4	91.6	56.7	21.8	157.4	18.8	4.4-157.4

^a Not Deployed

^b Deployed

^c Pilot-scale demonstrations completed

Table 4.43. Composite Thermal Power Equipment Costs (\$/kW)

Power (MW)	PHES	Sand	Conventional			Liquid Air		Composite
			Generic Single-Cycle Steam with High T Molten Salt	Liquid Salt Combined Cycle	Concrete	Conventional	With Fuel	
100	2,367.20	1,336.50	1,645.70	1,319.50	1,645.70	1,600.00	2,817.20	1337-2,817
1,000	1,751.10	851.60	1,029.60	834.60	1,029.60	1,278.30	2,354.60	852-2,351

Table 4.44. Composite Thermal Total Installed Costs (\$/kWh) by Duration

Power (MW)	Duration (hr)	PHES	Sand	Sensible Heat Based			Liquid Air		Composite
				Generic Single-Cycle Steam with High T Molten Salt	Combined Cycle with Low T Molten Salt	Concrete	Conventional	With Fuel	
100	4	452				589.80			452-590
	6	321				403.50	545.80		321-546
	8	252-315	13.20			310.30	463.90		13-464
	10	209-265	11.30	348.8	256.20	254.30	414.30	425.9	11-426
	24	100-208	7.00	220.9	153.50	123.40	295.50	177.5	7-296
	100	30-50	4.60	148.2	95.70	51.60	223.20	42.6	5-223
1000	4	298				388.30			298-388
	6	211				269.20	462.10		211-462
	8	169-215	12.9			207.60	396.20		13-396
	10	149-185	11.1	227.9	188.10	171.80	356.40	313.1	11-356
	24	76-168	6.80	155.0	122.30	88.00	260.50	130.4	7-261
	100	24-41	4.40	112.8	84.70	41.80	201.30	32.3	4-201

4.8.2 Operating Costs

Some developers provided a fixed O&M along with variable O&M that covered overhauls. In this study, both have been grouped under fixed O&M. As reported in (Lundy, 2020), the O&M for a CSP plant with molten salt storage was 3.6% of the system capital cost excluding CSP plant cost. Assuming the O&M for the plant excluding CSP is 55% of total O&M cost,⁵⁰ the O&M for a molten salt thermal energy system is assigned 2% of capital cost, with low-temperature molten salt assigned 1.5% of capital cost. The O&M for concrete-based storage is set at 50% of the low-temperature molten salt system O&M, while sand-based system O&M is set at 75% of low-temperature molten salt O&M due to lower complexity for these systems. 2030 O&M costs are assumed to be 90% of 2021 O&M costs. The RTE is assumed to increase by 2 percentage points, while calendar life is left unchanged. O&M costs for each of the thermal technology types in \$/kW-year is provided in the subsections below. The lowest O&M costs correspond to high power and low duration, while the highest O&M costs corresponds to low power and high duration. For the same duration, high-power systems have lower unit power costs, while at fixed power and increasing durations, the O&M costs expressed in \$/kW-year increase as expected.⁵¹

4.8.2.1 Pumped Heat Energy Storage

O&M costs were not provided for PHES systems; therefore, these costs were kept the same as that for a high-temperature molten salt plant (Lundy, 2020). A 10% decrease in O&M cost was assumed by 2030, related to experience gained from 2021 to 2030. Composite PHES fixed O&M for 2021 and 2030 are provided in Table 4.45.

Table 4.45. Composite PHES Fixed O&M (\$/kW-yr), 2021 and 2030

Cost Component	Year	Fixed O&M Cost (\$/kW/year)	Source
O&M (\$/kW-year)	2021	38-228 ^a	Lundy (2020)
	2030	34-205	

^a Not provided directly. Used the same O&M as for a high-temperature molten salt plant: \$38/kW/year at 1,000 MW, 8h and \$228/kW-year at 100 MW, 100h

4.8.2.2 Sensible Heat-based Thermal Storage with AC In, AC Out

The O&M costs are highest for conventional solar salt-based storage, with O&M decreasing in the following order: low-temperature salt, sand, and concrete-based storage. Note that solar salt is the only commercially deployed technology, with actual O&M cost data available. The O&M costs for the other technologies are estimates that need to be validated. However, solar salt with higher maximum temperature, is corrosive. To get around this, alternate storage media such as lower temperature salt, which is known to be less corrosive, and concrete, which is not corrosive, are considered.

Due to the relatively low TRL of thermal ESSs, only nominal cost drops were assigned with a reduction of 10% for O&M costs by 2030.

Composite conventional thermal fixed O&M costs for 2021 and 2030 are provided in Table 4.46.

⁵⁰ This is a conservative estimate since CSP plants have a large footprint, taking significant time to inspect the entire CSP array.

⁵¹ If O&M is expressed in \$/kWh-year, the O&M costs would decrease with increasing duration.

Table 4.46. Composite Conventional Thermal Storage Fixed O&M (\$/kW-yr), 2021 and 2030^a

Year	Sand	Generic Single-Cycle Steam With High T Molten Salt	Combined Cycle With Low T Molten Salt	Concrete	Composite	Source
2021	8-83 ^b	38-228	22-110 ^c	7-55 ^d	7-228	(Lundy, 2020)
2030	7-75	37-205	20-100	6-50	6-205	

^a O&M for high-temperature molten salt storage system estimated at 2% of direct capital cost, assuming it is 55% of O&M for CSP plant and molten salt thermal storage. O&M for low-temperature molten salt system estimated at 1.5% of direct capital cost, with sand- and concrete-based O&M 75% and 50% of this value, respectively.

^b Assumed to be 75% of low-temperature molten salt system O&M.

^c 1.5% of direct capital cost.

^d Assumed to be 50% of low-temperature molten salt system O&M.

4.8.2.3 Liquid Air Energy Storage

O&M costs were provided as a range for conventional LAES, with the higher end of the range applied to 100 MW and lower end to 1,000 MW. The LAES with fuel system O&M was assigned 1.5% of capital cost. Due to its more complex powertrain, the O&M for this system was 1.5–2 times higher than that for a conventional LAES.

Due to the relatively low TRL of thermal ESSs, only nominal cost drops were assigned with O&M dropping by 10% by 2030.

Composite liquid air fixed O&M costs for 2021 and 2030 are provided in Table 4.47.

Table 4.47. Composite Liquid Air Thermal Storage Fixed O&M (\$/kW-yr), 2021 and 2030

Year	Conventional ^a (Highview Power, 2021; Riley, 2021)	With Fuel ^b (Conlon, 2021a; Pintail Power, 2021)	Composite
2021	15-30	36-49	15-49
2030	13.5-27	32-44	13.5-44

^a O&M costs provided are constant at fixed power for various durations, implying energy component costs for hot, cold, and liquid air storage are negligible, which may not be realistic.

^b 1.5% of direct capital costs was recommended.

4.8.2.4 Composite Thermal Energy Storage

O&M costs are set at 2% and 1.5% of direct capital cost for high- and low-temperature molten salt plants, respectively, with sand-based and concrete system O&M set at 75% and 50%, respectively, of low-temperature molten salt system O&M. Costs for various technologies are shown in Table 4.48.

Table 4.48. Fixed O&M Costs for Thermal Storage Technologies and Composite Values by Duration

Power (MW)	Duration (hr)	PHES	Sand	Conventional			Liquid Air		Composite
				Generic Single-Cycle Steam with High T Molten Salt	Combined Cycle with Low T Molten Salt	Concrete	Conventional	With Fuel	
100	4					10.7			11
	6					11.3	30.0		11-30
	8	49.6	18.0			12.0	30.0		12-50
	10	53.7	22.1	53.7	29.4	14.7	30.0	49.0	15-54
	24	81.5	31.8	81.5	42.4	21.2	30.0	49.0	21-82
	100	227.8	82.7	227.8	110.3	55.1	30.0	49.0	30-228
1,000	4					6.9			7
	6					7.6	15.0		8-15
	8	37.6	8.2			8.2	15.0		8-38
	10	41.4	16.2	41.4	21.6	10.8	15.0	36.0	11-41
	24	67.6	25.3	67.6	33.7	16.9	15.0	36.0	15-68
	100	205.2	73.2	205.2	97.6	48.8	15.0	37.1	15-205

4.8.3 Decommissioning Costs

No decommissioning cost estimates have been provided for thermal ESSs. Additionally, given their long calendar life, decommissioning costs are considered to be very small on a present value basis. Thermal energy storage also benefits from easy recyclability of power equipment and for most of the thermal SB. For these reasons, decommissioning costs are not considered in this analysis.

4.8.4 Performance Metrics

RTE for various technologies were provided by developers and compared with thermodynamic efficiency (Thess, 2013); where the RTE was too high a percent of Carnot efficiency, it was reduced. A 42% RTE was used for thermal plants where data were not available.

Due to the relatively low TRL of thermal ESSs, only nominal changes were assigned for 2030. The RTE was increased by 2 percentage points, while calendar life was left unchanged.

4.8.4.1 Pumped Heat Energy Storage

The response time from standby to full generation was estimated at 15 minutes. The RTE had a wide range of 34–60%. The RTE for molten salt storage was 53–60% (Klochko & Lahaye, 2021), while that for sand storage was 60% (Held & Brennan, 2021). The ammonia-based system had an RTE of 31% (Klochko & Lahaye, 2021), hence the RTE of the molten salt-ammonia system was calculated as a weighted average of the molten salt and ammonia energy contents in the tanks, and is 34% for molten salt energy content of 10% of total energy. The calendar life of the PHES system is estimated at 30 years, with the electrolyzer for ammonia production needing to be replaced after 60,000 hours of operation (Klochko & Lahaye, 2021). Assuming continuous operation of the system and using RTE corresponding to various fractions of molten salt energy content, various charge/discharge duration ratios are obtained corresponding to replacement periods of 9–10 years for the electrolyzer stack.

The response time is left unchanged for 2030, while 2 percentage points were added to the RTE. There is not sufficient visibility to estimate calendar life increase for this low TRL technology. Composite PHES performance parameters for 2021 and 2030 are provided in Table 4.49.

Table 4.49. Composite PHES Performance Parameters for 2021 and 2030

Component	Year	Value	Comments	Source
RTE	2021	0.35-0.60	31% for ammonia system, 53-60% for molten salt, system RTE is weighted average.	Dufo-López et al. (2021), Klochko and Lahaye (2021), Held and Brennan (2021)
	2030	0.37-0.62		Dufo-López et al. (2021), Klochko and Lahaye (2021)
Response Time	2021	15 minutes from standby to full generation		Dufo-López et al. (2021)
	2030	5 minutes from standby to full generation	Improvement driven by system air volume reductions over time.	
Calendar Life (years)	2021 & 2030	9–10 years for electrolyzer stack, 30-33 years for system	60,000 hours for electrolyzer stack corresponds to 9–10 hours, 200,000 hours for rest of system corresponds to 30-33 years, based on RTE of 35 to 47%.	Dufo-López et al. (2021), Klochko and Lahaye (2021)

4.8.4.2 Conventional Thermal Storage with AC In, AC Out

The RTE for conventional thermal storage is in the 0.41–0.51 range, with combined-cycle plants corresponding to higher efficiency.⁵² The expected calendar life is 35 years. For 2030, the RTE was increased by 2 percentage points, while calendar life was left unchanged. Composite conventional thermal performance parameters for 2021 and 2030 are provided in Table 4.50.

Table 4.50. Composite Conventional Thermal Performance Parameters for 2021 and 2030

Component	Year	Conventional Thermal Storage with AC in, AC out				Composite
		Sand	Generic Single-Cycle Steam with High T Molten Salt	Combined Cycle with Low T Molten Salt	Concrete	
Source		Ma (2021a)	Lundy (2020)	W. Conlon (2021b)	Capp (2021)	
RTE	2021	0.5	0.42	0.514	0.41	0.41-0.51
	2030	0.52	0.44	0.534	0.43	0.43-0.53
Calendar Life	2021 & 2030	35	35	35	35	35

⁵² Note that this efficiency includes energy related to fuel consumed and electricity for resistance heating.

4.8.4.3 Liquid Air Energy Storage

The RTE for LAES was in the 0.5-0.55 range, while the calendar life was 35 years. Due to the relatively low TRL of thermal ESSs, only nominal changes were assigned for 2030. The RTE was increased by 2% percentage points while calendar life was left unchanged. Composite liquid air thermal storage performance parameters for 2021 and 2030 are provided in Table 4.51.

Table 4.51. Composite Liquid Air Performance Parameters for 2021 and 2030

Component	Year	LAES		Composite
		Conventional ^a	With Fuel ^b	
RTE	2021	0.50-0.55	0.514 ^a	0.5-0.55
	2030	0.52-0.57	0.534	.54-.59
Calendar Life (years)	2021 & 2030	35		35

^a Riley (2021)

^b Conlon (2021a)

4.8.4.4 Composite Thermal Energy Storage

Table 4.52 presents composite performance parameter values for thermal systems.

Table 4.52. Composite Performance Parameters for Thermal Systems, 2021 and 2030

Power (MW)	Year	PHES	Sand	Conventional			Liquid Air		Composite
				Generic Single-Cycle Steam with High T Molten Salt	Combined Cycle with Low T Molten Salt	Concrete	Conventional	With Fuel	
RTE	2021	0.35-0.60	0.50	0.42	0.514	0.41	0.50-0.55	0.514	0.35-0.60
	2030	0.37-0.62	0.52	0.44	0.534	0.43	0.52-0.57	0.534	0.37-0.62
Calendar Life (years)	2021 & 2030	30-33	35	35	35	35	35	35	30-35

4.8.5 Results

Figure 4.25 and Figure 4.26 show the 2021 and 2030 total installed cost and performance parameters for 100 MW and 1,000 MW; 4-, 10-, and 24-hour systems; and the installed cost ranges for all power capacity and energy durations, respectively, for thermal.

2021 & 2030 Thermal
Installed Costs & Performance Parameters

ESS Installed Cost	ESS	Storage System	2021 & 2030 Thermal											
			100 MW						1,000 MW					
			4 hr		10 hr		24 hr		4 hr		10 hr		24 hr	
		2021	2030	2021	2030	2021	2030	2021	2030	2021	2030	2021	2030	
		Thermal Capital (SB + BOS) (\$/kWh)	\$39.94	\$33.95	\$64.44	\$54.77	\$54.13	\$46.01	\$37.54	\$31.91	\$57.06	\$48.50	\$48.65	\$41.35
		Power Equipment (\$/kW)	\$1,662.70	\$1,579.57	\$1,613.59	\$1,532.91	\$1,780.59	\$1,691.56	\$1,046.60	\$994.27	\$1,101.53	\$1,046.45	\$1,268.53	\$1,205.10
		EPC Fee, Project Development, & Grid Integration (\$/kWh)	\$139.68	\$131.65	\$64.70	\$63.62	\$36.01	\$35.45	\$92.76	\$86.97	\$47.58	\$47.07	\$28.25	\$27.94
		Total Installed Cost (\$/kWh)	\$595.30	\$560.49	\$290.50	\$271.68	\$164.33	\$151.94	\$391.95	\$367.45	\$214.80	\$200.22	\$129.76	\$119.51
		Total Installed Cost (\$/kW)	\$2,381	\$2,242	\$2,905	\$2,717	\$3,944	\$3,647	\$1,568	\$1,470	\$2,148	\$2,002	\$3,114	\$2,868
Operating Costs														
		Fixed O&M (\$/kW-yr)	\$10.68	\$9.61	\$32.34	\$29.11	\$42.77	\$38.49	\$6.95	\$6.25	\$24.15	\$21.74	\$33.96	\$30.56
Performance Parameters														
		RTE (%)	51%	53%	52%	54%	50%	52%	51%	53%	52%	54%	50%	52%
		Cycle Life (#)	Unlimited		Unlimited		Unlimited		Unlimited		Unlimited		Unlimited	
		Calendar Life (yrs)	35.00	35.00	34.00	34.00	34.00	34.00	35.00	35.00	34.00	34.00	34.00	34.00
		DOD (%)	80%	80%	80%	80%	80%	80%	80%	80%	80%	80%	80%	80%

Figure 4.25. 2021 and 2030 Total Installed Cost Estimates – Thermal

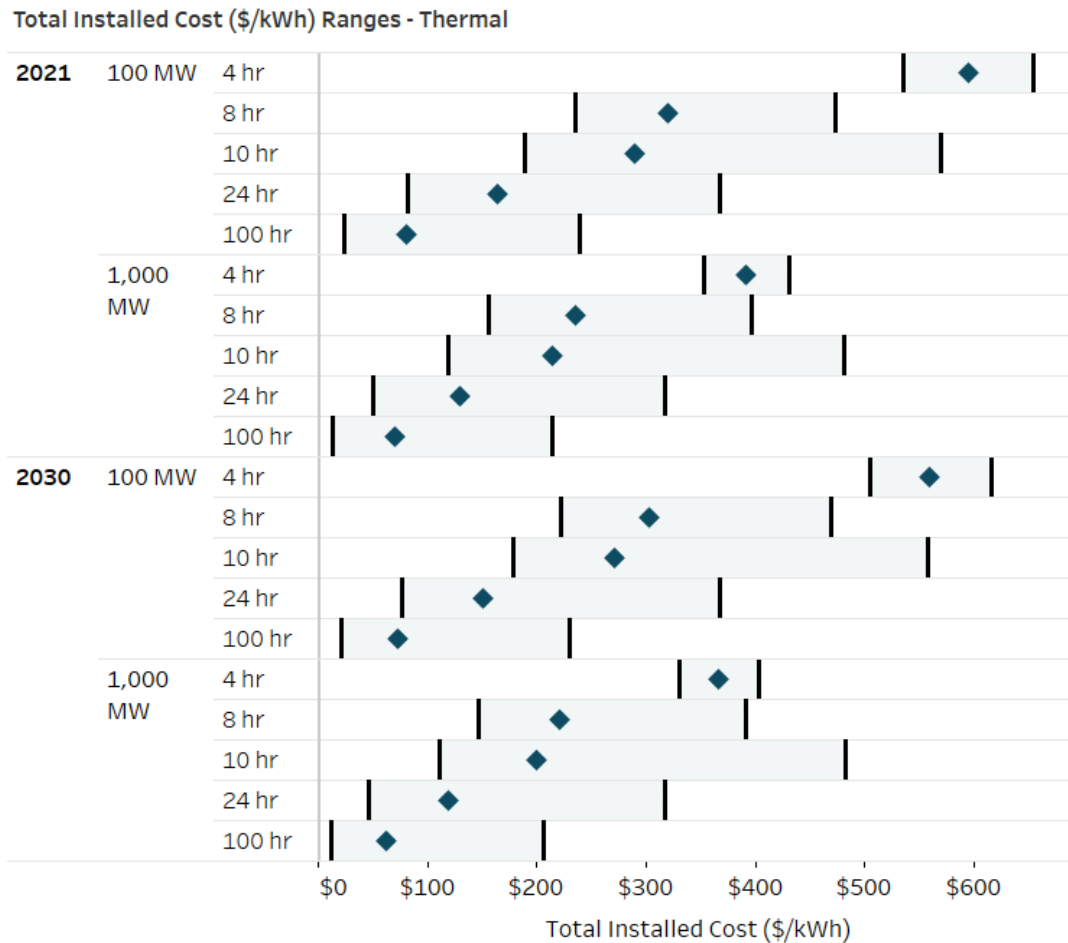


Figure 4.26. 2021 and 2030 Total Installed Cost Ranges – Thermal

4.9 Hydrogen

There are multiple HESS configurations that may be useful in different use cases. The configuration analyzed in this report, however, is bidirectional storage using fuel cells. This configuration further involves using a PEM electrolyzer to generate hydrogen from water with an electrical current (releasing oxygen as a byproduct) before compressing and storing the hydrogen in underground salt caverns until needed. The hydrogen is later re-electrified using the fuel cells to produce electricity.

HESS consists of three major components:

- Charging system includes electrolyzer modules, BOP, water-handling units, mass flow controllers, electrolyzer management system, compressor, and rectifier.
- Discharging system consists of stationary fuel cell modules, BOP, gas-handling units, blowers, mass flow controllers, fuel cell management system, and inverter.
- The storage system typically includes pipes or a cavern.

4.9.1 Capital Cost

Capital cost estimates for HESS for 2021 remain predominantly consistent with the 2020 report values for all cost elements except the cavern storage cost (\$/kWh) (Mongird et al., 2020b) and electrolyzer cost of \$1316/kW⁵³ (Rustagi, 2022). The fuel consumption per kWh for PEM fuel cell system is estimated at 0.052 kg H₂/kWh⁵⁴, from its electrochemical efficiency of 0.507 based on its high heating value (HHV) (Hunter et al., 2021), its HHV of 285.8 kJ/mole (Harrison et al., 2010), the thermoneutral potential for water decomposition of 1.482V (Barbir, 2005), and a combined one way efficiency of 0.96 for the inverter and transformer. Air consumption per kWh, along with CAES RTE were obtained from (Mongird et al., 2020b), using a molecular weight of 28.97 g/mole (Engineering ToolBox, 2014). The required moles (air/kWh) for CAES is 3.39 times higher than the required moles of hydrogen to generate the same amount of electricity (Barbir, 2005; Engineering ToolBox, 2014; Harrison et al., 2010; Scribner, 2017). This improves on the 2020 report assumption that the moles required would be equivalent for both air and hydrogen. However, despite hydrogen caverns being smaller for fixed-energy content, cavern cost per kWh of energy discharged for hydrogen can be slightly higher than for CAES due to the need for higher grade equipment (Howitt, 2021).

As described previously in the CAES section (Section 4.5.1), the average cavern storage cost for CAES is \$6.9/kWh, with low and high values of \$2.7/kWh and \$13.8/kWh, respectively. An additional data point for cavern costs for hydrogen storage was obtained for a cavern depth of 200 m, located 765 m below ground based on a cost of \$35.6/kg (Papadis & Ahluwalia, 2022) and 19.3 kWh/kg (Hunter et al., 2021), resulting in an estimated cavern cost of \$1.8/kWh. Adding this data point to the set of values for CAES cavern costs (Section 4.5.1) leads to an average of \$6.05/kWh for hydrogen (compared to \$6.9/kWh for CAES) for a 100 MW, 8-hour system. The low value for cavern cost is \$1.8/kWh, while the high value is unchanged at \$13.8/kWh. The wide range of cavern costs reported indicate a clear need for further study and refinement.

The DOE is establishing new goals and targets for electrolyzer capital costs and efficiency in support of DOE's Hydrogen Shot. These goals aim to reduce the cost of low-temperature electrolyzers to ≤ 250 /kW for PEM electrolyzers by 2026, assuming high-volume manufacturing, with an efficiency of 46 kWh/kg (Rustagi, 2022). For the fuel cell system, a \$900/kW cost target is established, with a 60% efficiency target (Rustagi, 2022).

In the current report, the future electrolyzer cost is assumed to be \$350/kW (Hunter et al., 2021; Rustagi, 2022), while the fuel cell system, rectifier and inverter costs are assumed to be \$425/kW, \$84/kW and \$38.9/kW respectively (Hunter et al., 2021). For this report, 2021 stationary fuel cell cost estimates remain consistent with the values presented in the 2020 report. While a pilot demonstration of HESS has not yet taken place, developments in the transportation sector for hydrogen fuel cell to power heavy duty vehicles are expected to accelerate grid-scale storage deployment. Future technology improvements have the potential to reduce costs; for example, shared power electronics between electrolyzer and fuel cell systems, or in a completely unitized reversible fuel cell that can both produce

⁵³ The electrolyzer + rectifier cost with mark-up is estimated at \$1300/kW (adapted from draft DOE record (Badgett, et. al., National Renewable Energy Laboratory, 2022). With rectifier cost of \$130/kW, this corresponds to \$1170/kW for electrolyzer. Adding 12.5% installation cost yields electrolyzer cost of \$1316/kW.

⁵⁴ This corresponds to 19.3 kWh/kg H₂

hydrogen and convert it to electricity in the same stack, depending on the controlled mode of operation, have the potential to reduce system costs (E. Miller, 2022).

4.9.2 Operating Costs

4.9.2.1 Fixed O&M

Fixed O&M costs for hydrogen consists of labor-related O&M (\$9/kW-year for 100 MW systems, and \$2.7/kW-year for 1,000 MW systems) following the same procedure as PSH; power equipment-related O&M (0.43% of the total CAPEX), storage-related O&M (0.43% of the additional storage-related CAPEX above 10 hours, 14 hours of additional storage for a 24 hour system), and power equipment augmentation every ten years at 30% of the power equipment cost. In combination, these items result in a fixed O&M cost range between \$17 and \$27/kW-year for 2021.

4.9.2.2 Warranty

No warranty information is included for HESS at this time due to data availability. The limited number of HESS in operation precludes mature business models including warranties.

4.9.3 Decommissioning Costs

No decommissioning information is included for HESS at this time. The limited number of HESS in operation precludes mature business models reaching the end of life.

4.9.4 Performance Metrics

4.9.4.1 Calendar Life

The plant life for HESS is estimated to remain the same as the 2020 estimate at 30 years. The calendar life for the electrolyzer and fuel cell stacks has been assumed to be 30 years, with a 20-25 year life assigned for BOP components such as compressors and air and fuel delivery systems. Replacement of BOP components are included in fixed O&M costs for hydrogen in order to reach a 30-year plant life. The calendar life is left unchanged for 2030.

4.9.4.2 Round-trip Efficiency

System efficiency for HESS depends on fuel cell and electrolyzer efficiency, along with energy required to compress hydrogen. Note that losses during storage have not been accounted for in the RTE calculation. Using the same fuel cell and electrolyzer efficiency of 50.7% and 72.5% respectively as stated in the 2020 report, and accounting for 5 kWh/kg electricity consumption by compressors for compression of hydrogen up to 200 bars (Rustagi, 2021), the RTE at the DC and AC levels drop by nearly 3 percentage points.

Table 4.53 provides information on the conversion from DC-DC RTE to AC-AC RTE inclusive of two-way transformer efficiency. The RTE used in this report for the final summary table, as well as the value used in the LCOS calculations later, is the AC-AC RTE inclusive of inverter and transformer efficiency losses. The RTE is left unchanged for 2030.

Table 4.53. Hydrogen DC-DC and AC-AC RTE Values

DC-DC RTE		AC-AC RTE at Inverter Level ¹		AC-AC RTE at Transformer Level ²	
2021	2030	2021	2030	2021	2030
34%	34%	32%	32%	31%	31%

¹. Assumes a two-way inverter efficiency of (.98)²

². Assumes a two-way transformer efficiency of (.98)²

4.9.5 Results

Figure 4.27 and Figure 4.28 show the 2021 and 2030 total installed cost and performance parameters for 100 MW and 1,000 MW, 10-hour, and 24-hour systems and the installed cost ranges for all power capacity and energy durations, respectively, for HESS.

2021 & 2030 Hydrogen
Installed Costs & Performance Parameters

		100 MW				1,000 MW					
		10 hr		24 hr		10 hr		24 hr			
		2021	2030	2021	2030	2021	2030	2021	2030		
ESS Installed Cost	ESS	Storage System	Fuel Cell (\$/kW)	\$1,320	\$425	\$1,320	\$425	\$1,320	\$425	\$1,320	\$425
			Electrolyzer (\$/kW)	\$1,316	\$350	\$1,316	\$350	\$1,316	\$350	\$1,316	\$350
			Cavern Storage (\$/kWh)	\$6.00	\$6.00	\$5.82	\$5.82	\$5.53	\$5.53	\$5.36	\$5.36
			Compressor (\$/kW)	\$39.30	\$39.30	\$39.30	\$39.30	\$39.30	\$39.30	\$39.30	\$39.30
			Inverter (\$/kW)	\$67.00	\$39.00	\$67.00	\$39.00	\$67.00	\$39.00	\$67.00	\$39.00
			Rectifier (\$/kW)	\$130.00	\$84.00	\$130.00	\$84.00	\$130.00	\$84.00	\$130.00	\$84.00
			C&C (\$/kW)	\$1.50	\$1.06	\$1.50	\$1.06	\$1.50	\$1.06	\$1.50	\$1.06
			Grid Integration (\$/kW)	\$19.89	\$16.30	\$19.89	\$16.30	\$19.89	\$16.30	\$19.89	\$16.30
			Total Installed Cost (\$/kWh)	\$295.37	\$101.46	\$126.39	\$45.60	\$294.90	\$101.00	\$125.93	\$45.13
			Total Installed Cost (\$/kW)	\$2,954	\$1,015	\$3,033	\$1,094	\$2,949	\$1,010	\$3,022	\$1,083
Operating Costs											
	Fixed O&M (\$/kW-yr)	\$23.21	\$14.30	\$23.90	\$15.00	\$16.89	\$7.98	\$17.52	\$8.62		
Performance Parameters											
	RTE (%)	31%	31%	31%	31%	31%	31%	31%	31%		
	Cycle Life (#)	Unlimited		Unlimited		Unlimited		Unlimited			
	Calendar Life (yrs)	30	30	30	30	30	30	30	30		
	DOD (%)	80%	80%	80%	80%	80%	80%	80%	80%		

Figure 4.27. 2021 and 2030 Installed Costs and Performance Parameters – Hydrogen

Total Installed Cost (\$/kWh) Ranges - Hydrogen

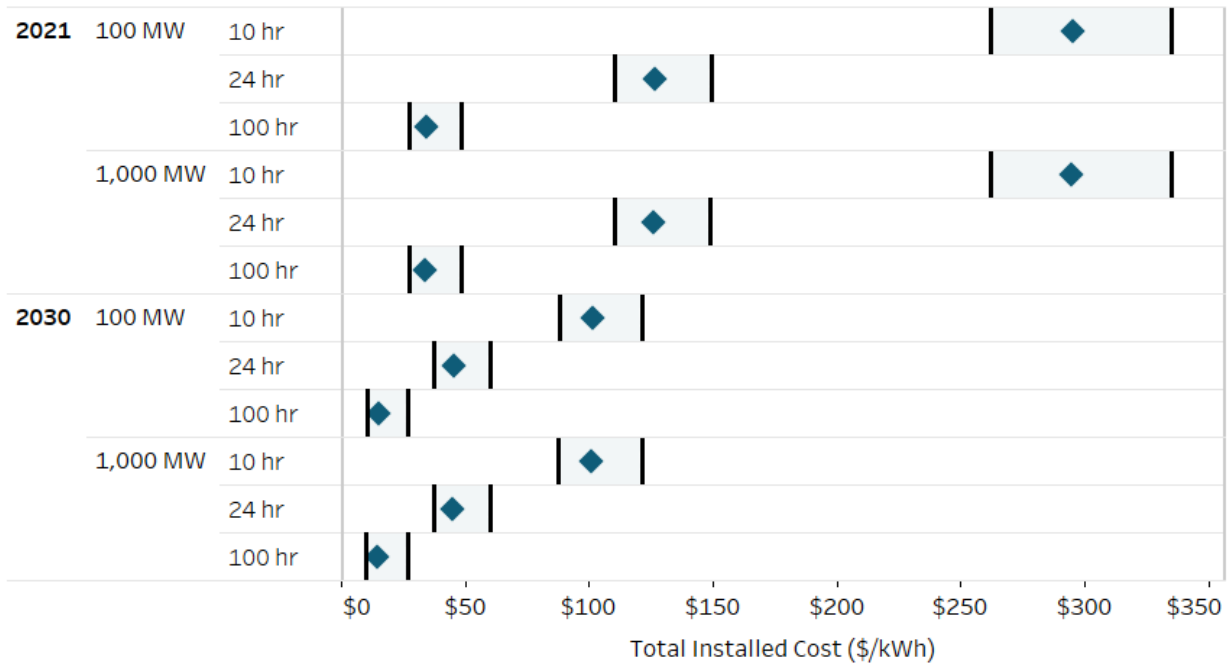


Figure 4.28. 2021 and 2030 Total Installed Costs Ranges – Hydrogen

5 Comparative Results

5.1 Total Installed Cost

Figure 5.1 shows total installed ESS costs (\$/kWh) for all storage systems, power capacities, and energy duration combinations for 2021. Estimates shown represent the point estimates for each technology. Figure 5.2 shows the same information as Figure 5.1 but for the year 2030. Some high-level observations and takeaways from these results include the following:

- BESSs remain mostly in the range of \$300-\$600/kWh across all power capacity and energy duration combinations. Non-battery systems, on the other hand, range considerably more depending on duration. Looking at 100 MW systems, at a 2-hour duration, gravity-based energy storage is estimated to be over \$1,100/kWh but drops to approximately \$200/kWh at 100 hours.
- Li-ion LFP offers the lowest installed cost (\$/kWh) for battery systems across many of the power capacity and energy duration combinations. At higher durations, however, vanadium RFBs appear to be highly competitive with these systems.
- The total installed cost for battery systems decreases as duration increases, with the narrowest range of costs appearing for a 100-hour system, mainly due to sharp drop of redox flow battery cost.
- CAES offers the lowest total installed cost (\$16/kWh for a 1,000 MW, 100-hour system), followed by hydrogen (\$34/kWh), PSH (\$69/kWh), thermal (\$70/kWh), and gravitational (\$131/kWh). Battery systems offer a significantly higher cost at this power capacity and duration combination, in the range of \$296/kWh (RFB) and \$354/kWh (Li-ion NMC). This cost trend remains in place for 100 MW, 100-h systems as well.
- For the 100 MW and 1000 MW power levels, CAES is the lowest cost option for ≥ 4 hours, with thermal, PSH and HESS being more cost effective than batteries at ≥ 8 hours. The cross-over for gravity occurs at ≥ 24 hours for 100 MW, and ≥ 6 hours for 1000 MW, due to its higher energy related scaling effect.
- Looking at 2030 estimates, battery systems are expected to decrease to within the range of approximately \$230-\$690/kWh, with Li-ion LFP at the lower end of the range.
- LFP systems are expected to become roughly equivalent to or lower than both PSH and thermal systems in total installed cost at the 100 MW, 10-hour duration by 2030.

2021 Total Installed Cost Comparison, \$/kWh

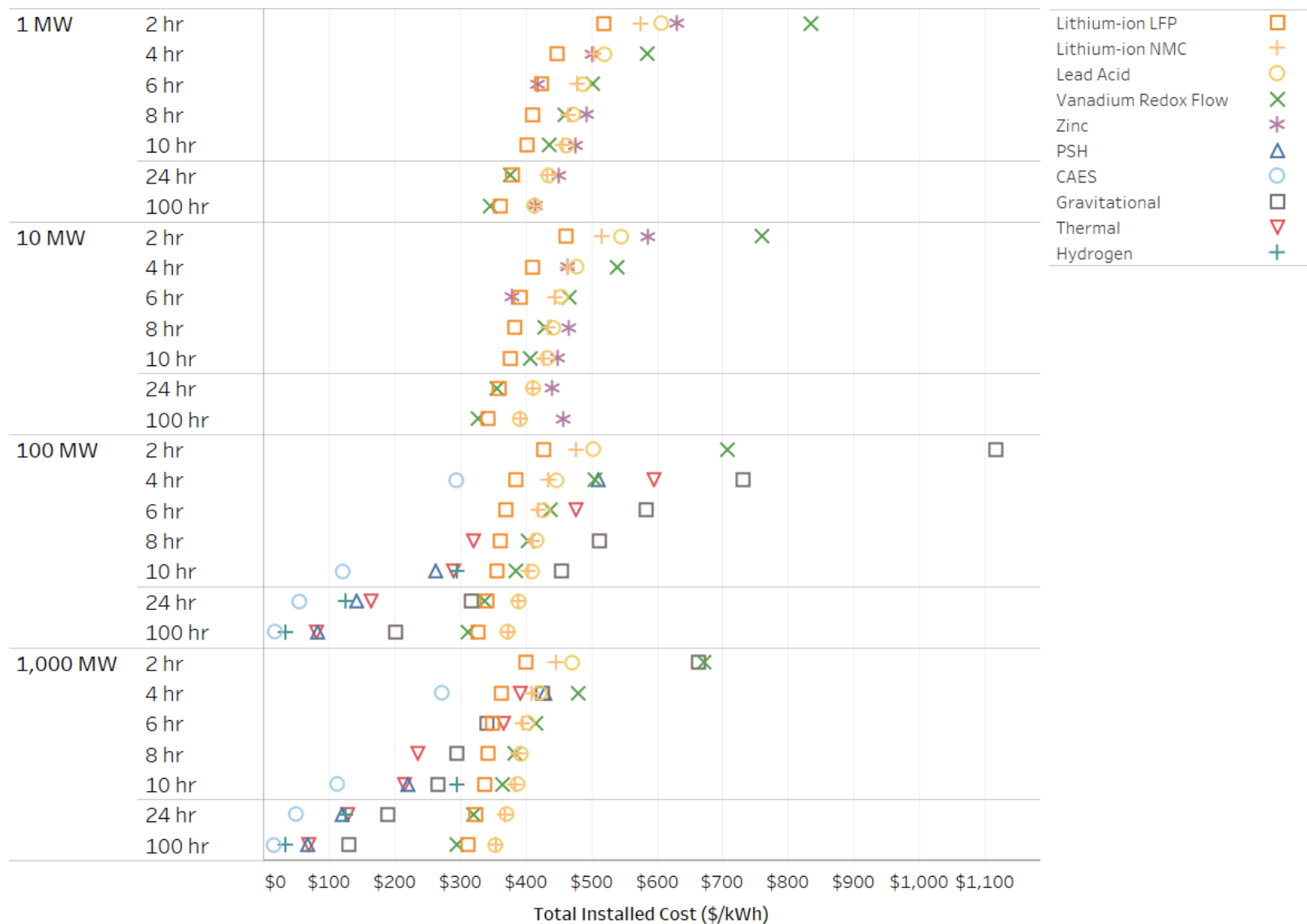


Figure 5.1. Comparison of Total Installed ESS Cost Point Estimates by Technology, 2021 Values

2030 Total Installed Cost Comparison, \$/kWh

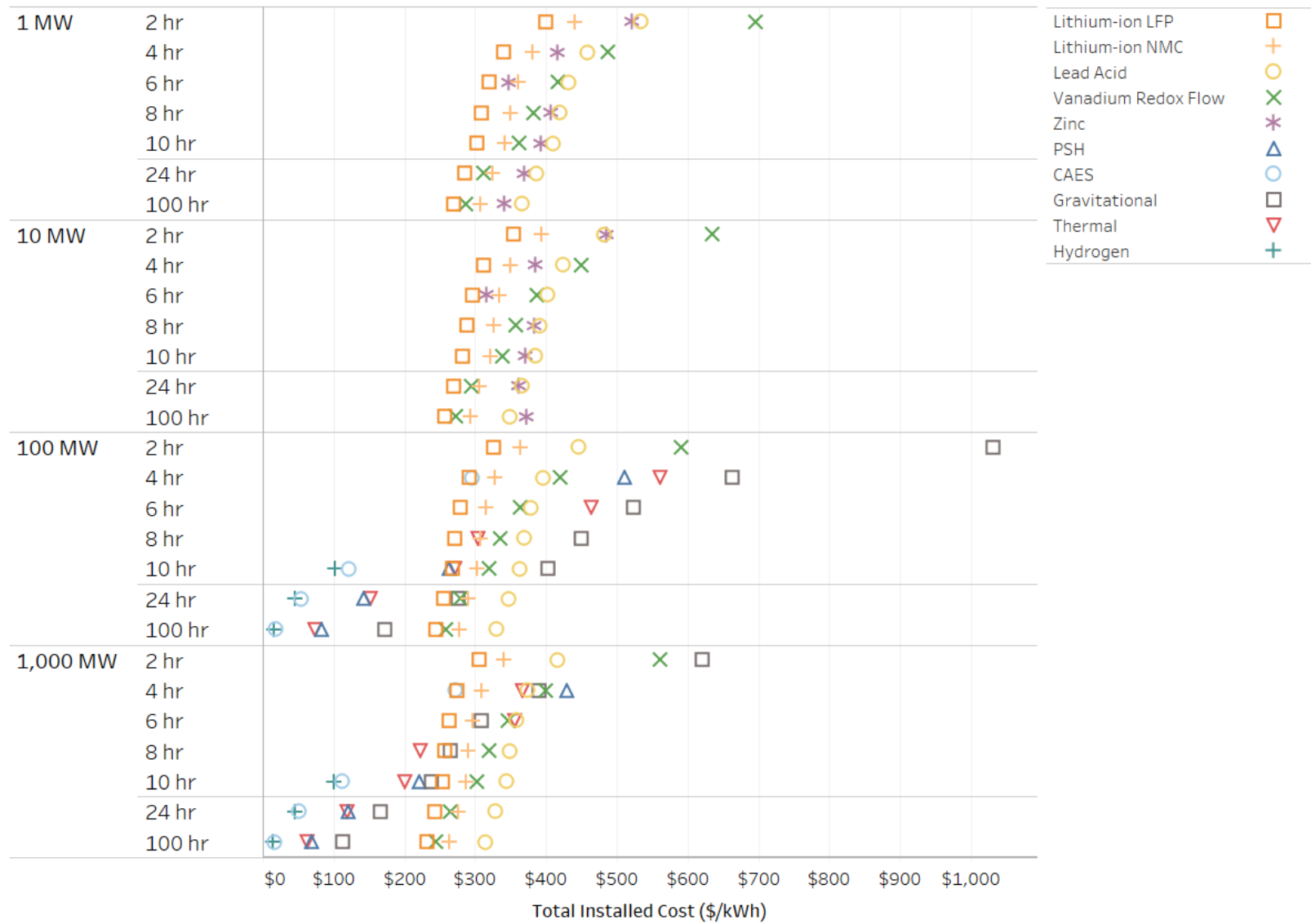


Figure 5.2. Comparison of Total Installed ESS Cost Point Estimates by Technology, 2030 Values

5.2 Performance Parameters

The performance parameters that impact LCOS the most are RTE, cycle life and calendar life. As seen in Table 6.4, vanadium RFB and all non-battery technologies have unlimited cycle life. Plotting the RTE vs. calendar life and cycle life can provide a snapshot of the energy storage performance.

Figure 5.3 shows RTE vs. calendar life for 100 MW, 10-hour systems. Battery systems generally have a calendar life in the range of 10–15 years and higher RTEs than nonelectrochemical storage systems, while the latter have calendar life in the 30–60 year range. LFP and NMC have the highest RTE of any storage system included at approximately 84%. Vanadium RFBs have the lowest RTE of the battery systems of approximately 65%. Note that the 12-year calendar life for vanadium RFBs only applies to stacks, since the electrolyte life is unlimited. Zinc does not have cost and performance estimates at 100 MW, and the values shown in the figure represent a 10 MW, 10-hour system instead. At this power capacity and energy duration, zinc falls between vanadium RFB and lead acid in terms of RTE and has the highest calendar life of all battery systems at just over 17 years. Of the non-battery systems, gravitational storage has the highest RTE (83%) and the second highest calendar life (49 years), while PSH with an RTE of 80% and calendar life of 60 years offers both high RTE and life. HESS has the lowest RTE of the included systems at 31%.

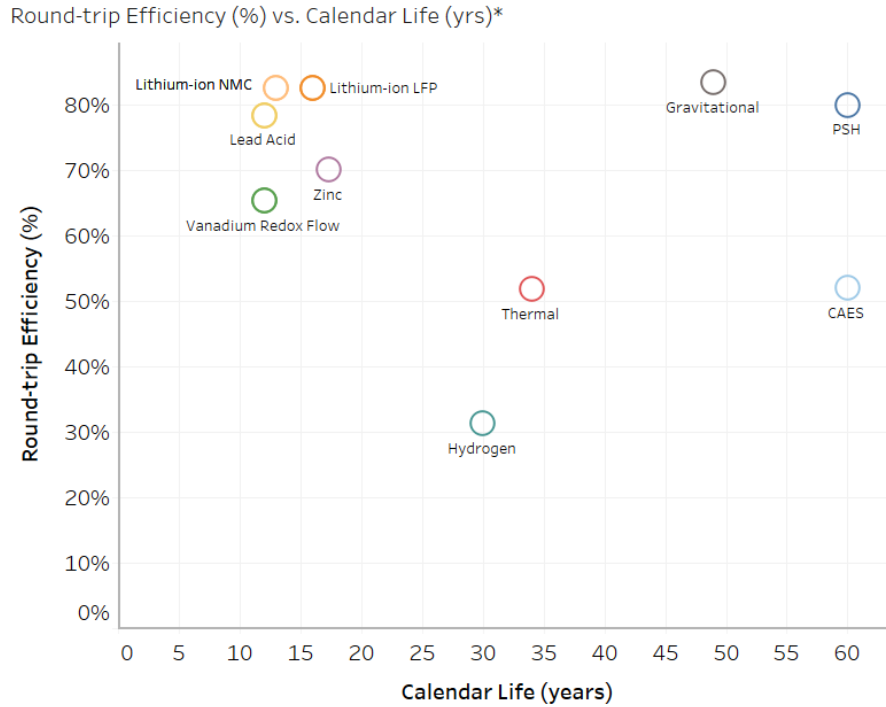
The RTE vs. calendar life plot doesn't take into account the fact that vanadium redox flow battery has unlimited cycle life for the electrolyte. It also doesn't consider the fact that at the 80% DOD selected in this report, batteries need augmentation or replacement well before the calendar life is reached. Figure 5.4 shows RTE vs. cycle life for battery technologies with finite cycle life. As discussed earlier, the end of life for Li-ion batteries is reached when available energy decreases linearly to 60% of rated energy. Hence, batteries cycled at 80% DOD can provide at least the same energy throughput from the end of 80% DOD cycling to battery end of life. These batteries are cycled at 60% DOD once available energy decreases to 80% of rated energy at the end of 80% DOD cycling. The cycle life for these batteries at 80% DOD to end of life is estimated by adding the cycle life at 80% DOD to half the cycle life at 60% DOD with adjustments as given by cycle life at 80% DOD to end of life being equal to the cycle life at 80% DOD to 50% State of Health⁵⁵ + 0.5*(cycle life at 60% DOD) * (60/80).⁵⁶

For lead-acid and zinc batteries, end of life corresponds to when available energy decreases to 80% of rated energy. Note that since zinc batteries have a wide range of cycle life for different durations, the average cycle life at all duration is used in this figure.

While zinc batteries have cycle life comparable to Li-ion NMC technology, this high cycle life is influenced by data from one developer which was on the high end and needs further validation. The advantage of Li-ion technology is apparent from this figure, with 4-5 times the cycle life of lead-acid batteries, with the latter requiring multiple replacements during project life.

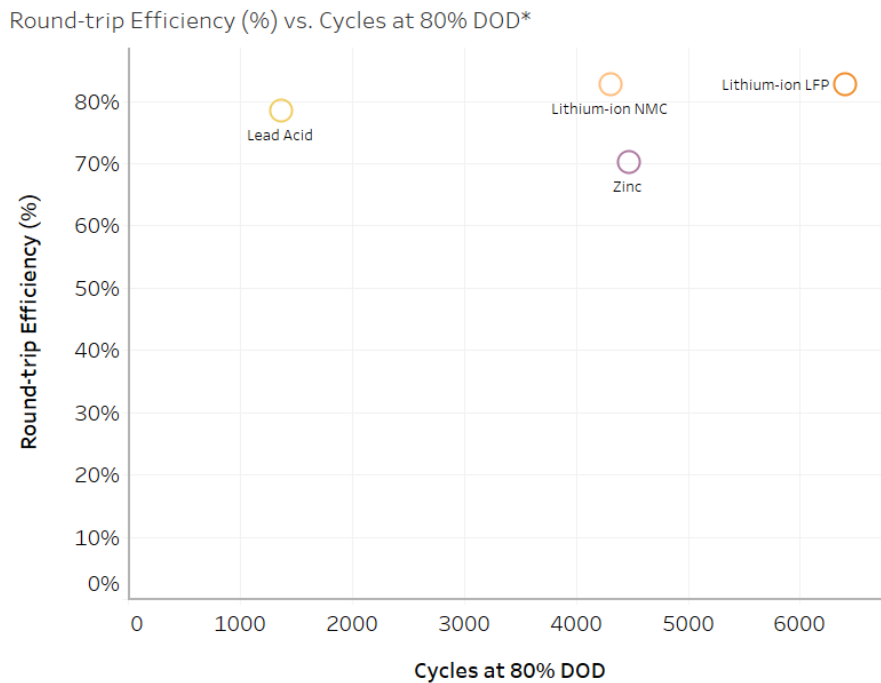
⁵⁵ 50% state of health is reached when available energy after full charge is 80% of rated energy

⁵⁶ This converts cycles at 60% DOD to equivalent cycles at 80% DOD.



* All systems shown are 100 MW, 10 hours except for zinc which does not have estimates at that power capacity. Zinc estimates correspond to a 10 MW, 10 hour system.

Figure 5.3. RTE vs. Calendar Life for 100 MW, 10-hour Systems



* All RTE values shown are associated with 100 MW, 10 hour systems except for zinc which does not have estimates at that power capacity. Zinc RTE corresponds to a 10 MW, 10 hour system.

Figure 5.4 RTE vs. Cycles at 80% Depth of Discharge

6 Levelized Cost of Storage

The 2022 report moves from reporting a levelized cost of energy to an LCOS to better capture the attributes of storage and align with DOE cost targets for the Long-Duration Energy Storage Earthshot. LCOS still represents a cost per unit of energy (\$/kWh or \$/MWh) metric that can be used to compare different storage technologies on a more equal footing than comparing their installed costs. Different systems have different calendar life, cycle life, DOD limitations, and O&M costs, and may require various capital expenditures over time in the form of major overhauls and replacements. Each of these characteristics and parameters, in addition to taxes, costs due to debt, and others, ultimately define the total cost of a storage system over the lifetime of a project.

6.1 Methodology

6.1.1 Overview

The LCOS methodology follows that of the previous cost and performance analysis in (Mongird et al., 2020b) with a number of adaptations that have been made to better represent operation of the various storage assets, investment decisions, and other factors. These adaptations, which impact the LCOS, include the following:

- This analysis built on the previous report to include augmentation and replacements to meet a specific project life. These replacements have been incorporated into the 2021 analysis and are described in more detail later in this section.
- The previous analysis, given that it did not include augmentations and replacements, set the economic life (years to pay off assets) to the technology life. The 2021 analysis now sets a baseline assumption that the economic life for each project is 20 years with a 30-year economic life considered for a sensitivity analysis.
- Additional adaptations have been made to account for construction time of projects and associated financing. This, along with a selection of financial parameter inputs, were adapted from the LCOS methodology presented in NREL (2021).
- An enhanced methodology for the annual cumulative energy discharged from the storage system has been developed and incorporated into the LCOS calculation. The improved methodology considers factors such as cycle life related limitations on maximum allowable annual cycles and includes rest time assumptions for each technology after charging and discharging. More information on this methodology is provided later in this section.

The LCOS determined from this analysis provides a \$/kWh value that can be interpreted as the average \$/kWh price that energy output from the storage system would need to be sold at to break even on total costs.

Equation 1 below shows the LCOS calculation.

$$LCOS = \frac{[(FCR \times CAPEX_{PV}) + O\&M_{Fixed}]}{AH} + ECC \quad (1)$$

Where:

$LCOS$ = Levelized cost of storage (\$/kWh)

FCR = Fixed Charge Rate (%)

$CAPEX_{PV}$ = Present value of capital expenditures (\$/kW)

$O\&M_{Fixed}$ = Annual fixed O&M (\$/kW-year)

AH = Annual hours discharged

ECC = Electricity charging cost (\$/kWh-discharge) inclusive of costs due to losses (ECC = charging cost for purchased energy [\$/kWh] divided by system RTE [%]).

A more detailed explanation of each of the parameters and variables included in the LCOS calculation along with definitions of variables in Equation 1 can be found in the appendix.

6.1.2 Assumptions and Parameters

Inputs into the LCOS model consist of (1) capital cost data, (2) operational data, and (3) various financial parameters. The first and second of these were presented in the individual technology sections of this report. The assumed financial parameters for the LCOS calculation are shown in Table 6.1. The inflation rate assumed for the analysis is taken from the 2021 U.S. Congressional Budget Office Budget and Economic Outlook report (Swagel, 2021). The interest rate and cost of equity parameter assumptions follow those provided in NREL (2021).⁵⁷ The assumed tax rate follows the same rate used in Mongird et al. (2020b).

Table 6.1. Financial Parameters and Assumptions

Parameter	Value
Inflation rate	2.80%
Interest rate – nominal	8.00%
Interest rate – real	5.06%
Cost of equity – nominal	13.00%
Cost of equity – real	9.92%
Debt fraction	50.0%
Tax rate (Federal and State)	24.873%
Weighted average cost of capital (WACC) – nominal	9.51%
WACC – real	6.52%
Electricity charging cost (\$/kWh)	\$0.03/kWh ⁵⁸

There are multiple timespans that must be properly accounted for depending on technology. These include:

- Construction period – The assumed number of years necessary to complete construction prior to operation.

⁵⁷ The financial assumptions adapted from NREL (2021) follow those used in the Regional Energy Deployment System model.

⁵⁸ The electricity cost of \$0.03/kWh used in the LCOS calculation are closely aligned with the ARPA-E DAYS program and the SunShot Initiative –

https://arpa-e.energy.gov/sites/default/files/documents/files/DAYS_ProgramOverview_FINAL.pdf

<https://www.energy.gov/eere/solar/sunshot-2030>

- Calendar life – The maximum number of years of operation available before storage system (e.g., DC SB in the case of Li-ion) replacement or decommissioning is necessary, regardless of cycle life.
- Project life – The total number of years, inclusive of construction and operation, until project decommissioning. For non-batteries, this is equivalent to the calendar life plus construction time. For battery systems (not including RFB) this is a variable value between 20–25 years of operation in addition to construction time and will depend on the frequency of SB augmentation/replacement. That is, if the augmentation/replacement is slated to occur in year 20-25, the project life is concluded in that year. Note that for RFBs, the electrolyte and tank are assumed to not need augmentation/replacement, while the stacks are replaced every 12 years, leading to a project life of the sum of construction time and two times the stack replacement time.
- SB replacement period – The minimum of cycle life in years⁵⁹ and calendar life for a given battery system operating at a specified DOD, not considering augmentation. Augmentation is discussed in greater detail later in this section.
- Economic life – Length of time to pay off assets (assumed 20 years for all technologies in this report).
- Tax depreciation period – The number of years in the tax depreciation schedule,⁶⁰ variable by technology.

The assumed project life and construction period of each ESS are listed in Table 6.1. Construction period varies by technology, with batteries assumed to require only one year of construction prior to operation. Systems that may require land excavation, solution mining, and/or power plant construction (gravitational, CAES, thermal, and hydrogen) are assumed to take 3 years. PSH projects typically require more intensive land excavation and construction and are assumed to have a construction period of 5 years. Note that, historically, larger projects such as PSH have taken more than 5 years due to environmental assessments or unforeseen construction delays. The value used here is considered moderately optimistic for some projects.

Table 6.2. Assumed Project Life and Construction Period for Each Energy Storage Technology

Storage Technology	Project Life (years)	Construction Period (years)
Li-ion LFP	20-25	1
Li-ion NMC	20-25	1
Lead-acid	20-25	1
Vanadium RFB	24	1
Zinc	20-25	1
PSH	60	5
CAES	60	3

⁵⁹ Cycle life is number of cycles at a specific DOD. Cycle life in years is equal to the number of cycles at a specific DOD/cycles per year.

⁶⁰ As related to the modified accelerated cost recovery system, half-year convention

Storage Technology	Project Life (years)	Construction Period (years)
Hydrogen	30	3
Gravitational	52	3
Thermal	30-35	3

For the tax depreciation period, battery storage projects that are not tied to another use (as is the case in solar plus storage) are classified as a 7-year property (Elggqvist, Anderson, & Settle, 2018). For non-batteries, projects with initial “clearing and grading land improvements with respect to any electric utility transmission and distribution plant” are assumed to be 20-year properties (Cornell Law School, 2021). The latter assumption additionally follows the depreciation period used in NREL (2021) for PSH.

Cycle life and DC SB replacement and augmentation periods vary by DOD, storage duration, RTE, and recommended rest after charge and discharge. More information on how the DC SB replacement and augmentation period is determined is provided in the next section. As mentioned, the project life for battery systems is a variable value between 20–25 years. Flexible project durations were built into account for variable DC SB replacement and augmentation periods.

6.1.3 Cycles Per Day and Annual Discharge Methodology

The number of cycles per year depends on DOD and the maximum annual allowable discharge energy based on developer’s warranty and technological characteristics such as duration of charge, discharge, and rest per cycle. The cycles per year determine the annual cumulative energy output and annual hours discharged of the storage system. Typically, there are limitations placed on the total number of equivalent cycles at 100% DOD that a storage system can operate without violating the terms of the developer’s warranty. For this report, that value is assumed to be 365 cycles per year at 100% DOD per year for all technologies.

Storage systems typically are cycled at less than 100% DOD, with the actual number of allowable cycles per year a function of the DOD. For this report, the baseline DOD is set at 80%. Additional information for each technology is provided in the next section. The total annual allowable cycles at any DOD is calculated by Equation 2, taking into account the duration for each cycle, including rest time after charge and discharge.

The total annual cycles are determined as the maximum 100% DOD cycles allowed (assumed to be 365 here) multiplied by the minimum of (1) one equivalent cycle at 100% DOD per day and (2) maximum number of cycles possible per day. As an example, for a 2-hour system operating at 80% DOD, the maximum number of cycles per day is greater than $1/0.8$ or 1.25 cycles, hence, the daily cycles are limited to 1.25 cycles at 80% DOD (condition 1), whereas a 100-hour system operating at 100% DOD takes approximately 9 days to complete a cycle and the daily cycles are limited to 0.11 cycles per day (condition 2).

Equation 2 shows the calculation for the number of cycles per year for each storage technology.

$$Cycles_{annual} = Cycles_{max} \times \min\left(\frac{1}{DOD}, \frac{24}{CT+Rest+DT+Rest}\right) \quad (2)$$

Where:

$Cycles_{max}$ = Maximum 100% DOD equivalent cycles allowed annually, typically included as part of system warranty

DOD = DOD (%)

CT = Time required to charge (hours)

$Rest$ = Rest required after charge and after discharge (hours), varies by technology and duration

DT = Time required to discharge (hours)

Where:

$$DT = DOD (\%) \times \text{Rated Energy Duration}^{61} (\text{hrs}) \quad (2.1)$$

$$CT = \frac{DT}{RTE (\%)} \quad (2.2)$$

The hours of rest required after charge and discharge depends on the battery technology and duration. For non-battery systems, rest time is assumed to be zero hours as the powertrain is designed to operate continuously. For battery systems, rest time required decreases with increased duration of the system, related to lower temperature increase during operation at the lower rates associated with high durations. The assumed rest times are provided in Table 6.3.

Table 6.3. Required Rest Time (hours) for Battery Systems by Duration

Duration (hr)	Required Rest Time (hrs)			
	Lead-acid	Li-ion	Zinc	Redox Flow
2	1.77	3.60	2.68	1.00
4	1.04	1.39	1.21	0.50
6	0.56	0.83	0.70	0.0
8	0.53	0.65	0.59	0.0
10	0.44	0.53	0.49	0.0
24	0.00	0.23	0.11	0.0
100	0.00	0.06	0.03	0.0

Equation 3 determines the total number of discharge hours used in the LCOS calculation.

$$\text{Annual Hours Discharged (AH)} = \frac{\text{Cycles}_{\text{annual}} \times DOD (\%) \times \text{Rated Energy (kWh)}}{\text{Rated Power (kW)}} \quad (3)$$

6.1.4 Depth of Discharge and Cycle Life Assumptions

The cycle life of conventional batteries depends on DOD. For LFP chemistry, the discharge throughput at 60% DOD is 25% greater than the throughput at 80% DOD, while the corresponding number for NMC is 37%. To ensure the desired energy is obtained at the rated power throughout the design life, Li-ion batteries are typically cycled at $\leq 80\%$ DOD to account for degradation. The cycle life and DOD relationship for Li-ion batteries has been described in detail in Section 4.1.4.2. For lead-acid batteries, the rated energy is available typically at the 50–100 hour rate, the exception being the high-power

⁶¹ Rated Energy Duration is simply the duration at rated power to discharge the rated energy, and is equal to Rated Energy/Rated Power.

batteries used for starting, lighting and ignition. At lower durations or higher rates, the available energy is lower, limited by the DC SB's internal resistance, thus limiting the DOD.

Table 6.4 provides the cycle life for each system, with the DOD limitations provided for lead-acid batteries at durations ≤ 10 hours.

Table 6.4. DOD Assumptions by Storage Technology and Duration

Technology	Power (MW)	Duration (hrs)	DOD	2021 Cycle Life at DOD ⁶²	2030 Cycle Life at DOD	
Li-ion LFP	All	All	80%	2,400	2,640	
			60%	8,000	8,800	
Li-ion NMC		All	80%	1,520	1,672	
			60%	5,573	6,130	
Lead-acid		All	2	58%	1,951	
			4	68.1%	1,634	
			6	75%	1,470	
			8	77.5%	1,371	
			10	79.9%	1,370	
			24	80%	1,370	
	100		80%	1,370		
Vanadium RFB	All	All	80%	Unlimited		
Zinc	1 MW	2	80%	2,146	2,360	
		4		3,066	3,372	
		6		1,800	1,980	
		8		6,000	6,600	
		10		6,000	6,600	
		24		6,000	6,600	
	10 MW	2		2,969	3,266	
		4		3,854	4,240	
		6		2,000	2,200	
		8		6,000	6,600	
		10		6,000	6,600	
		24		6,000	6,600	
CAES	All	All	80%	Unlimited		
PSH						
Hydrogen						
Gravitational						
Thermal						

⁶² For Li-ion, this cycle life is to the point where available energy as % of rated energy = DOD%.

6.1.5 Augmentation, Replacement, and Warranty Methodology

To achieve a specified project life, various components of an ESS will need to be replaced or augmented at various time intervals. Costs for these replacements and augmentations are factored into the total costs used in the LCOS calculation. The cost of each component is determined as the present value of the capital expenditure as a function of the year it is incurred. The present value of replacements and future expenditure decreases the further out the investment. The list of expenditures and warranty payments required to reach the determined project life are outlined in Table 6.5.

Each of these costs is incurred at specified timesteps until the final project life of the storage system is reached. For batteries, a variable project life is used with a minimum of 20 years and a maximum of 25. The project life is determined by the number of DC SB augmentations or replacements, which depend on the associated calendar and cycle life. For example, if the cycle life of the DC SB for a lead-acid system is 6 years, then the last rack replacement will take place in year 18 of operation (three replacements in total) and the project life will be 24 years. For a 7-year replacement frequency, the last rack replacement is in year 14 of operation and the project life is set to 21 years. The replacement frequency is determined by the cycle life of the DC SB associated with the DOD divided by the calculated number of cycles per year (Equation 2) at the specified DOD and varies for each power and duration combination.

Table 6.5. Augmentation, Replacement, and Warranty Schedule by Technology

Technology	Component	Frequency
All Batteries, not including Redox Flow	DC SB rack augmentation and/or Replacement	Minimum of cycle life associated with average DOD and calendar life
Vanadium Redox Flow	Stack Replacement	End of calendar life
	Pump Replacement	End of calendar life
	Warranty	Every year of battery life
Li-ion NMC	Warranty	Every year starting four years after each DC SB replacement
Gravitational	Power Equipment Replacement	Every 30 years
Hydrogen	BOP Replacement	Every 15 years
	Fuel Cell Stack Replacement	Every 40,000 stack operating hours ^a
	Electrolyzer Replacement	Every 60,000 electrolyzer operating hours ^b

^a Adapted from Hunter et al. (In Press); (Hunter et al., 2021)

^b Based on 7 years of operation at 97% capacity factor (Hunter et al., 2021) (Hunter et al., In Press)

As previously discussed, Li-ion systems are augmented when available energy reaches the discharge energy corresponding to DOD. It is assumed that the DC SB is operated at an average DOD of 80% at the beginning of the project and 60% once the first augmentation occurs to capture remaining available energy. Additional augmentations are done each time the available energy of SB reaches 60% of rated energy. The amount required for each augmentation takes into account available energy of the SB and the additional energy needed to ensure the required discharge energy at 80% DOD based on rated energy of the unaugmented BESS is available at 60% DOD based on rated energy of the augmented BESS. The augmentation cost is estimated by using the DC SB cost (\$/kWh) specified in the Li-ion capital cost section, with net present value for these augmentations calculated using the appropriate discount

rate. Augmentations continue to occur until the end of life of an augmentation falls between 20–25 years (see Figure 6.1).

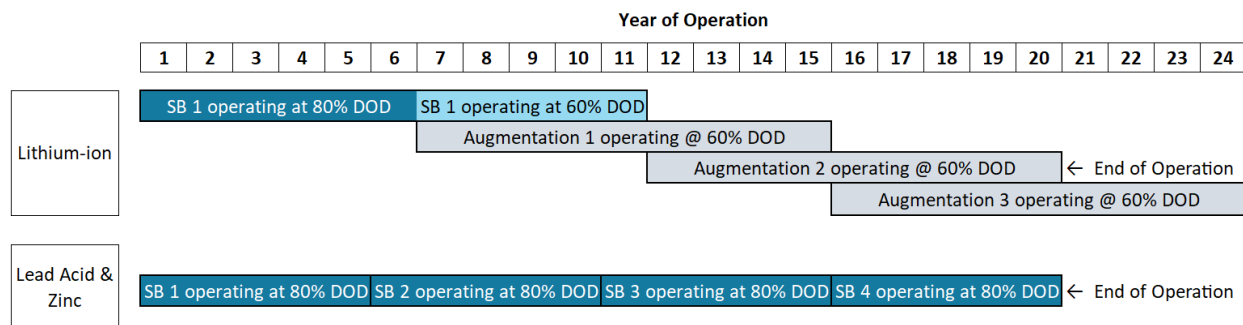


Figure 6.1. Example SB Augmentation and Replacement Schedule

For lead-acid and zinc systems, end of life for each DC SB is assumed to be when available energy reaches 80% of rated energy. For this reason, the rack must be replaced in its entirety when it reaches this point.⁶³ Figure 6.1 is an example of the augmentation and replacement process for Li-ion, lead-acid, and zinc systems. Note that this analysis assumes all DC SB racks are uniform in energy capacity degradation. In reality, there may be some racks that degrade more rapidly, while others last longer. Note that the years between augmentation and replacement are demonstrative and are not reflective of the true values. Additionally, the figure does not include construction period prior to operation. For Li-ion systems it is assumed that the SB used for the last replacement will have some useful energy remaining or available at the end of the project life that remains unused.

6.2 Results

The subsections below discuss the LCOS outcomes for both 2021 and 2030 as well as high-level takeaways from each.

6.2.1 2021 LCOS Values

Figure 6.2 and Figure 6.3 provide 2021 LCOS results. Figure 6.2 shows results for 1 MW and 10 MW systems across all durations. LCOS values presented in the base case are not inclusive of recycling costs due to inconsistency of data availability across technologies. Recycling costs and their effect on LCOS for the technologies that had estimates available are presented in the next section as a sensitivity analysis. Figure 6.3 shows results for 100 MW and 1,000 MW systems across all durations. Note that both figures reflect point estimate values.

High-level takeaways from the 2021 results include the following:

- Looking at 1 MW and 10 MW systems, the LCOS for all battery systems falls between approximately \$0.20–\$0.40/kWh for durations less than or equal to 10 hours. Li-ion LFP has the lowest LCOS across all durations for both power capacity sizes, due to its high cycle life and high

⁶³ If the Li-ion battery is cycled at $\leq 60\%$ DOD, the SB has to be replaced at the end of its cycle life at that DOD.

RTE while lead-acid and zinc systems have the highest LCOS due to lower cycle life and lower RTE.

- At durations greater than 24 hours, the LCOS begins to increase substantially for battery systems. At 24 hours, LFP batteries, for example, have an LCOS of approximately \$0.30/kWh for 1 MW systems and \$0.29/kWh for 10 MW. At 100 hours, those values increase to \$1.05/kWh and \$1.00/kWh, respectively. Longer duration battery systems face higher \$/kWh output costs given that they are limited in the number of cycles they can discharge in a year (less than one cycle per day for the 24- and 100-hour durations). This pattern holds for all battery systems across all power capacities. The lowest point of the LCOS values occurs at approximately 10 hours for all batteries, showing that, given current capital costs for these systems, 10-hour systems are where the lowest ratio of cost to energy output occurs. At lower durations, cycle life limitations necessitate frequent augmentation or replacement, while at higher durations, the number of cycles per day is reduced, reducing the cumulative discharge throughput for the battery. The LCOS increases by 25-100% when the duration is increased from 10 hours to 24 hours and increases by 200-250% when duration is increased from 24 hours to 100 hours.
- The gaps between LCOS values across battery technologies except for lead acid narrow as duration increases from 2 to 10 hours. This happens for different reasons in each system. The flow battery LCOS decreases as stack capital and replacement costs become less significant. Li-ion battery LCOS decreases as the power equipment cost is distributed over a greater energy content, while the 6-10 hour duration allows efficient use of the cycle life of the batteries while reducing augmentation costs. LCOS for zinc batteries decreases because their cycle life increases by nearly 3X in this range. Lead-acid battery LCOS, on the other hand, decreases only marginally due to its low cycle life. At 10 hours, all battery systems except for lead-acid begin to coalesce around the same \$0.20/kWh cost and are within approximately \$0.03/kWh of one other. Lead-acid is the only system that does not drop substantially enough at higher durations to meet the other values.
- Looking at 100 MW and 1,000 MW systems (Figure 6.3) shows that CAES systems offer the lowest LCOS of all technologies included in this report for 2021 due to its lower unit energy capital cost and higher cycle/calendar life, reaching a minimum of \$0.10/kWh for a 1,000 MW, 10-hour system. PSH offers the second lowest at \$0.11/kWh for the same power and duration combination due to the same reasons as CAES in addition to its high RTE. These values are followed by gravitational, thermal, Li-ion LFP, vanadium RFB, and Li-ion NMC which fall in a tight range of \$0.13-\$0.20/kWh. Lead-acid at \$0.33/kWh and hydrogen (\$0.35) have high LCOS due to low cycle life of lead-acid batteries and low RTE and high fuel cell and electrolyzer stack costs for hydrogen.

2021 LCOS (\$/kWh) Comparison - 1 MW & 10 MW

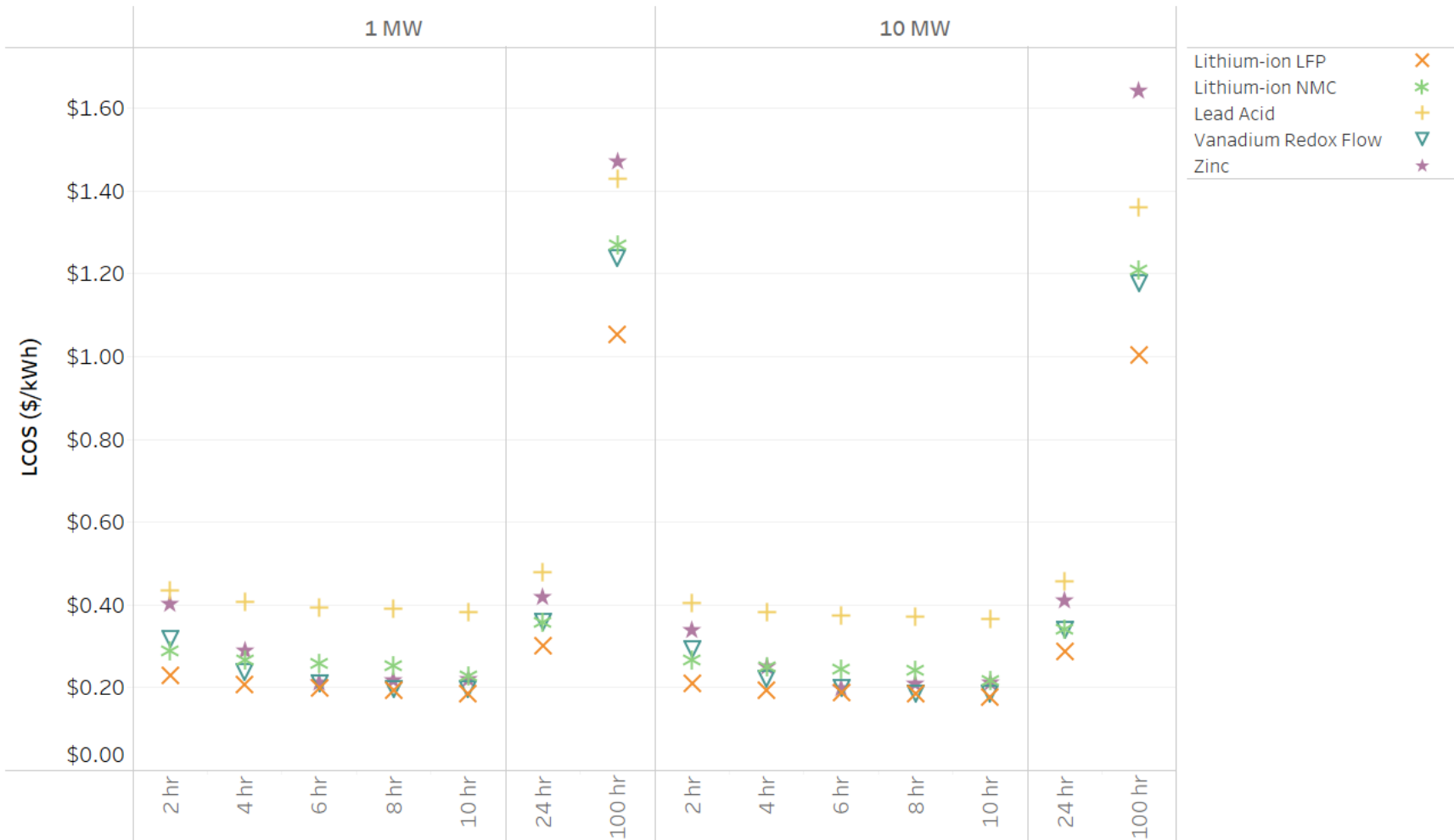


Figure 6.2. LCOS Results for 1 MW and 10 MW Storage Systems, 2021 Values

2021 LCOS (\$/kWh) Comparison - 100 MW & 1,000 MW

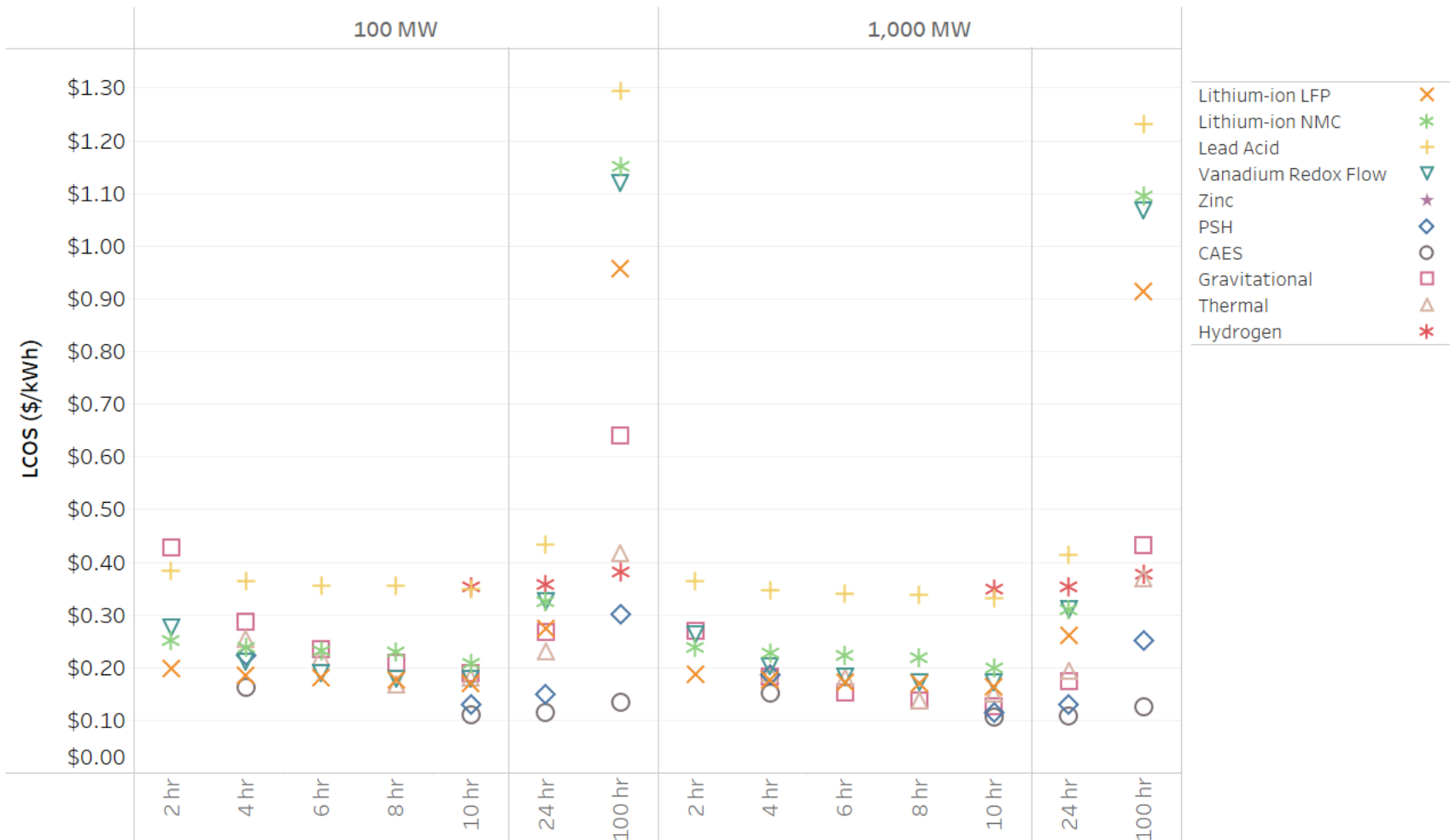


Figure 6.3. LCOS Results for 100 MW and 1,000 MW Storage Systems, 2021 Values

6.2.2 2030 LCOS Values

Figure 6.4 and Figure 6.5 provide 2030 LCOS results. Figure 6.4 shows results for 1 MW and 10 MW systems across all durations. Figure 6.5 shows results for 100 MW and 1,000 MW systems across all durations. Note that both figures reflect point estimate values.

High-level takeaways from the 2030 results include the following:

- The LCOS for 1 MW and 10 MW battery systems is expected to be approximately \$0.15–\$0.40/kWh for systems 10-hours or less by 2030. LCOS trends for durations < 10 hours are similar to 2021 trends, with LFP and NMC establishing the lower end of this range while lead-acid remaining at the high end. Similar to 2021 trends, vanadium RFB and zinc close the gap with Li-ion at duration > 4 hours. Vanadium RFB and zinc are narrowly above the Li-ion systems for systems of 6 to 10 hours and fall between Li-ion NMC and lead acid at lower durations.
- Looking at 1 MW and 10 MW systems, battery storage sees an approximate \$0.03-0.05/kWh drop in LCOS between 2021 and 2030, depending on technology, for lower duration (≤ 8 -hour) systems. At higher durations, the difference between 2021 and 2030 LCOS values is more substantial, with an approximate \$0.08/kWh drop for 24-hour systems and \$0.25/kWh drop for 100-hour systems for batteries. This is due to the fact that at a lower 2030 capital cost, limitations in cumulative energy discharged at high durations do not have as severe an impact on LCOS.
- By 2030, the order of lowest to highest LCOS is estimated to remain predominantly the same as the order established from the 2021 values for 1 MW and 10 MW systems. For 100 MW and 1,000 MW systems, however, the order changes at various durations based on expected cost decreases and performance enhancements. Li-ion systems are estimated to provide the lowest LCOS for nearly all durations up to 8 hours by 2030 at both 100 MW and 1,000 MW, only being narrowly surpassed by gravitational at 1,000 MW, 8 hours. Note that CAES and PSH analysis were not done for 6 and 8 hours.
- Non-battery LCOS values are not expected to change substantially by 2030 with the exception of hydrogen, which sees a drop of approximately \$0.17/kWh across included durations for 100 MW and 1,000 MW systems, mainly related lower fuel cell and electrolyzer stack costs.

2030 LCOS (\$/kWh) Comparison - 1 MW & 10 MW

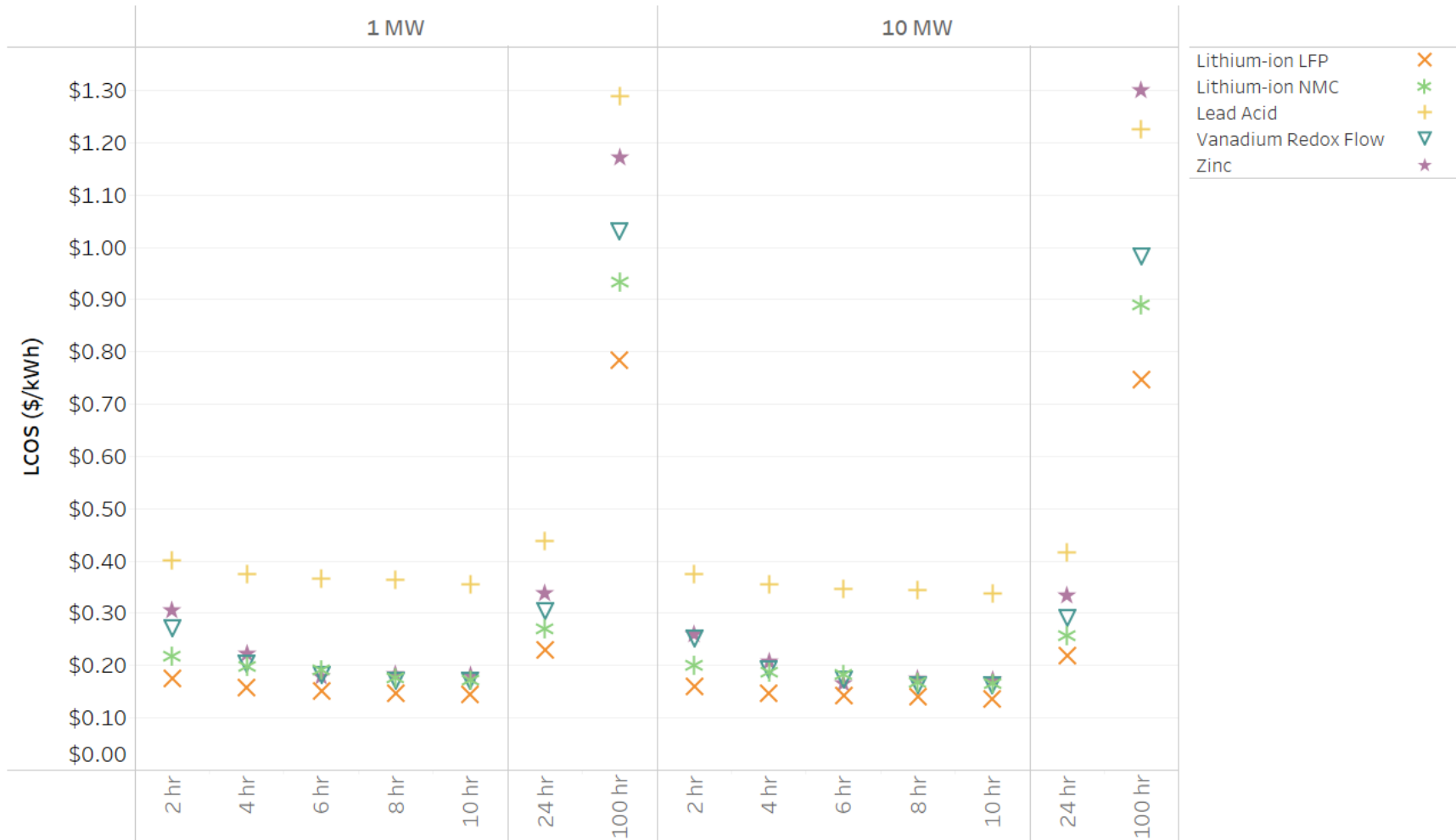


Figure 6.4. LCOS Results for 1 MW and 10 MW Storage Systems, 2030 Values

2030 LCOS (\$/kWh) Comparison - 100 MW & 1,000 MW

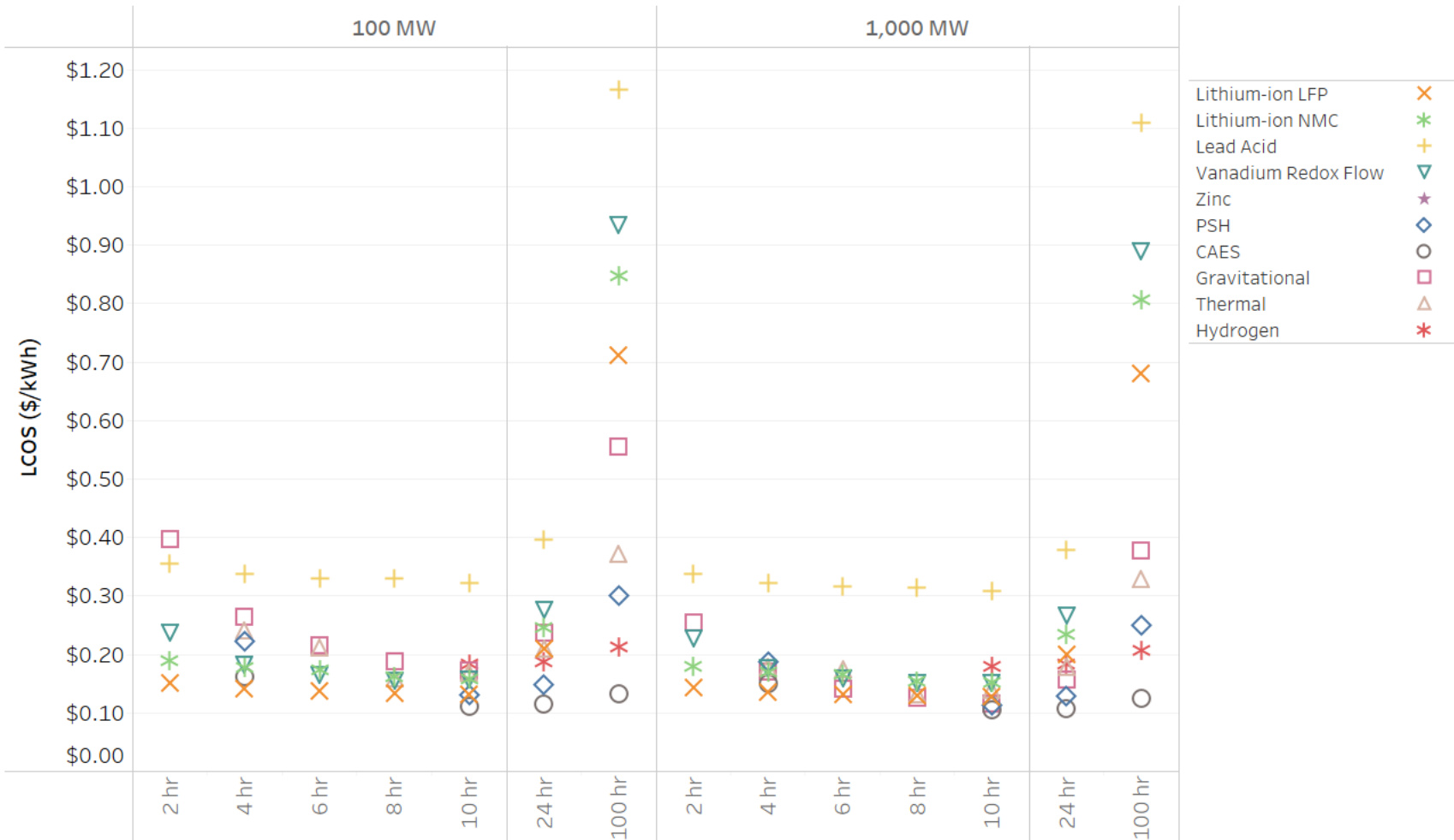


Figure 6.5. LCOS Results for 100 MW and 1,000 MW Storage Systems, 2030 Values

6.3 Sensitivity Analyses

This section provides a summary of the sensitivity of the LCOS values to changes in various parameters or assumptions.

6.3.1 Recycling Cost

The base case LCOS analysis does not include recycling cost estimates due to inconsistency of data availability across all technologies. As a result, recycling costs, as shown in the technology sections for LFP, lead-acid, and vanadium RFB are included in a separate LCOS sensitivity analysis. Note that for NMC and zinc-based systems, material value recovered from recycling is expected to cover SB disposal costs.

Recycling costs are provided on a \$/kWh basis for the aforementioned technologies. The cost to recycle the battery system components is assumed to be incurred at the end of life for each component. For LFP and lead-acid, the years in which recycling occurs coincides with the end of life for each SB up to the end of the project life. For RFB, recycling is assumed to occur at the end of the stack and pump calendar life up to the end of the project life, and recycling of electrolyte, tanks, piping and valves at the end of project life.

Figure 6.6 shows the results of the sensitivity analysis in the form of the net increase in LCOS (\$/kWh) over the base case.

Increase in LCOS with the Addition of Recycling Costs

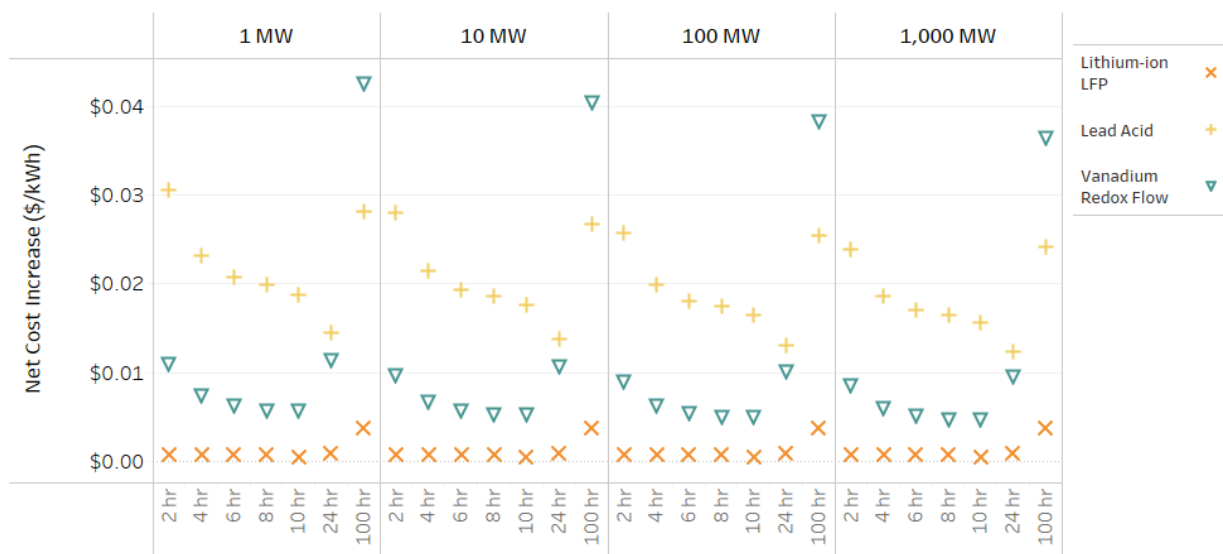


Figure 6.6. Sensitivity Analysis Results Showing Net Cost Increase due to Recycling Costs by Power Capacity (MW) and Duration (hr)

This diagram shows that recycling costs generate a \$0.0325/kWh increase or less for all three technologies across durations up to and including 24 hours. Vanadium RFBs see a larger \$/kWh increase in LCOS at 100-hour durations for each power capacity, related to high disposal cost for an underutilized asset. LFP LCOS values see almost no change across all durations due to low recycling costs. Lead-acid sees a decline in LCOS increase as duration increases up to 24 hours, related to lower replacements

needed as duration increases, with associated recycling costs distributed over a large cumulative discharge energy. At 100-hour duration, the recycling costs are distributed over a lower energy base, resulting in increase in LCOS.

6.3.2 Extended Economic Life

The economic life (i.e., time to pay back debt) assumed in the base case analysis is 20 years. As an additional sensitivity analysis for the LCOS value, the model was run with an economic life of 30 years.

The results of the sensitivity analysis for 100 MW systems are shown in Figure 6.7.

Decrease in LCOS with Extended Economic Life, 100 MW Systems

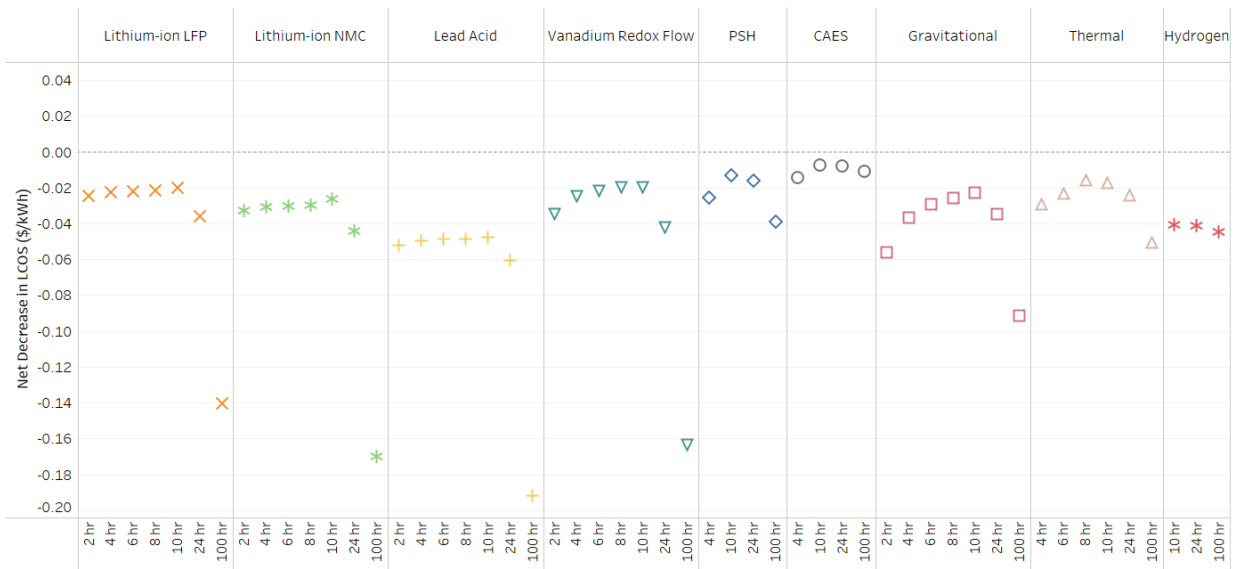


Figure 6.7. Sensitivity Analysis Results for Extended Economic Life on LCOS Value

Takeaways from the economic life sensitivity analysis show that nearly all battery systems see a large (\$0.14-0.20/kWh) decrease in LCOS at 100-hour durations by extending the economic life. At lower durations they receive more consistent drops in LCOS of approximately \$0.02-0.06/kWh. CAES sees the lowest difference in LCOS from a longer economic life, reaching only a \$0.02/kWh decrease.

7 Conclusion

This report has provided detailed cost and performance metrics for the following energy storage technologies across a range of energy-to-power (h) ratios:

- LFP batteries
- NMC batteries
- Lead-acid batteries
- Vanadium RFBs
- CAES
- PSH
- HESS (bidirectional)
- Zinc-based batteries
- Gravity energy storage
- Thermal energy storage

The high-level results are provided below:

- The dominant grid storage technology, PSH, has a 2021 cost estimate of \$263/kWh for a 100 MW, 10-hour installed system. The most significant cost components are the reservoir (\$76/kWh) and powerhouse (\$742/kW). For a 24-hour system, the total installed cost is reduced to \$143/kWh.
- Battery grid storage solutions, which have seen significant growth in deployments in the past decade, have projected 2021 costs for fully installed 100 MW, 10-hour battery systems of Li-ion LFP (\$356/kWh), Li-ion NMC (\$405/kWh), vanadium RFB (\$385/kWh), and lead-acid (\$409/kWh). Zinc-based systems are not available at the 100 MW scale; for a 10 MW, 10-hour system, the total installed cost for 2021 is \$449/kWh, putting it at a higher cost than the other systems at the same scale.
- CAES is estimated to be the lowest cost storage technology at durations ≥ 4 hours (\$122/kWh for a 100 MW, 10-hr system) but is highly dependent on siting near naturally occurring caverns that greatly reduces overall project costs. PSH is projected to be the second or third lowest cost storage technology on an installed cost basis for durations of 10, 24, and 100 hours at the same scale.
- Regarding projected 2030 installed ESS costs for 100 MW 4-hour systems, LFP (\$291/kWh) and CAES (\$295/kWh) installed costs are nearly the same. CAES retains a low cost status at higher durations due to low cavern costs, but is narrowly surpassed by HESS at durations greater than 10 hours. For 100 MW, 100-hour systems, installed costs for CAES and HESS systems are estimated at \$18/kWh and \$15/kWh, respectively.
- When looking at levelized costs across projects, BESSs fall within an LCOS range of approximately \$0.20 to \$0.40/kWh for systems of 10 hours or less, with LFP at the low end and

lead-acid at the high end. At longer durations (24 and 100 hr), the LCOS for batteries begins to increase, falling approximately between \$0.30 and \$0.45/kWh for a 1 MW, 24-hour system and \$1.05 to \$1.50/kWh for 1 MW, 100-hour systems. The lowest point of the LCOS values occurs at approximately 10 hours for all batteries, showing that, given current capital costs for these systems, 10-hour systems are where the lowest ratio of cost-to-energy output occurs. At lower durations, cycle life limitations necessitate frequent augmentation or replacement, while at higher durations, the number of cycles per day is reduced.

- At higher power capacities (100 MW+), CAES provides the lowest LCOS at all durations for which values were estimated (\$0.10/kWh for 1,000 MW, 10 hr). This is mainly related to the lower unit energy cost for caverns. At 1,000 MW, 10 hours, CAES is followed closely by PSH (\$0.11/kWh) and gravitational (\$0.13/kWh), with lead-acid and HESS offering the highest LCOS at \$0.33/kWh and \$0.35/kWh, respectively.

Technologies selected for the second iteration of the report were based on availability of current data from multiple sources and/or specific interest from industry stakeholders. The 2020 report focused on technologies capable of providing bidirectional electrical power exchange with the grid (electrons input from the grid, electrons output to the grid). In this report, thermal energy storage covers thermal energy input while providing electrical output. Additional efforts will focus on capturing multiple output vectors of certain technologies like hydrogen, which may be used as transportation fuel or for chemical synthesis to provide more valuable services than electricity generation. Thermal technology options will be expanded to include cold (ice storage) or heat output instead of electricity.

The cost projections provided here represent an initial attempt at accurately defining and capturing the entire cost structure of these storage systems. The cost and performance data were compiled for the components under the defined categories based on conversations with developers and other stakeholders, literature, and costs of systems procured at sites across the United States. Detailed cost, cost ranges, and performance estimates are presented for 2021 and projected out to 2030 for each of the technologies described, using learning rates for the well-established Li-ion batteries and fixed-cost reduction for other technologies.

In addition to expanding the number of technologies tracked, future updates will be focused on refining and updating the current and 2030 cost and performance values based on stakeholder feedback. These values will be regularly updated on the ESGC Cost and Performance website (currently at <https://www.pnnl.gov/ESGC-cost-performance>), which has been established to make the energy storage cost and performance metrics both accessible to a wide audience and easily updatable as costs change over time.

Areas for research that may be explored in additional phases of this initiative include:

- Establishing further fidelity on cycle life for all BESS at various DOD with associated RTE to facilitate technology selection across a suite of grid services.
- Developing a standardized way of estimating O&M costs for ESSs through expert collaboration and discussion.
- Developing a standardized way of estimating C&C costs for ESSs, taking into account power and energy content.

- Using projected annual demand for nonlithium technologies as well to project 2030 costs based on appropriate choice of learning rates.
- Gathering additional input and feedback from industry stakeholders to update and firm up cost numbers and performance metrics.
- Collecting information and data to develop additional costs related to decommissioning of ESS.

This project has also developed a standardized framework of the cost components for ESS in order to establish a method that accurately compares costs across various technologies. Terminology is often applied inconsistently resulting in confusion over which components are associated with specific cost categories. The standardized framework will hopefully enable an equitable way to compare across technologies.

This effort provides an agile resource for industry to understand the current cost and performance metrics of different technologies while providing a standardized framework to track longer term cost projections. The standardized methodology and long-term cost projections can be used to identify valuable research and development areas for DOE and industry to lower the overall cost of each technology and provide a suite of cost-competitive storage options that industry can choose from.

8 References

- Abrams, A., Farzan, F., Lahiri, S., & Masiello, R. (2014). *Optimizing concentrating solar power with thermal energy systems in California* (CEC-500-2015-078). Retrieved from Chalfont, PA:
- Advanced Rail Energy Storage. (Undated). The Power of Gravity. Retrieved from <https://aresnorthamerica.com/>
- Airthium. Airthium Energy Storage. Retrieved from <https://www.airthium.com/>
- Albrecht, K. J., Bauer, M. L., & Ho, C. K. (2019). *Parametric Analysis of Particle CSP System Performance and Cost to Intrinsic Particle Properties and Operating Conditions*. <https://doi.org/10.1115/ES2019-3893>
- Allison, T. C. (2021). Communication between Tim Allison of Southwest Research Institute and PNNL. In.
- Anwer, U., Cowles, G., & Yadav, G. (2021). Correspondence between Umer Anwer, Gabe Cowles and Gautam Yadav of Urban Electric Power and PNNL. In.
- Aquino, T., Zuelch, C., & Koss, C. (2017). *Energy Storage Technology Assessment* Retrieved from <https://www.pnm.com/documents/396023/1506047/11-06-17+PNM+Energy+Storage+Report+-+Draft+-+RevC.pdf/04ca7143-1dbe-79e1-8549-294be656f4ca>
- Atlas ESS. (2020). 24V 200 Ah 5.1 kWh CA180 Universal Battery Specification. In A. ESS (Ed.). Blaine, Washington: Atlas ESS.
- Augustine, C., Kesseli, D., & Turchi, C. (2020). *Technoeconomic Cost Analysis of NREL Concentrating Solar Power Gen3 Liquid Pathway*. Paper presented at the 26th SolarPACES Conference 2020, Online. <https://www.nrel.gov/docs/fy22osti/77852.pdf>
- Bailie, R. (2020). *Correspondence between Robert Bailie of Siemens Energy and PNNL*.
- Barbir, F. (2005). *PEM Fuel Cells: Theory and Practice*: Academic Press.
- Battery Equivalents. Retrieved from [https://www.batteryequivalents.com/group-31-batteries-dimensions-features-and-recommendations.html#:~:text=Group%2031%20Batteries%20Dimensions%2C%20Weight,\(lead%2Dacid%20batteries\)](https://www.batteryequivalents.com/group-31-batteries-dimensions-features-and-recommendations.html#:~:text=Group%2031%20Batteries%20Dimensions%2C%20Weight,(lead%2Dacid%20batteries)).
- Bauer, T., Odenthal, C., & Bonk, A. (2021). Molten Salt Storage for Power Generation. *Chem. Ing. Tech.*, 93(4), 534-546. doi:10.1002/cite.202000137
- Baxter, R. (2021a). *2020 Energy Storage Pricing Survey* (SAND2021-14700). Retrieved from Albuquerque, NM:
- Baxter, R. (2021b) *Li-ion Warranty, Cycle Life, Calendar Life, and Business Practices/Interviewer: R. Franks*.
- Berron, R. O., & Edley, S. (2021). Communications between Roberto Berron and Steve Edley of Zinc8 Energy Solutions and PNNL. In.
- BG Materials. (Undated). BG Materials. In B. Materials (Ed.): BG Materials.
- Blair, C., & Apps, R. (2021). Communications between Charlie Blair and Ruth Apps of Gravitricity and PNNL. In.

- BNEF. (2020). *2020 Lithium-Ion Battery Price Survey*. Retrieved from
- Brayton Energy. (2021). Gen3 Gas Phase System Development and Demonstration. Retrieved from <https://www.energy.gov/sites/default/files/2021-08/Executive%20Summary%20-%20Gen3%20Gas%20Phase%20System%20Development%20and%20Demonstration%20-%20Brayton%20Energy.pdf>
- Brown, R. (2021). Communication between Rob Brown of Invinity Energy Systems and PNNL. In.
- Buchanan, J. (2021) *Deka Manufacturing Co. Pb-acid Cost and Performance/Interviewer: R. Franks*.
- Burz, M., Macher, M., & Baker, P. (2021). Communication between Michael Burz, Meinrad Macher, Philip Baker of Enzinc and PNNL. In.
- Butler, P. C., Eidler, P. A., Grimes, P. G., Klassen, S. E., & Miles, R. C. (1995). Zinc/Bromine Batteries. In D. Linden (Ed.), *Handbook of Batteries* (Second ed., pp. 37.33, 37.35). New York: McGRAW-HILL, Inc.
- C&D Technologies. Carbon Battery. In C. D. Technologies (Ed.): C&D Technologies.
- Capp, B. (2021). Communication between Bill Capp of StorWorks Power and PNNL. In.
- Caraballo, A., Galán-Casado, S., & Serena, S. (2021). Molten Salts for Sensible Thermal Energy Storage: A Review and an Energy Performance Analysis *Energies*, 14. doi:10.3390/en14041197
- Choi, D. (2021). Input on upper SOC limit for NMC from Daiwon Choi of PNNL. In.
- Cipriano, G. (2021). Correspondence between Greg Cipriano of WattJoule Corporation and PNNL. In.
- Coastal Chemical Co., L. (2022). HITEC Heat Transfer Salt. Retrieved from <https://coastalchem.com/products/heat-transfer-fluids/hitec-heat-transfer-salt/>
- Collins, L. (2019). Retrieved from <https://www.rechargenews.com/transition/siemens-gamesa-launches-revolutionary-thermal-storage-pilot/2-1-619939>
- Conlon, W. (2021a). Correspondence between William Conlon of Pintail Power and PNNL on Liquid Air Combined Cycle technology.
- Conlon, W. (2021b). Correspondence between William Conlon of Pintail Power and PNNL on Liquid Salt Combined Cycle technology. In.
- Conlon, W. (2022). Communication between William Conlon of Pintail Power, LLC and PNNL. In.
- Cornell Law School. (2021). 26 U.S. Code § 168 - Accelerated cost recovery system. Retrieved from <https://www.law.cornell.edu/uscode/text/26/168>
- Crawford, A., Viswanathan, V., Stephenson, D., Wang, W., Thomsen, E., Reed, D., . . . Sprenkle, V. (2015). Comparative analysis for various redox flow batteries chemistries using a cost performance model. *Journal of Power Sources*, 293, 388-399. doi:<https://doi.org/10.1016/j.jpowsour.2015.05.066>
- Davitti, A. (2018). Project cost modelling for Hydropower schemes in developing countries. *International Journal on Hydropower and Dams*, 25(6), 56 - 64.

- Delamarche, B. (2018). VRB Energy invents vanadium leasing. Retrieved from <https://www.usinenouvelle.com/article/vrb-energy-securise-son-approvisionnement-et-invente-le-leasing-de-vanadium.N713154>
- Designing Buildings. (2021). Design life. Retrieved from https://www.designingbuildings.co.uk/wiki/Design_life
- Doll, S. (2021, October 26, 2021). BYD to reportedly raise battery prices by 20% due to raw material costs. Retrieved from <https://electrek.co/2021/10/26/byd-to-reportedly-raise-battery-prices-by-20-due-to-raw-material-costs/>
- Dufo-López, R., Cortés-Arcos, T., Artal-Sevil, J. S., & Bernal-Agustín, J. L. (2021). Comparison of Lead-Acid and Li-Ion Batteries Lifetime Prediction Models in Stand-Alone Photovoltaic Systems. *Applied Sciences*, 11(3). doi:<https://doi.org/10.3390/app11031099>
- EASE. (2016). Technologies. Retrieved from <https://ease-storage.eu/energy-storage/technologies/>
- Echogen Power Systems. (Undated). Energy Storage. Retrieved from <https://www.echogen.com/energy-storage/etes-benefits/>
- Eguchi, T. (2021). Correspondence between Tak Eguchi of NGK and PNNL. In.
- EIA. (2021). Hydropower explained: Hydropower and the environment. Retrieved from <https://www.eia.gov/energyexplained/hydropower/hydropower-and-the-environment.php>
- Elgqvist, E., Anderson, K., & Settle, E. (2018). *Federal Tax Incentives for Energy Storage Systems*. Retrieved from Golden, CO: <https://www.nrel.gov/docs/fy18osti/70384.pdf>
- Energy, S. G. R. (2020). Electric Thermal Energy Storage (ETES) – Industrial Decarbonization. Retrieved from <https://www.siemensgamesa.com/en-int/-/media/siemensgamesa/downloads/en/products-and-services/hybrid-power-and-storage/etes/siemens-gamesa-etes-ad-teaser-industrial-decarbonization.pdf>
- Energy Vault. (2021). Energy Vault, the Technology Company Using Gravity-based, Grid-Scale Energy Storage to Accelerate Global Decarbonization, to List on the NYSE Through Merger with Novus Capital Corporation II. EV DOC ID. EVPR-20210909.
- Engineer, T. (2019). Newcastle University connects first grid-scale pumped heat energy storage system. Retrieved from <https://www.theengineer.co.uk/grid-scale-pumped-heat-energy-storage/>
- Engineering ToolBox. (2014). Air - Molecular Weight and Composition. Retrieved from https://www.engineeringtoolbox.com/molecular-mass-air-d_679.html
- ESS, A. (2020). 24V 200 Ah 5.1 kWh CA180 Universal Battery Specification. In A. ESS (Ed.): Atlas ESS.
- Farley, J. (2020). *Correspondence between Jack Farley of Apex Compressed Air Energy Storage and PNNL*.
- Fernández, A. G., Gomez-Vidal, J., Oró, E., Kruizenga, A., Solé, A., & Cabeza, L. F. (2019). Mainstreaming commercial CSP systems: A technology review. *Renewable Energy*, 140, 152-176. doi:<https://doi.org/10.1016/j.renene.2019.03.049>
- Fiske, J. (2021). Correspondence between Jim Fiske of Gravity Power and PNNL. In.
- Forsberg, C., Sabharwall, P., & Sowder, A. (2020). *Separating Nuclear Reactors from the Power Block with Heat Storage: A New Power Plant Design Paradigm* (MIT-ANP-TR-189). Retrieved from Cambridge, MA:

- Forsberg, C., Stack, D., & McDaniel, P. (2021, August 4-6). *Nuclear Air-Brayton COmbined Cycles using Electrically-Heated Conductive Firebrick Heat Storage and Hydrogen for Peak Power*. Paper presented at the 28th International Conference on Nuclear Engineering, Virtual, Online.
- Forsberg, C. W. (2020). Market Basis for Salt-Cooled Reactors: Dispatchable Heat, Hydrogen, and Electricity with Assured Peak Power Capacity. *Nuclear Technology*, 206(11), 1659-1685. doi:10.1080/00295450.2020.1743628
- Forsberg, C. W., McDaniel, P. J., & Zohuri, B. (2021). Nuclear Air-Brayton Power Cycles with Thermodynamic Topping Cycles, Assured Peaking Capacity, and Heat Storage for Variable Electricity and Heat. *Nuclear Technology*, 207(4), 543-557. doi:10.1080/00295450.2020.1785793
- Gan, P. G., Wang, Y., & Pye, J. (2021). *System modelling and optimisation of a particle-based CSP system*. Retrieved from Canberra, Australia:
- Gas Turbine World. (2020). *2020 Combined Cycle Plant Price*. In.
- Geissbühler, L., Mathur, A., Mularczyk, A., & Haselbacher, A. (2019a). An assessment of thermocline-control methods for packed-bed thermal-energy storage in CSP plants, Part 1: Method descriptions. *Solar Energy*, 178, 341-350. doi:https://doi.org/10.1016/j.solener.2018.12.015
- Geissbühler, L., Mathur, A., Mularczyk, A., & Haselbacher, A. (2019b). An assessment of thermocline-control methods for packed-bed thermal-energy storage in CSP plants, Part 2: Assessment strategy and results. *Solar Energy*, 178, 351-364. doi:https://doi.org/10.1016/j.solener.2018.12.016
- Georgiou, S., Shah, N., & Markides, C. N. (2018). A thermo-economic analysis and comparison of pumped-thermal and liquid-air electricity storage systems. *Applied Energy*, 226, 1119-1133. doi:https://doi.org/10.1016/j.apenergy.2018.04.128
- Gravitricity. Fast, long-life energy storage. Retrieved from <https://gravitricity.com/technology/>
- Gravitricity. Gravity energy storage - A new form of renewable energy storage to power a cleaner world. Retrieved from <https://gravitricity.com/>
- Gravitricity. (2021). Fast, long-life energy storage. Retrieved from <https://gravitricity.com/technology/>
- Gravity Power. (2021). Gravity Power - A Revolution in Energy Storage. Retrieved from <https://www.gravitypower.net/>
- Gritsevskiy, A., & Nakićenovi, N. (2000). Modeling uncertainty of induced technological change. *Energy Policy*, 28(13), 907-921. doi:https://doi.org/10.1016/S0301-4215(00)00082-3
- Guo, J., Cai, L., Chen, J., & Zhou, Y. (2016). Performance optimization and comparison of pumped thermal and pumped cryogenic electricity storage systems. *Energy*, 106, 260-269. doi:https://doi.org/10.1016/j.energy.2016.03.053
- Harrison, K. W., Remick, R., Martin, G. D., & Hoskin, A. (2010). *Hydrogen Production: Fundamentals and Cas Study Summaries* Paper presented at the 18th World Hydrogen Energy Conference, Essen, Germany. <https://www.nrel.gov/docs/fy10osti/47302.pdf>
- Heindl Energy. (2017). Gravity Storage. A new solution for large scale storage. In H. Energy (Ed.).
- Heindl Energy. (2021). Gravity Storage A new StoreAge. Retrieved from <https://heindl-energy.com/>
- Held, T., & Brennan, P. (2021). Communication between Tim Held, Philip Brennan of Echogen Power Systems and PNNL. In.

- Hickey, S. (2021). Correspondence between Steven Hickey of Redflow and PNNL. In.
- Hickley, M. (2021) *Li-Cycle Li-ion Recycling Costs/Interviewer: R. Franks*.
- Highview Power. (2021, March 10). *Liquid Air Energy Storage*. Paper presented at the DOE Long Duration Energy Storage Workshop, Online.
- Ho, C. (2022). [Correspondence between Clifford Ho of Sandia National Laboratory and Pacific Northwest National Laboratory].
- Ho, C. K. (2016). A review of high-temperature particle receivers for concentrating solar power. *Applied Thermal Engineering*, 109, 958-969. doi:<https://doi.org/10.1016/j.applthermaleng.2016.04.103>
- Ho, C. K., Carlson, M., Garg, P., & Kumar, P. (2016). Technoeconomic Analysis of Alternative Solarized s-CO₂ Brayton Cycle Configurations. *Journal of Solar Energy Engineering*, 138(5). doi:10.1115/1.4033573
- Ho, C. K., Sment, J., Albrecht, K., Mills, B., Schroeder, N., Laubscher, H., . . . Wang, Y. (2021). *Gen 3 Particle Pilot Plant (G3P3) – High-Temperature Particle System for Concentrating Solar Power (Phases 1 and 2)* (SAND2021-14614). Retrieved from Albuquerque, New Mexico:
- Hoivik, N., Greiner, C., Barragan, J., Iniesta, A. C., Skeie, G., Bergan, P., . . . Calvet, N. (2019). Long-term performance results of concrete-based modular thermal energy storage system. *Journal of Energy Storage*, 24, 100735. doi:<https://doi.org/10.1016/j.est.2019.04.009>
- Howitt, M. (2021). Communication between Mark Howitt of Storelectric Ltd. and PNNL. In.
- Hume, S. (2020). Re: Integration of Heat Storage with Fossil Energy Systems
- Hunter, C. A., Penev, M., Reznicek, E. P., Eichman, J., Rustagi, N., & Baldwin, S. F. (In Press). *Techno-Economic Analysis of Long-Duration Energy Storage and Flexible Power Generation Technologies to Support High Variable Renewable Energy Grids*. Retrieved from <https://ssrn.com/abstract=3720769>
- Hunter, C. A., Penev, M. M., Reznicek, E. P., Eichman, J., Rustagi, N., & Baldwin, S. F. (2021). Techno-economic analysis of long-duration energy storage and flexible power generation technologies to support high-variable renewable energy grids. *Joule*, 5(8), 2077-2101. doi:<https://doi.org/10.1016/j.joule.2021.06.018>
- International, B. (2021, February 14). WIRTZ INVESTS IN NICKEL-ZINC BATTERY MAKER ZAF ENERGY SYSTEMS. Retrieved from <https://www.batteriesinternational.com/2019/02/14/wirtz-invests-in-nickel-zinc-battery-maker-zaf-energy-systems/>
- IRENA. (2020). Innovation Outlook: Thermal Energy Storage. In. Abu Dhabi: International Renewable Energy Agency.
- John, J. S. (2019, August 15). Energy Vault Lands \$110M From SoftBank's Vision Fund for Gravity Storage. Retrieved from <https://www.greentechmedia.com/articles/read/energy-vault-lands-110m-from-softbanks-vision-fund-for-gravity-energy-stora>
- Kahl, C. (2021) *OHM Inc. Li-ion Recycling Costs/Interviewer: R. Franks*.
- Kelly, B. (2021a, April 28). [Discussion on Thermal Energy Storage].
- Kelly, B. (2021b). *Nitrate Salt Thermal Storage*. Paper presented at the DOE Long-Duration Energy Storage Workshop, Online. Presentation retrieved from

- Klein, M., & McLarnon, F. (1995). Nickel-Zinc Batteries. In D. Linden (Ed.), *Handbook of Batteries* (Second ed., pp. 29.181995). New York: McGRAW-HILL, Inc.
- Klochko, A., & Lahaye, F. (2021). Correspondence between Andrei Klochko and Franck Lahaye of Aitthium and PNNL. In.
- Kokam. (2020). High Energy Type 5.3 kWh Battery Module. In K. b. SolarEdge (Ed.).
- Largo. (2021). Maracás Menchen Mine. Retrieved from <https://largoinc.com/English/about-us/maracas-menchen-mine/default.aspx>
- Lee, A., & Tian, Y. (2021, November 4, 2021). The Commodity Boom Is Starting to Push Battery Prices Higher. Retrieved from <https://www.bloomberg.com/news/articles/2021-11-04/the-commodity-boom-is-starting-to-push-battery-prices-higher>
- Li, L., Kim, S., Wang, W., Vijaykumar, M., Nie, Z., Chen, B., . . . Yang, G. (2010). *A New Vanadium Redox Flow Battery Using Mixed Acid Electrolytes*. Paper presented at the US DOE Energy Storage Systems Program Review, Washington, DC. <https://www.energy.gov/sites/default/files/ESS%202010%20Update%20Conference%20-%20A%20New%20Vanadium%20Redox%20Flow%20Battery%20Using%20Mixed%20Acid%20Electrolytes%20-%20Liyu%20Li%20C%20PNNL.pdf>
- Lithionics Battery. (2019). Frequently Asked Questions. In L. Battery (Ed.), (Rev.1 ed.): Lithionics Battery.
- Lithium Werks. (2019). U24-12XP Group 24, 12 Volt, 118 Ah Lithium Ion Battery Module. In L. Werks (Ed.): Lithium Werks.
- Lundy, S. (2020). *Capital Cost and Performance Characteristic Estimates for Utility Scale Electric Power Generating Technologies*. Retrieved from Washington, DC:
- Ma, Z. (2021a, March 16). [Email correspondence on Thermal Energy Storage to V. V. Viswanathan of PNNL].
- Ma, Z. (2021b). *Long-Duration Electricity Storage by Low-Cost Thermal Energy Storage and High-Efficiency Power Generation*. Paper presented at the DOE Long-Duration Energy Storage Workshop, Virtual, Online. <https://www.sandia.gov/ess-ssl/ldes/>
- Ma, Z., Wang, X., Davenport, P., Gifford, J., & Martinek, J. (2021, June 16-18). *Economic Analysis of an Electric Thermal Energy Storage System using Solid Particles for Grid Electricity Storage*. Paper presented at the ASME 2021 15th International Conference on Energy Sustainability, Virtual, Online.
- Manwaring, M., Mursch, D., & Erpenbeck, D. (2020). [Correspondence between NHA Members (Michael Manwaring of McMillen Jacobs Associates, Debbie Mursch of GE Renewables, Don Erpenbeck of Stantec, Inc.) and PNNL; July 22, 2020].
- Materials, B. BG Materials. In B. Materials (Ed.): BG Materials.
- May, G. J., Davidson, A., & Monahov, B. (2018). Lead batteries for utility energy storage: A review. *Journal of Energy Storage*, 15, 145-157. doi:<https://doi.org/10.1016/j.est.2017.11.008>
- Mehos, M., Price, H., Cable, R., Kearney, D., Kelly, B., Kolb, G., & Morse, F. (2020). *Hami CSP Project* (NREL/TP-5500-75763). Retrieved from
- Mehos, M., Turchi, C., Vidal, J., Wagner, M., Ma, Z., Ho, C., . . . Kruizenga, A. (2017). *Concentrating Solar Power Gen3 Demonstration Roadmap* (NREL/TP-5500-67464). Retrieved from

- Miller, E. (2022). Communication between Eric Miller of Hydrogen and Fuel Cell Technologies Office and PNNL. In.
- Miller, R. (2020). [Correspondence between Rick Miller of HDR Inc. and PNNL; June 30, 2020].
- Mills, B. H., Ho, C. K., Schroeder, N. R., Shaeffer, R., Laubscher, H. F., & Albrecht, K. J. (2022). Design Evaluation of a Next-Generation High-Temperature Particle Receiver for Concentrating Solar Thermal Applications. *15*(5), 1657.
- Minopoli, S. (2021). *Practical examples of flow batteries in long duration applications*. Paper presented at the International Flow Battery Forum, Virtual. <https://flowbatteryforum.com/session/session-1-successful-flow-battery-deployment/>
- Mittal, V. (2021). Correspondence between Vishal Mittal of Delectrik Systems Pvt. Ltd. and PNNL. In.
- Mongird, K., Viswanathan, V., Alam, J., Vartanian, C., Sprenkle, V., & Baxter, R. (2020a). *2020 Grid Energy Storage Technology Cost and Performance Assessment (DOE/PA-0204 PNNL-31956)*. Retrieved from <https://www.pnnl.gov/sites/default/files/media/file/Final%20-%20ESGC%20Cost%20Performance%20Report%2012-11-2020.pdf>
- Mongird, K., Viswanathan, V., Alam, J., Vartanian, C., Sprenkle, V., & Baxter, R. (2020b). *2020 Grid Energy Storage Technology Cost and Performance Assessment (PNNL-31956)*. Retrieved from
- Mongird, K., Viswanathan, V., Balducci, P., Alam, J., Fotedar, V., Koritarov, V., & Hadjeriouaa, B. (2019). *Energy Storage Technology and Cost Characterization Report*. Retrieved from Richland, Washington, USA: https://www.energy.gov/sites/prod/files/2019/07/f65/Storage%20Cost%20and%20Performance%20Characterization%20Report_Final.pdf
- Moore, S. K. (2021). Gravity Energy Storage Will Show Its Potential in 2021. Retrieved from <https://spectrum.ieee.org/energy/batteries-storage/gravity-energy-storage-will-show-its-potential-in-2021>
- National Renewable Energy Laboratory. (2022). Concentrating Solar Power Projects. Retrieved from <https://solarpaces.nrel.gov/>
- NREL. (2021). *2021 Annual Technology Baseline*. Retrieved from Golden, CO: <https://atb.nrel.gov/>
- Nunes, V., Queiros, C., Lourenco, M., Santos, F., & Castro, C. N. d. (2016). Molten salts as engineering fluids - A review: Part I. Molten alkali nitrates. *Applied Energy*, *183*, 603-611. doi:10.1016
- Odayar, T. (2021). PFR Energy Storage Roundtable 2021. Retrieved from <https://www.powerfinancerisk.com/article/28pgbjhm5o2k60bw57ym8/pfr-energy-storage-roundtable-2021>
- Odenthal, C., Klasing, F., Knodler, P., Zunft, S., & Bauer, T. (2019). Experimental and numerical investigation of a 4 MWh high temperature molten salt thermocline storage system with filler. *AIP Conference Proceedings*, *2303*. doi:10.1063/5.0028494
- Paiss, M. (2021). [Communication between Matthew Paiss of PNNL and authors].
- Papadis, D. D., & Ahluwalia, R. K. (2022). *Bulk Storage of Hydrogen*.
- Papageorgopoulos, D. (2021). *Fuel Cell Technologies Overview*. Paper presented at the 2021 Annual Merit Review and Peer Evaluation Meeting, Washington, DC. Presentation retrieved from

- Pedretti, A. (2021). *Long Duration Energy Storage - Gravity*. Paper presented at the DOE Long-Duration Energy Storage Workshop, Online. Presentation retrieved from
- Perles, T. (2021). Correspondence between Terry Perles of US Vanadium and PNNL. In.
- Pintail Power. (2021). Liquid Air Combined Cycle. Retrieved from <https://www.pintailpower.com/technology/liquid-air-combined-cycle/>
- Plautz, K. (2021). Communication between Kirk Plautz and PNNL. In.
- Raiford, M. (2020). Correspondence between Matt Raiford of Battery Innovation and PNNL. In.
- Reed, D. M., Thomsen, E. C., Li, B., Wang, W., Nie, Z., Koepfel, B. J., . . . Sprenkle, V. L. J. J. o. T. E. S. (2016). Stack Developments in a kW Class All Vanadium Mixed Acid Redox Flow Battery at the Pacific Northwest National Laboratory. 163.
- Richey, F. (2021). Correspondence between Francis Richey of Eos and PNNL In.
- Riley, R. (2021). Communication between Richard Riley of Highview Power and PNNL. In.
- Rustagi, N. (2021). Email Correspondence between Neha Rustagi of US DOE Fuel Cell Technology Office and PNNL. In.
- Rustagi, N. (2022). Correspondence between Neha Rustagi of The Hydrogen and Fuel Cell Technologies Office and PNNL. In.
- Saft, J. M. (2021) *Li-ion Cost and Performance Assessment Data/Interviewer: V. V. Ryan Franks*.
- Salomoni, V. A., Majorana, C. E., Giannuzzi, G. M., Miliozzi, A., Di Maggio, R., Girardi, F., . . . Lucentini, M. (2014). Thermal storage of sensible heat using concrete modules in solar power plants. *Solar Energy*, 103, 303-315. doi:<https://doi.org/10.1016/j.solener.2014.02.022>
- Samsung SDI. (2018). ESS Batteries by Samsung SDI. In S. SDI (Ed.).
- Sapien, T. (2020). Grid Scale Storage: where does flow fit in. In: International Battery Virtual Seminar.
- Schoenfeldt, A. (2021). Communication between | Alexander Schoenfeldt of CellCube and PNNL. In.
- Schumacher, M., Rupprecht, C., & Kayaalp, B. (2021). Communication between Maximilian Schumacher, Clemens Rupprecht, Bugra Kayaalp and PNNL. In.
- Sciacovelli, A., Smitha, D., Navarro, H., Lia, Y., & Dinga, Y. (2016). *Liquid air energy storage – Operation and performance of the first pilot plant in the world*. Paper presented at the ECOS 2016 - THE 29TH INTERNATIONAL CONFERENCE ON EFFICIENCY, COST, OPTIMIZATION, SIMULATION AND ENVIRONMENTAL IMPACT OF ENERGY SYSTEMS, PORTOROŽ, SLOVENIA.
- Scribner. (2017). How To Estimate Required Fuel Flow For PEM Cells. Retrieved from <https://www.scribner.com/faq/3-how-to-estimate-required-fuel-flow-for-pem-cells/>
- SimpliPhi Power, I. (2019). PHI 3.8 TM Battery. In I. SimpliPhi Power (Ed.): SimpliPhi Power, Inc.
- Smith, N. (2021, March 1-2). *Small-Scale PHES Demonstration*. Paper presented at the DAYS Annual Meeting.
- Solutions, Z. E. (2020). Zinc8 is redefining long-duration energy storage. Retrieved from <https://www.zinc8energy.com/>

- Spector, J. (2018, NOVEMBER 14). Can Newcomer Energy Vault Break the Curse of Mechanical Grid Storage? Retrieved from <https://www.greentechmedia.com/articles/read/energy-vault-stacks-concrete-blocks-to-store-energy#gs.wja8ed>
- Storage, A. R. E. (2020, October 29, 2020). Gravity Power: non-explosive, non-flammable, non-degrading and freely available.
- Stover, J. (2021). Communication between Jim Stover of VRB Energy and PNNL. In.
- Strahan, D. (2013). *Liquid Air in the energy and transport systems* (Report No. 021). Retrieved from
- Sullivan, S., & Frinze, K. (2022). [Correspondence between Shaun Sullivan and Jack Frinze of Brayton Energy and Pacific Northwest National Laboratory].
- Sullivan, S. D. (2018, June 25). *Gen3 Gas Phase System Development and Demonstration*. Paper presented at the DOE Concentrating Solar Power Gen3 Kickoff, Orlando, FL.
- Sumitomo Electric Industries, L. Introduction of Vanadium Flow Battery System (VFB). In (Vol. RP-21-005): Sumitomo Electric Group.
- Sumitomo Electric Industries, L. Redox Flow Battery. Retrieved from https://sumitomoelectric.com/sites/default/files/2021-04/download_documents/Redox_Flow_Battery_En.pdf
- Sumitomo Electric Industries, L. Vanadium Flow Battery System for Energy Efficiency. Retrieved from http://www.unido.or.jp/en/technology_db/2984/
- Swagel, P. L. (2021). *An Update to the Budget and Economic Outlook: 2021 to 2031*. U.S. Congressional Budget Office Retrieved from <https://www.cbo.gov/system/files/2021-07/57218-Outlook.pdf>
- Systems, E. P. Energy Storage. Retrieved from <https://www.echogen.com/energy-storage/etes-benefits/>
- TECH, S. (2021). How Does Wind Influence Crane Safety? Retrieved from <https://scarlet-tech.com/how-does-wind-influence-crane-safety/>
- Terruzzin, M. (2021). Communications between Marco Terruzzin of Energy Vault and PNNL. In.
- The Engineering Toolbox. (2003). Specific Heat of some common Substances. Retrieved from https://www.engineeringtoolbox.com/specific-heat-capacity-d_391.html
- Thess, A. (2013). Thermodynamic Efficiency of Pumped Heat Electricity Storage. *Physical Review Letters*, 111(11), 110602. doi:10.1103/PhysRevLett.111.110602
- Torikai, K., & SHIBATA, T. (2021). Communication between Keisuke Torikai, Toshikazu Shibata and PNNL. In.
- Urban, M., Brunner, M., & Oldacre, P. (2021). *The results and benefits of long duration flow battery energy storage*. Paper presented at the International Flow Battery Forum, Virtual. <https://flowbatteryforum.com/session/session-1-successful-flow-battery-deployment/>
- Ürlings, N., & Pereira, E. L. (2020). Design of a direct thermal oil based thermocline thermal energy storage for a concentrating solar power plant. 2303(1), 190031. doi:10.1063/5.0028920
- Vanadium Price. (2021). V2O5 Vanadium Pentoxide Flake 98% Price USD / lb. Retrieved from <https://www.vanadiumprice.com/>
- Vartanian, C. (2021). [Communication between Charlie Vartanian of PNNL and authors].
- Vault, E. (2021). Enabling a Renewable World. Retrieved from <https://energyvault.com/>

- Watson, E. (2021). Communication between Eric Watson of Largo Clean Energy and PNNL. In.
- Weed, R. (2021). Correspondence between Russ Weed ARES North America and PNNL. In.
- Wei, M., Smith, S. J., & Sohn, M. D. (2017). Non-constant learning rates in retrospective experience curve analyses and their correlation to deployment programs. *Energy Policy*, *107*, 356-369. doi:<https://doi.org/10.1016/j.enpol.2017.04.035>
- Werner, R. (2021). Correspondence between Robert Werner of Heindl Energy and PNNL. In.
- Westlake, B. (2021). Battery Energy Storage System Recycling and Disposal Investigation: Industry Overview and Cost Estimates.
- Wright, S. (2012). *Compressed Air Energy Storage: Proven US CAES Plant Cost Achievements and Potential Engineering, Design & Project Management Based Cost Reductions*. (1024286). Retrieved from Palo Alto, CA: <https://www.epri.com/research/products/1024286>
- Yang, Z., Zhang, J., Kintner-Meyer, M. C. W., Lu, X., Choi, D., Lemmon, J. P., & Liu, J. (2011). Electrochemical Energy Storage for Green Grid. *Chem. Rev.*, *111*(5), 3577-3613. doi:<https://doi.org/10.1021/cr100290v>
- Zhang, L., Jansen, A., Smith, N., Yang, G., Pepper, S., Britton, C., . . . Schanfein, M. (2017). *Battery Technologies for Unattended Monitoring Systems* (ANL/CSE-17/1). Retrieved from https://www.google.com/search?q=ANL%2FCSE-17%2F1&rlz=1C1GCEJ_enUS922US922&oq=ANL%2FCSE-17%2F1&aqs=chrome..69i57j69i58.897j0j7&sourceid=chrome&ie=UTF-8
- Zhongeng Technology. (2019). Product Specification In Z. Technology (Ed.): Zhongeng Technology.

Appendix 1: LCOS Methodology and Definitions

LCOS Equation

Equation (1) in Section 6.1.1 provides the formula to determine the LCOS (\$/kWh). This appendix provides supplemental equations that offer information on how to calculate the various inputs.

CAPEX

The present value of capital expenditures ($CAPEX_{PV}$) is used to determine the total investment in the storage system in present year dollars. While the bulk of the CAPEX cost is assumed to be incurred in year 0 for this report, various capital investments for augmentations and replacements will be incurred in future years. Equation (4) shows the present value equation for capital expenditures over the project life of the system. The year in which augmentation, major overhauls, and replacements for battery systems take place will be dependent on the cycle life, calendar life, DOD, and other factors for each system, as specified in the LCOS section of the report.

$$CAPEX_{PV} = \sum_{n=0}^N \frac{CF_n}{(1+d)^n} = CF_0 + \frac{CF_1}{(1+d)^1} + \frac{CF_2}{(1+d)^2} + \dots + \frac{CF_N}{(1+d)^N} \quad (4)$$

Where:

$CAPEX_{PV}$ = Present value of capital expenditures

CF_n = Cash flow in year n

N = Project Life

d = $WACC_{Real}$

Information on the major overhauls and replacement frequency and cost (CF_n) as well as the project life (N) for each storage technology can be found in Section 6. The $WACC_{Real}$ is calculated below.

Weighted Average Cost of Capital

The real WACC is presented in Equation 5. This value represents the rate paid to financial assets as a weighted average after adjustment for inflation.

$$WACC_{Real} = \frac{(1+WACC_{Nominal})}{(1+inflation)} - 1 \quad (5)$$

$$WACC_{Nominal} = DF \times i_{nom} \times (1 - \tau) + (1 - DF) \times COE_{nom} \quad (5.1)$$

Where:

Table A4.1. WACC Equation Variable List and Definition

Variable	Name	Definition
$inflation$	Inflation rate (%)	Assumed rate of inflation. Assumed to be 2.8% in this report.
DF	Debt Fraction (%)	Percent of total capital expenditures financed with debt.
i_{nom}	Nominal interest rate (%)	Interest rate assumed on expenditures financed with debt.
τ	Tax rate (federal and state)	Federal and state combined tax rate (%).
COE_{nom}	Nominal cost of equity (%)	Rate of return paid on assets financed with equity.

Fixed Charge Rate

The fixed charge rate gives the percent of capital expenditures that must be recovered on an annual basis to cover annual revenue requirements. It is a function of the capital recovery factor (CRF) and the construction finance factor (CFF), defined below. The tax depreciation method is the modified accelerated cost recovery system (MACRS), half-year convention. More information on the term used to determine the present value of depreciation for each technology can be found in Section 6.

$$FCR = CRF \times \frac{(1-\tau \times PVD_{MACRS})}{(1-\tau)} \times CFF \quad (6)$$

Where:

CRF = Capital recovery factor (%)

τ = Tax rate (federal and state)

PVD_{MACRS} = Present Value of Depreciation (MACRS)

CFF = Construction finance factor (%)

Capital Recovery Factor

The CRF represents the constant annual payment necessary to amortize a loan over a specific lifetime. It is a function of the assumed economic life (t) and $WACC_{Real}$ (d). This equation returns the CRF as a fraction of the original principle that must be paid annually.

$$CRF = \frac{d}{1-(1+d)^{-t}} \quad (7)$$

Where:

CRF = Capital Recovery Factor (%)

t = Economic life (years)

$d = WACC_{Real}$, see Equation (5)

The economic life (t) is the assumed number of years to pay off asset costs. This value is assumed to be 20 years for all technologies in this report for the base case.

Construction Finance Factor

The CFF represents the financing costs that are incurred during the construction period of the project and is shown in Equation 8.

$$CFF = \sum_{c=0}^C (AI_c \times CF_c \times LC) + \sum_{c=0}^C (AE_c \times CF_c \times EC) \quad (8)$$

Where:

CFF = Construction Finance Factor (%)

c = Year of construction period

C = Total construction period (years)

AI_c = Accumulated interest during construction in year c

CF_c = Capital fraction (%) in year c

LC = Percent of leverage

EC = Percent of equity

AE_c = Accumulated equity during construction

Where:

$$AI_c = 1 + ((1 + i_{nom})^{c+0.5} - 1) \quad (8.1)$$

$$AE_c = 1 + ((1 + COE_{nom})^{c+0.5} - 1) \quad (8.2)$$

i_{nom} = nominal interest rate

COE_{nom} = nominal cost of equity

The ESGC is a crosscutting effort managed by DOE's Research Technology Investment Committee (RTIC). The Energy Storage Subcommittee of the RTIC is co-chaired by the Office of Energy Efficiency and Renewable Energy and Office of Electricity and includes the Office of Science, Office of Fossil Energy, Office of Nuclear Energy, Office of Technology Transitions, ARPA-E, Office of Strategic Planning and Policy, the Loan Programs Office, and the Office of the Chief Financial Officer.

